

JINDŘICH NEČAS CENTER FOR MATHEMATICAL MODELING
LECTURE NOTES

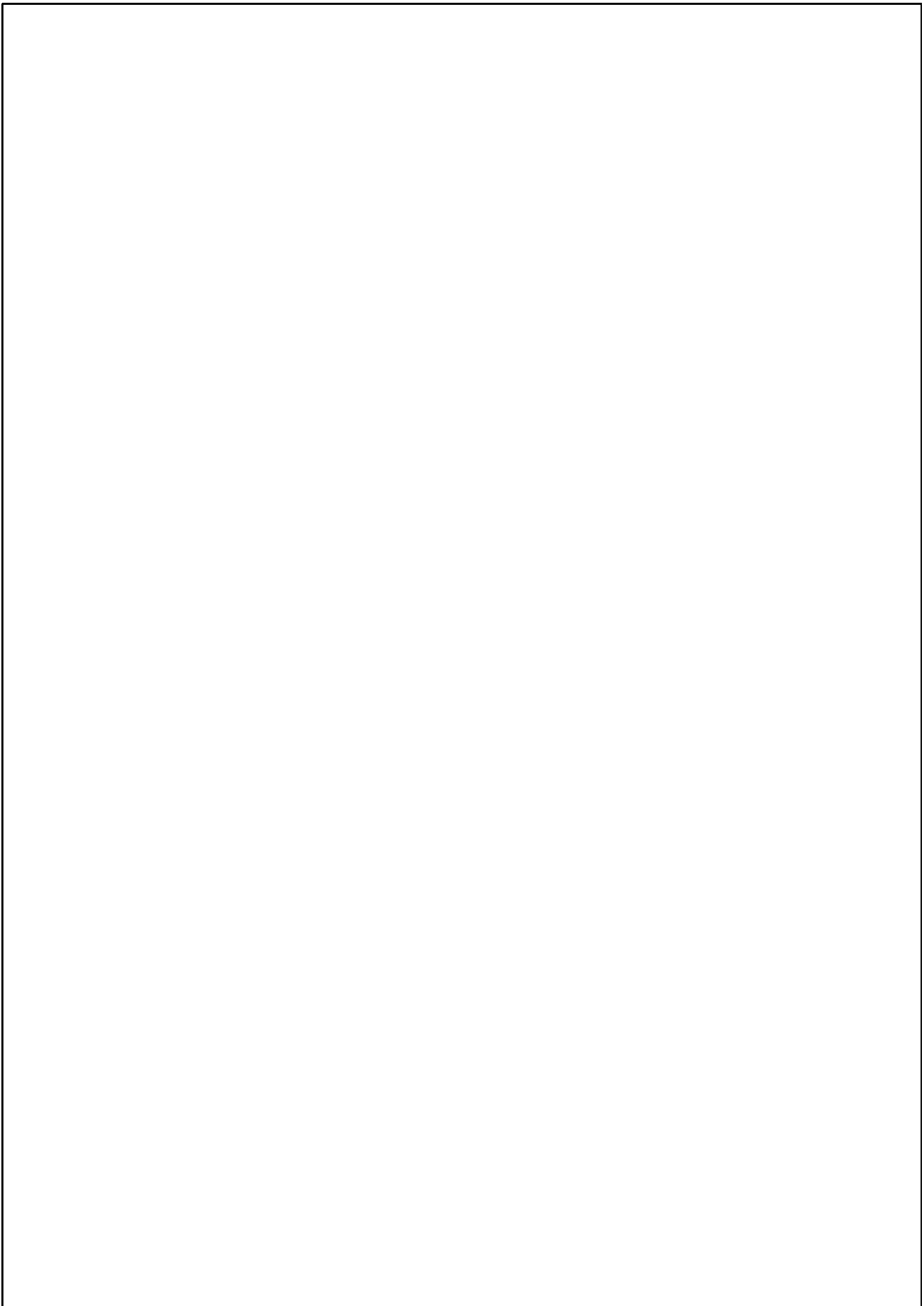
Volume 3

Reviews in geomechanics

Volume edited by J. MÁLEK, V. PRŮŠA and K. R. RAJAGOPAL

***matfyz*press**

VYDAVATELSTVÍ MATEMATICKO-FYZIKÁLNÍ FAKULTY
UNIVERZITY KARLOVY V PRAZE



JINDŘICH NEČAS CENTER FOR MATHEMATICAL MODELING
LECTURE NOTES

Volume 3

Editorial board

Michal BENEŠ
Pavel DRÁBEK
Eduard FEIREISL
Miloslav FEISTAUER
Josef MÁLEK
Jan MALÝ
Šárka NEČASOVÁ
Jiří NEUSTUPA
Antonín NOVOTNÝ
Kumbakonam R. RAJAGOPAL
Hans-Georg ROOS
Tomáš ROUBÍČEK
Daniel ŠEVČOVIČ
Vladimír ŠVERÁK

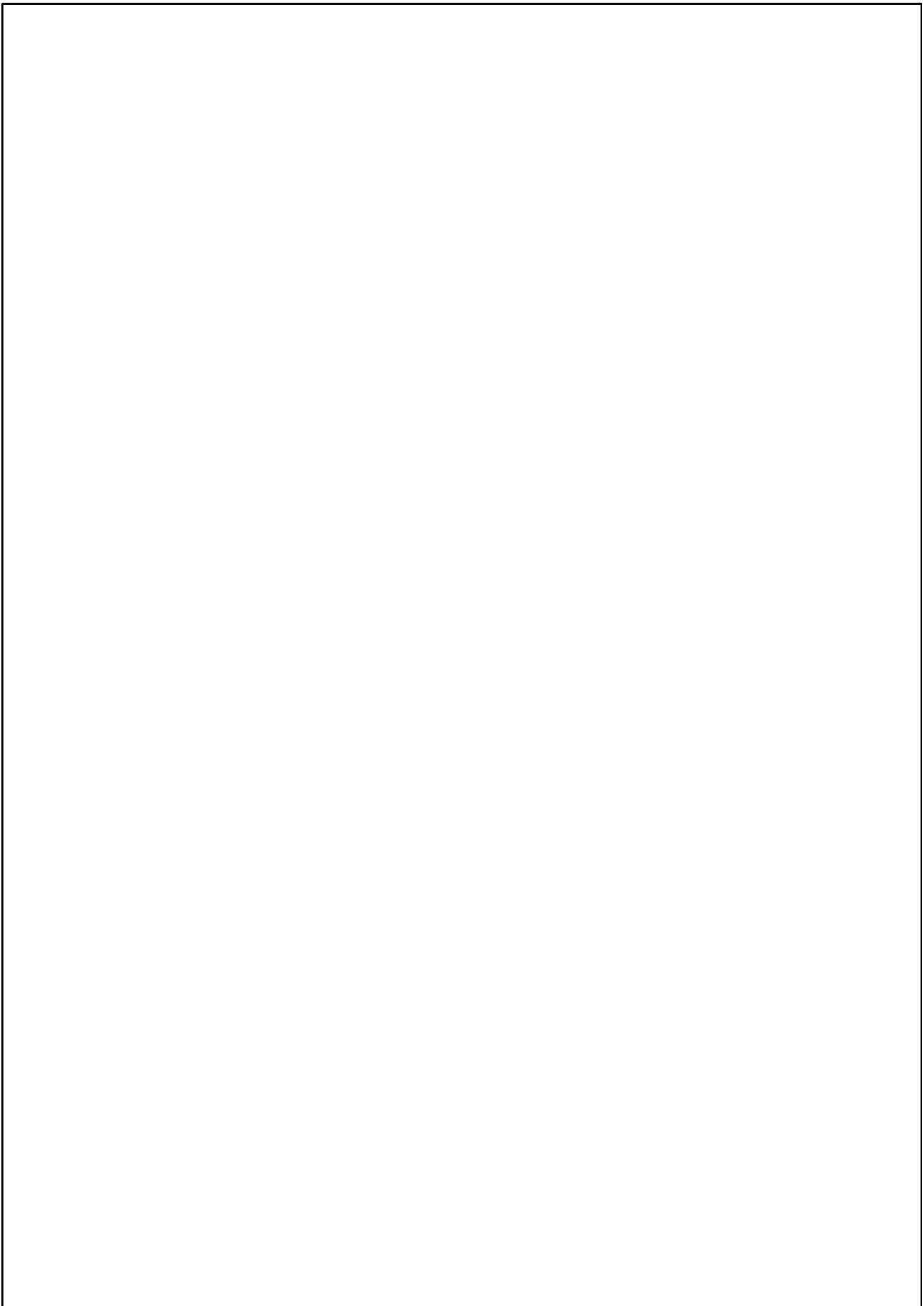
Managing editors

Petr KAPLICKÝ
Vít PRŮŠA



matfyzpress

VYDAVATELSTVÍ
MATEMATICKO-FYZIKÁLNÍ FAKULTY
UNIVERZITY KARLOVY V PRAZE



Jindřich Nečas Center for Mathematical Modeling
Lecture notes

Reviews in geomechanics

B. BERNSTEIN

Department of Chemical and
Environmental Engineering
Illinois Institute of Technology
Chicago, Illinois 60616, USA

E. MASAD

Department of Civil Engineering
Texas A&M University
College Station, Texas 77843, USA

I. F. COLLINS

Department of Engineering Science
University of Auckland
Auckland 1142, New Zealand

K. R. RAJAGOPAL

Department of Mechanical Engineering
Texas A&M University
College Station, Texas 77843, USA

J. M. KRISHNAN

Department of Civil Engineering
Indian Institute of Technology
Madras, Chennai 600036, India

R. G. ROBINSON

Department of Civil Engineering
Indian Institute of Technology
Madras, Chennai 600036, India

Volume edited by J. MÁLEK, V. PRŮŠA and K. R. RAJAGOPAL

2000 *Mathematics Subject Classification.* 74-06, 74Lxx, 74Axx

Key words and phrases. mathematical modeling, continuum mechanics, soil, granular materials, asphalt

ABSTRACT. The text provides a record of lectures given at Workshop on Geomaterials held in September 2006 under the auspices of the Jindřich Nečas Center for Mathematical Modeling. The text surveys a wide variety of topics in the theory of geomaterials such as asphalt, bitumen and soil. Contributions are mainly focused on description of physical properties of such materials and on suggestions how to mathematically describe these materials.

All rights reserved, no part of this publication may be reproduced or transmitted in any form or by any means, electronic, mechanical, photocopying or otherwise, without the prior written permission of the publisher.

© Jindřich Nečas Center for Mathematical Modeling, 2007

© MATFYZPRESS Publishing House of the Faculty of Mathematics and Physics
Charles University in Prague, 2007

ISBN 978-80-7378-032-6

Preface

Workshop on the mechanics of geomaterials

Despite the wide spread use of sand, soils, stones, asphalt and other geomaterials from times immemorial there is no reliable theoretical framework for the description of the behavior of such materials. However, in virtue of the ubiquitous use of such materials there has always been an abiding interest in developing models to describe the response of geomaterials. A workshop was organized at the Nečas Center for Mathematical Modeling in Prague, September 2006, with the aim to provide a forum for geologists, physicists, engineers, mathematical modelers and mathematical analysts to put their diverse backgrounds together to understand, interpret, and model the behavior of geomaterials. The format for the workshop consisted in six experts in various aspects concerning geomaterials lecturing on their areas of expertise, with sufficient time between the lectures for a meaningful interaction to take place between the participants and the lecturers.

This book presents the main lectures that were given at the workshop. The first chapter, after identifying the materials that are referred to as asphalt, provides an introduction into the physical and chemical structure of asphalt, a complex heterogeneous mixture of hydrocarbons found naturally in geological structures and also as a byproduct of the refining process of oils. The lectures also provide a brief sketch of the history of the usage of asphalt and its availability.

This is followed by a chapter by Murali Krishnan concerning the mechanical response of asphalt. The multi-component and heterogeneous nature of asphalt and the challenges it provides with respect to mathematical modeling is discussed in some detail. One feature of asphalt that makes its modeling particularly difficult is the change that occur in both its chemical and physical structure in time. A brief description of a thermodynamical framework is presented within which mathematical models can be developed for the behavior of the asphalt. Rate type viscoelastic models that possess multiple relaxation mechanisms are developed. The chapter ends with a brief discussion of the applications of asphalt.

In the third chapter Eyad Masad provides a detailed presentation of a variety of experimental methods which are being used to determine the internal structure of asphalt. Special emphasis is placed on experimental imaging techniques and the mathematical analysis used for data reduction. The effect of compaction on material properties and issues concerning modeling are also discussed.

The next chapter by Robinson deals with the behavior of soils. Different types of apparatus used to measure the friction in soils and the methodologies developed for characterizing the various attributes such as size, shape, roughness, density, etc., are discussed. Some empirical correlations are provided for the quantification of the

roughness of soils and some of the issues that are yet to be resolved concerning the internal friction in soils is presented.

The fifth chapter deals with the consolidation behavior of land fills. A detailed discussion is provided concerning the swelling of lumpy clays and methods for measuring their shear strength.

Ian Collins, in the sixth chapter, provides a historical introduction concerning the modeling of the behavior of soils and granular solids. The reader is introduced to the seminal ideas of Reynolds concerning “dilatancy”. Experimental techniques for measuring material properties of granular solid are discussed in detail. A systematic and critical discussion of the various theoretical models that have been used in the past and those that are currently in use is presented. Coulombs models, Double shearing models, Cap models, Critical state models are some of the models that are discussed. An interesting thermodynamic approach for modeling rate independent inelastic bodies that is appropriate for granular materials is presented.

The reader is introduced to the concept of Hypoelasticity in the next to the last chapter, written by Bernstein. The behavior of such materials is contrasted against the response of hyperelastic and plastic bodies by appealing to a simple one dimensional response. This is followed by the development of a rigorous thermodynamic basis for describing the behavior of such materials. The final chapter of the book concerns the viscoelastic response of materials. Bernstein discusses a very general class of viscoelastic materials that have memory, namely, the Bernstein-Kearsley-Zapas model that has been found to be quite successful in describing the response of viscoelastic fluids and which seems to have the potential to describe certain classes of geological materials.

The topics covered in the book have a wide ambit: solids, fluids and granular materials; bodies that are elastic, viscoelastic and inelastic. Numerous important problems pertinent to geomaterials have been omitted, for example earthquake engineering, liquefaction of soils, etc. However, it is hoped that the collection of essays will not only provide an introduction to the thermomechanics of a variety of geophysical materials but will also serve as a useful reference book for practitioners in geomechanics.

August 2007

J. Málek
V. Průša
K. R. Rajagopal

Contents

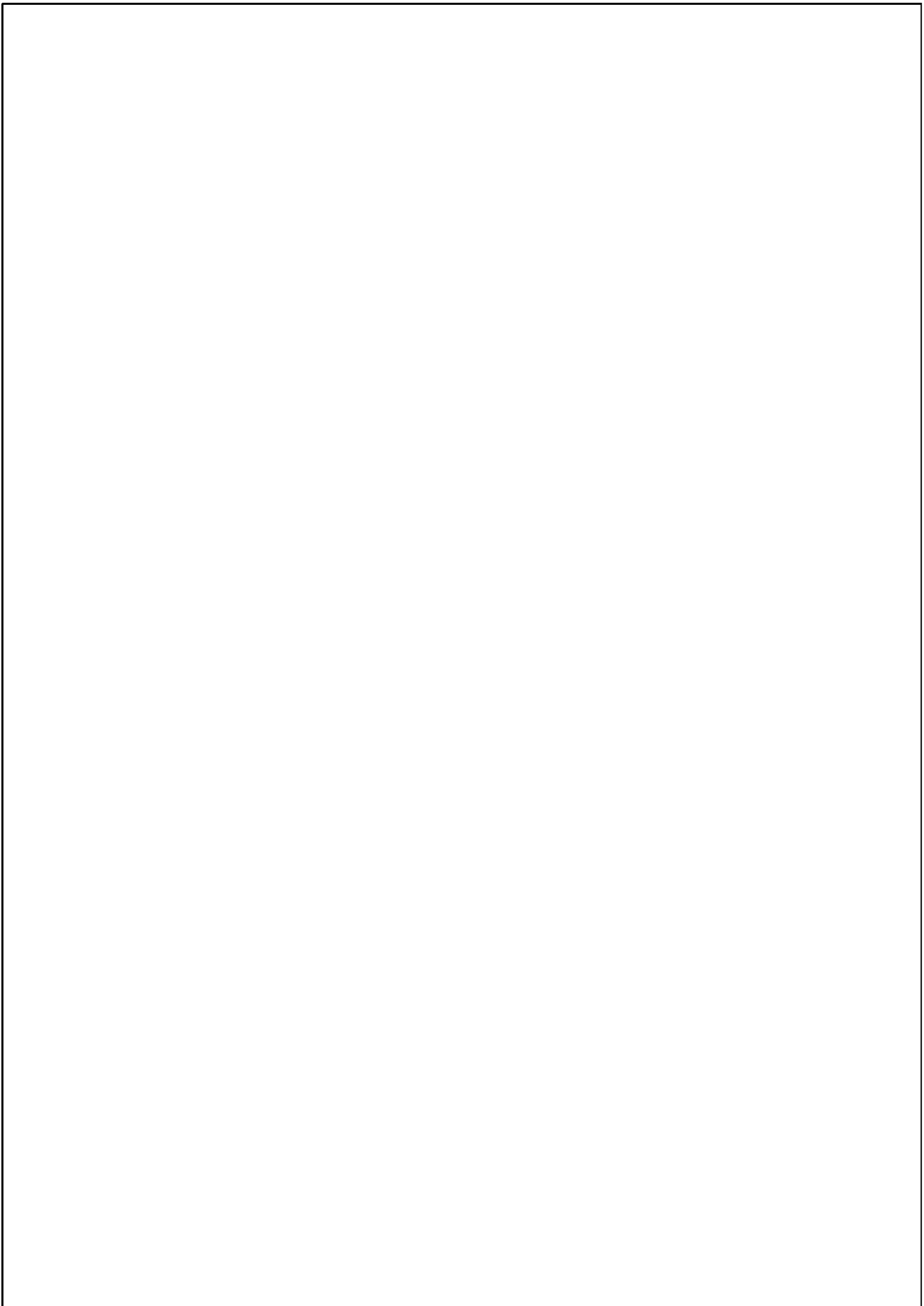
Preface	vii
Workshop on the mechanics of geomaterials	vii
Part 1. Modeling of asphalt	1
Chapter 1. The physical and chemical structure of asphalt: with a brief history of their usage and availability	
J. M. KRISHNAN, K. R. RAJAGOPAL	5
1. What are bitumen and asphalt?	5
2. On the abundance of bitumen in nature	7
3. Uses of bitumen from prehistory to modern times	8
4. Uses of bitumen in modern times	9
5. Physical chemistry of asphalt	13
Bibliography	29
Chapter 2. The mechanical behavior of asphalt	
J. M. KRISHNAN	39
1. Introduction	39
2. Issues related to modeling of asphalt	41
3. Modeling of asphalt	45
4. Applications	48
5. Conclusions	49
Bibliography	51
Chapter 3. Internal structure and modeling of asphalt mixtures	
E. MASAD	57
1. Introduction	57
2. Imaging methods for measuring the internal structure distribution	57
3. Applications of image analysis techniques	58
4. Summary	64
Bibliography	65
Part 2. Soil and granular materials	69
Chapter 1. Interface behaviour of soils	
R. G. ROBINSON	73

1. Introduction	73
2. Apparatus types reported in the literature	73
3. Factors influencing interfacial friction	75
4. Quantification of interface roughness and empirical correlations	79
5. Limiting values of δ	80
6. Analysis of past studies	81
7. Effect of mode of shear on shear stress-movement curves	82
8. Modeling of interfaces	83
9. Looking forward	84
Bibliography	85
Chapter 2. Consolidation behaviour of reclamation fill made of lumps	
R. G. ROBINSON	89
1. Introduction	89
2. Experimental programme	90
3. Results and discussions	92
4. Some research issues	98
5. Conclusions	98
Bibliography	101
Chapter 3. Modelling the behaviour of soils and granular materials	
I. F. COLLINS	103
1. Historical introduction	103
2. Material properties and experimental techniques	106
3. Some extant theories of soil mechanics	109
4. Thermomechanical approaches to the constitutive modelling of soils	115
5. Conclusions	124
Bibliography	127
Part 3. Hypoelasticity and viscoelasticity	131
Chapter 1. Hypoelasticity	
B. BERNSTEIN	135
1. Introduction	135
2. Equations of hypoelasticity	136
3. Plasticity	137
4. Hypoelasticity	141
5. Concluding Remarks	144
Bibliography	145
Chapter 2. Viscoelasticity	
B. BERNSTEIN	147
1. Introduction	147
2. Elastic solid	148
3. Viscous fluid	149

CONTENTS

xi

4. Viscoelasticity	149
5. Energy	150
6. General theory	152
7. Conclusion	154
Bibliography	155



Part 1

Modeling of asphalt

2000 *Mathematics Subject Classification.* 74L10, 74E99, 74A20

Key words and phrases. asphalt, bitumen, constitutive relations

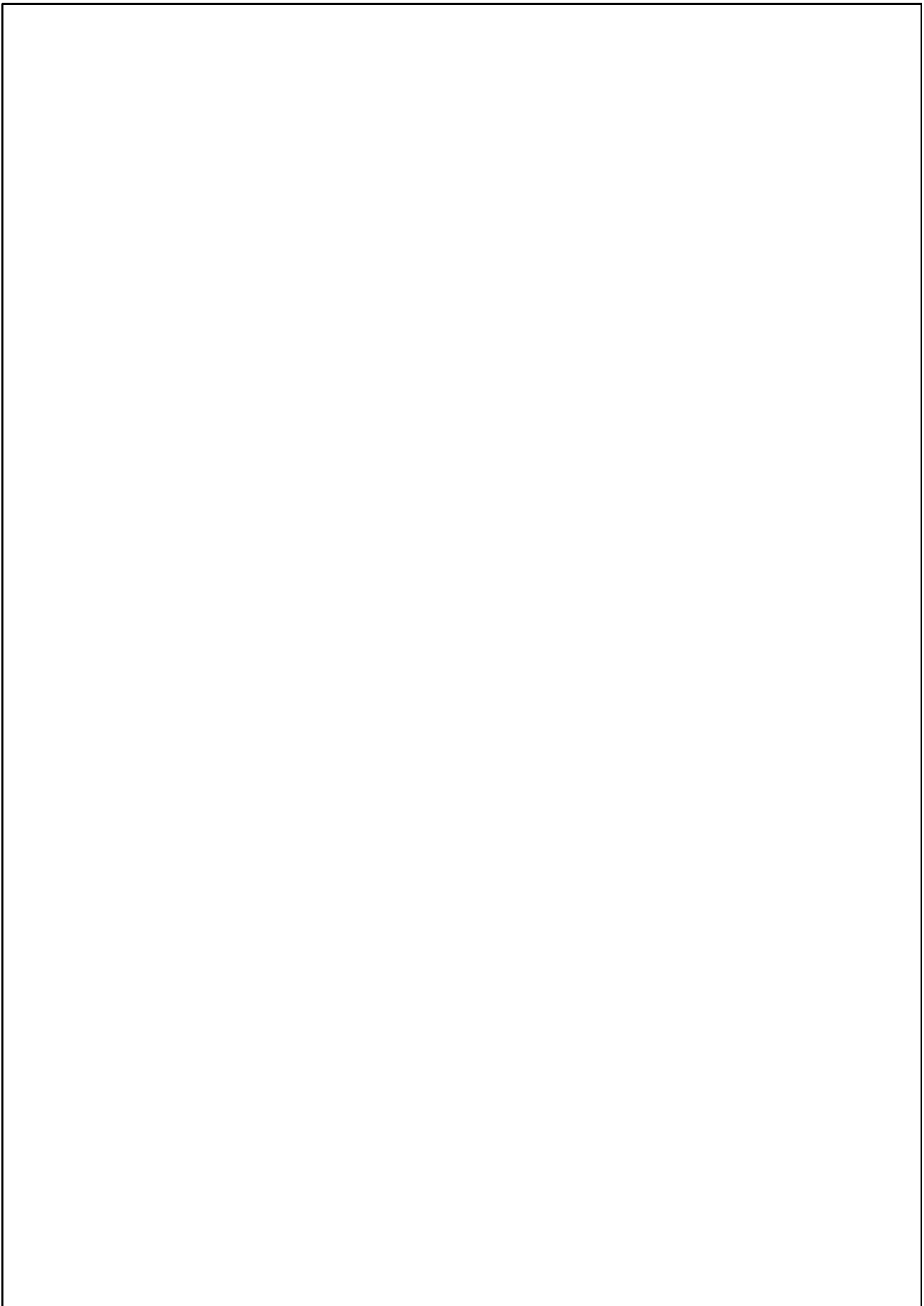
ABSTRACT. The first two chapters discuss various aspects of modeling of asphalt. The first chapter provides a short historical overview of usages of asphalt and of physical chemistry of asphalt. The second chapter is devoted to modeling of asphalt in the framework of continuum mechanics. Various physical features of asphalt are discussed, and finally a thermodynamic framework for the constitutive modeling of asphalt is suggested – the merit of the framework is that it recognizes the fact that materials like asphalt can exist in more than one natural configuration (for instance, stress free configuration).

The third chapter discusses various methods for analysis of the internal structure of asphalt, and the influence of the internal structure on the performance of hot mix asphalt used in construction works.

ACKNOWLEDGEMENT. [J. Murali Krishnan] J. Murali Krishnan thanks the Mathematical Institute of Charles University, Prague for giving an opportunity to present this work and J. Murali Krishnan and K. R. Rajagopal thank the National Science Foundation, USA for its support of this work.

Contents

Chapter 1. The physical and chemical structure of asphalt: with a brief history of their usage and availability J. M. KRISHNAN, K. R. RAJAGOPAL	5
1. What are bitumen and asphalt?	5
2. On the abundance of bitumen in nature	7
3. Uses of bitumen from prehistory to modern times	8
4. Uses of bitumen in modern times	9
5. Physical chemistry of asphalt	13
5.1. Early studies on the chemistry of bitumen	14
5.2. Chemistry of straight run bitumen	15
Bibliography	29
Chapter 2. The mechanical behavior of asphalt J. M. KRISHNAN	39
1. Introduction	39
2. Issues related to modeling of asphalt	41
2.1. ‘Multi-constituent’ nature of asphalt	41
2.2. Asphalt transitions	42
2.3. Internal structure change of asphalt with time	43
3. Modeling of asphalt	45
3.1. Preliminaries	45
3.2. Modeling asphalt with multiple relaxation mechanisms	46
4. Applications	48
5. Conclusions	49
Bibliography	51
Chapter 3. Internal structure and modeling of asphalt mixtures E. MASAD	57
1. Introduction	57
2. Imaging methods for measuring the internal structure distribution	57
3. Applications of image analysis techniques	58
3.1. Compaction and mechanical properties	58
3.2. Fluid flow and permeability	59
3.3. Modeling	62
4. Summary	64
Bibliography	65



CHAPTER 1

The physical and chemical structure of asphalt: with a brief history of their usage and availability

J. M. KRISHNAN, K. R. RAJAGOPAL

1. What are bitumen and asphalt?

Amongst the earliest of construction materials, asphalt was used aplenty in all the early civilizations: Babylonia, Mesopotamia, Sumeria, Chaldea, Mohenjodaro and Harappa, Phoenicia, China and later in Greece and Rome, and unlike other construction materials its use has become ever more common. Finding ever-increasing use in the unlikeliest of applications, asphalt has become indispensable, as it is the material of choice for the construction of roadways and runways that serve as the circulatory system for the world economy.

According to the Oxford English Dictionary (OED) [137], asphalt is “*A bituminous substance, found in many parts of the world, a smooth, hard, brittle, black or brownish-black resinous mineral, consisting of a mixture of different hydrocarbons; called also mineral pitch, Jew’s pitch and in the Old Testament ‘slime’*”. The Oxford English Dictionary [137] defines Bitumen as “*Originally, a kind of mineral pitch found in Palestine and Babylon, used as mortar, etc. The same as asphalt, mineral pitch, Jew’s pitch, Bitumen Judaicum*”. It also provides the following more scientific definition “*In modern scientific use, the generic name of certain inflammable substances, native hydrocarbons more or less oxygenated, liquid, semi-solid and solid, including naphtha, petroleum, asphalt, etc. Elastic Bitumen: Mineral Caoutchouc or Elaterite*”. Today, both these words are used to describe the same class of materials, asphalt being the word of choice in the United States and bitumen in the European countries and countries in the East (see also [35] and [153]). Concerning the controversies surrounding the usage of the word asphalt and bitumen in United States of America and Europe, we refer the reader to the book by Jaccard [73] and an elaborate discussion related to the usage of these words in the review by Peckham [109].

The Webster’s Dictionary [148] defines asphalt as “*A brown or black, tarlike, bituminous substance that consists mainly of hydrocarbons, found in large flat beds or made by refining petroleum*” and bitumen as “*1) asphalt found in natural state, 2) any of various black, combustible, solid to semisolid mixtures of hydrocarbons that are usually obtained from the distillation of petroleum, used to make roofing materials, sealants, paints, etc*”. The above definitions do little to clearly delineate the class of materials that are referred to as “bitumen”.

On turning our attention to definitions offered by scientific organizations, we find that there is no clear consensus as to what one exactly denotes by the terms bitumen and asphalt. The American Society for Testing and Materials (ASTM) in its standard ASTM D 8- 97 [10] has promulgated the following definitions for asphalt and bitumen:

Bituminous materials (Relating in general to bituminous materials): a class of black or dark-colored (solid, semi-solid or viscous) cementitious substances, natural or manufactured, composed principally of high molecular weight hydrocarbons, of which asphalts, tars, pitches, and asphaltites are typical.

Relating specifically to Petroleum or Asphalts: Asphalt, a dark brown to black cementitious material in which the predominating constituents are bitumens which occur in nature or are obtained in petroleum processing.

The *Réunion Internationale des Laboratoires d'Essais et de recherche sur les Matériaux et les Constructions* (RILEM – International Union of Laboratories and Experts in Construction Materials, Systems and Structures) proposed a different set of definitions for asphalt and bitumen [52, 123]. In this set of definitions, RILEM chose to use a very general terminology for categorizing asphalt and bitumen. They were called as *hydrocarbon binders* and most of the standards pertaining to asphalt and bitumen were referred to by the name hydrocarbon binders (see, for instance [124, 125]). As per the RILEM standards,

Bitumen is the heaviest fraction of petroleum and can be:

- (i) petroleum bitumen obtained by refinery processes from crude petroleum;
- (ii) natural bitumen occurring in mixtures, such as Trinidad Lake Asphalt, which were formed during natural processes of decantation, evaporation or absorption. Natural Bitumen often occurs in the form of natural asphalt, asphalt being a natural or artificial mixture of bitumen with mineral matter.

In all the above classifications, bitumen is clearly differentiated from asphalt. However, it is unclear what exactly the framers of the ASTM definition meant by solid, liquid and viscous. Similarly the latest ASTM definition for bitumen that allows it to be either solid, semi-solid or viscous implies that a solid cannot be viscous, and clearly this is not a tenable position within the context of modern mechanics that allows for viscoelastic solids. Not to accept the possibility that materials could be viscoelastic solids or viscoelastic fluids is rather odd given the great strides made in viscoelasticity by the time these definitions were put in place by the Permanent International Association of Road Congresses as well as the current ASTM definitions. The above definitions would leave the modern day student of mechanics none the wiser with respect to the response characteristics of the material being described.

The recent tools of science such as Gas Chromatography, Mass Spectrometry and Differential Scanning Calorimetry have advanced the classification of asphalt and bitumen to a sound footing and while the chemistry of asphalt and bitumen

have been re-examined by using these tools, the translation of such information into modeling the thermomechanical response of these materials has not kept pace [38, 39, 53, 86, 93, 117]. Early papers that deserve special mention in view of their attention to detail are those by Richardson (1898) [121] on the nature and origin of asphalt found in Trinidad and Venezuela (a discussion of the composition of the material is provided in a detail that is most impressive) and that by Abraham (1912) [1] on the classification of bitumens.

2. On the abundance of bitumen in nature

We shall discuss briefly the availability of natural bitumen in various parts of the world. Bitumen occurs naturally in seas, lakes, ponds and rivers, on mountainsides, in coal pits and iron mines; practically in all forms of flora and fauna. A compendious tabular presentation of the various sources of bitumen: volcanoes, sandstones, limestones, coal deposits, shales, calcareous rocks, etc., their location and geological position has been compiled by Whittlesey (1853) [151].

Bitumen seems to have been available naturally aplenty. Agricola [2] remarks “*Liquid bitumen, if there is much floating on springs, streams and rivers, is drawn up in buckets or other vessels; but, if there is little, it is collected with goose wings, pieces of linen, ralla, shreds of reeds and other things to which it easily adheres, and it is boiled in large brass or iron pots by fire and condensed*”. Asphalt was also found in other parts of Europe, a lengthy description of the asphaltic mine of the Val-de-Travers in the canton of Neufchatel is provided by Henri Fournel¹ (1838) [51].

The Hebrews harvested the Dead Sea for bitumen. Agricola [2] observes “*of this kind is the lake which the Hebrews call the Dead Sea, and which is quite full of bituminous fluids*”.

While practically devoid of life, the Dead Sea was a great source of economic activity in antiquity². In addition to being a source of Salt, Bromine and Potash obtained by evaporating the Brines, the land locked Dead Sea was a source for asphalt which was harvested in plenty. A detailed study of the Geochemistry of the Dead Sea asphalt as well as a discussion of the trade of the Dead Sea asphalt to

¹Asphalt was available in a mineral rock called *Asphaltic Calcaire* with the proportion of bitumen being up to 10 percent in these rocks. From the making of a vase for the King of France in the year 1740 to the caulking of ships belonging to the East India Company in the same year, it was used in diverse applications. However, it was not until the year 1835 the asphaltic rock from this mine was used for the construction of footways in the Port Royal, followed by the footways of *Pont du Carousel* in Paris.

²A detailed report of the geology of the several parts of Western Asia was carried out by Hitchcock in 1842 [66]. In this report, Hitchcock detailed a variety of limestone found on the western shore of Dead Sea which according to the compositional analysis that he carried out consisted of 25 percent of bitumen. His remarks related to the possible use of this bituminous limestone is very interesting and we quote “. . . if this rock can be obtained in abundance, it may prove valuable in the formation of a cement for pavements.” [66, page 363]. These specimens of rocks and minerals that Hitchcock mentions were sent to him by the American Missionaries located in Western Asia.

Canaan and Egypt in the early Bronze age can be found in Connan, Nissenbaum and Dessort (1992) [33] (see also [80])³.

Peckham [111] discusses in great detail the geographical distributions of the various types of “*semi-solid bitumens and bituminous rocks*” in the United States⁴. He mentions that the different types of materials that go under the name of bitumen are to be found in the valley of the Connecticut river, in the eastern portion of the state of New York, in New Jersey, in Ritchie county in West Virginia, in numerous counties in Texas (in the valleys of the Brazos in Brazos county) and in the valley of the Red River in Montage county, in Burnett county and Uvalde county, in the area of Upper Willow Creek and white river in Colorado, in parts of Utah adjoining northwestern Colorado, Breckenridge, Hogan and Carter Counties in Kentucky, the banks of the Washita River and the Prairie adjoining the Arbuckle mountains in Okalahoma, in the vicinity of Santa Cruz, San Luis Obispo, Los Alamos, Santa Barbara, Los Angeles, San Francisco, Carpinteria and many other locations in California (see also [42]).

Today, we rarely, if ever get our asphalt from natural sources. It is available in large quantities at the end of the refining process for petroleum. For instance, the total production of hot mix asphalt in Europe and USA was around 900 million tones during the year 2000 [47].

3. Uses of bitumen from prehistory to modern times

Few natural materials are put to as many diverse uses as bitumen. Clear evidence exists concerning the use of Bitumen from the Hummalian period from around 180,000 BC [18, 19]. It was used as the adhesive of choice to construct hunting implements out of stick and stone, the success of the hunt critically depending on how well the sharpened flint stuck to the stick that was flung at a fleeing animal. Forbes [50] quotes a passage from Pliny that specifically addresses this point “*Some authors include naphtha (as described in Book two) under the category of bitumen, but its inflammability and close relationship to fire precludes it from any useful employment*”. Now the lighter bituminous oil and their distillates are used as much, or more, than the more solid family members. A detailed discussion of the uses of bitumen from the remote ages to the early eighteen hundreds, with copious quotations from the historians of yore, can be found in the essay on bitumen published in 1839 [138]. A thorough treatment of the practical aspects concerning the properties and uses of bitumen, its varieties, geological characterization of asphaltic rock, its preparation for different uses, a cost analysis of different mastics and a catalogue of numerous experiments carried out in Europe and the United States can be found

³We also refer the reader to the works of Nissenbaum and Goldberg (1980) [103], Rullkötter *et al.*, [128], and Tannenbaum and Aizenshtat [136] on the geochemical aspects of bitumen found in and around the Dead Sea area and the use of biological marker parameters in ranking the maturity of bitumens found in these areas.

⁴An exhaustive document concerning the production, technology and uses of petroleum and its products was prepared by Peckham as part of the Unites States of America’s tenth census during 1880 [108]. The phrase petroleum used in this report was used literally to include solid - asphaltum, semi-fluid - maltha, fluid - petroleum and gaseous - natural gas. This impressive report includes almost all the references that are pertinent to petroleum (totaling more than 1000 in number) starting from *circa* 450 BC to 1880 AD.

in the authoritative article by Halleck⁵ (1841) [59]. Another detailed and thorough discussion of the uses of asphalt in roadways, as a coating for bridges and viaducts, as an insulator, coatings for masonry, roofs, in silos, etc., can be found in the book by Delano (1893)[40].

We now consider its multifarious uses in the unlikeliest of places. Bitumen was used by the Egyptians for embalming. As Greenhill [55] observes “*there are several kinds of embalming, viz., with asphalt or pissasphalt, with Oyl or Gum of cedar, with aromatics and spices*”. However, that asphalt was invariably one of the many ingredients is clear from the very use of the word Mummy. The word Mummy is derived from the Persian word *mumiya*, the word for asphalt in Persian (See Pettigrew [115]). For instance, Forbes [50] states that . . . *mûmijâ*, a word which in the Persian language denotes “wax”, and in Arabic “bitumen”. In recent times, Connan and Desort [31] used Gas chromatography and mass spectrometry to trace the presence of Dead Sea asphalt in the skull, knees and viscera of a mummy from the Guimet Museum in Lyon. They were even able to detect the differences in the molecular composition of the three bitumens to conclude that the embalmers had used *different sources* for their bitumen. They followed their study of 1989 with a study in 1991 [32] wherein they investigated 12 balms of Egyptian mummies and once again found bitumen from different sources from the Dead Sea and Iraq. In any event there is unmistakable evidence for the use of bitumen in mummification in these and many other techniques using petroleum geochemistry studies. The analysis of Koller *et al.*, [79] indicated that the clavicle fragment of the mummy of Idu II contained significant amount of wood tar. The Gas Chromatography - Mass Spectrometric studies of Colombini *et al.* [30] of an Egyptian mummy from the 17th century showed that the main components of the mummy are “*mastic resins, bees wax, an unidentified vegetable oil and most likely Dead Sea asphalt*”. These and other studies would lead us to conclude that bitumen was used in mummification. Such a view has been aptly expressed by Bahn (1992) [13] as follows: “*The lid has, it seems, finally been put on a controversy about whether the ancient Egyptians used bitumen when mummifying the dead. In their recent paper on the topic J. Connan and D. Dessort show unequivocally that bitumen was indeed generally used in mummification, and far earlier than hitherto suspected, and they also pinpoint the most likely sources of the material.*”

4. Uses of bitumen in modern times

The Shell Bitumen Handbook [150] lists over 250 known current uses for bitumen in agriculture, construction, hydraulics, erosion control, automobile industry, electrical industry, railways, paving industry, etc. (see Table 1, and also [8, 132]).

⁵Halleck [59] set out to write as complete an article as possible concerning the properties and uses of bitumen. He remarks “*The following article is an abstract of all the important publications, within the compiler’s reach on the properties and uses of bitumen; and will be found to contain, it is believed, most of value that is now known upon the subject.*”

Table 1: More than 250 known uses of Bitumen [150]

<p>Agriculture Damp-proofing and water-proofing buildings, structures, Disinfectants, Fence post coating, Mulches, Mulching paper, Paved barn floors, barnyards, feed platforms, etc., Protection tanks, vats, etc., Protection for concrete structures, Tree paints, Water and moisture barriers, (above and below ground) Wind and water erosion control, Weather modification areas.</p> <p>Buildings <i>Floors</i> Damp-proofing and water proofing, Floor compositions, tiles, coverings, Insulating fabrics, papers, Step treads. <i>Roofing</i> Building papers, Built-up roof adhesives, felts, primers, Caulking Compounds, Cement waterproofing compounds, Cleats for roofing, Glass wool compositions, Insulating fabrics, felts,</p>	<p><i>Miscellaneous</i> Air drying paints, varnishes, Artificial timber, Ebonized timber, Insulating paints, Plumbing, pipes, Treated awnings.</p> <p>Hydraulic and erosion control Hydraulic and erosion control Canal linings, sealants, Catchment area, basins, Dam groutings, Dam linings, protection, Dike protection, Ditch linings, Drainage gutters, structures, Embankment protection, Groynes, Jetties, Levee protection, Mattresses for levee and bank protection, Membrane linings, water proofing, Reservoir Revetments, Sand dune stabilization, Sewage lagoons, oxidation ponds, Swimming pools, Waste ponds, Water barriers.</p> <p>Industrial <i>Aluminum foil compositions using bitumen</i> Backed felts, Conduit insulation, Lamination, Insulating Boards, Paint Compositions, Papers, Pipe wrappings, Roofing, Shingles.</p>	<p><i>Compositions</i> Black grease, Buffing compounds, Cable splicing compound, Coffin linings, Embalming, Etching compositions, Extenders, Explosives, Fire extinguisher compounds, Joint fillers, Lap cement, Lubricating grease, Pipe coatings, dips, joint seals, Plastic cements, Plasticisers, Preservatives, Printing inks, Well drilling fluid, Wooden cask liners. <i>Impregnated, treated materials</i> Armored bituminized fabrics, Burlap impregnation, Canvas treating, Carpeting medium, Deck cloth impregnation, Fabrics, felts, Mildew prevention, Packing papers, Pipes and pipe wrapping, Planks, Rugs, asphalt base, Sawdust, cork, asphalt composition, Treated leather, Wrapping papers. <i>Paints, Varnishes, etc.</i> Acid-proof enamels, mastics, varnishes, Acid-resistant coatings, Air-drying paints, varnishes, Anti-corrosive and anti-fouling</p>	<p>Paving (See also Hydraulics, Agriculture, Railways, Recreation) Airport runways, taxiways, aprons, etc. Asphalt blocks, Brick fillers, Bridge deck surfacing, Crack fillers, Curbs, gutters, drainage ditches, Floors for buildings, Warehouses, garages, etc. Highways, roads, streets, shoulders, Parking lots, driveways, Portland cement concrete underseal, Roof-deck parking, Sidewalks, footpaths, soil stabilization.</p> <p>Railways Ballast treatment, Curve lubricant, Dust laying, Paved ballast, sub-ballast, Paved crossings, Freight yards, Station platforms, Rail fillers,</p>
--	--	--	--

Table 1: *continued*

<p>papers, Joint filler compounds, Laminated roofing shingles, Liquid-roof coatings, Plastic cements, Shingles. <i>Walls, siding, ceilings</i> Acoustical blocks, compositions, felts, Architectural decoration, Bricks, Brick siding, Building blocks, papers, Damp-proofing coatings, compositions, Insulating board, fabrics, felts, paper, Joint filler compounds, Masonry coatings, coatings, Plaster boards, Putty, Siding Compositions, Soundproofing, Stucco base, Wallboard.</p>	<p><i>Automotive</i> Acoustical compositions, felts, Brake linings, Clutch facings, Floor sound deadeners, Friction elements, Insulating felts, Panel Boards, Shim strips, Tacking strips, Underseal. <i>Electrical</i> Armature carbons, windings, Battery boxes, carbons, Electrical insulating compounds, papers, tapes, wire coatings, Junction box compound, Moulded Conduits.</p>	<p>paints, Anti-oxidants and solvents, Bases for solvent compositions, Baking and heat resistant enamels, Boat deck sealing compound, Lacquers, japans, Marine enamels <i>Miscellaneous</i> Belting, Blasting fuses, Briquette binders, Burial vaults, Casting moulds, Clay articles, Clay pigeons, Depilatory, Expansion joints, Flower pots, Foundry cores, Friction tape, Fuel, Gaskets, Gramophone records, Mirror backing, Rubbers, Moulded compositions, Shoe fillers, soles, Table tops.</p>	<p>Railway sleepers, Sleeper impregnating, stabilization. Recreation <i>Paved surfaces for:</i> Dance pavilions, Drive-in movies, Gymnasiums, sport arenas, Playground, school yards, Race tracks, Running tracks, Skating tracks, Swimming and wading pools, Tennis courts, handball courts. <i>Bases for:</i> Synthetic playing field and running track surfaces</p>
---	---	---	--

Asphalt is used in large quantities in the construction of dams. Many embankment dams have been waterproofed with asphaltic concrete for the facings and core walls. A long list of advantages to asphalt facings and asphalt core walls can be found in the Shell bitumen hydraulic engineering handbook [132] (see also [7]).

Bituminization of radioactive waste is being carried out in practically all developing countries [70]: *“At present practically all developed countries and also several developing countries are carrying out research and developing works on the bituminization process.”* Belgium, France, Germany, Hungary, India, Japan, Pakistan, Poland, United Arab Republic, United States of America and the former Union of Soviet Socialist Republics bituminize low level radioactive waste. The competing processes for storing low level radioactive wastes are cementation and vitrification. The process of bituminization has advantages over the other processes as well as disadvantages. The advantages are that bitumen is cheap, the process requires moderate temperatures and the process is much simpler than vitrification. Also, the resistance of bitumen to leaching by water is quite high, and the activity range is reasonably broad. On the other hand the disadvantages are that the radiation effects decrease the level of activity that can be incorporated in the bitumen, nitrites and nitrates can lead to the lowering of the self-ignition temperature and this could be dangerous (we shall discuss this in what follows), and the properties expected of the bituminized block limit the amount of solids in the blocks (see [70] for a detailed discussion of the same). As bituminization seems to be a very viable means for storing low and medium level radioactive wastes a serious evaluation of its suitability was instituted⁶ (see [70]): *“For these reasons the IAEA organized a research co-ordination meeting at Dubna (USSR) in December 1968 to discuss in greater detail the properties of the most suitable bituminous materials for incorporation of waste, the properties of the wastes themselves from the standpoint of whether they can be incorporated into bitumen, the activity level permissible for such incorporation, the additives required to improve the properties of bituminous materials, amelioration of the process through the addition of emulsifiers, considerations involved in the design of basic bituminization equipment, and problems related to the burials of materials produced.”*

Little did the IAEA recognize that the bituminized waste could self-ignite with catastrophic consequences, and that is what transpired in 1997.

Bitumen is finding ever increasing use as an insulator in electrical appliances such as transformers. It is also used to insulate cables and the fact that it does not mix with water could make it an insulator of choice for underwater cables, especially in virtue of its inexpensiveness. For more details on the use of asphalt in

⁶IAEA issued reports in the year 1983 [71] and in 1993 [72] (see also [105]). Of interest to the reader is the remark related to the self-ignition characteristics of bituminized waste in the 1993 report [72]: *“Bitumen waste products can support combustion, but they cannot self-ignite during handling, transportation, storage or disposal, e.g. large sources of energy are required to ignite bitumen waste products under these conditions.”* This report also outlines the state-of-the-art for characterization of bitumen for use in the conditioning of radioactive wastes and the specification of empirical testing procedures. It is interesting to note that these testing procedures have been discarded by the pavement engineering community for testing bitumen for the construction of roadways and runways.

electrical appliances and the issues related to it, the reader is referred to [29, 41, 83, 94, 95, 139, 152].

The most widespread use of asphalt today is in the construction of roadways and runways. For the discussion of the first use of bitumen in road construction, the reader is referred to the excellent monograph by Forbes [49].

5. Physical chemistry of asphalt

It is not surprising, as bitumen denotes a class of materials than a single material, that its exact structure is still shrouded in mystery. However, it is astonishing, that given bitumen’s continued use since times immemorial that it may appear that there has not been more effort expended in defining the material and its several sub-classes with more precision and exactitude. This inadequacy is no accident and is a consequence of various reasons that render such classifications inherently complex. Different sources of the crude subjected to different refining processes give rise to different grades of bitumen. Furthermore, the structure of bitumen continually changes from when it leaves the refinery till the final mixing in the hot mix asphalt plant, due to the repeated heating and cooling during its transportation. As new tools of science are being put to use in the exploration of the true nature of bitumen, old erroneous notions are laid to rest, however, new information, that needs to be carefully analyzed and digested, arise that bring with them attendant problems related to modeling. In the following section, we discuss the chemical and physical analysis of bitumen. We have, however, restricted ourselves to the literature which is of relevance to the phenomenological modeling of bitumen, because this impacts on our interests in describing the mechanical response of bitumen. Moreover, as the general literature concerning the chemistry of bitumen is vast and more importantly way beyond our area of expertise, requiring a person with far greater knowledge of chemistry. Hence, most of our discussion will be limited insofar as it impacts on the efforts of a constitutive model builder interested in its mechanical response, information that helps him/her in making some valid assumptions about the material’s mechanical and thermodynamic behavior.

The nature and chemical makeup of bitumen is much too complex to be amenable to a detailed discussion that is definitive, at least not in a single volume of reasonable length devoted to purely issues of chemistry. Here we shall rest content with a discussion of some of the interesting studies that have been carried out in the last few decades by the Asphalt Technologists and Geochemists primarily pertaining to the chemistry of ‘straight run bitumen’ (the bitumen obtained through refining operations of petroleum). These recent findings seems to have been largely ignored by the research investigators interested in the constitutive modeling of asphalt and also by those that develop different modifiers to enhance the performance of asphalt. Given that the response of asphalt can be radically altered by the addition of modifiers, it is quite surprising that this issue has not been rewarded the importance that it deserves by the phenomenological modeler.

Since the overall makeup of the naturally occurring bitumen (in terms of the molecular structure of the fractions which constitute these species) are similar to that of the straight run bitumen, our discussion will also include some of the features related to natural bitumen. However, we hasten to add that at this point of time,

very little is known about the nature of interactions of the different fractions of these two varieties of bitumen and hence we urge the reader to bear this fact in mind lest he/she make unwarranted generalizations concerning natural bitumens based on comments made here concerning straight run bitumens.

5.1. Early studies on the chemistry of bitumen. There have been numerous interesting studies on the nature of bitumen and the several theories have been advanced as to its creation. Charles Hatchett made significant contributions to unraveling the mystery of bitumen and bituminous materials. We cite here three of his many important works on the nature of bitumen, the first one published in the year 1797 on bituminous substances with a description of *elastic bitumen* [60], the second one published in the year 1804 on the nature of conversion of vegetables into bitumen [61] and the third paper on the nature of pitch obtained from the Island of Trinidad (the Trinidad pitch was also called as *Parianite* [110]) in the year 1807 [62]. Hatchett [60] classified the bituminous substances as consisting of Naphtha, Petroleum, Mineral Tar, Mineral Pitch, Asphaltum, Jet, Pit Coal, Bituminous Wood, Turf, Peat and Bituminous Ores, a combination of oxides of certain minerals with bitumen. Hatchett’s another important contribution to the understanding of bitumen was his study of different specimens from the Pitch lake of the Island of Trinidad [62]. He concluded that these bitumens were not *simple bitumens* but “... *in reality only a porous stone of the argillaceous genus, much impregnated with bitumen.*”

Research on the chemistry of bitumen during the later half of the nineteenth century, following Hatchett’s pioneering studies, were mostly related to alterations in the classification system as envisaged by Hatchett. Some of the earliest experiments on *solid bitumens* were carried out by Peckham and his monograph devoted to this subject [111] contains a wealth of information, not only related to the origin, physical and chemical nature of bitumen, but also the controversies related to the classification of bitumen, on the use of word asphaltum, bitumen etc., and the characterization of bitumen by means of different chemical constituents. In the classification system proposed by Peckham, the source and the manner in which one can distill bitumen was taken into account. Accordingly, Peckham classified bitumen into three categories: Class A, pure bitumens as they occur in nature (it had 11 different types of bitumen as they exist in nature); Class B, pyro-bitumens (for the first time referred to as *pyroschists* by Hunt in 1863 [69]) or substances which yield products resembling bitumen on the application of heat (7 different substances ranging from Coal, Peat etc.) and Class C, the artificial bitumens obtained by distillation and other chemical processes from pure bitumens and pyro-bitumens (with 12 different varieties).

Boussingault [20, 21, 22, 23] carried out some of the early experiments on the composition of bitumen and classified it into two groups, namely *petrolene* and *asphaltene* depending upon the type of solvents used to separate these hydrocarbons. He used the bitumen of Becherlbronn for testing. Upon subjecting the above specimen to distillation, the volatile oily matter formed was called by him as *petrolene*. By purifying the bitumen with ether and then subjecting it to a temperature of 250 °C, Boussingault obtained a solid portion of the bitumen which he called *asphaltene*. According to such a procedure, the bitumen of Becherlbronn contained

0.854 portion of petrolene and 0.146 portion of asphaltene. The following comment by Boussingault found in the English translation rendered by Peckham gives a clear idea of what Boussingault perceived as the source for an important physical characteristic of bitumen, namely its fluidity: *“In conclusion, it is seen that the glutinous bitumens may be considered as mixtures, probably in all proportions, of two principles, each of which has a definite composition. One of these principles (asphaltene) fixed and solid, approaches asphalt in its nature. The other (petrolene) liquid, oily and volatile, resembles in some of its properties, certain varieties of petroleum. It may, then, be conceived that whilst the consistency of bitumen varies, it may be said to infinity; it suffices that one or the other of the two principles dominates the mixture, thereby giving such or such a degree of fluidity.”*

5.2. Chemistry of straight run bitumen. Kayser in 1879 (see [111] for details) isolated asphalt into three components and called them the ‘ α ’, ‘ β ’ and ‘ γ ’ asphalts. He also assigned different molecular formulae with an increasing percentage of sulphur. The ‘ α ’ asphalt was supposed to be oily, the ‘ β ’ asphalt was a solid gummy substance melting at 60 °C and the ‘ γ ’ asphalt had the same consistency as ‘ β ’ asphalt but melted at 165 °C. Richardson [122] carried out a study of the composition of Trinidad asphalt and he systematically looked into the mineral content and investigated its colloidal nature. Richardson in his paper in 1915 [122] discussed the relation between the colloidal chemistry and what he called ‘*perfect sheet asphalt*’ in that both rely on the studies of the behavior of surfaces and films. He also recognized the increase of the surface energy due to the increase in the number of colloidal particles and thus the increase of the cementing power of bitumen. The classification of bitumen into its different constituents was carried out by Marcussou in a systematic way [88, 89, 90, 91, 92]. He classified asphaltic bitumen into carboids, carbenes, asphaltenes, asphaltic resins, oily constituents, asphaltic acids and their anhydrides. The studies by Rosinger [126] and Errera [46] emphasized the colloidal nature of asphalt on the basis of a variety of physical and chemical analysis. For instance, the following observation by Errera [46] is worth repeating (here he uses the terminology proposed by Kayser about the classification of the constituents of asphalt into its ‘ α ’, ‘ β ’, ‘ γ ’ asphalts): *“Modern theories seem to admit in sensitive asphalt the existence of three substances chemically defined as ‘ α ’, ‘ β ’, ‘ γ ’ asphalt. The latter is alone sensitive to light. When studying the question from a colloid point of view, it would appear more correct to say that asphalt is a ‘polydispersoid’; the sensitive part is the one which is found in a state of colloidal dispersion. When chemically analysed, this colloidal part proves to be the richer in sulphur, the valencies of which are a factor in polymerisation. According as their degree of association is greater or smaller we find in asphalt the intermediate stages between molecular and colloidal asphalt. Sunlight seems to have a coagulating action.”* Rosinger [126] earlier also had come to the same conclusion concerning the coagulating effect of sunlight. Lord [81] seems to have recognized that the colloidal character of asphalt can be modified by adding inorganic solids or clay. Nichols conducted one of the first investigations in 1902 on the optical properties of asphalt [102]. He used asphalt films of thickness 0.003 cm and used a one-prism spectrocope. He concluded that asphalt can be considered to be suspensions of carbon-like particles in a liquid and he compared his experiments on the opacity

and transparency of asphalt with the measurements of carbon black conducted by Ångström⁷.

Nellensteyn [97] analyzed the constitution of asphalt and remarks on the fact that different bitumens behave differently as they congeal – some crystallize while other remain amorphous. He says “*Asphalt when solidifying shows a very marked increase in viscosity without crystallization. Other bitumens show either crystallization or a general increase in viscosity*”. In this widely quoted paper, he concludes that “*asphalt contains elementary carbon in colloidal form and that this colloidal form is the essential constituent of asphalt*”. Observations of the Tyndall effect and Brownian motion using ultramicroscopic examinations of asphaltenes and the synthesis of asphalt from carbon and hydrocarbons have confirmed his findings (See also the discussion of this paper by Hackford [57]).

Kirk and Reuerson [78] discuss the important studies up to 1925 in which the colloidal nature of asphalt was recognized. The colloidal nature imparted to asphalt by the presence of inorganic matter (Richardson in 1915 [122]), by the addition of either clay or certain inorganic salts (Lord in 1919 [81]), or the sheer nature of pure asphalt to exist in both molecular and colloidal dispersion (Rosinger in 1914 [126] and Errera in 1923 [46]) were discussed by them. They showed that the influence of the addition of copper sulfate on the colloidal nature of Trinidad asphalts is such that it increased the number of the colloidal particles but decreased their size. They also showed that by dispersing a certain oil asphalt in carbon disulphide, carbon tetrachloride and acetone, there were dispersions of the inorganic material as well as the organic portion of the asphalt. Their remark that “*It would seem probable from these experiments that the solvents used is at least as important a factor as the character of the asphalt*”, points to the difficulties inherent to characterizing asphalt and thereby modeling it.

The principles of colloidal chemistry as it applies to the various processes related to the petroleum industry and in particular to the preparation of asphalt emulsions were discussed by Dunstan [43] and Morrell and Egloff [96]. Nellensteyn [97, 98, 99] classified asphaltic bitumens within the context of the colloidal chemistry into the following groups:

- (1) the medium,
- (2) a lyophile part: the protective bodies and
- (3) a lyophobe part: the ultramicrons.

According to his observations, the dispersed phase consists of the last two groups, these being the constituents of the asphalt micelles. Also he talks about the stability of this system: “*The stability of the whole system in the first place depends upon the relation between the micelles and the medium. Changes in this stability, which are known as flocculate and peptizing reactions, give rise to a ‘reversible flocculation’. If, however, the micelle itself is destroyed, the micelles cannot be repeptized, at least not directly. In this case we have an ‘irreversible flocculation’.*” The

⁷Knut Johan Ångström is the son of the famous Swedish physicist Anders Jonas Ångström. He was also an accomplished physicist in his own merit and he did some early experiments on solar radiation, devised lot of apparatus one of which is the well known photographic representation of infrared spectrum.

observation takes on particular significance in view of the numerous practical applications related to polymer modified asphalt and asphalt emulsion. For instance, if as per Nellensteyn's view point, asphalt can be considered as a two-phase system, what really causes the precipitation of the asphaltenes during emulsification? Is it due to the change of the interfacial tension of the micelle-medium? This is of much practical significance as summed up by Nellensteyn [99] “. . . *it is certainly very mysterious that the coagulated bitumen easily expels the water, while molten bitumen adheres very poorly to moistened surfaces of mineral matter*”. The notion of irreversible flocculation as described by Nellensteyn has considerable merit especially when it comes to describing the aging of asphalt. This also explains the anomalous behavior related to some “hard bitumens” having excellent service life as opposed to “soft bitumen”. Kalichevsky and Fulton [75] have summed up the important developments in research related to the chemical composition of asphalt along the lines of the classification proposed by Marcusson [88, 89, 90, 91, 92]. They proposed that asphalt should be considered as a three constituent mixture consisting of asphaltenes, asphaltic resins and oils; asphaltenes imparting hardness and high melting point to the mixture, asphaltic resins responsible for the ductility and tensile strength of the mixture as well as playing the role as a stabilizer and the oily constituents acting as the dispersing phase (see also Schneider and Just [131]). Mack [84, 85] extended the ideas of Marcusson [88, 89, 90, 91, 92] but considered only two constituents for the asphalt: asphaltenes as the dispersed phase and the mixture of asphaltic resins and oils as the dispersion medium. He used Einstein's formula in trying to find the molecular weight of the asphaltenes by using the relation between relative viscosity (ratio of the viscosity of suspension and the viscosity of the dispersion medium) and the concentration. However his estimate of the molecular weight of the asphaltenes and his generalization that asphaltenes have relatively low molecular weight does not agree well with the recent estimates of the constitution and makeup of asphaltenes.

Baskin [17] was well ahead of his time when he discussed the chemistry of asphalt and the significance of the source of asphalt on its properties. His observations relating to the specific properties of asphalt and their dependence on the source, the oxidation of asphalt and on the various empirical tests which were used during his time (which are still in use now) were right on the mark and can be of assistance in modeling asphalt or for that matter in writing out the specifications of asphalt for practical engineering purposes. Various studies carried out concerning the chemistry of asphalt during and before the time of this paper seem to have concluded that asphalt was a mixture. However, the influence of the individual constituents on the overall behavior of asphalt depends to a large extent on the source, the manufacturing processes etc., and this was very clearly enunciated by Baskin. His remarks that “*Asphalt is in no sense a distinct group by itself, but rather a portion of the crude petroleum containing several groups in form of a mixture or mutual solution. The character and makeup of each group to start with depends to a great extent on source. For any given consistency, the oily constituents in a California crude residue are different in physical and chemical properties from those extracted from the same consistency Panuco residual. This likewise, undoubtedly holds true of the resins and the asphaltenes.*” pinpoint the need for taking the source of asphalt into account and the need for the same has been borne out by the recent

use of biomarkers in characterizing asphalts from different sources. His observations concerning the various empirical tests on asphalt will be discussed in a later section.

Hillman and Barnett [64] separated asphalt into different constituents by means of fractional precipitation and concluded that the molecular weight of asphaltenes from a cracked residue was lower than that of the un-cracked residue. Nellensteyn [100] building on the work done by him on the colloidal structure of bitumens used microscopic and ultramicroscopic pictures of bitumen, natural and artificial asphalt and tar and found that the colloidal structure of natural bitumen is the same as the artificial bitumen mixed with mineral fillers (see also Nellensteyn and Kuipers [101] for a discussion of the *difference asphaltenes*). Identification and the classification of bitumen by using *The Panchrometer* which essentially uses the comparison of the color of the bitumen being tested with that of a standard sample was carried out by Attwood and Broome [11]. This method is capable of detecting the changes in the structure of bitumen during aging and the settlement of the straight run bitumen, changes that are undetectable by routine tests such as the penetration test, viscosity test, softening point test etc. (See also Csanyi and Fung [37] for a discussion of the possible use of ultraviolet light identification as a rapid means for determining the constituents of asphalt.) In a detailed study of the dependence of the rheological behavior of the bitumen on molecular considerations such as the molecular structure, weight, etc., Oliensis [106] summarized the complex response of the bitumen when subjected to high temperatures thus:

- (1) There is an increase in the molecular weight at certain stages and decrease at certain other stages and
- (2) the complexity of the internal structure is increased at certain stages and simplified at certain other stages.

Corbett and his co-workers have made significant contributions to the understanding of the composition of asphalt and its change over time when subjected to specific tests or field applications. In his joint paper with Swarbrick in 1960 [36] and in his subsequent paper in 1969 [34], a systematic study of the composition of asphalt was undertaken leading to what are now called as “*Corbett fractions*”⁸. Corbett and Swarbrick [36] used a new procedure for the separation of asphalt into its different constituents (they separated asphalt into three constituents such as paraffins plus naphthalenes, aromatic oils and asphaltenes) and then used Nuclear

⁸There were quite a few attempts prior to Corbett in the fractionation of asphalt some of which were discussed in detail in the preceding pages. Similar studies worth mention are those due to Hubbard and Stanfield [68] who separated asphalts into three fractions viz., asphaltenes, resins and oils; Hoiberg and Garris [67] who separated asphalts into five fractions viz., hexane-insolubles, hard resins, soft resins, oils and waxes. Noteworthy of mention is also the study by O’Donnell in 1951 [104] in which asphalt was fractionated into paraffins, naphthenes, aromatics, resins and asphaltenes. O’Donnell carried out an interesting study on the molecular weight distribution of these fractions. Traxler and Schweyer [140, 141, 142, 143, 144, 145, 146] developed procedures that employed the solvent action of *n-butanol* and acetone to separate asphaltic materials into asphaltics, paraffinic oils and cyclic oils. Helm [63] for the first time reported the use of reversed phase partition and adsorption chromatography for the separation of asphaltic materials. Similarly Altgelt and Hirsch [4] reported one of the earliest results on high and low molecular weight asphaltenes. Ramijak [119] in 1977 reported a study in which acids were extracted from an air blown asphalt, maltene and asphaltenes.

TABLE 2. Summary of composition and characterization as found in typical 85/100 straight reduced asphalt [34]

Component	Wt % range	Physical Nature	Density 20/4 °	Molecular Weight (Av)
Saturates	5-15	Colorless liquid	0.87	650
Naphthene-Aromatics	30-45	Yellow to Red Liquid	0.99	725
Polar-Aromatics	30-45	Black Solid	1.07	1150
Asphaltenes	5-20	Brown to Black Solid	1.15	3500

TABLE 3. Effect of crude source on composition [34]

	Venezuelan	USA	Mexico	Mid-East
Saturates	14.0 %	10.5 %	8.5 %	8.0 %
Naphthene-Aromatics	34.5 %	38.5%	29.8 %	38.5 %
Polar-Aromatics	36.3 %	33.4%	42.6 %	37.0 %
Asphaltenes	14.1 %	16.8 %	28.3 %	15.5 %
Penetration @ 77 °F	90	92	88	85
Soft Point, °F	114	114	116	115

Magnetic Resonance Imaging, Electron Paramagnetic Resonance Imaging, Infrared Radiation, Mass Spectrometry, Ultraviolet Radiation etc., to study the characteristics of each of these fractions. Using these techniques, they conducted the thin film oven test that is normally used for simulating the short-term aging behavior of asphalt. They found that there was no change in the paraffin plus naphthalenes constituent but some portion of the aromatic oils were converted into asphaltenes. Corbett in his landmark paper in 1969 [34] described a method for determining the composition of asphalt based on fractionation into its four generic components. The following tables taken from this paper will help us in understanding the composition of asphalt and its dependence on the source of crude.

For instance, Table 2 shows that asphalt is a mixture of four constituents, two of them are liquids and the other two are solids. Also, a perusal of Table 3 makes it abundantly clear that the empirical tests used for characterizing asphalt such as penetration and ring and ball softening point test are completely silent concerning the consistency of asphalt and contrariwise mislead one into believing that all asphalts having either the same penetration or softening point respond essentially in the same manner.

Within the context of modeling the behavior of asphalt, it is clear from the above studies that

- (1) asphalt is a mixture of different reacting and diffusing components,
- (2) asphalt from different sources of crude have different amounts of constituents and possibly different ability for reactions and
- (3) each and every manifestation of change in the behavior of asphalt (such as aging etc.) is due to the inter-conversion of one type of constituent to the other type.

In a related development, Griffin et al., [56] and Simpson et al., [133] looked into the influence of the chemical composition of asphalt on various empirical measures such as penetration, softening point, penetration index and some of the physical properties such as viscosity and viscosity-temperature susceptibility. Assuming asphalt to be a linear viscoelastic material, they also looked into the influence of different constituents on the complex modulus. Since our intent in this section is to restrict our discussion to the developments in the research related to the chemical composition of asphalt, we desist from making observations concerning the appropriateness of their assumption that asphalt can be modeled as a linear viscoelastic solid (see the definitions proposed by Van der Poel [147]) which is grossly inadequate as will become apparent from later discussions). The importance of the work by Griffin et al., [56] and Simpson et al., [133] lies in their suggestion concerning the need for the blending of the different constituents to get the desired properties and hence the desired physical response characteristics (though the properties used by them to benchmark were empirical measures which did not capture the complex makeup of bitumen).

Starting with the work of Boussingault in 1837 to the work of Corbett in 1969, it has taken over 100 years to come to grips with an acceptable description for the compositional structure of asphalt (see [9] for the ASTM standard for test methods for separation of asphalt into four fractions). Most of the works after 1970 were carried out by Geochemists and Petroleum Chemists interested in the chemical structure of asphaltenes and with the advent of new tools for studying the same, there have been numerous publications related to these issues. Our aim, as we emphasized earlier, is in discussing the composition of asphalt and the interaction mechanisms of its constituents so as to highlight the complexity that confronts a modeler. Being aware of the variety of issues that influence the structure of asphalt, would place us in a better position to describe phenomena such as aging, fracturing and healing, and thereby describe better the many complex response characteristics exhibited by bitumen.

Lot of investigations have been carried out to validate the correlations between the chemical composition and the performance of asphalt in the field. An excellent summary of these results can be found in [54]. The bewildering variety of testing procedures and equipments used now to fractionate asphalt often confuses the modeler rather than clarifying the issues. For instance, as of now the following are the procedures which are being used to analyze the composition of asphalt: solvent precipitation, chemical precipitation, adsorption liquid chromatography, ion exchange liquid chromatography, coordination liquid chromatography, thin-layer chromatography, gas-liquid chromatography, size-exclusion chromatography, high pressure gel permeation chromatography, vapor pressure osmometry, mass spectrometry, electrophotometric spectroscopy, nuclear magnetic resonance spectroscopy, electron spin resonance spectroscopy, spectrochemical analysis, elemental analysis, distillation fractionation, wax content determination, photochemical reactions of asphalt, acid number determination, internal dispersion stability, titrimetric/gravimetric analysis etc [3, 16, 54, 135].

Asphalt has a wide ranging molecular weight distribution with carbon molecules ranging from 24 to 150 [54]. Also, asphalt includes in its composition a large amount of heteroatoms such as nitrogen, oxygen, sulphur, vanadium, nickel, iron etc. These

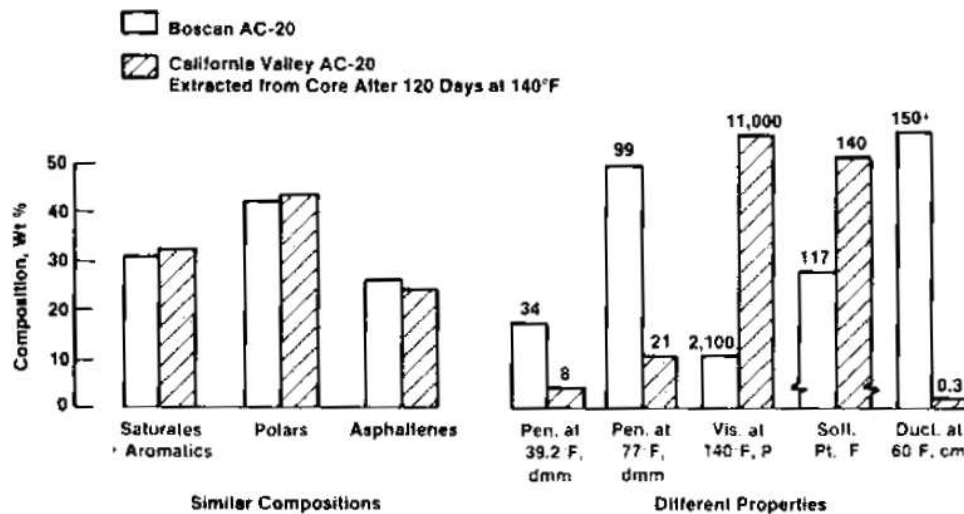


FIGURE 1. Asphalts with similar compositions but different properties from Goodrich, 1986 [54]. The compositions are compared with penetration at 39.2 °F, penetration at 77 °F, viscosity at 140 °F, softening point in F and ductility at 60 °F.

heteroatoms play a significant part in the physical properties of asphalt cements. This complexity is increased by the fact that crude from different sources are blended together in the refinery for optimum production and this in a way confounds the characterization of asphalt. A very revealing remark made by Goodrich *et al.* in 1986 [54] more or less sums up the status of the different fractionation studies : “Some believe that today’s sophisticated analytical tools, computer-controlled instruments that work with milligrams of asphalt, should make the connection between asphalt composition and performance properties. These instruments are being applied to asphalt research and well-defined field problems. Fundamental chemical explanations of asphalt aging, adhesion, structure, and rheology have been proposed. Yet the complex chemical mix of even a single asphalt may never be adequately described.”

Do the fractional separation techniques tell us anything about the physical/rheological characteristics of the asphalt being tested? Also, if the correlations between elemental composition of asphalt and the so called rheological tests do not agree for even a single asphalt, do we blame the complexity of the asphalt and look for yet another fractionation procedure or do we reevaluate the usefulness or otherwise of a penetration test, ductility test etc.? For instance, the Figure 1 (adapted from [54]) reveals the extent of the disparity between asphalt composition and the different tests which are in vogue. While the empiricism related to these tests will be discussed in a later chapter, we wish to emphasize that unless proven to the contrary,

any correlation between a reasonable fractionation procedure and the values of the empirical tests should be viewed with great degree of skepticism⁹.

There have been several studies which have attempted to construct a model for asphalt essentially based on the fractionation methods for asphalt. These models aim to construct a hypothetical structure of asphalt mostly based on presupposed notions of the interactions and associations of the different fractions of asphalt. The usefulness or otherwise of these hypothetical models on the formulation of constitutive models are debatable. However, the experimental methods which led to the proposition of these models give useful insight into the microstructure of asphalt and we will review some of the important models here. These studies are different from the several studies which we reviewed in the earlier sections of this chapter in the sense that these investigations try to explain the behavior of asphalt as a manifestation of the different fractions of asphalt¹⁰.

One of the earliest of such models was due to Pfeiffer and Saal [116] (see Figure 2)¹¹. Experimenting with different bitumens and using low-boiled saturated hydrocarbons, Pfeiffer and Saal [116] fractionated bitumen into asphaltenes (the insoluble part) and maltenes (the soluble part). In the model constructed by them (figure 2), the asphalts are visualized as colloidal system, with asphaltenes forming the centers of micelle and having a more pronounced aromatic nature. The asphaltenes were assumed to be surrounded by lighter constituents of less aromatic nature, and Pfeiffer and Saal further conjectured that there were no distinct interphases between the micelles and the medium surrounding it¹². In the case of the shortage of ‘resins’ (compounds in the immediate vicinity of asphaltenes), a mutual attraction of the micelles is facilitated resulting in an irregular open packing system (see, however the investigations of Speight and Moschopedis [134] wherein hydrogen bonding between resins and asphaltenes are postulated for resin-asphaltene interactions). Pfeiffer and Saal claimed that this system had “*all the characteristics*

⁹A study conducted on Athabasca and Utah tar sand bitumens by Bukka *et al.*, [27] revealed that assumptions about the direct relationship between the amount of asphaltenes and the ‘viscosity’ of these two different bitumens do not hold good. On the other hand, studies conducted by Chatergoon *et al.*, [28] reveals that the size distribution of the micelles have a simple relationship with the viscosity. However, it is hard to understand what Chatergoon *et al.*, mean by non-Newtonian, elastic behavior.

¹⁰See also [149] regarding the difficulties associated with fractionation schemes for natural bitumen.

¹¹In 1928-29, Auer [12] proposed that fatty oils, an ‘asphalt-like’ system resembled ‘isocolloids’. He also conjectured that in the isocolloidal fatty oil system, the disperse phase may increase with respect to the dispersion medium due to the following (different) reasons : action of ultra-violet and X-rays, action of heat, action of external aggregators such as organic solvents and action of gases such as oxygen. If we conceptualize the disperse phase as asphaltenes and the dispersing medium as resins and oils within the context of the isocolloidal system, we can appreciate the researches of Auer [12] specifically when we are interested in aging or for that matter in the influence of the organic solvents in the precipitation of asphaltenes (see also the criticism of ‘isocolloids’ by Sachanen [130]).

¹²Several different studies have come out with different structures for the micelles, for instance one such study conducted by Lozano and Rodríguez [82] assumes the micelles to be composed of asphaltenes, resins and waxes in a base of oil. The study by Sachanen [130] points to the presence of neutral resins which form true solutions. These neutral resins are different from the adsorbed resins which causes the peptization of asphaltenes.

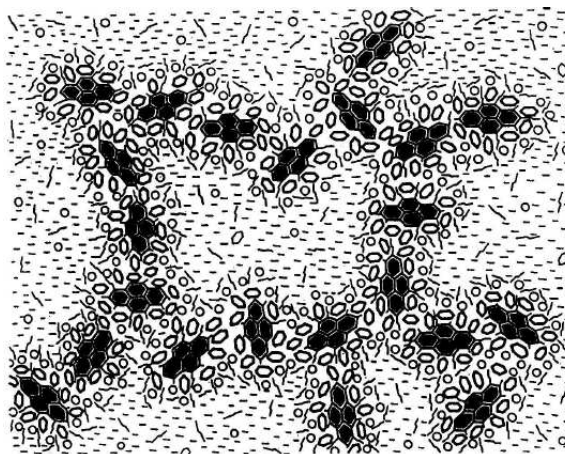


FIGURE 2. Schematic representation of the structure of an asphaltic bitumen of the blown type, from Pfeiffer and Saal [116]. The filled hexagons represents central part of asphaltenes, the open hexagons represent compounds of higher and lower molecular weights and of aromatic in nature, the hollow circles represent compounds of mixed aromatic-naphthenic nature, the rod like structures represent compounds of mixed naphthenic-aliphatic nature and the dashes represent compounds of a preponderantly aliphatic nature.

of complex flow, such as elasticity and thixotropy” and further remarked that the “. . . the elasticity is composed of intramicellar and intermicellar elasticity” [116]. Synthesizing bitumens by combining maltenes and asphaltenes and testing these products in a conicylindrical viscometer, Pfeiffer and Saal concluded that: “The intramicellar elasticity decreases with increasing C/H ratio of the asphaltenes; this may be attributed to smaller micelles, or to more compact structure of the micelles, or to combinations of these.” (See also the paper by Saal and Labout [129] on the different rheological tests carried out on bitumen, Everett [48] for a discussion on the use of different rheological tests for the characterization of colloids, and the lengthy exposition of Bancroft [14, 15] on the state of colloid chemistry with more than 400 references on the subject.

The second important investigation in this series is due to Katz¹³ and Beu [76]. Katz and Beu examined thin films of asphalt and oil using the electron microscope in search of the colloidal asphaltenes¹⁴ (see also [45]). While these films were

¹³This is one of the papers that was way ahead of its time in terms of clarity and the logical experimental procedure followed. Till the paper by Rozeveld *et al.*, [127] was published in 1997, no one knew whether asphaltenes really existed in asphalt or whether it was some kind of a solvent induced artifact, and even today ASTM defines asphaltene based on the solvent used for fractionating it. Had Katz and Beu shone the electron beam for more than 10 minutes on the asphalt films, they would have observed the ladder network observed by Rozeveld *et al.*

¹⁴Preckshot *et al.*, in a related study used an electron microscope, in one of its very early uses, to observe the formation of asphaltic particles during the flow of crude oil from the reservoir to

free of such particles, the same particles appeared in their study when they observed suspensions of asphalt in benzene and petroleum ether. They also carried out a systematic study of the appearance of asphalt during the various stages of manufacturing operations in a refinery. One of their important conclusions is that “... *colloidal particles or micelles do not appear in any of the asphalt products examined by the electron microscope but made to appear by the use of solvents.*” They also characterized asphaltenes as “*potential colloids and that solutions containing them easily convert into colloidal systems from changes in the composition of the solution (solvents) or from electrical effects.*” In this context, it is worth recognizing the very recent study on the network morphology of straight and polymer modified asphalts conducted by Rozeveld *et al.*, [127] in more or less the same manner as Katz and Beu [76]. Rozeveld *et al.*, conducted a systematic study of asphalt using an environmental scanning electron microscope (ESEM), high performance gel permeation chromatography and a thermogravimetric analyzer. Asphalt films of thickness 0.005 inch were observed under the ESEM and the asphalt films were featureless initially, however, after several minutes of beam exposure, the network entanglement of the strands were revealed. They conducted several other experiments to conclusively prove that the network morphology was not a beam-induced artifact but due to the volatilization of low molecular weight oils in the asphalt due to localized heating of the electron beam, thereby revealing the asphaltenes and resins after the upper surface layer of the oils have been removed [127] (see Figure 3). These two investigations were more or less identical in nature but due to the sophistication in technology available to Rozeveld *et al.*, the asphaltene and resin network structure was captured in their investigations and this was not possible in the study of Katz and Beu [76] which resulted in their questioning the existence of asphaltene.

The difficulties associated with the fractionation procedures increase as the individual molecular weights become larger. To circumvent this problem, some ‘mean structural types’ are assumed and using NMR and molecular unit sheet weight measurements, different varieties of analytical models have been proposed. Few of the studies which have proceeded in this direction are Altgelt and Hirsch [65], Haley [58], Ramsey *et al.*, [120] using the structural parameters derived by Brown and Ladner [26] and Kiet *et al.*, [77]. The study carried out by Petersen [112] discusses an analytical method for the quantitative analysis of select chemical functionalities using differential infrared spectrometry and some chosen chemical reactions on an aged asphalt and this kind of studies reveal a great lot of information concerning the important interactions that take place in asphalt. However, the integration of these ideas into a constitutive modeling is far from easy.

During the Arab oil embargo of 1972, the refineries in North America processed crude from several other sources and the pavement industry perceived that the asphalt quality had deteriorated (see for instance the study by Anderson and Dukatz [6] in which more than 400 asphalts produced during the period 1950-1970 were compared with more than 100 asphalts from the period of 1978-1979). The

the stock tank [118]. The influence of streaming potential in facilitating the formation of the precipitates of asphaltic substances during the flow through sand was also studied by them. This is a problem which plagues the processing and production of petroleum even today. See [87] and the references cited therein on the causes of asphaltene and other heavy organic depositions.

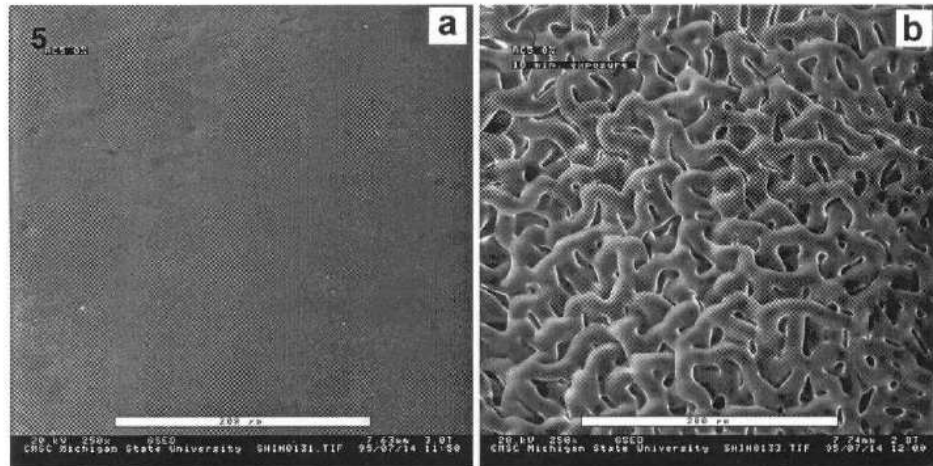


FIGURE 3. Environmental scanning electron microscope images of an unmodified AC-5 asphalt binder film a) before and b) after beam exposure. From Rozeveld *et al.*, [127].

unexpected pavement failures added to the increase of vehicle tire pressures during the same time resulted in the rethinking the formulation of different specifications for asphalt cements and asphalt concrete. This culminated in the formation of the strategic highway research program (SHRP) in the United States of America and the ‘performance related specifications’ for asphalt cements. The SHRP spent a total of \$150 million on research on asphalt concrete out of which \$50 million was spent on asphalt research, a five year research program that started in 1987 [154]. The aim of this research effort was to develop ‘performance-based’ binder and asphalt concrete mixture specifications which will help the highway agencies in the country in getting better performances from the hot-mix asphalt concrete pavements. This effort of the SHRP resulted in the publication of several important reports which looked into the chemistry, physical characterization, development of testing methods for asphalts and also resulted in a SHRP material reference library (see for instance some of the references [5, 24, 25, 44, 74, 107, 113, 114]). The SHRP research effort critically examined the available colloidal models for asphalt in the light of the advances made in the field of colloid chemistry and came to the conclusion that *asphalt cement is a relatively homogeneous and randomly distributed collection of molecules differing in polarity and molecular size* [113] and *asphalt is a single phase mixture of many different polar and non-polar molecules, all of which interact with one another* [154]¹⁵. Ion exchange chromatography (IEC) was used to separate asphalt into strong and weak acids, strong and weak bases, neutrals and

¹⁵The use of the word *phase* leaves much to be desired especially with respect to asphalt. Many of the studies have pointed that polar molecules in asphalt have solid-like characteristics and the non-polar molecules have fluid-like characteristics, and most of the important manifestations of asphalt’s physical behavior such as aging, steric hardening etc., are due to the inter-conversion among these groups.

amphoterics - compounds with both acid and base functionalities. These fractions along with the parent asphalt were also subjected to rheometry in an attempt to link the physical properties of asphalt with the various chemical fractions. The entire methodology specifically related to the physical characterization is summarized by SHRP in the following manner: [113, page 5-6]

A major effort has been the study of the rheology, or the viscoelastic properties, to determine the effects of shear, shear rate, and temperature. This effort has resulted in description of asphalt in terms of rheological master curves that show the variation in viscous and elastic components with shear and temperature. In general, all asphalts exhibit a glass like behavior at very low temperature, and are relatively fluid at high temperature, but the pathway from glass to fluid, or vice versa varies substantially from one asphalt to another. Historically, this variation was known as *temperature susceptibility*, but a single temperature susceptibility is a straight-line relationship of log viscosity between two temperatures. The classic idea of temperature susceptibility was shown to be substantially in error. The master curve shows that there are a series of temperature susceptibilities for each asphalt and that the sets vary among asphalts. The master curve varies with asphalt source. Hence, no two-point measurement can describe the variation in viscoelastic properties for asphalts. Determining rheological master curves in detail is a time-consuming process. During the A-002A project, a set of three points at appropriate temperatures, was chosen, and it was demonstrated that a reliable simulation of the master curve for any asphalt could be obtained relatively rapidly.

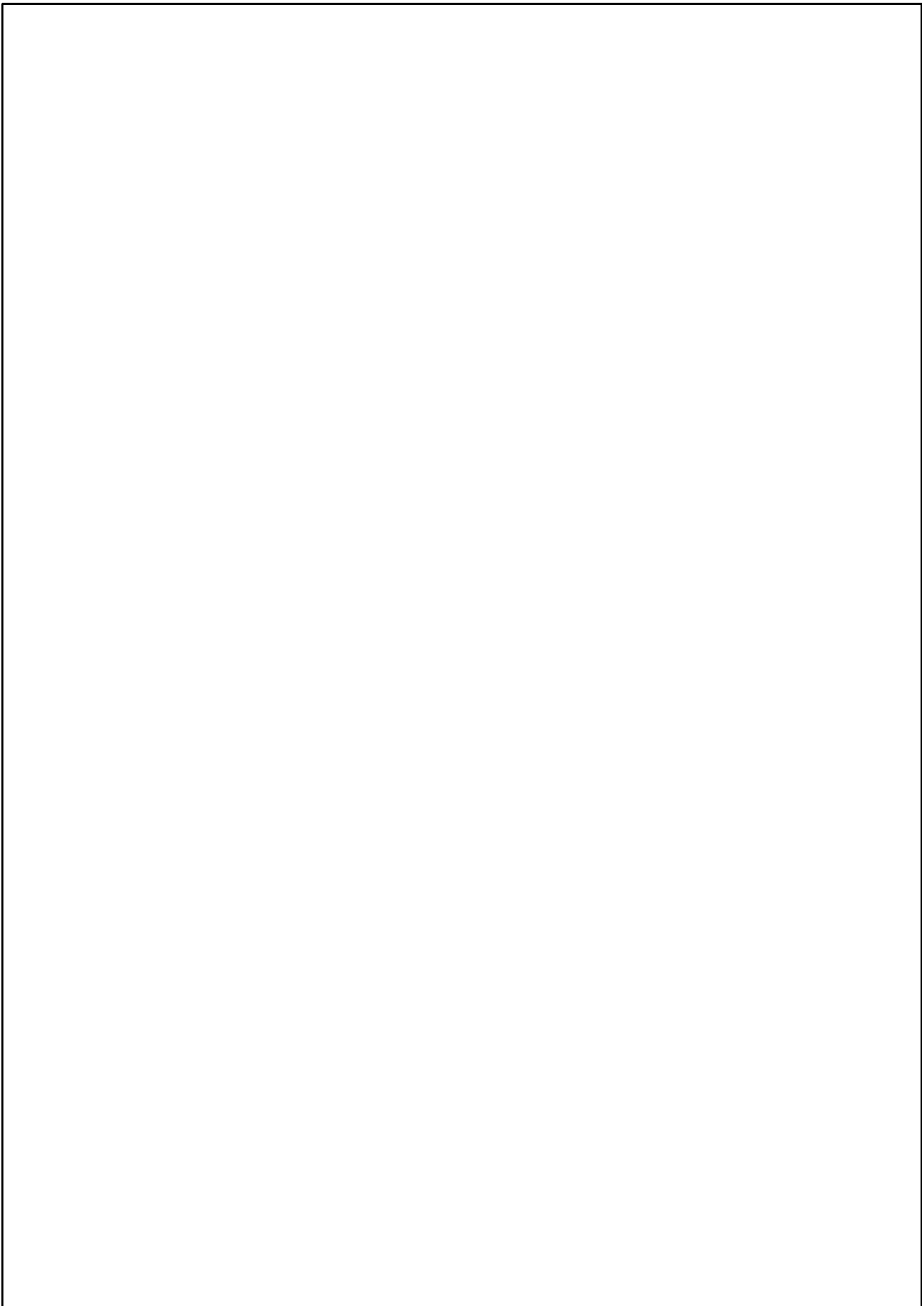
It was also further assumed that polar molecules (mainly acidic, basic and amphoteric fractions) interact and are responsible for the elastic characteristics of asphalt and the non-polar molecules (the neutrals) influence the viscous behavior and the low-temperature characteristics of asphalt. These observations were based on the results of experiments on asphalt and the different fractions of asphalt separated by the IEC procedure. One such interesting experimental data is shown below to illustrate the rationale behind these assumptions. The following table details the viscosity measurement of asphalt and asphalts blended with IEC fractions and measured at 60 °C, 1 rad/s (see Table 4).

Based on this data, the SHRP concluded that “. . . as a fraction, the amphoteric are the components of the asphalts governing high viscosities . . .”; “These results do not mean that no viscosity-enhancing species exist in acid, base, or neutral materials, or that no viscosity-reducing species exist in the amphoteric fractions.”[24, page 11] and “. . . addition of amphoteric materials has a very large effect on the elastic character of the asphalt” [154, page 15]. These conclusions are very simplistic in nature and do not really explain anything about the nature of asphalts and the influence of the fractions on the physical behavior of asphalt. We conclude this paper with a brief comment in the SHRP report that attests to the difficult task

TABLE 4. Viscosity (Pa·s) of Asphalts and Asphalts blended with IEC fractions at 60 °C, 1 rad/s from [154], see also [24, Table 1.13, page 35]

SHRP Asphalt	AAD-1	AAG-1	AAK-1	AAM-1
Asphalt	131	240	413	258
Asphalt + Neutrals	40	131	117	137
Asphalt + Bases	327	346	656	399
Asphalt + Acids	174	285	517	292
Asphalt + Amphoterics	2,638	1,440	6,796	3,967

that a modeler faces “*Quite simply, the word asphalt refers to a large collection of quite variable materials.*”



Bibliography

- [1] H. Abraham. The classification of bituminous and resinous substances. In *Eighth International Congress of Applied Chemistry*, pages 7–15, Washington and New York, 1912. Volume 10, Section VC, Fuels and Asphalt.
- [2] G. Agricola. *De Re Metallica*. Dover Publications, Inc., New York, 1950. Translated from the first Latin edition of 1556 by H. C. Hoover and L. H. Hoover.
- [3] K. H. Altgelt and T. H. Gouw. Chromatography of heavy petroleum fractions. In J. C. Giddings, E. Grushka, R. A. Keller, and J. Cazes, editors, *Advances in Chromatography*, pages 71–175. Marcel Dekker, Inc., New York, 1975. Volume 13.
- [4] K. H. Altgelt and E. Hirsch. GPC separation and integrated structural analysis of petroleum heavy ends. *Separation Science*, 5(6):855–862, December 1970.
- [5] D. A. Anderson, D. W. Christensen, H. U. Bahia, R. Dongre, M. G. Sharma, C. E. Antle, and J. W. Button. Binder Characterization and Evaluation: Volume 3: Physical Characterization. Report number SHRP-A-369, Strategic Highway Research Program, Washington, D. C., USA, 1994.
- [6] D. A. Anderson and E. L. Dukatz. Asphalt Properties and Composition: 1950 - 1980. *Association of Asphalt Paving Technologists*, 49:1–29, 1980.
- [7] Anonymous. Asphalt success on the banks of the river Ware. *International Water Power & Dam Construction magazine*, 51:4, October 1999.
- [8] W. F. van Asbeck. *Bitumen in Hydraulic Engineering*. Elsevier Publishing Company, Amsterdam, 1964. Volume 2.
- [9] ASTM:D4124. *Standard Test Methods for Separation of Asphalt into Four Fractions*, 2000. American Society for Testing and Materials, Annual Book of ASTM Standards, Section 4, Volume 4.03, Philadelphia, USA.
- [10] ASTM:D8-02. *Standard terminology relating to materials for roads and pavements*, 2000. American Society for Testing and Materials, Annual Book of ASTM Standards, Philadelphia, USA.
- [11] A. W. Attwooll and D. C. Broome. The identification of bitumen in paving mixtures. *AAPT*, 11:60–76, 1940.
- [12] L. Auer. Colloid Chemical Changes in Rubber and Fatty Oils. *Transactions of the Institute of Rubber Industry*, 4:499–520, 1928-29.
- [13] P. G. Bahn. The making of a mummy. *Nature*, 356:109, 1992.
- [14] W. D. Bancroft. Outline of Colloid Chemistry – I, II, III. *Journal of the Franklin Institute*, 185(1,2,3):29–57 (Part I), 199–230 (Part II), 373–387 (Part III), January, February, March 1918.

- [15] W. D. Bancroft. The Development of Colloid Chemistry. *Journal of the Franklin Institute*, 199(6):727–760, June 1925.
- [16] B. N. Barman, V. L. Cebolla, and L. Membrado. Chromatographic Techniques for Petroleum and Related Products. *Critical Reviews in Analytical Chemistry*, 30:75–120, 2000.
- [17] C. M. Baskin. Asphalt, its chemistry, significance of source and effect of modern processes on present day specifications. *Proceedings of Association of Asphalt Paving Technologists*, 3:71–92, 1932.
- [18] E. Boëda, J. Connan, D. Dessort, S. Muhesen, N. Mercier, H. Valladas, and N. Tisnerat. Bitumen as hafting material on middle palaeolithic artefacts. *Nature*, 380:336–338, 1996.
- [19] E. Boëda, J. Connan, and S Muhesen. Bitumen as a hafting material on middle palaeolithic artifacts from the El Kowm Basin, Syria. In T. Akazawa, K. Aoki, and O. Bar-Yosef, editors, *Neandertals and Modern Humans in Western Asia*. Plenum Press, New York and London, 1998.
- [20] M. Boussingault. Memoire sur la composition des bitumes. *Annales de Chimie et de Physique*, LXIV:141–151, 1837.
- [21] M. Boussingault. On the composition of bitumen. *Journal of the Franklin Institute*, 24:138–139, 1837.
- [22] M. Boussingault. On the composition of bitumen. *The Edinburgh New Philosophical Journal, exhibiting a view of the progressive discoveries and improvements in the sciences and the arts*, XXII:77–79, 1837.
- [23] M. Boussingault. Analyse de quelques substances bitumineuses. *Annales de Chimie et de Physique*, LXXIII:442–445, 1840.
- [24] J. F. Branthaver, J. C. Petersen, R. E. Robertson, J. J. Duvall, S. S. Kim, P. M. Harnsberger, T. Mill, E. K. Ensley, F. A. Barbour, and J. F. Schabron. Binder Characterization and Evaluation: Volume 2: Chemistry. Report number SHRP-A-368, Strategic Highway Research Program, Washington, D. C., USA, 1993.
- [25] J. F. Branthaver, R. E. Robertson, and J. J. Duvall. Relationship Between Molecular Weights and Rheological Properties of Asphalts. *Transportation Research Record*, 1535:10–14, 1996.
- [26] J. K. Brown and W. R. Ladner. A Study of the Hydrogen Distribution in Coal-like Materials by high-resolution Nuclear Magnetic Resonance Spectroscopy ii - A Comparison with Infra-red Measurement and the Conversion to Carbon Structure. *Fuel*, 39:87–96, 1960.
- [27] K. Bukka, J. D. Miller, and A. G. Oblad. Fractionation and Characterization of Utah Tar Sand Bitumens : Influence of Chemical Composition on Bitumen Viscosity. *Energy & Fuels*, 5:333–340, 1991.
- [28] L. Chatergoon, R. Whiting, L. Grierson, T. Peters, and C. Smith. Use of size distribution and viscosity to distinguish asphalt colloidal types. *Fuel*, 74(2): 301–304, 1995.
- [29] F. M. Clark. *Insulating materials for design and engineering practice*. Wiley, New York, 1962.
- [30] M. P. Colombini, F. Modugno, F. Silvano, and M. Onor. Characterization of the Balm of an Egyptian Mummy from the Seventh Century B.C. *Studies in Conservation*, 45:19–29, 2000.

- [31] J. Connan and D. Dessort. Du bitume de la Mer Morte dans les baumes d’une momie égyptienne: identification par critères moléculaires. *Comptes Rendus De l’Académie Des Sciences, Série II*, 309:1665–1672, 1989.
- [32] J. Connan and D. Dessort. Du bitume dans les baumes de momies égyptiennes (1 295 av. J.-C.-300 ap. J.-C.): détermination de son origine et évaluation de sa quantité. *Comptes Rendus De l’Académie Des Sciences, Série II*, 312: 1445–1452, 1991.
- [33] J. Connan, A. Nissenbaum, and D. Dessort. Molecular archaeology: Export of Dead Sea asphalt to Canaan and Egypt in the Chalcolithic-early bronze age (4th–3rd millennium BC). *Geochimica et Cosmochimica Acta*, 56:2743–2759, 1992.
- [34] L. W. Corbett. Composition of Asphalt based on Generic Fractionation, using solvent Deasphalting, Elution-Adsorption Chromatography, and densimetric Characterization. *Analytical Chemistry*, 41:576–579, 1969.
- [35] L. W. Corbett and R. Urban. Asphalt and bitumen. In *Ullmann’s Encyclopedia of Industrial Chemistry*, pages 169–188. VCH, Germany, Fifth edition, 1985. A3.
- [36] L.W. Corbett and R. E. Swarbrick. Composition analysis used to explore asphalt hardening. *AAPT*, 29:104–113, 1960.
- [37] L. H. Csanyi and Fung H.-P. A rapid means of determining the constituents of asphalts. *AAPT*, 23:64–77, 1954.
- [38] J. A. Curiale. Origin of solid bitumens, with emphasis on biological marker results. *Organic Geochemistry*, 10:559–580, 1986.
- [39] J. A. Curiale. Biological markers in graphamites and pyrobitumens. In T. F. Yen and J. M. Moldowan, editors, *Geochemical Biomarkers*, pages 1–24. Harwood Academic Publishers, New York, 1988.
- [40] W. H. Delano. *Twenty years’ Practical Experience of Natural Asphalt and Mineral Bitumen*. E. & F. N. Spon, London, 1893.
- [41] J. Densley. Ageing mechanisms and diagnostics for power cables - an overview. *IEEE Electrical Insulation Magazine*, 17(1):14–22, 2001.
- [42] E. T. Dumble. Texas asphaltum. *Science*, 13:295, 1889.
- [43] A. E. Dunstan. Colloid Chemistry of Petroleum. In J. Alexander, editor, *Colloid Chemistry - Theoretical and Applied*, pages 491–502. The Chemical Catalog Company Inc., New York, 1931. Volume 3.
- [44] J. J. Duvall, G. Miyake, M. W. Catalfomo, S. S. Kim, D. C. Colgin, and J. F. Branthaver. Size exclusion chromatography and ion exchange chromatography separations of asphalts. Topical Report SHRP-A-663, Strategic Highway Research Program, Washington, D. C., U. S. A., 1993.
- [45] H. Dykstra, K. Beu, and D. L. Katz. Precipitation of Asphalt from Crude Oil by flow through Silica. *The Oil and Gas Journal*, 43(21):79, 82, 102, 104, September 1944.
- [46] J. Errera. The sensitiveness to light of asphalt as a function of its degree of dispersion. *Transactions of the Faraday Society*, 19:314–317, 1923. Published as part of ‘The Physical Chemistry of the Photographic Process. A General Discussion’.
- [47] European Asphalt Pavement Association. Asphalt in figures 2000. The Netherlands, 2001.

- [48] D. H. Everett. *Basic Principles of Colloid Science*. Royal Society of Chemistry, London, 1989. Royal Society of Chemistry Paperbacks.
- [49] R. J. Forbes. *Notes on the history of ancient roads and their construction*. N.V. Noord-Hoollandsche Uitgevers-MIJ, Amsterdam, 1934.
- [50] R. J. Forbes. *Bitumen and petroleum in antiquity*. E. J. Brill, Leiden, 1936.
- [51] M. H. Fournel. *Description of the Asphaltic Mine of the Val-De-Travers in the Canton of Neufchatel with Introductory Observations by the Count De Saasenay to which are appended, remarks on the works executed by the Seyssel and other Companies in Paris, and throughout France by P. Muldoon, Esq.* A. H. Baily & Co., London, 1838.
- [52] H. W. Fritz, J. Huet, and R. Urban. English-French-German dictionary of technical terms related to Hydrocarbon binders, Hydrocarbon composite materials, Processes for removing pavement material and for the rehabilitation of asphalt pavements. *Materials and Structures*, 25:171–185, 1992.
- [53] Z-N. Gao, Y-N. Chen, and F. Niu. Compressively matured solid bitumen and its geochemical significance. *Geochemical Journal*, 35:155–168, 2001.
- [54] J. L. Goodrich, J. E. Goodrich, and W. J. Kari. Asphalt Composition Tests: Their Application and Relation to Field Performance. *Transportation Research Record*, 1096:146–167, 1986.
- [55] T. Greenhill. Nekpokhaeia: Or, the art of embalming; wherein is shewn the right of burial and funeral ceremonies, especially that of preserving bodies after the egyptian method. together with an account of the egyptian mummies, pyramids, subterranean vaults and lamps, and their opinion of the metempsychosis, the cause of their embalming: As also a geographical description of egypt, the rise and course of the Nile, the temper, constitution and physick of the inhabitants; their inventions, arts, sciences, stupendious works and sepulchres, and other curious observations any ways relating to the physiology and knowledge of this art. part i. illustrated with a map and fourteen sculptures. *Philosophical Transactions*, 24:1101–2109, 1704-1705.
- [56] R. L. Griffin, W. C. Simpson, and T. K. Miles. Influence of composition of paving asphalt on viscosity, viscosity-temperature susceptibility, and durability. *Journal of Chemical Engineering and Data*, 4:349–354, 1959.
- [57] J. E. Hackford. Discussion on the constitution of asphalt by F. J. Nellensteyn. *The Journal of the Institution of Petroleum Technologists*, 10:717–719, 1924.
- [58] G. A. Haley. Unit Sheet Weights of Asphalt Fractions Determined by Structural Analysis. *Analytical Chemistry*, 44(3):580–585, March 1972.
- [59] H. W. Halleck. *Bitumen: Its Varieties, Properties, and Uses*. U. S. Corps of Engineers, Washington, 1841. Papers on Practical Engineering, U. S. Corps of Engineers under the Direction of Col. J. G. Totten, Chief Engineer.
- [60] C. Hatchett. Observations on Bituminous Substances with a Description of the Varieties of the Elastic Bitumen. *Transactions of the Linnean Society*, 4: 129–154, 1798. Read May 2, June 6, and July 4, 1797.
- [61] C. Hatchett. Observations on the change of the proximate principles of vegetables into bitumen; with analytical experiments on a peculiar substance which is found with the bovey coal. *Philosophical Transactions of the Royal Society of London*, 94:385–410, 1804.

- [62] C. Hatchett. Some Account of the Pitch-lake in the Island of Trinidad in Two Letters: The first from Samuel Span, Esq. to James Tobin, Esq. F. L. S. and the other from Mr. Tobin to Charles Hatchett, Esq. F. R. S. & L. S. with Observations by Mr. Hatchett. *Transactions of the Linnean Society*, pages 251–269, 1807. Read April 17, 1804.
- [63] R. V. Helm. Separation of Asphaltic Materials by Reversed Phase Partition and Adsorption Chromatography. *Analytical Chemistry*, 41(10):1342–1344, August 1969.
- [64] E. S. Hillman and B. Barnett. The constitution of cracked and uncracked asphalts. *Proceedings of the 40th Meeting of ASTM*, 37:558–568, 1937. Part II, Technical Papers.
- [65] E. Hirsch and K. H. Altgelt. Integrated Structural Analysis. A Method for the Determination of Average Structural Parameters of Petroleum Heavy Ends. *Analytical Chemistry*, 42(2):1330–1339, October 1970.
- [66] E. Hitchcock. Notes on the Geology of several parts of Western Asia: founded chiefly on specimens and descriptions from American Missionaries. *Proceedings and Transactions of the Association of American Geologists and Naturalists*, pages 348–321, 1842. Reports of the first, second (1840, 1841 at Philadelphia, USA) and the third (1842 at Boston, USA) meetings of the Association.
- [67] A. J. Hoiberg and W. E. Garris. Analytical Fractionation of Asphalts. *Industrial and Engineering Chemistry Analytical Edition*, 16(5):294–302, May 1944.
- [68] R. L. Hubbard and K. E. Stanfield. Determination of Asphaltenes, Oils, and Resins in Asphalt. *Analytical Chemistry*, 20(5):460–465, May 1948.
- [69] T. S. Hunt. Contributions to the chemical and geological history of bitumens, and of pyroschists or bituminous shales. *The American Journal of Science and Arts*, XXXV:157–171, 1863. Second Series.
- [70] IAEA. Bituminization of Radioactive wastes. Technical Reports Series 116, International Atomic Energy Agency, Vienna, 1970. Review of the present state of the development and industrial application.
- [71] IAEA. Conditioning of Low-and Intermediate-Level Radioactive Wastes. Technical Reports Series 222, International Atomic Energy Agency, Vienna, 1983.
- [72] IAEA. Bituminization Processes to Condition Radioactive Wastes. Technical Reports Series 352, International Atomic Energy Agency, Vienna, 1993.
- [73] A. Jaccard. *Le Pétrole, l’asphalte et le bitumen, au point de vu géologique*. Bibliothèque Scientifique Internatioanle, Paris, 1895. Anceinne librairie Germer Bailliere et cie.
- [74] D. R. Jones. SHRP Materials Reference Library: Asphalt Cements: A Concise Data Compilation. Report SHRP-A-645, Strategic Highway Research Program, Washington, D. C., U. S. A., 1993.
- [75] V. Kalichevsky and S. C. Fulton. Chemical Composition of Asphalts and Asphaltic Materials. *National Petroleum News*, 23(51):33–36, 1931.
- [76] D. L. Katz and K. E. Beu. Nature of Asphaltic Substances. *Industrial and Engineering Chemistry*, 37(2):195–200, February 1945.

- [77] H. H. Kiet, S. L. Malhotra, and L-P. Blanchard. Structure Parameter Analyses of Asphalt Fractions by a Modified Mathematical Approach. *Analytical Chemistry*, 50(8):1212–1218, July 1978.
- [78] R. E. Kirk and L. H. Reyerson. Some observations on the colloidal character of asphalt. *Journal of Physical Chemistry*, 29:865–871, 1925.
- [79] J. Koller, U. Baumer, Y. Kaup, H. Etspüler, and U. Weser. Embalming was used in Old Kingdom. *Nature*, 391:343–344, January 1998.
- [80] B. Kreiger. *The Dead Sea: Myth, History, and Politics*. Brandeis University Press, Hanover, New England, 1997. pages 130–132.
- [81] E. C. E. Lord. Ultra-microscopic examination of Disperse Colloids present in Bituminous Materials. *Journal of Agricultural Research*, 27:167–176, 1919.
- [82] J. A. F. Lozano and Y. M. Rodríguez. Rheological and Conductometric Properties of Two Different Crude Oils and of Their Fractions. *Industrial and Engineering Chemistry Process Design and Development*, 23(1):115–121, 1984.
- [83] D. S. MacDonald, J. W. Weatherley, and D. J. Hollick. A modern jointing system for medium voltage distribution cables. *3rd IEEE International Conference on Power cables and Accessories 10kV-500 kV*, pages 82–86, 1993.
- [84] C. Mack. Colloid Chemistry of Asphalts. *Journal of Physical Chemistry*, 36: 2901–2914, 1932.
- [85] C. Mack. Physico-chemical aspects of asphalts. *AAPT*, 5:40–52, 1933.
- [86] A. S. Mackenzie. Applications of biological markers in petroleum geochemistry. In J. Brooks and D. Welte, editors, *Advances in Petroleum Geochemistry*, pages 115–214. Academic Press, London, 1984. Volume 1.
- [87] G. A. Mansoori. Modeling of asphaltene and other heavy organic depositions. *Journal of Petroleum Science and Engineering*, 17:101–111, 1997.
- [88] J. Marcusson. Beiträge zur chemie und Analyse der Asphalte. *Chemiker-Zeitung*, 76:813–815, 1914.
- [89] J. Marcusson. Beiträge zur chemie und Analyse der Asphalte. *Chemiker-Zeitung*, 77:822–823, 1914.
- [90] J. Marcusson. Der chemische Aufbau der Naturasphalte. *Zetischrift für Angewandte Chemie*, 29:346–351, 1916.
- [91] J. Marcusson. Der chemische Aufbau der Kunstasphalte. *Zetischrift für Angewandte Chemie*, 31:113–115, 1918.
- [92] J. Marcusson. *Die Natuerlichen und Kuenstlichen Asphalte*. Engelmann, Leipzig, Second edition, 1931.
- [93] J-F. Masson and G. M. Polomark. Bitumen microstructure by modulated differential scanning calorimetry. *Thermochimica Acta*, 374:105–114, 2001.
- [94] K. N. Mathes. A brief history of development in electrical insulation. *Proceedings of the IEEE 20th Electrical Electronics Insulation Conference*, pages 147–150, 1991. Boston, USA.
- [95] W. McDermid. Dielectric absorption characteristics of generator stator insulation. *Conference Record of the 2000 IEEE International Symposium on Electrical Insulation*, pages 516–519, 2000. Anaheim, CA, USA.
- [96] J. C. Morrel and Egloff G. Colloid Chemistry of Petroleum. In J. Alexander, editor, *Colloid Chemistry - Theoretical and Applied*, pages 503–522. The Chemical Catalog Company Inc., New York, 1931. Volume 3.

- [97] F. J. Nellensteyn. *Bereiding En Constitutie Van Asphalt*. Ph.D. Thesis, Technische Hoogeschool, Delft, 1923.
- [98] F. J. Nellensteyn. Neuere asphalttheorien. In *Congrès International Pour L’Essai Des Matériaux*, La Haye, 1928. Martinus Nijhoff. Volume Two.
- [99] F. J. Nellensteyn. Asphalt. In J. Alexander, editor, *Colloid Chemistry - Theoretical and Applied*, pages 535–546. The Chemical Catalog Company Inc., New York, 1931. Volume 3.
- [100] F. J. Nellensteyn. The Colloidal Structure of Bitumens. In A. E. Durnstan, A. W. Nash, B. T. Brooks, and H. Tizard, editors, *The Science of Petroleum 4*. Oxford University Press, London, 1938.
- [101] F. J. Nellensteyn and J. P. Kuipers. Researches on asphaltenes: Part i. *Journal of the Institute of Petroleum*, 26:400–406, 1940.
- [102] E. L. Nichols. One some optical properties of asphalt. *Physical Review*, 14: 204–213, 1902. Series I.
- [103] A. Nissenbaum and M. Goldberg. Asphalts, heavy oils, ozocerite and gases in the Dead Sea Basin. *Organic Geochemistry*, 2:167–180, 1980.
- [104] G. O’Donnell. Separating Asphalt into its Chemical Constitutents. *Analytical Chemistry*, 23(6):894–898, June 1951.
- [105] OECD. Bituminization of low and medium level radioactive wastes Proceedings. Technical Report 18-19/V/1976, OECD Nuclear Energy Agency and the Eurochemich Company, Antwerp, 1976. Proceedings of a Seminar organised jointly by the OECD Nuclear Agency and the Eurochemic Company.
- [106] G. L. Oliensis. Reaction to “partial solvents” as a criterion of structure in bitumen. *AAPT*, 17:1–25, 1948.
- [107] P. C. Painter. The Characterization of Asphalt and Asphalt Recyclability. Report SHRP-A-675, Strategic Highway Research Program, Washington, D. C., U. S. A., 1993.
- [108] S. F. Peckham. *Report on the Production, Technology, and uses of Petroleum and its Products*. Department of the Interior, Census Office, Government Printing Office, Washington, USA, 1884. The Miscellaneous Documents of the House of Representatives for the Second Session of the forty-seventh Congress, Final Report of the Tenth Census of United States of America, Volume 13, Part 10, 1882-’83, 319 pages.
- [109] S. F. Peckham. Review of le pétrole, l’asphalte et le bitumen, au point de vu géologiqu. *Science*, 2:237–238, 1895.
- [110] S. F. Peckham. What is Parianite? *Journal of the Franklin Institute*, 149(3): 161–193, March 1900.
- [111] S. F. Peckham. *Solid Bitumens: Their physical and chemical properties and chemical analysis together with a treatise on the chemical technology of bituminous pavements*. The Myron C. Clark Publishing Co., London, 1909.
- [112] J. C. Petersen. Quantitative Functional Group Analysis of Asphalts using Differential Infrared Spectrometry and Selective Chemical Applications. *Transportation Research Record*, 1096:1–11, 1986.
- [113] J. C. Petersen, R. E. Robertson, P. M. Branthaver, J. F. Harnsberger, J. J. Duvall, S. S. Kim, D. A. Anderson, D. W. Christiansen, and H. U. Bahia. Binder characterization and evaluation: Volume 1. Report SHRP-A-367, shrp, Washington, D. C., U. S. A, 1994.

- [114] J. C. Petersen, R. E. Robertson, P. M. Branthaver, J. F. Harnsberger, J. J. Duvall, S. S. Kim, D. A. Anderson, D. W. Christiansen, H. U. Bahia, R. Dongre, M. G. Sharma, C. E. Antle, J. W. Button, and C. J. Glover. Binder Characterization and Evaluation: Volume 4: Test methods. Report SHRP-A-370, shrp, Washington, D. C., U. S. A, 1994.
- [115] T. J. Pettigrew. *A History of Egyptian Mummies*. North American Archives, Los Angeles, 1834. Library of Archaeology Classics, Republished in 1983.
- [116] J. Ph. Pfeiffer and R. N. J. Saal. Asphaltic Bitumen as Colloid System. *The Journal of Physical Chemistry*, 44(2):139–149, February 1940.
- [117] N. Pieri, F. Jacquot, G. Mille, J. P. Planche, and J. Kister. GC-MS identification of biomarkers in road asphalt and in their parent crude oils. Relationship between crude oil maturity and asphalt reactivity towards weathering. *Organic Geochemistry*, 25:51–68, 1996.
- [118] G. W. Preckshot, N. G. DeLisle, C. E. Cottrekk, and D. L. Katz. Asphaltic Substances in Crude Oils. *Transactions of the American Institute of Mining and Metallurgical Engineers*, 151:188–205, 1943.
- [119] Z. Ramijak, A. Šolc, P. Arpino, J-M. Schmitter, and G. Gulochon. Separation of Acids from Asphalts. *Analytical Chemistry*, 49(8):1222–1225, July 1977.
- [120] J. W. Ramsey, F. R. McDonald, and J. C. Petersen. Structural Study of Asphalts by Nuclear Magnetic Resonance. *Industrial and Engineering Chemistry Product Research and Development*, 6(4):231–236, December 1967.
- [121] C. Richardson. On the nature and origin of asphalt. Bulletin 2, The Barber Asphalt Paving Company, Long Island City, New York, October 1898. Contributions to the chemistry of the natural hydro-carbons and their derivatives, Number 1; Reprinted, with corrections and additions, from an article in the Journal of the Society of Chemical Industry for January, 1898, 63 pages.
- [122] C. Richardson. The theory of the perfect sheet asphalt surface. *The Journal of Industrial and Engineering Chemistry*, 7:463–465, 1915.
- [123] RILEM. *BM1: Terminology of hydrocarbon binders*. International Union of Testing and Research Laboratories for Materials and Construction, 1994. Final 2nd Edition March 1989.
- [124] RILEM. *BM3: Determination of density or relative density of hydrocarbon binders - capillary stoppered pyknometer method*. International Union of Testing and Research Laboratories for Materials and Construction, 1994. Final Edition April 1984.
- [125] RILEM. *BM4: Determination of needle penetration of hydrocarbon binders*. International Union of Testing and Research Laboratories for Materials and Construction, 1994. Final Edition October 1984.
- [126] A. Rosinger. Beitrage zur kolloidchemie des asphalts. *Kolloid-Zeitschrift*, 15: 177–179, 1914.
- [127] S. J. Rozeveld, E. E. Shin, A. Bhurke, L. France, and L. T. Drzal. Network morphology of straight and polymer modified asphalt cements. *Microscopy Research and Technique*, 38:529–543, 1997.
- [128] J. Rullkötter, B. Spiro, and A. Nissenbaum. Biological marker characteristics of oils and asphalts from carbonate source rocks in a rapidly subsiding graben, Dead Sea, Israel. *Geochimica et Cosmochimica Acta*, 49:1357–1370, 1985.

- [129] R. N. J. Saal and J. W. A. Labout. Rheological Properties of Asphaltic Bitumens. *The Journal of Physical Chemistry*, 44(2):149–165, February 1940.
- [130] A. N. Sachanen. *The Chemical Constituents of Petroleum*. Reinhold Publishing Corporation, New York, U. S. A., 1945.
- [131] W. Schneider and I. Just. Ultramikroskopie der Oleosole. *Zeitschrift für wissenschaftliche Mikroskopie und mikroskopische Technik*, 2:501–530, 1905.
- [132] E. Schönian. *The Shell Bitumen Hydraulic Engineering Handbook*. Shell Bitumen, United Kingdom, 1999.
- [133] W. C. Simpson, R. L. Griffin, and T. K. Miles. Relationship of asphalt properties to chemical composition. *Journal of Chemical Engineering Data*, 6:426–429, 1961.
- [134] J. G. Speight and S. E. Moschopedis. On the Nature of Petroleum Asphaltenes. In J. W. Bunger and N. C. Li, editors, *Chemistry of Asphaltenes*, pages 1–15. American Chemical Society, Washington, D. C., U. S. A., 1981. Advances in Chemistry Series 195.
- [135] A. F. Stock. Review of the Application of High-Pressure Liquid Chromatography to Pavements. *Transportation Research Record*, 1096:100–105, 1986.
- [136] E. Tannenbaum and Z. Aizenshtat. Formation of immature asphalt from organic-rich carbonate rocks - I. Geochemical correlation. *Organic Geochemistry*, 8(2):181–192, 1985.
- [137] The Oxford English Dictionary. Oxford university press. Oxford, United Kingdom, 1989. 20 volumes.
- [138] Theoretical and Practical Essay on Bitumen. Theoretical and Practical Essay on Bitumen setting forth its Uses in Remote Ages and Revival in Modern Times and demonstrating its Applicability to Various Purposes. E. Wilson, London, 1839. Goldsmiths’-Kress library of economic literature; no. 30916.
- [139] J. E. Timperley and J. R. Michalec. Estimating the remaining service life of asphalt-mica stator insulation. *IEEE Transactions on Energy Conversion*, 9(4):686–694, 1994.
- [140] R. N. Traxler and H. E. Schweyer. Asphalt Analysis-2 : How to make component analysis? *The Oil and Gas Journal*, 52(19):158, 1953.
- [141] R. N. Traxler and H. E. Schweyer. Asphalt Analysis-3 : How do different methods compare? *The Oil and Gas Journal*, 52(21):143–144, 1953.
- [142] R. N. Traxler and H. E. Schweyer. Asphalt Analysis-4 : Refractive Index can be a useful tool. *The Oil and Gas Journal*, 52(23):167, 1953.
- [143] R. N. Traxler and H. E. Schweyer. Asphalt Analysis-5 : Making empirical correlations. *The Oil and Gas Journal*, 52(24):157, 1953.
- [144] R. N. Traxler and H. E. Schweyer. Asphalt Analysis-6 : Effect of processing on composition. *The Oil and Gas Journal*, 52(25):151, 1953.
- [145] R. N. Traxler and H. E. Schweyer. Asphalt Analysis-7 : What is asphalt composition? *The Oil and Gas Journal*, 52(26):133, 1953.
- [146] R. N. Traxler and H. E. Schweyer. Separating Asphalt Materials ... N-Butanol-Acetone Method. *The Oil and Gas Journal*, 52(17):133, 1953.
- [147] C. Van der Poel. A general system describing the visco-elastic properties of bitumens and its relation to routine test data. *Journal of Applied Chemistry*, 4:221–236, 1954.

- [148] Webster’s Basic English Dictionary. Merriam-webster. Springfield, U.S.A., 1995.
- [149] C. S. Wen, G. V. Chilingarian, and T. F. Yen. Properties and Structures of Bitumen. In G. V. Chilingarian and T. F. Yen, editors, *Bitumen, Asphalts and Tar Sands*, pages 155–190. Elsevier Scientific Publishing Company, Amsterdam, 1978. Developments in Petroleum Science, 7.
- [150] D. Whiteoak. *The Shell Bitumen Handbook*. Shell Bitumen, United Kingdom, 1990.
- [151] C. Whittlesey. Origin of the bitumen of stratified rocks. *Annals of Science*, 1:153–157, 1853.
- [152] M. Wilkinson. Material progress in cable accessories up to 33 kv. *Power Engineering Journal*, pages 89–91, April 1994.
- [153] T. F. Yen. Asphaltic materials. In *Encyclopedia of Polymer Science and Engineering*, pages 1–10. John Wiley and Sons, New York, 1990. Index Volume, A.
- [154] J. S. Youtcheff and D. R. Jones. Guideline for asphalt refiners and suppliers. Report SHRP-A-686, SHRP, Washington, D. C., U. S. A., 1994.

CHAPTER 2

The mechanical behavior of asphalt

J. M. KRISHNAN

1. Introduction

Asphalt¹ is a complex heterogeneous mixture of hydrocarbons usually collected as a byproduct of the refining process of crude oil in petroleum refineries. Asphalt has numerous applications and one of its major uses is as a binder for aggregate materials in the construction of highways and runways [38]. The mechanical properties of asphalt mixtures depend to a large extent on the type and quantity of asphalt used and hence it is imperative that one develops a better understanding of asphalt. Modifiers in the form of polymer, crumb tire rubber, fillers etc., are being added to asphalt in an attempt to improve its mechanical properties. As each and every modifier can interact with asphalt in a widely different manner, the complexity in modeling the constitutive behavior of modified asphalt is increased. However, even before one attempts the modeling of modified asphalt, the behavior of straight-run asphalt needs to be better understood. In this study, we focus our attention on modeling the mechanical behavior of asphalt for a specific temperature range in which its behavior is predominantly viscoelastic. The reason for modeling the behavior of asphalt in this specific range will become clear as we discuss in detail the nature of asphalt and the various complex manifestations of its behavior. Several experimental investigations have been carried out on asphalt, however, most of the information that is required to make reasonable assumptions concerning the nature of asphalt for the entire temperature range of interest is still lacking. For instance, reliable information related to the glass transition temperature, influence of temperature and pressure on the apparent viscosity, influence of different source/processing method etc., on the mechanical and thermodynamical behavior of asphalt are not available.

Most of the current as well earlier modeling attempts with regard to asphalt have characterized asphalt as a linear viscoelastic or a Newtonian fluid and have invariably used assumptions such as time-temperature superposition, and have modeled them as thermorheologically simple fluids which obey the Arrhenius type rate equations. While these models have served the purpose in characterizing distress measurements for asphalt concrete to a reasonable degree, none of them could be considered as rigorous constitutive models with the constitutive equations reflecting the complexity of asphalt. Some of the attempts describe the behavior of asphalt in

¹An extended version of this paper is available in *Mechanics of Materials*, 37(11), 1085-1100, 2005

a piecemeal fashion with different empirical equations describing the material behavior for different temperature regimes. As details about the complexity of asphalt are being revealed by the use of tools such as gas chromatography, mass spectrometry, differential scanning calorimetry etc., there is a need to develop constitutive models which have a rigorous basis and which have the ability to take into account the information that is gleaned as a consequence of these sophisticated experiments.

One of the popular models for describing the mechanical behavior of asphalt is due to Burgers [6]. Saal and Labout [58] used a modified form of the Burgers’s model to characterize asphalt as a mixed gel-sols and predicted with reasonable accuracy certain experimental results. Lethersich [31] used a model based on a mechanical analog consisting of two springs and two dashpots to characterize the response of bitumen and observed the need for more than one relaxation time to describe the response of asphalt. One of the earliest attempts in deriving a fully three dimensional theory for rate type viscoelastic fluids is due to Frohlich and Sack [17]. Motivated by the experimental results on bitumen of Lethersich [31], they developed constitutive models for the viscoelastic response of dispersions. Van der Poel [66] assumed that asphalt behaved like a linearized elastic material at low temperatures and for short loading times and behaved like a Newtonian fluid for long loading times and sufficiently high temperatures. While his nomographs using penetration index and softening point measurements of asphalt are very widely used, use of measures like ‘stiffness’ for charactering the Newtonian response of asphalt is questionable at best. Brodnyan *et al.*, [4] and Gaskins *et al.*, [18] in a series of papers investigated the rheological characteristics of asphalt. They used time-temperature superposition along with the William-Landel-Ferry equations. Using de Waele-Ostwald’s empirical equations, Majidzadeh and Schwyer tried to characterize the non-Newtonian behavior of asphalts [33]. The structural degradation of asphalt was modeled by them using a Eyring rate process theory. Most of the later studies concerning asphalt were dedicated to the development of simple linear viscoelastic models for asphalt and data reduction with respect to such models which led to the determination of the complex modulus, phase angle etc., obtained by correlating with tests on asphalt in different kinds of rheometers. For instance, they developed relations between the dynamic modulus and phase angle [29], master curves for the complex shear modulus with frequency and temperature [15], linear viscoelastic models for thin bituminous films in tension and compression [14]. The limitations of using the assumption of time-temperature superposition at high temperatures were reported in the study of Lesueur *et al.*, [30]. Crystallization and the nature of asphaltenes present in asphalt were ascribed, by Lesueur *et al.*, as the reasons for the failure of time temperature superposition for describing the behavior of asphalt. Assuming asphalt to be a dispersion of asphaltene particles peptized by resins, a bimodal model was developed by these authors. Cheung and Cebon [8] used the “Eyring plasticity model” at temperatures below glass transition with a temperature dependence of the Arrhenius type at temperatures above glass transition, and they also assumed that asphalt obeyed time-temperature superposition at high temperatures.

In the following sections, we elaborate on some of the issues related to the modeling of asphalt. We then detail a thermodynamic framework for modeling asphalt. This framework takes into account the fact that materials like asphalt can exist in

different natural (stress-free) configurations and it has been successfully used for modeling diverse material behavior. The final section of this paper is related to testing the efficacy of the predictions of the model by making a comparison of the prediction with some of the experimental data that is available in the literature.

2. Issues related to modeling of asphalt

2.1. ‘Multi-constituent’ nature of asphalt. The multi-constituent nature of asphalt has been explored in different degrees of sophistication and the procedures related to the different fractionation schemes are still evolving. One of the earliest studies which addressed the multi-constituent nature of asphalt is due to Boussingault [3] and he classified the bitumen of Bechelbronn into *petrolene* and *asphaltene*. Nellensteyn [41] suggested characterizing asphalt as a colloidal system and significant investigations on the colloidal nature of asphalt were conducted by Pfeiffer and Saal [46]. In a similar vein to earlier attempts that were concerned with understanding the micro-structure of asphalt, Dickie and Yen [13] conceptualized that asphaltenes and resins are repeating elements of similar composition with the difference in their chemical structure ascribable to solubility and aromaticity. There have been innumerable studies related to fractionating asphalt into different distinct chemical species and the fractionation schemes due to Rostler’s [57] and Corbett’s [11] deserve special mention here. In the light of the above developments, it is interesting to observe here the research conducted as part of the Strategic Highway Research Program (SHRP) in the United States of America. The SHRP research effort critically examined the available colloidal models for asphalt in the light of the advances made in the field of colloid chemistry and came to the conclusion that “*asphalt cement is a relatively homogeneous and randomly distributed collection of molecules differing in polarity and molecular size*” [45] and “*asphalt is a single phase mixture of many different polar and non-polar molecules, all of which interact with one another*” [67]. They also used Ion Exchange Chromatography to separate asphalt into strong and weak acids, strong and weak bases, neutrals and *amphoteric*s - compounds with both acid and base functionalities. These fractions along with the parent asphalt were also tested in rheometers in an attempt to link the physical properties of asphalt with the various chemical fractions.

Based on the above cited studies, some general conclusions about the nature of asphalt can be reached. We can conclude without any loss of generality that asphalt is a mixture of different chemical species and the different manifestations of the mechanical behavior of asphalt depend on the relative proportions of each of these species. The change of behavior of asphalt over time, such as aging, internal structure change etc., are due to the interconversion of the different chemical species constituting asphalt. The proportion of these different constituents as well as the potential for chemical interconversion depends to a large extent on the source of asphalt (crude source), the processing method etc. A complete and rigorous constitutive model should then be able to take into account the multi-constituent nature of asphalt, the ability to interconvert as well as the influence of the crude source on the mechanical behavior of asphalt. To construct such a model is a difficult but achievable task using the framework we have in hand, but due to the paucity of experimental information such an attempt may not be feasible at the moment.

Hence, in this investigation we ignore the influence of the different chemical species that constitute asphalt as far as its mechanical behavior is concerned.

2.2. Asphalt transitions. Different temperature regimes have been associated with the different types of mechanical response of asphalt. For instance, Schwyer [59] classified asphalt behavior in the following manner: high temperature ($> 60^{\circ}\text{C}$) – Newtonian fluid, near-transition region (between 0 and 60°C) – viscoelastic and far-transition range (between glass transition temperature and 0°C) – elastic. More insight into the transitory nature of asphalt has been gained recently due to the studies by Storm *et al.*, [62]. Using asphalts from three different sources and testing them over a wide range of temperature, Storm *et al.*, concluded that at a temperature range of $65\text{-}150^{\circ}\text{C}$, these asphalts behaved as Newtonian fluids and in the temperature range of $25\text{-}65^{\circ}\text{C}$, the behavior was essentially viscoelastic. Storm *et al.*, hypothesized that the solvation of the asphaltene shells becomes larger during this temperature transition imparting a new microstructure for asphalt. This is in addition to the crystallization that is generally considered as being responsible for this transitory behavior. Hence as the temperature of an asphalt sample is varied from a specific value, the internal structure changes giving rise to different mechanical behavior. As discussed earlier, this is due to the fact that asphalt is in essence a mixture of different chemical species, each of them exhibiting solid-like or fluid-like characteristics as the temperature is varied. One can also view asphalt as a mixture of amorphous and crystalline phases and the influence of temperature is in the melting of crystalline phases as the temperature is increased or in the formation of crystalline phases as the temperature is decreased. Different studies have addressed the issues related to the existence of amorphous and crystalline phases in asphalt and their role in the transitory nature of asphalt. Most of these studies have concluded that the low temperature properties of asphalt binders depend to a large extent on the amount of crystallizable fractions and the glass transition temperature of asphalt. For instance, increased crystallized fractions in asphalt lead to reduced ductility, reduced adhesion to the mineral aggregates and increased brittleness at low temperatures. Unlike the literature in polymers, there have been few studies devoted to understanding the crystallization kinetics of asphalt. Some of the studies which have concerned themselves with the role of amorphous and crystalline fractions of asphalts include Smith *et al.*, [60], Noel and Corbett [43], Giavarini and Pochetti [19], Albert *et al.*, [1], Claudy *et al.*, [9], Daly *et al.*, [12], Netzel [42], Michon *et al.*, [37], Masson *et al.*, [34], and Edwards and Redelius [16].

The fact that asphalts exhibit more than one glass transition temperature has been recorded in different experimental investigations [7, 34, 35]. From an initial condition, different cooling rates induce different internal structural changes in asphalt resulting in glass transitions which are several orders apart. Masson and co-workers [34, 35] investigated the microstructure of bitumen by means of modulated DSC (MDSC) and came to the conclusion that the degree of polymerization of asphalts is of the order 10 and hence asphalt could be classified as an oligomer. On the basis of MDSC of bitumen with different annealing history, these studies concluded that asphalt had a mesophase structure similar to that encountered in liquid crystals.

To summarize the above discussion on the transitory nature of asphalt, we can consider asphalt as a mixture of two complex amorphous phases at roughly 100°C. We hasten to add here that by phase we mean ‘a homogeneous, physically distinct portion of matter’. As the temperature is reduced, one phase of this mixture starts crystallizing while the other remains in the amorphous phase. At the field service temperature of interest, asphalt can be assumed to consist of amorphous and crystalline phases. The viscoelastic behavior of asphalt then is influenced by the volume/mass fractions of these different phases and the tendency for the crystalline phase to either dissolve or solidify depending upon whether the pavement temperature increases or decreases. As of now, there are not enough experimental data available discussing the *inter-conversion* between amorphous and crystalline phases as asphalt is subjected to a wide range of temperatures and loading. Also, the crystallization kinetics of asphalt is not well understood. For instance, it is not clear as to what causes the crystallization of some fractions of asphalt as the temperature is reduced or what the influence of the different asphalt sources and processing methods are on the crystallization. We can make reasonable assumptions on the conditions for the initiation of crystallization and the evolution for the growth of the crystallized fractions only when we have an answer to the above question. In this investigation, we assume that the amorphous and crystalline phases give rise to different relaxation mechanisms and hence we will model asphalt with multiple relaxation mechanisms. We ignore the actual process of crystallization/dissolution of the crystalline phase as the temperature is varied and also the presence of an interfacial phase which can be considered to have characteristics that lies in between that for the amorphous and crystalline phases.

2.3. Internal structure change of asphalt with time. The complex response of asphalt is directly related to the evolution of its internal structure in the absence of external forces. The internal structure of asphalt can develop and evolve if it is left undisturbed at a constant temperature. This internal structure develops rapidly at first and then evolves in an asymptotic manner over time. Essentially, this evolution of internal structure can consist of a reversible and an irreversible portion. The irreversible portion can be ascribed to the aging of asphalt that results in the loss of chemical species due to the evaporation/volatilization and depends on the temperature at which asphalt is held. It also depends on the source of asphalt, the ‘consistency’ of asphalt and the specific fractional composition of asphalt. The more interesting change in the internal structure is due to the reversible portion and is similar to the ‘physical aging’ of polymers [27]. This specific phenomenon is the change in the property (density, mechanical response characteristics, dielectric properties, etc.,) of asphalt when maintained at a constant temperature for considerable time in the absence of any external forces and without any appreciable change in its chemical composition. Thermal and/or external forces acting on asphalt can revert the internal structure to the original condition in which it existed. As of now, two different kinds of reversible internal structural change have been identified. The first one occurs at room temperature and is an extremely slow process taking from days to weeks to reach equilibrium conditions. The second one which is observed at temperatures near glass transition for asphalt is much more rapid and experimental investigations have reported that it takes normally 1 - 2 days at the temperature

range of -15 to -35°C [32]. Hence the simple Arrhenius kind of relationship between rates and temperatures do not apply for asphalt, as according to this assumption one would expect faster hardening rate at higher temperatures [34]. Several studies have investigated the reversible internal structural change of asphalt (see for instance [2, 5, 10, 23, 24, 25, 32, 44, 61, 63, 64, 65]). This reversible change in the internal structure has been identified at room temperature as ‘steric hardening’ [5] and at glass transition temperature as ‘low temperature physical hardening’ [2]. The need for subjecting asphalt to identical test conditions before starting any kind of experimentation is due to this change in internal structure that occurs, as any such deviation may result in measurement of properties of asphalt from a transient configuration and not from its natural configuration. For instance, Traxler and coworkers [63, 65] while measuring the viscosity of several different asphalts in falling coaxial cylinder viscometers noticed that the viscosities of asphalt kept in the viscometers for considerable time exhibited increased viscosity. Traxler *et al.*, ascribed this structure formation due to the two-phase nature (asphaltene and petrole) of asphalt in which a gradual isothermal sol-gel transformation occurs as asphalt is kept steady at a specific temperature. Similar results were reported by Brown *et al.*, [5] who chose to call this phenomenon steric hardening. Brown *et al.*, attributed the formation of internal structure to the asphaltene fraction of asphalt. The change in the internal structure of asphalt when held for sufficient time near the glass transition temperature has been characterized as that due to low temperature physical hardening in the work of Bahia and Anderson [2]. They tried to explain this behavior due to the collapse of ‘free volume’ as asphalt passes through glass transition [2]. Claudy *et al.* [10] investigated the low temperature physical hardening of asphalt and concluded that molecular agglomerations of crystalline phases at low temperature could be one reason for this behavior. They were also the first to observe that ‘spinodal decomposition’ a phenomenon in which a ‘homogeneous’ liquid separates into two liquid phases as the material is cooled [22] is characteristic of asphalt and is another possible reason for the low temperature physical hardening of asphalt. Continuing on these lines, Masson *et al.*, ascribed a four stage internal structural development process for asphalt [34]. Each of the fractions of asphalt influence in their own way, depending on their tendency for crystallization in the formation of reversible internal structure (see Masson *et al.*).

Within the context of what we have discussed in the earlier sections, it is clear that a) the mechanical behavior of asphalt in the temperature regime of interest is quite complicated and not well understood, b) a comprehensive theory for modeling asphalt even with the limited information that is available is lacking and c) each and every facet of the modeling of the mechanical behavior of asphalt requires fusing ideas from physics and chemistry. A rigorous framework for modeling asphalt with the ability to take into account the microstructural details and reflect them in a macroscopic sense, is lacking. Such a framework should take into account the fact that the internal structure of asphalt evolves with time (in the presence or otherwise of external influences such as load, temperature etc). In this study we take a first step in this direction. We visualize asphalt as a material possessing multiple relaxation mechanisms. These different relaxation times could be associated with the amorphous and crystalline phases and the type and changes in the internal structure, i.e., the interaction between the phases. We assume that each of these

relaxation mechanisms can be modeled by a rate type viscoelastic fluid model with multiple sets of natural configurations. The key element of the framework that we use is that a body can exist stress free in numerous natural configurations. The underlying natural configurations can change during any process to which the body is subjected and the change of the internal microstructure is captured by this evolution of the natural configuration. The response of the body from these natural configurations is elastic when subjected to external forces. This particular framework has been used for modeling different types of phenomena, for instance, multi-network theory [52], plasticity [47, 48], crystallization of polymers [54, 55, 56], solid to solid phase transition [49], viscoelastic liquids [50], anisotropic fluids [51], and growth of biological materials [26, 53]. We refer the interested reader to [38, 39, 40] with regard to the application of this theory to asphalt mixtures.

3. Modeling of asphalt

3.1. Preliminaries. Consider a body \mathcal{B} in a configuration $\kappa_{\mathbf{R}}(\mathcal{B})$. We shall, for the ease of notation refer to the configuration as $\kappa_{\mathbf{R}}$. Let \mathbf{X} denote a typical position of a material point in $\kappa_{\mathbf{R}}$. Let κ_t be the configuration at a time t , then the motion $\chi_{\kappa_{\mathbf{R}}}$ assigns to each particle in configuration $\kappa_{\mathbf{R}}$ a particle in the configuration κ_t at time t , i.e.,

$$\mathbf{x} = \chi_{\kappa_{\mathbf{R}}}(\mathbf{X}, t). \quad (2.1)$$

The deformation gradient $\mathbf{F}_{\kappa_{\mathbf{R}}}$ is defined through

$$\mathbf{F}_{\kappa_{\mathbf{R}}} \equiv \frac{\partial \chi_{\kappa_{\mathbf{R}}}}{\partial \mathbf{X}}. \quad (2.2)$$

The left and right Cauchy-Green stretch tensors $\mathbf{B}_{\kappa_{\mathbf{R}}}$ and $\mathbf{C}_{\kappa_{\mathbf{R}}}$ are defined through

$$\mathbf{B}_{\kappa_{\mathbf{R}}} \equiv \mathbf{F}_{\kappa_{\mathbf{R}}} \mathbf{F}_{\kappa_{\mathbf{R}}}^{\mathbf{T}}, \quad (2.3)$$

$$\mathbf{C}_{\kappa_{\mathbf{R}}} \equiv \mathbf{F}_{\kappa_{\mathbf{R}}}^{\mathbf{T}} \mathbf{F}_{\kappa_{\mathbf{R}}}. \quad (2.4)$$

Now the balance of mass is given by

$$\dot{\rho} + \rho \operatorname{div} \mathbf{v} = 0, \quad (2.5)$$

where ρ is the density and \mathbf{v} is the velocity. Experimental studies on the compressibility of asphalt have pointed out that the change in the density is of the order of only 1.5 percent under normal temperatures and pressures [36] and hence in this study, we assume asphalt to be incompressible. In the light of the assumption of incompressibility, the balance of mass reduces to

$$\operatorname{div} \mathbf{v} = 0. \quad (2.6)$$

The balance of linear momentum is

$$\rho \left[\frac{\partial \mathbf{v}}{\partial t} + (\nabla \mathbf{v}) \mathbf{v} \right] = \operatorname{div} \mathbf{T} + \rho \mathbf{g}, \quad (2.7)$$

where \mathbf{T} is the Cauchy stress and \mathbf{g} is the acceleration due to gravity. For an incompressible material, the Cauchy stress tensor \mathbf{T} reduces to

$$\mathbf{T} = -p\mathbf{I} + \mathbf{T}^{\mathbf{E}} \quad (2.8)$$

where p is the Lagrange multiplier due to the constraint of incompressibility and \mathbf{T}^E is the constitutively determined extra stress. The balance of angular momentum for a body in the absence of internal couples implies that the stress tensor is symmetric. In the formulation of the constitutive equations derived in this study, the reduced-dissipation equation is used and for isothermal conditions it is given by [21, 49]

$$\mathbf{T} \cdot \mathbf{L} - \rho \dot{\psi} = \rho \theta \zeta \equiv \xi \geq 0, \quad (2.9)$$

where ψ is the Helmholtz potential, ζ is the rate of entropy production and ξ is the rate of dissipation. In the present attempt we ignore radiation [38].

3.2. Modeling asphalt with multiple relaxation mechanisms. We model asphalt as a rate type viscoelastic fluid. We follow the methodology of Rajagopal and Srinivasa [50] for developing constitutive relations for the stress. Referring to figure 1, κ_R is a reference configuration, $\kappa_{c(t)}$ is the configuration currently occupied by the material and $\kappa_{p_i(t)}$ is the preferred natural configuration once the tractions on $\kappa_{c(t)}$ are removed. It is possible for the material to possess more than one natural configuration and we assume that we can associate the natural configurations with different relaxation mechanisms. Let us for the sake of discussion assume that we have an asphalt sample at 100°C and we cool the sample to room temperature at a rate such that the crystalline phase develops. If we leave this sample at room temperature for sufficient time, the relaxation of asphalt will be due to the two different phases, the amorphous and crystalline phases. Due to the fact that the internal structure of asphalt evolves over a period of time (‘steric hardening’), there can be one more relaxation time associated with this change and this relaxation time will be of the order of days. Hence, the configuration $\kappa_{p_i(t)}$ in this case can be thought of being made up of a body with which we can associate three different relaxation times, one pertaining to the amorphous phase, one to the crystalline phase and the other that is related to the time scale of the steric hardening at room temperatures. The same material can exhibit different relaxation mechanisms if it is cooled to near the glass transition temperature. To take into account all these possibilities, we assume that asphalt possesses multiple relaxation mechanisms, each of them triggered by a different physical/chemical process. We also assume that the response from each of these natural configurations is elastic. Referring to figure 1, \mathbf{F}_{κ_R} denotes the mapping between the tangent space associated with κ_R , at a point in the reference configuration to the tangent space associated with the same material point in $\kappa_{c(t)}$. $\mathbf{F}_{\kappa_{p_i(t)}}$ refers to the mapping between the tangent space associated with the configuration $\kappa_{p_i(t)}$, at a material point to the tangent space associated with the current configuration $\kappa_{c(t)}$ at the same point. Here the index ‘i’ ranges from ‘1, . . . n’ where ‘n’ signifies the number of relaxation mechanisms. We also define the following mapping \mathbf{G}_i between the appropriate tangent spaces of κ_R and $\kappa_{p_i(t)}$,

$$\mathbf{G}_i \equiv \mathbf{F}_{\kappa_R \rightarrow \kappa_{p_i(t)}} = \mathbf{F}_{\kappa_{p_i(t)}}^{-1} \mathbf{F}_{\kappa_R}, \quad i = 1, 2, \dots n. \quad (2.10)$$

We define the velocity gradient $\mathbf{L}_{\kappa_{p_i(t)}}$ and the symmetric part of $\mathbf{L}_{\kappa_{p_i(t)}}$, $\mathbf{D}_{\kappa_{p_i(t)}}$ as follows,

$$\mathbf{L}_{\kappa_{p_i(t)}} = \dot{\mathbf{G}}_i \mathbf{G}_i^{-1}, \quad \mathbf{D}_{\kappa_{p_i(t)}} = \frac{1}{2} \left(\mathbf{L}_{\kappa_{p_i(t)}} + \mathbf{L}_{\kappa_{p_i(t)}}^T \right), \quad i = 1, 2, \dots n. \quad (2.11)$$

Now, one can view the tensors $\mathbf{B}_{\kappa_{p_i}(t)}$ as containing information about the deformations of the amorphous, crystalline phases as well as the specific internal structural changes that take place as the material is unloaded. Also, as the recent studies of Masson *et al.* [34, 35] have suggested asphalt could have a microstructure similar to liquid crystals, one could also model asphalt as an anisotropic fluid. In that case, how the stored energy depend on the tensor $\mathbf{B}_{\kappa_{p_i}(t)}$, contains information about the anisotropy of asphalt, of course in a macroscopic sense. Now it can be shown that (see [50] for details),

$$\overset{\nabla}{\mathbf{B}}_{\kappa_{p_i}(t)} \equiv \overset{\cdot}{\mathbf{B}}_{\kappa_{p_i}(t)} - \mathbf{L}\mathbf{B}_{\kappa_{p_i}(t)} - \mathbf{B}_{\kappa_{p_i}(t)}\mathbf{L}^T = -2\mathbf{F}_{\kappa_{p_i}(t)}\mathbf{D}_{\kappa_{p_i}(t)}\mathbf{F}_{\kappa_{p_i}(t)}^T, \quad i = 1, 2, \dots, n, \quad (2.12)$$

where the inverted triangle is the ‘upper convected’ Oldroyd derivative and the superposed dot signifies the material time derivative. Since we have assumed asphalt to be incompressible, the motions associated with the natural configurations are isochoric and hence

$$\text{tr}\left(\mathbf{D}_{\kappa_{p_i}(t)}\right) = 0, \quad i = 1, 2, \dots, n. \quad (2.13)$$

We assume the following form for the Helmholtz potential,

$$\psi = \psi(\mathbf{I}_i, \mathbf{II}_i), \quad i = 1, 2, \dots, n, \quad (2.14)$$

where

$$\mathbf{I}_i = \text{tr}\left(\mathbf{B}_{\kappa_{p_i}(t)}\right), \quad \mathbf{II}_i = \text{tr}\left(\mathbf{B}_{\kappa_{p_i}(t)}^2\right), \quad i = 1, 2, \dots, n. \quad (2.15)$$

Since the material is assumed to be isotropic, the configurations $\kappa_{p_i}(t)$ can be chosen such that

$$\mathbf{F}_{\kappa_{p_i}(t)} = \mathbf{V}_{\kappa_{p_i}(t)}, \quad i = 1, 2, \dots, n, \quad (2.16)$$

where $\mathbf{V}_{\kappa_{p_i}(t)}$, $i = 1, 2$ are the right stretch tensors in the polar decomposition. We also assume the following form for the rate of dissipation

$$\xi = \xi(\mathbf{B}_{\kappa_{p_i}(t)}, \mathbf{D}_{\kappa_{p_i}(t)}), \quad i = 1, 2, \dots, n. \quad (2.17)$$

Also, we can assume that for motions where the natural configurations do not change, the rate of dissipation is zero and hence,

$$\xi = \xi(\mathbf{B}_{\kappa_{p_i}(t)}, \mathbf{0}) = 0, \quad i = 1, 2, \dots, n. \quad (2.18)$$

Following the procedure setout in Rajagopal and Srinivasa [50], we arrive at the following representation for stress,

$$\mathbf{T} = -p\mathbf{1} + \sum_{i=1}^n \left(\mu_i \mathbf{B}_{\kappa_{p_i}(t)} + \bar{\eta}_i \mathbf{D} \right), \quad (2.19)$$

and the following evolution equation for $\mathbf{B}_{\kappa_{p_i}(t)}$,

$$\frac{1}{2} \overset{\nabla}{\mathbf{B}}_{\kappa_{p_i}(t)} = \frac{\mu_i}{\eta_i} \left[\frac{3}{\text{tr}\left(\mathbf{B}_{\kappa_{p_i}(t)}^{-1}\right)} \mathbf{1} - \mathbf{B}_{\kappa_{p_i}(t)} \right], \quad i = 1, 2, \dots, n. \quad (2.20)$$

This completes the development of the model for asphalt. In the remaining part, we use this model and examine the efficacy of its predictions vis-à-vis some of the experimental results available in the literature.

4. Applications

In this section, we investigate the application of this model. A constant extension rate test is simulated using this model and the results are compared with the experimental data. Assuming the deformation to be homogeneous, the kinematics of deformation in cylindrical polar coordinate system is given by

$$\mathbf{r} = \frac{1}{\sqrt{\Lambda(t)}}\mathbf{R}, \quad \theta = \frac{1}{\sqrt{\Lambda(t)}}\Theta, \quad z = \Lambda(t)Z. \quad (2.21)$$

Here a point in the reference configuration is denoted by (\mathbf{R}, Θ, Z) and the same point in the current configuration is denoted by (\mathbf{r}, θ, z) and $\Lambda(t)$ denotes the stretch along the Z direction. The deformation gradient for this motion is given by

$$\mathbf{F}_{\kappa_{\mathbf{R}}} = \text{diag} \left(\frac{1}{\sqrt{\Lambda(t)}}, \frac{1}{\sqrt{\Lambda(t)}}, \Lambda(t) \right), \quad (2.22)$$

and thus

$$\mathbf{B}_{\kappa_{\mathbf{R}}} = \text{diag} \left(\frac{1}{\Lambda(t)}, \frac{1}{\Lambda(t)}, \Lambda^2(t) \right). \quad (2.23)$$

The components of $\mathbf{B}_{\kappa_{\mathbf{p}(t)}}$ are assumed to be $\text{diag} \left(\frac{1}{B(t)}, \frac{1}{B(t)}, B^2(t) \right)$. This assumption is consistent with the stipulation that the stress-free state for the material is achieved via a motion of the form given by equation (2.21).

For the current problem, we assume that asphalt has a single relaxation time. This essentially means that there is a single natural configuration associated with asphalt. The constitutive model detailed in the earlier section is very general in nature and takes into account the different relaxation mechanisms possible for asphalt. However, since the details related to the volume/mass fractions of amorphous and crystalline phases as well as the specific influence of the internal structure change such as steric hardening on the mechanical behavior of asphalt are not available with regard to the experimental studies that we shall use for correlation, it is proposed to solve the problem related to the above two deformation with a single relaxation time. For the case with single relaxation time, the constitutive equation is given by

$$\mathbf{T} = -p\mathbf{1} + \mu\mathbf{B}_{\kappa_{\mathbf{p}(t)}} + \bar{\eta}\mathbf{D}, \quad (2.24)$$

and the evolution equation for the natural configuration is given by

$$\frac{1}{2}\nabla \mathbf{B}_{\kappa_{\mathbf{p}(t)}} = \frac{\mu}{\eta} \left[\frac{3}{\text{tr}(\mathbf{B}_{\kappa_{\mathbf{p}(t)}}^{-1})} \mathbf{1} - \mathbf{B}_{\kappa_{\mathbf{p}(t)}} \right]. \quad (2.25)$$

For the problem under consideration, the stresses in the lateral directions are zero and hence the stress in the z direction is given as follows,

$$T_{zz} = \mu(B_{zz} - B_{rr}) + \bar{\eta}(D_{zz} - D_{rr}). \quad (2.26)$$

The evolution equation for the natural configuration in the z direction is given by

$$\frac{\partial B_{zz}}{\partial t} + v_z \frac{\partial B_{zz}}{\partial z} = \frac{2\mu}{\eta} \left[\frac{2B_{zz}(B_{rr} - B_{zz})}{2B_{zz} + B_{rr}} \right] + 2L_{zz}B_{zz}. \quad (2.27)$$

In the constant extension rate experiments, normally a ‘dumb-bell’ shaped specimen is mounted between the cross-heads and the cross-heads are then pulled at a constant speed. In such a case, the stretch is given as follows,

$$\Lambda(t) = 1 + Kt, \quad (2.28)$$

where K is a constant. The velocity gradient for this motion is given by,

$$\mathbf{L} = \text{diag} \left[\frac{-1}{2} \frac{K}{1+Kt}, \frac{-1}{2} \frac{K}{1+Kt}, \frac{K}{1+Kt} \right]. \quad (2.29)$$

The velocity gradient \mathbf{L} is diagonal and hence \mathbf{D} the symmetric part of the velocity gradient is the same as \mathbf{L} . Also, we assume the following form for the viscosities,

$$\eta = \eta_0 \left[N \left(\text{tr} \mathbf{B}_{\kappa_p(t)} - 3 \right)^m + 1 \right] \exp(\beta), \quad (2.30)$$

$$\bar{\eta} = \bar{\eta}_0. \quad (2.31)$$

The initial condition for this motion is given as follows,

$$\mathbf{B}_{\kappa_p(t)} = \mathbf{1}, \quad \text{for } t = 0. \quad (2.32)$$

With this initial condition, equation (2.27) is solved ignoring inertial terms and the stress in the asphalt specimen is given by (2.26). Experimental studies on bitumen conducted by Cheung and Cebon [8] are compared with the model predictions in Figure 2 and it is seen that the model predicts the experimental observations reasonably well.

5. Conclusions

In this paper, we have developed a framework for the constitutive modeling of straight run asphalt. The developed constitutive model is based on the framework of evolving natural configurations. By choosing specific forms for the Helmholtz potential, rate of dissipation and using the reduced energy-dissipation equation and maximization of the rate of dissipation, we have obtained constitutive relations for the stress and the evolution equations for the underlying natural configurations. We have assumed asphalt to have multiple relaxation mechanisms and modeled each of these relaxation mechanisms by a rate type viscoelastic fluid model. We illustrated the efficacy of the model by comparing its predictions with experimental observations.

Acknowledgment: I thank the Mathematical Institute of Charles University, Prague for giving me an opportunity to present this work and I thank National Science Foundation, USA for its support of this work.

2. THE MECHANICAL BEHAVIOR OF ASPHALT

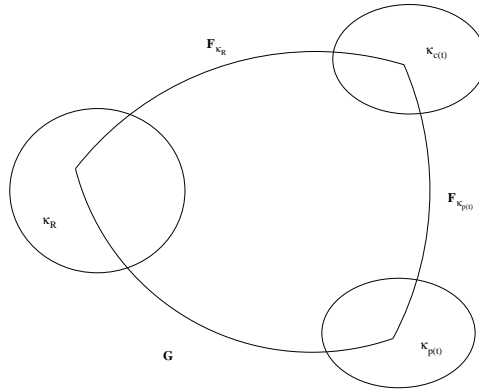


FIGURE 1. Natural configurations associated with asphalt

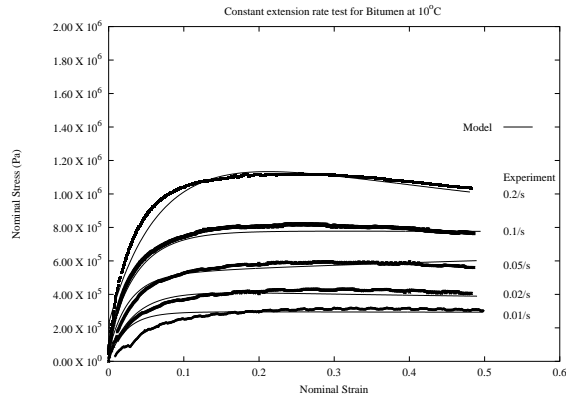


FIGURE 2. Comparison of the constant extension rate tests at 10°C of bitumen B1 reported in Cheung and Cebon [8] with model predictions. The model parameters used are $\mu = 5\text{MPa}$, $\eta_0 = 6.2\text{MPa s}$, $\bar{\eta}_0 = 0.75\text{MPa s}$, $N = 0.75$, $m = 0.5$, $\beta = 0.55$.

Bibliography

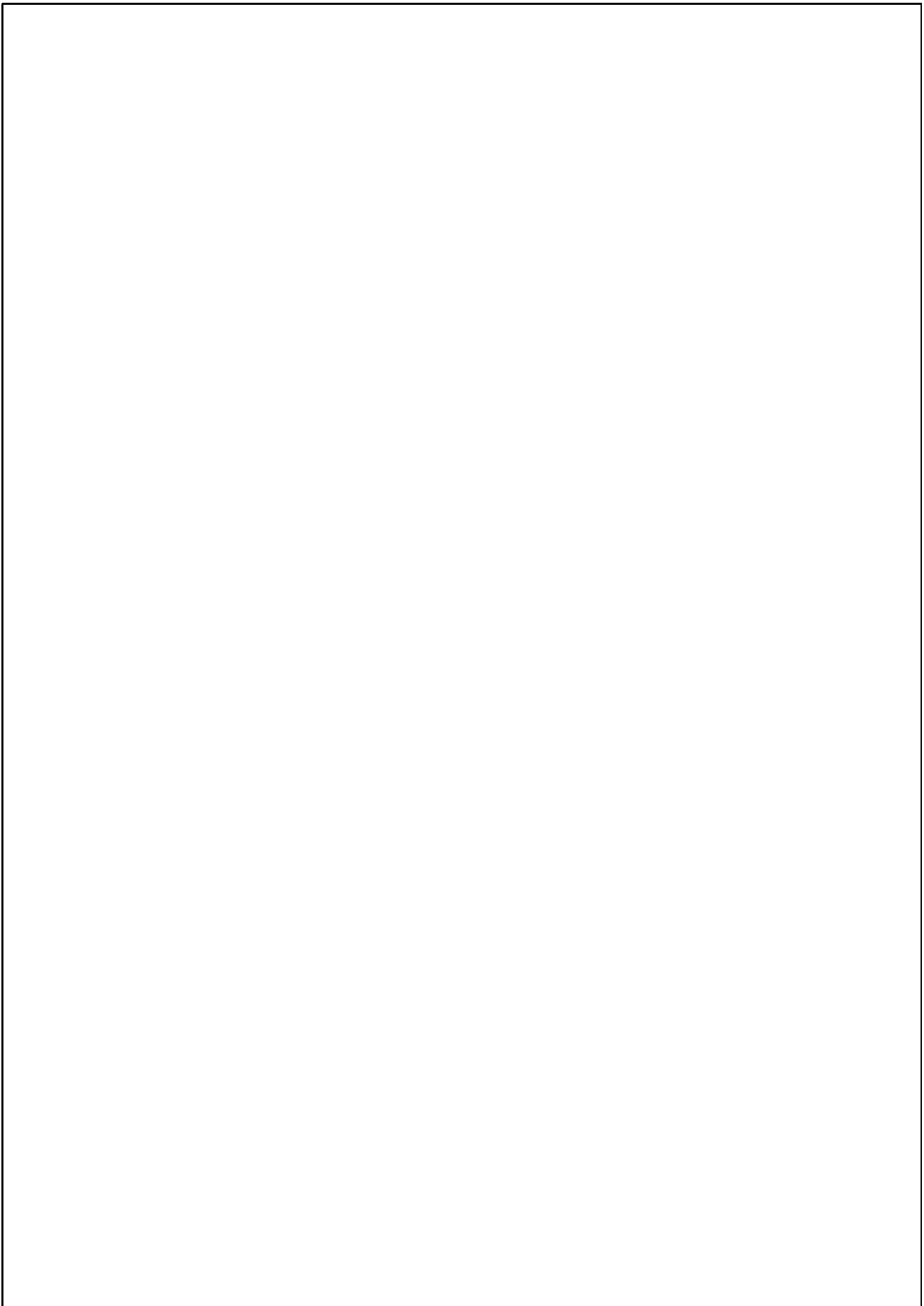
- [1] M. Albert, F. Bosselet, P. Claudy, J. M. Letoffe, E. Lopez, B. Damin, and B. Neff. Comportement Thermique Des Bitumes Routiers. Determination Du Taux De Fractions Cristallisees Par Analyse Calorimetrique Differentielle. *Thermochimica Acta*, 84:101–110, 1985.
- [2] H. U. Bahia and D. A. Anderson. Physical hardening of paving grade asphalts as related to compositional characteristics. *Preprints, Division of Fuel Chemistry, American Chemical Society*, 37(3):1397–1407, August 1992.
- [3] M. Boussingault. Memoire sur la composition des bitumes. *Annales de Chimie et de Physique*, LXIV:141–151, 1837.
- [4] J. G. Brodnyan, F. H. Gaskins, W. Philippoff, and E. Thelen. The Rheology of Asphalt III, Dynamic Mechanical Properties of Asphalt. *Transactions of the Society of Rheology*, IV:279–296, 1960.
- [5] A. B. Brown, J. W. Sparks, and F. M. Smith. Steric Hardening of Asphalts. *Proceedings of the Association of Asphalt Paving Technologists*, 26:486–494, 1957.
- [6] J. M. Burgers. Mechanical considerations - model systems - phenomenological theories of relaxation and of viscosity. In *First report on viscosity and plasticity*. Nordemann Publishing Company, Inc., New York, 2nd edition, 1939. Prepared by the committee for the study of viscosity of the academy of sciences at Amsterdam.
- [7] P. Chambrion, R. Bertau, and P. Ehrburger. Characterization of bitumen by differential scanning calorimetry. *Fuel*, 75(2):144–148, 1996.
- [8] C. Y. Cheung and D. Cebon. Experimental study of pure bitumens in tension, compression, and shear. *Journal of Rheology*, 41(1):45–73, January/February 1997.
- [9] P. Claudy, J. M. Létoffé, G. N. King, and J. P. Planche. Characterization of Asphalts Cements by Thermomicroscopy and Differential Scanning Calorimetry: Correlation to Classic Physical Properties. *Fuel Science and Technology International*, 10(4-6):735–765, 1992.
- [10] P. Claudy, J. M. Letoffe, F. Rondelez, L. Germanaud, G. King, and J. P. Planche. A new interpretation of time-dependent physical hardening in asphalts based on dsc and optical thermoanalysis. *Preprints, Division of Fuel Chemistry, American Chemical Society*, 37(3):1408–1426, August 1992.
- [11] L. W. Corbett. Composition of Asphalt based on Generic Fractionation, using solvent Deasphaltening, Elution-Adsorption Chromotography, and densimetric Characterization. *Analytical Chemistry*, 41:576–579, 1969.

- [12] W. H. Daly, Z. Qiu, and I. Negulescu. Differential Scanning Calorimetry Study of Asphalt Crystallinity. *Transportation Research Record*, 1535:54–60, 1996.
- [13] J. P. Dickie and T. F. Yen. Macrostructure of Asphaltic Fraction by Various Instrumental Methods. *Analytical Chemistry*, 39(14):1847–1852, December 1967.
- [14] E. J. Dickinson and H. P. Witt. The Dynamic Shear Modulus of Paving Asphalts as a Function of Frequency. *Transactions of the Society of Rheology*, 18(4):591–606, 1974.
- [15] G. R. Dobson. The Dynamic Mechanical Properties of Bitumen. *Proceedings of the Association of Asphalt Paving Technologists*, 38:123–139, 1969.
- [16] Y. Edwards and P. Redelius. Rheological Effects of Waxes in Bitumen. *Energy & Fuels*, 17(3):511–520, 2003.
- [17] H. Frohlich and R. Sack. Theory of the Rheological Properties of Dispersions. *Proceedings of the Royal Society of London, Series A, Mathematical and Physical Sciences*, 185:415–430, April 1946.
- [18] F. H. Gaskins, J. G. Brodnyan, W. Philippoff, and E. Thelen. The Rheology of Asphalt II, Flow Characteristics of Asphalt. *Transactions of the Society of Rheology*, IV:265–278, 1960.
- [19] C. Giavarini and F. Pochetti. Characterization of Petroleum Products by DSC Analysis. *Journal of Thermal Analysis*, 5:83–94, 1973.
- [20] J. L. Goodrich, J. E. Goodrich, and W. J. Kari. Asphalt Composition Tests: Their Application and Relation to Field Performance. *Transportation Research Record*, 1096:146–167, 1986.
- [21] A. E. Green and P. M. Naghdi. On thermodynamics and the nature of the second law. *Proceedings of the Royal Society of London*, A357:253–270, 1977.
- [22] J. E. Hilliard. Spinodal decomposition. In *Phase Transformations*, pages 497–560. American Society for Metals, Metals Park, Ohio, U. S. A., 1970. Papers Presented at a Seminar of the American Society of Metals, October, 1968.
- [23] S-C. Huang, R. E. Robertson, J. F. Branthaver, and J. F. McKay. Study of Steric Hardening Effect of Thin Asphalt Films in Presence of Aggregate Surface. *Transportation Research Record*, 1661:15–21, 1999.
- [24] P. Hubbard and F. P. Pritchard. Effect of Controllable Variables upon the Penetration Test for Asphalts and Asphalts Cements. *Journal of Agricultural Research*, V(17):805–818, January 1916.
- [25] P. Hubbard and C. S. Reeve. The Effect of Exposure on Bitumens. *Industrial and Engineering Chemistry*, 5(1):15–18, 1913.
- [26] J. D. Humphrey and K. R. Rajagopal. A constrained mixture model for growth and remodeling of soft tissues. *Mathematical Models and Methods in Applied Sciences*, 12:1–24, 2002.
- [27] J. M. Hutchinson. Physical Aging of Polymers. *Progress in Polymer Science*, 20:703–760, 1995.
- [28] Asphalt Institute. *Performance Graded Asphalt Binder Specification and Testing*, 1994. Superpave Series No. 1 (SP-1).
- [29] R. Jongepier and B. Kuilman. Characteristics of the Rheology of Bitumens. *Proceedings of the Association of Asphalt Paving Technologists*, 38:98–122, 1969.

- [30] D. Lesueur, J-F. Gerard, P. Claudy, J-M. Letoffe, J-P. Planche, and D. Martin. A structure-related model to describe asphalt linear viscoelasticity. *Journal of Rheology*, 40(5):813–836, September/October 1996.
- [31] W. Lethersich. The Mechanical Behavior of Bitumen. *Journal of the Society of Chemical Industry*, 61:101–108, 1942.
- [32] X. Lu and U. Isacsson. Laboratory study on the low temperature physical hardening of conventional and polymer modified bitumens. *Construction and Building Materials*, 14:79–88, 2000.
- [33] K. Majidzadeh and H. E. Schweyer. Non-Newtonian Behavior of Asphalt Cements. *Proceedings of the Association of Asphalt Paving Technologists*, 34:20–44, 1965.
- [34] J-F. Masson, Polomark G. M., and P. Collins. Time-Dependent Microstructure of Bitumen and Its Fraction by Modulated Differential Scanning Calorimetry. *Energy & Fuels*, 16:470–476, 2002.
- [35] J-F. Masson and G. M. Polomark. Bitumen microstructure by modulated differential scanning calorimetry. *Thermochimica Acta*, 374:105–114, 2001.
- [36] A. K. Mehrotra and W. Y. Svrcek. Viscosity of Compressed Cold Lake Bitumen. *The Canadian Journal of Chemical Engineering*, 65:672–675, August 1987.
- [37] L. C. Michon, D. A. Netzel, T. F. Turner, D. Martin, and J-P. Planche. A ^{13}C NMR and DSC Study of the Amorphous and Crystalline Phases in Asphalt. *Energy & Fuels*, 13(3):602–610, 1999.
- [38] J. Murali Krishnan and K. R. Rajagopal. Review of the uses and modeling of bitumen from ancient to modern times. *Applied Mechanics Review*, 56(2):149–214, 2003.
- [39] J. Murali Krishnan and K. R. Rajagopal. A thermodynamic framework for constitutive modeling of asphalt concrete - theory and applications. *ASCE Journal of Materials in Civil Engineering*, 16(2):155–166, April 2004.
- [40] J. Murali Krishnan and K. R. Rajagopal. Triaxial testing and stress relaxation of asphalt concrete. *Mechanics of Materials*, 36(9):849–864, 2004.
- [41] F. J. Nellensteyn. The Constitution of Asphalt. *The Journal of the Institution of Petroleum Technologists*, 10:311–325, 1924.
- [42] D. A. Netzel. Low Temperature Studies of Amorphous, Interfacial, and Crystalline Phases in Asphalts using Solid-State ^{13}C Nuclear Magnetic Resonance. *Transportation Research Record*, 1638:23–30, 1998.
- [43] F. Noel and L. W. Corbett. A Study of the Crystalline Phases in Asphalt. *Journal of the Institute of Petroleum*, 56(551):261–268, September 1970.
- [44] W. W. Pendleton. The penetrometer method for determining the flow properties of high viscosity fluids. *Journal of Applied Physics*, 14:170–180, April 1943.
- [45] J. C. Petersen, R. E. Robertson, P. M. Branthaver, J. F. Harnsberger, J. J. Duvall, S. S. Kim, D. A. Anderson, D. W. Christiansen, and H. U. Bahia. Binder characterization and evaluation: Volume 1. Report SHRP-A-367, Strategic Highway Research Program, Washington, D. C., U. S. A, 1994.
- [46] J. Ph. Pfeiffer and R. N. J. Saal. Asphaltic Bitumen as Colloid System. *The Journal of Physical Chemistry*, 44(2):139–149, February 1940.

- [47] K. R. Rajagopal and A. R. Srinivasa. Mechanics of the inelastic behavior of materials -Part II:inelastic response. *International Journal of Plasticity*, 14:969–995, 1998.
- [48] K. R. Rajagopal and A. R. Srinivasa. Mechanics of the inelastic behavior of materials-Part I, theoretical underpinnings. *International Journal of Plasticity*, 14:945–967, 1998.
- [49] K. R. Rajagopal and A. R. Srinivasa. On the thermodynamics of shape memory wires. *ZAMP*, 50:459–496, 1999.
- [50] K. R. Rajagopal and A. R. Srinivasa. A thermodynamic framework for rate type fluid models. *Journal of Non-Newtonian Fluid Mechanics*, 88:207–227, 2000.
- [51] K. R. Rajagopal and A. R. Srinivasa. Modeling anisotropic fluids within the framework of bodies with multiple natural configurations. *Journal of Non-Newtonian Fluid Mechanics*, 88:207–227, 2001.
- [52] K. R. Rajagopal and A. S. Wineman. A constitutive equation for nonlinear solids which undergo deformation induced micro-structural changes. *International Journal of Plasticity*, 8:385–395, 1992.
- [53] I. J. Rao, J. D. Humphrey, and K. R. Rajagopal. Biological growth and remodeling: A uniaxial example with possible application to tendons and ligaments. *Computer Modeling in Engineering & Sciences*, 4:439–456, 2003.
- [54] I. J. Rao and K. R. Rajagopal. Phenomenological modeling of polymer crystallization using the notion of multiple natural configurations. *Interfaces and free boundaries*, 2:73–94, 2000.
- [55] I. J. Rao and K. R. Rajagopal. A study of strain-induced crystallization of polymers. *International Journal of Solids and Structures*, 38:1149–1167, 2001.
- [56] I. J. Rao and K. R. Rajagopal. A thermodynamic framework for the study of crystallization in polymers. *ZAMP*, 53:365–406, 2002.
- [57] F. S. Rostler and R. M. White. Composition and Changes in Composition of Highway Asphalts, 85 - 100 Penetration Grade. *Proceedings of the Association of Asphalt Paving Technologists*, 31:35–89, 1962.
- [58] R. N. J. Saal and J. W. A. Labout. Rheological Properties of Asphaltic Bitumens. *The Journal of Physical Chemistry*, 44(2):149–165, February 1940.
- [59] H. E. Schwyer. Asphalt Rheology in the Near-Transition Temperature Range. *Highway Research Record*, 468:1–15, 1973.
- [60] C. D. Smith, C. C. Schuetz, and R. S. Hodgson. Relationship between Chemical Structures and Weatherability of Coating Asphalts as shown by Infrared Absorption Spectroscopy. *Industrial and Engineering Chemistry Product Research and Development*, 5(2):153–161, June 1966.
- [61] F. Stinsky. Thixotropie des bitumen routiers. In V. Takacs, editor, *Proceedings of the Second International Symposium devoted to Tests on Bitumens and Bituminous Materials*, pages 197–209, Budapest, September 1975. International Union of Testing and Research Laboratories for Materials and Structures, OMKDK-Technoinform.
- [62] D. A. Storm, R. J. Barresi, and E. Y. Sheu. Development of Solid Properties and Thermochemistry of Asphalt Binders in the 25 - 65°C Temperature Range. *Energy & Fuels*, 10:855–864, 1996.

- [63] R. N. Traxler and C. E. Coombs. Development of Internal Structure in Asphalts with Time. *Proceedings of the American Society for Testing and Materials*, 37:549–557, 1937. Part II.
- [64] R. N. Traxler and C. E. Coombs. Structure in Asphalts. Indicated by Solvent-Treated Surfaces. *Industrial and Engineering Chemistry*, 30(4):440–443, 1938.
- [65] R. N. Traxler and H. E. Schweyer. Increase in Viscosity of Asphalts with Time. *Proceedings of the American Society for Testing and Materials*, 36:544–551, 1936. Part II.
- [66] C. Van der Poel. A general system describing the visco-elastic properties of bitumens and its relation to routine test data. *Journal of Applied Chemistry*, 4:221–236, 1954.
- [67] J. S. Youtcheff and D. R. Jones. Guideline for asphalt refiners and suppliers. Report SHRP-A-686, Strategic Highway Research Program, Washington, D. C., U. S. A., 1994.



CHAPTER 3

Internal structure and modeling of asphalt mixtures

E. MASAD

1. Introduction

The internal structure of asphalt mixes refers to the directional and spatial arrangement of the mix constituents (aggregates, asphalt, and air voids) as well as the chemical and physical interactions among these constituents. The arrangement of the aggregate particles in terms of spatial distribution, directional distribution, contact points, and packing is referred to as the aggregate skeleton. This chapter summarizes the methods used in characterizing and quantifying the internal structure distribution in hot mix asphalt (HMA). The implications of the internal structure analysis on the performance and modeling of HMA are also discussed.

The internal structure distribution is the result of proportions and properties of materials as well as compaction methods used in preparing the mix. This has been long recognized in mix design methodologies through requiring certain aggregate gradations, aggregate shape and mechanical properties, compaction methods and limits, and mix volumetrics.

Recently, there has been emphasis on developing methods to quantitatively assess some aspects of the internal structure distribution (Yue et al. 1995, Masad et al. 1999a, Masad et al. 1999b, Tashman et al. 2001). These methods utilize imaging techniques to quantify the distribution of the aggregate skeleton and air voids by analyzing two-dimensional (2-D) and three-dimensional (3-D) images of the internal structure. The mathematical functions used to describe the internal structure directional and spatial distributions are useful for providing inputs for models that describe mixture performance.

2. Imaging methods for measuring the internal structure distribution

Digital image analysis has been used to quantify the internal structure distribution of HMA. It involves three major steps: image acquisition, image processing, and image analysis as illustrated in Figure 1. 2-D images of the internal structure can be captured using a setup that consists of a microscope and a camera. X-ray computed tomography (CT) has also been used to capture the internal structure of HMA. It is a unique nondestructive tool for obtaining 3-D images of the internal structure based on differences in density between the mix constituents. The X-ray CT system consists of an X-ray source and a detector with a test specimen placed in between. The source transmits X-ray radiation with certain intensity (I_0). Some

the X-rays penetrate through a specimen while other X-rays get absorbed or scattered. The intensities of these transmitted X-rays (I) are recorded with an array of detectors placed at the other side of the specimen. The line between the X-ray source focal spot and a single detector is called a ray, and the integral of this ray is called a ray integral. At each point within a specimen, the amount of radiation energy scattered and absorbed is a function of a constant called the linear attenuation coefficient, which is a property of the material occupying that point. The attenuation coefficient varies as a function of material density which makes it possible to differentiate between the mix constituents. The X-rays can be applied in different geometries as described in ASTM E 1441 procedure.

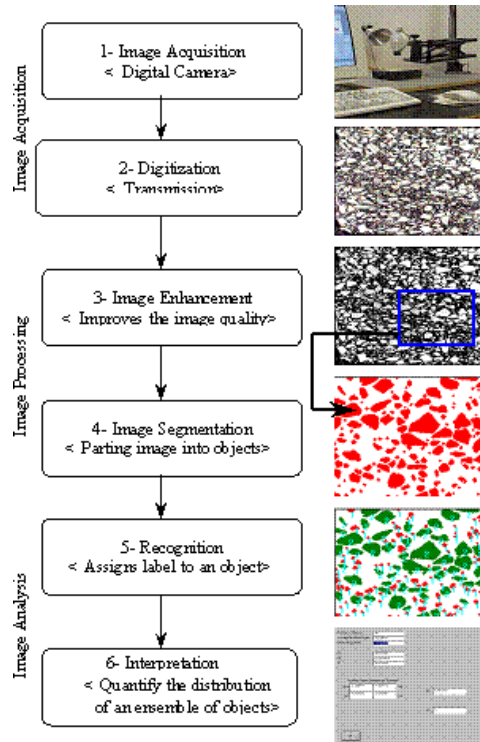


FIGURE 1. The steps involved in the image analysis techniques

3. Applications of image analysis techniques

3.1. Compaction and mechanical properties. Masad et al. (1999a) measured aggregate orientations in specimens compacted to different numbers of gyrations and in field cores. They found that the anisotropy (preferred orientation of particles towards the horizontal direction) in gyratory specimens became more pronounced with an increase in the compaction effort up to a certain point. However, further increase in the compaction effort caused a reduction in the anisotropy level and a tendency for particles to exhibit random orientation.

These findings suggest that the aggregate structure can sustain the applied compaction loads up to a certain level. During this period, the aggregate structure develops a higher level of anisotropy. However, further increase in the compaction effort associated with high shear stresses among particles leads to sliding, rotation, and consequently, random distribution of the aggregate structure.

Air void distribution was studied using X-ray CT images. An example of air void distribution in HMA is shown in Figure 2. X-ray CT images helped to discover the nature of air void distribution in laboratory specimens and field cores. Figure 3 shows the vertical air void distribution in two different laboratory compaction methods (Superpave gyratory compactor (SGC) and linear kneading compactor (LKC) specimens.) Field cores were found to have higher percent air voids towards the pavement surface. Efforts have been initiated recently in order to improve compaction methods such that more uniform distribution of air voids are achieved in laboratory specimens and field cores.

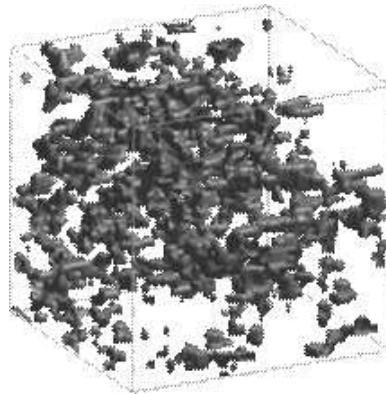


FIGURE 2. An example of three-dimensional distribution of air voids in HMA

The results discussed above have direct implications on the design, compaction, and performance of HMA. It can be used to quantify the differences between the laboratory and field compacted mixes and evaluate the influence of different compaction techniques on reducing these differences. The anisotropy of the aggregate distribution in HMA influences the validity of the response and performance models. Contact analysis can be used to ensure the development of stone-to-stone contact in rut-resistance mixes. The nonuniform air void distribution affects the stress and strain distribution in a test specimen, the size of the representative volume element needed for experimental characterization, and field density measurements to mention a few examples.

3.2. Fluid flow and permeability. Al-Omari et al. (2002) used image analysis techniques to measure percent of connected air voids (n), specific surface area of air voids, and air void tortuosity and related these properties through the Kozeny-Carman (K-C) equation to measured permeability. Comparison between the permeability calculated using the K-C equation and laboratory measurements is shown

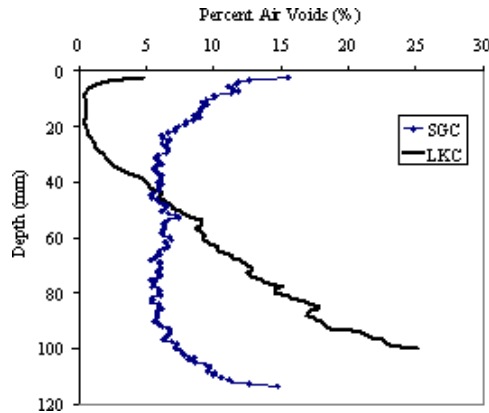


FIGURE 3. Void distribution in SGC and LKC specimens (after Masad et al. 1999b)

in Figure 4. Masad et al. (2006a) and Kutay et al. (2006) developed numerical models for the simulation of fluid flow in three dimensional images of HMA. Figures 5 and 6 show simulations of fluid flow in HMA specimens. These models also provide the HMA permeability in different directions. The permeability values computed using the models were found to correlate well with experimental measurements (Figure 7). The major and minor principal directions of the permeability tensor were found to correspond to the horizontal and vertical directions, respectively. The results indicated that the non-uniform spatial distribution of air voids created more open flow paths in the horizontal direction than the vertical direction, and hence was the much higher permeability in the horizontal direction.

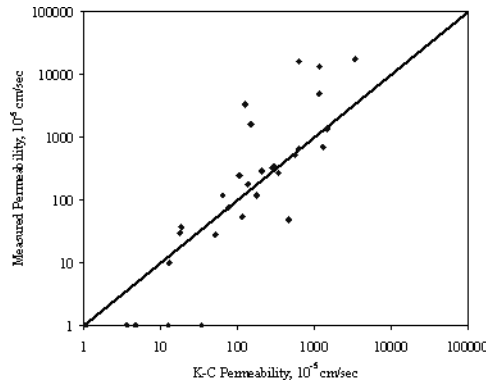


FIGURE 4. Comparison between the predicted and measured permeability values for field cores (after Al-Omari et al. 2002)

Masad et al. (2006b) analyzed the air void distribution in different HMA specimens and related the distribution to the resistance to moisture damage. The results showed that there are “pessimum” air void size and permeability values at which the mix has the least resistance to moisture damage. Researchers suggested

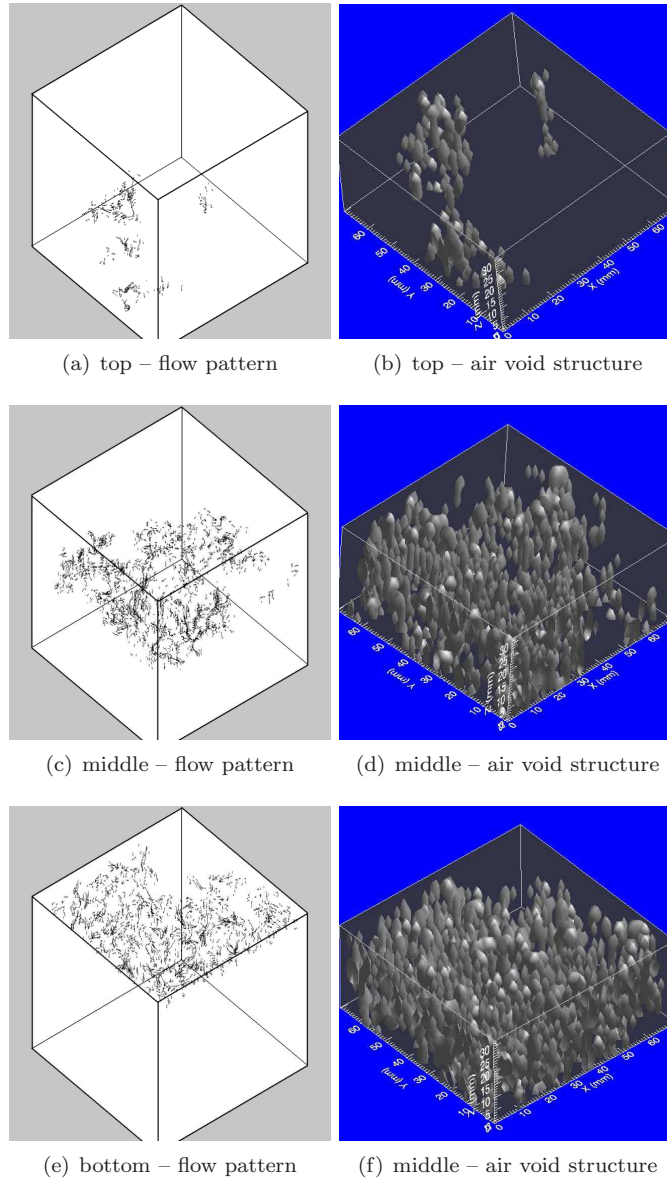


FIGURE 5. Flow patterns (left) and the corresponding air void structures (right) for the top, middle, and bottom parts of LKC specimen (after Masad et al. 2006a)

that small air void sizes associated with low permeability reduce infiltration of water within the mix, while large air voids make it easier for the water to drain out of the mix. Hence, acceptable resistance to moisture damage occurs at these two levels of air void sizes. At the “pessimum” air void size, water permeates the mix and

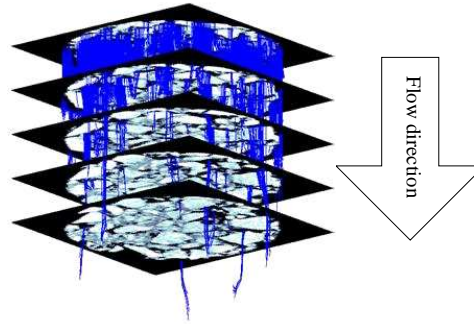


FIGURE 6. Simulation of fluid flow in three-dimensional image of an asphalt mix (after Kutay et al. 2006)

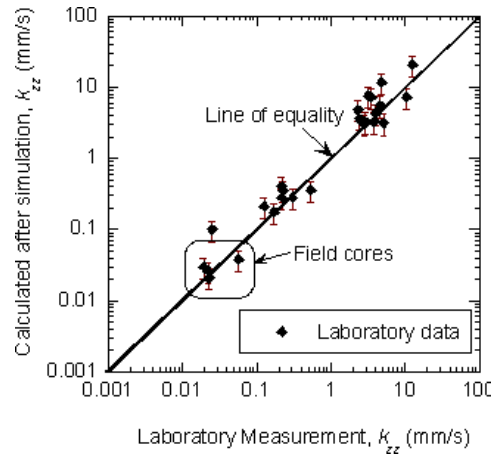


FIGURE 7. A comparison between calculated permeability and laboratory measurements (after Kutay et al 2006)

it is difficult for water to drain out of the mix, leading to more moisture damage. This concept can be used to design mixes outside the “pessimum” range in order to improve the resistance to moisture damage.

3.3. Modeling. A critical factor that determines the validity of mixture performance models is the realistic representation of the internal structure distribution. Image analysis techniques have been used for this purpose in both micromechanical finite element and discrete element simulations. Figure 8 shows an example of an image of the internal structure in which the asphalt and aggregate phases are identified. In a finite element model, material properties are assigned to each of these phases. In a discrete element model, properties are assigned for the different contact types (aggregate-aggregate, asphalt-asphalt, and aggregate-asphalt) that are present in the model as shown in Figure 9. Image analysis techniques coupled with micromechanical models have been used to study strain distribution in the mix

and its influence on the nonlinear response (Kose et al. 2000, Papagiannakis et al. 2002, Abbas et al. 2004), analyze micro fracture (Guddati et al. 2002, Sadd et al. 2003, Buttlar and You 2001, Kim et al. 2005), analyze stress localization in the mix and its influence on performance (Wang et al. 2001, Wang et al. 2003), and study the deformational behavior of asphalt mixtures under conditions simulating those used in different testing methods in the laboratory (Abbas et al. 2006, You and Buttlar 2006). Image analysis techniques have also been used to obtain properties of the internal structure distribution for continuum models. Tashman et al. (2005) developed a continuum performance model for HMA, which includes parameters describing the directional distribution of aggregate particles, air void distribution and damage. The results showed that better predictions of performance are achieved by including internal structure parameters in these models.

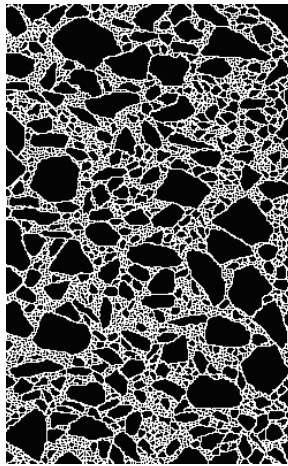


FIGURE 8. An image of HMA internal structure digitized to aggregate and asphalt phases

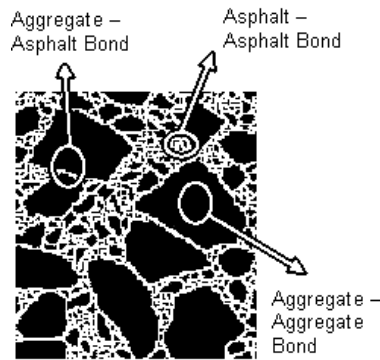


FIGURE 9. Types of bonds in DEM

There is a pressing need to develop a comprehensive approach for mathematical modeling of asphalt mixtures. This approach needs to consider the nonlinear response of the mixture and should be able to predict mixture failure mechanisms such as fatigue cracking, low temperature cracking and permanent deformation. This modeling approach needs to consider the influence of environmental conditions such as temperature and moisture on material properties and mixture behavior. In addition, mathematical models are needed to accurately describe the compaction process of asphalt mixtures. It is well established that the quality of compaction is a very important factor that influences asphalt pavement performance.

Krishnan and Rajagopal (2004) presented a thermodynamic framework for constitutive modeling of asphalt mixtures. This approach has been extended recently to model the process of asphalt mixture compaction in the laboratory (Koneru et al. 2007). The readers are referred to the comprehensive review by Krishnan and Rajagopal (2003) for the different uses, applications and modeling approaches of asphalt mixtures.

4. Summary

The internal structure distribution has long been recognized as a critical factor influencing the performance of HMA. This has been reflected in design methodologies through specifying requirements on the volumetrics of asphalt mixes. Recently, there has been emphasis on the development of methods to quantify the internal structure distribution.

Developments of computer technology, image analysis techniques, and non-destructive imaging have lead to the developments of methods that can directly quantify the internal structure distribution. These methods have been applied recently in studying the differences among different laboratory compaction methods, improving the simulation of laboratory compaction to field compaction, and predicting the permeability of HMA mixtures.

These advances in imaging techniques for measuring the internal structure are expected to provide very useful information about the internal structure distribution. This information can be useful for determination of parameters for mathematical models and verify the model predictions based on measurements conducted at the microstructure level.

Bibliography

Abbas, A., Papagiannakis, T., and Masad, E. (2004). “Linear and Non-Linear Viscoelastic Analysis of the Microstructure of Asphalt Concretes,” *Journal of Materials in Civil Engineering*, ASCE, Vol. 16, No. 2, pp. 133-139

Abbas, A., Masad, E., Papagiannakis, T., and Harman, T. (2006). “Micromechanical Modeling of the Viscoelastic Behavior of Asphalt Mixtures Using the Discrete Element Method,” *International Journal of Geomechanics*, ASCE (Accepted for Publication).

Al-Omari, A., Tashman, L., Masad, E., Cooley, A., and Harman, T. (2002). “Proposed Methodology for Predicting HMA Permeability,” *Journal of the Association of Asphalt Paving Technologists*, Vol. 71, pp. 30-58

Brown, E. R., and Mallick, R. B. (1994). *Stone Matrix Asphalt-Properties Related to Mixture Design*, NCAT Report No. 94-2, Auburn, Alabama.

Buttlar, W.G., and You, Z. (2001). “Discrete Element Modeling of Asphalt Concrete: A Micro-Fabric Approach,” *Transportation Research Record 1757*, *Journal of the Transportation Research Board*, National Research Council, Washington, D.C., pp. 111-118.

Dessouky, S., Masad, E., Bayomy, F. (2003). “Evaluation Of Asphalt Mix Stability Using Compaction Properties and Aggregate Structure Analysis,” *International Journal of Pavement Engineering*, (In Press).

Guddati, M. N., Feng, Z., and Kim, R. (2002). “Toward a micromechanics-based procedure to characterize fatigue performance of asphalt concrete.” *Transportation Research Record 1789*, TRB, National Research Council, Washington, D.C., 121-128.

Kim, Y. R., Allen, D., and Little, D. N. (2005). “Damage-Induced Modeling of Asphalt Mixtures through Computational Micromechanics and Cohesive Zone Fracture,” *Journal of Materials in Civil Engineering*, Vol. 17, No. 5, pp. 477-484.

Kose, S., Guler, M., Bahia, H., and Masad, E. (2000). “Distribution of Strains within Hot-Mix Asphalt Binders,” *In Transportation Research Record*, *Journal of the Transportation Research Board 1728*, pp. 21-27.

Koneru, S., Masad, E., and Rajagopal, K. (2007). “Modeling of Asphalt Mix Compaction Using a Thermodynamic Material Model,” *International Journal of Mechanics of Materials*, (In Review).

Krishnan, J. M., and Rajagopal, K. R. (2003). “A Review of the Uses and Modeling of Bitumen from Ancient to Modern Times,” *Applied Mechanics Review*, Vol. 56, No. 2, pp. 149-214.

Krishnan, J. M., and Rajagopal, K. R. (2004). “A Thermodynamic Framework for the Constitutive Modeling of Asphalt Concrete – Theory and Applications,” *Journal of Materials in Civil Engineering*, ASCE, Vol. 16, No. 2, pp. 155-166.

Kutay, E. M., Aydilek, M., Masad, E., and Harman, T. (2006). “Evaluation of Hydraulic Conductivity Anisotropy in Asphalt Specimens,” *International Journal of Pavement Engineering*.

Masad, E., Muhunthan, B., Shashidhar, N., and Harman T. (1999a). “Internal Structure Characterization of Asphalt Concrete Using Image Analysis,” *Journal of Computing in Civil Engineering (Special Issue on Image Processing)*, ASCE, Vol. 13, No. 2, pp. 88-95.

Masad, E. A., Muhunthan, B., Shashidhar, N., and Harman, T. (1999b). “Quantifying Laboratory Compaction Effects on the Internal Structure of Asphalt Concrete,” In *Transportation Research Record, Journal of the Transportation Research Board* 1681, pp. 179-184.

Masad, E., Al-Omari A., and Chen, H. C. (2006a). “Computations of Permeability Tensor Coefficients and Anisotropy of Hot Mix Asphalt Based on Microstructure Simulation of Fluid Flow,” *Journal of Engineering Mechanics*, ASCE.

Masad, E., Castelblanco, A., and Birgisson, B. (2006b). “HMA Moisture Damage as a Function of Air Void Size Distribution, Pore Pressure and Bond Energy,” *Journal of Testing and Evaluation*, American Society for Testing and Materials, Vol. 34, No. 1, pp. 15-23.

Papagiannakis, T, Abbas, A., and Masad, E. (2002). “Micromechanical Analysis of the Viscoelastic Properties of Asphalt Concretes,” In *Transportation Research Record, Journal of the Transportation Research Board* 1789, pp. 113-120.

Saaddeh, S., Tashman, L., Masad, E., and Mogawer, W. (2002). “Spatial and Directional Distributions of Aggregates in Asphalt Mixes,” *Journal of Testing and Evaluation*, American Society for Testing and Materials, ASTM, Vol. 30, No. 6, pp. 483-491.

Sadd, M.H., Dai, Q., Parameswaran, V., and Shukla, A. (2003). “Simulation of asphalt materials using finite element micromechanical model with damage mechanics.” *Transportation Research Record*, 1832, *Journal of the Transportation Research Board*, National Research Council, Washington, D.C., 86-95.

Tashman, L., Masad, E., Peterson, B., and Saleh, H. (2001). “Internal Structure Analysis of Asphalt Mixes to Improve the Simulation of Superpave Gyrotory Compaction to Field Conditions,” *Journal of the Association of Asphalt Paving Technologists*, Vol. 70, pp. 605-645.

Tashman, L., Masad, E., Zbib, H., Little, D., Kaloush, K. (2005). “Microstructural Viscoplastic Continuum Model for Asphalt Concrete,” *Journal of Engineering Mechanics*, American Society of Civil Engineers, Vol. 131, No. 1, pp. 48

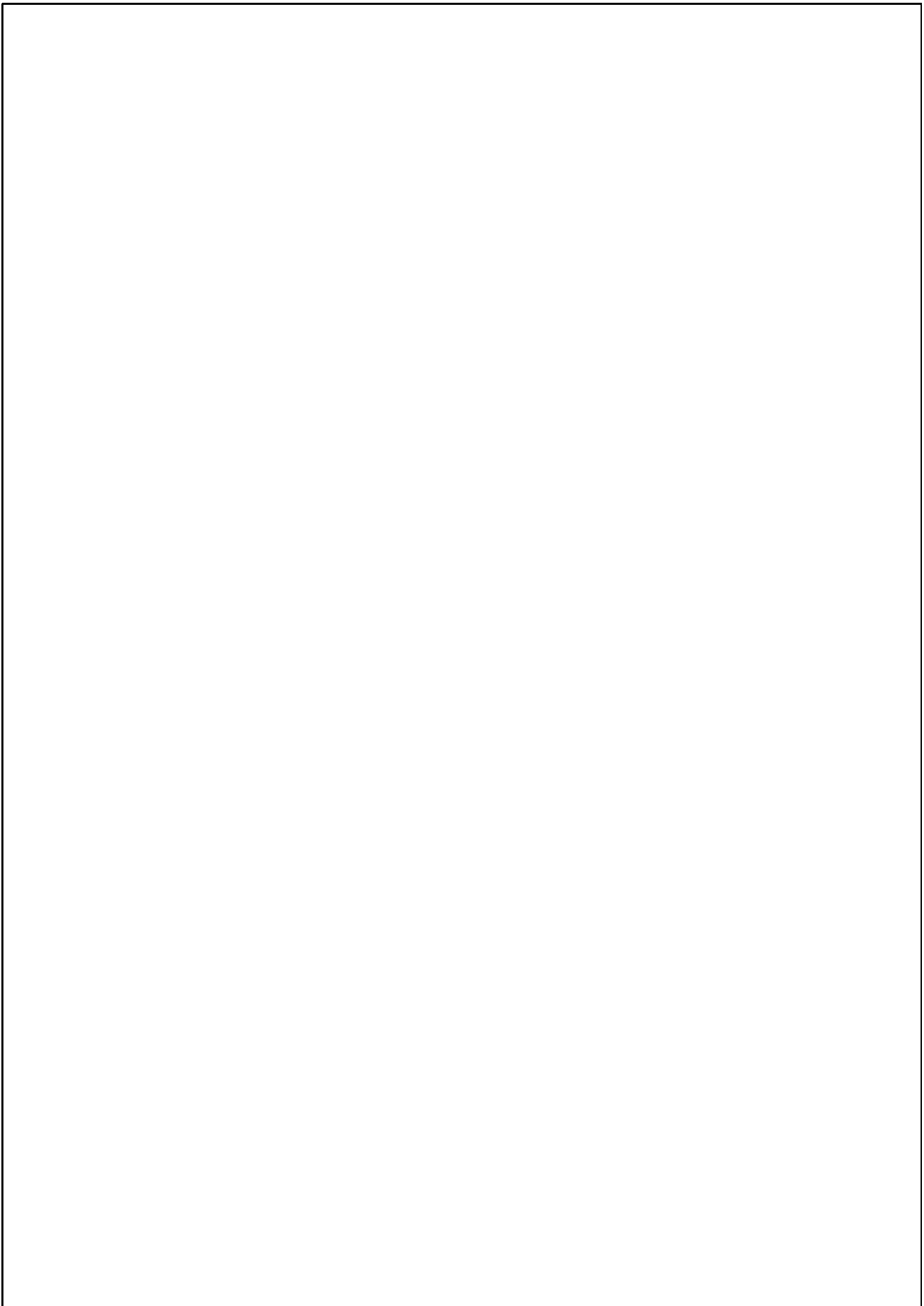
Wang, L., Frost, D., and Shashidhar, N. (2001). “Microstructure Study of West-track Mixes From X-Ray Tomography Images,” *Transportation Research Record* 1767, *Journal of the Transportation Research Board*, National Research Council, Washington, D.C., pp. 85-94.

Wang, L. B., Myers, L. A., Mohammad, L. N., and Fu, Y. R. (2003). “A Micromechanics Study on Top-Down Cracking,” In *Transportation Research Record* 1853, *Journal of the Transportation Research Board*, National Research Council, Washington, D.C., pp. 121-133.

Watson, D., Masad, E., Moore, K. A., Williams, K., and Cooley L. A. (2004). “Verification of VCA Testing to Determine Stone-On-Stone Contact of HMA Mixtures,” In Transportation Research Record 1891, Journal of the Transportation Research Board, pp. 182-190.

You, Z. and Buttlar, W.G. (2006). “Micromechanical Modeling Approach to Predict Compressive Dynamic Moduli of Asphalt Mixture Using the Distinct Element Method,” Journal of the Transportation Research Board, National Research Council, Washington, D.C., Accepted for publication.

Yue, Z. Q., Bekking, W., and Morin, I. (1995). “Application of digital image processing to quantitative study of asphalt concrete microstructure.” In Transportation Research Record 1492, TRB, National Research Council, Washington, D.C., pp. 53-60



Part 2

Soil and granular materials

2000 *Mathematics Subject Classification.* 74L10, 74E20, 74A20, 74A55

Key words and phrases. soil, granular materials, constitutive relations, interfacial friction

ABSTRACT. The first chapter discusses the complex behavior of interface between soils and solid surfaces. It introduces several experimental setups used to measure various characteristics of soil-solid surfaces, and it presents a comprehensive analysis of past experiments.

The second chapter is a report on experiments made with lumpy fill within the context of a land reclamation project in Singapore. The experiments were mainly focused on the influence of degree of swelling on the behavior of lumpy fill.

The last chapter provides an up-to-date historical overview of several models used for modeling of soils and granular materials. The merits and demerits of the models are thoroughly commented with a special attention to the role of thermodynamics in the development of such models.

ACKNOWLEDGEMENT. [R. G. Robinson, Consolidation behaviour of reclamation fill made of lumps] The results reported in this paper are part of the research project “Optimisation of the use of waste soils from construction for large scale land reclamation” funded by the National Science and Technology Board of Singapore (MCE/99/03). The financial assistance provided is gratefully acknowledged. Prof. Tan Thiam Soon is the principal investigator of this project with whom the author has worked on this project. The author takes this opportunity to thank him for all the useful discussions and suggestions he had throughout the course of the project.

Contents

Chapter 1. Interface behaviour of soils	73
R. G. ROBINSON	
1. Introduction	73
2. Apparatus types reported in the literature	73
3. Factors influencing interfacial friction	75
3.1. Density	75
3.2. Normal stress	76
3.3. Deformation rate	77
3.4. Size of apparatus	77
3.5. Grain size and shape	77
3.6. Type of apparatus	78
4. Quantification of interface roughness and empirical correlations	79
5. Limiting values of δ	80
6. Analysis of past studies	81
7. Effect of mode of shear on shear stress-movement curves	82
8. Modeling of interfaces	83
9. Looking forward	84
Bibliography	85
Chapter 2. Consolidation behaviour of reclamation fill made of lumps	
R. G. ROBINSON	89
1. Introduction	89
2. Experimental programme	90
3. Results and discussions	92
3.1. Fully swollen state	92
3.2. Influence of degree of swelling	94
3.3. Swelling of clay lumps	95
3.3.1. Finite element analysis	96
3.4. Shear strength profiles of the lumpy fill	97
4. Some research issues	98
5. Conclusions	98
Bibliography	101
Chapter 3. Modelling the behaviour of soils and granular materials	
I. F. COLLINS	103
1. Historical introduction	103

2. Material properties and experimental techniques	106
2.1. Material properties	106
2.2. Laboratory experiments	106
2.3. Discrete element methods of simulation (DEM)	108
3. Some extant theories of soil mechanics	109
3.1. Coulomb models	109
3.2. Double shearing models	111
3.3. Cap models	111
3.4. Critical state models	112
4. Thermomechanical approaches to the constitutive modelling of soils	115
4.1. The Cambridge approach	115
4.2. A critique of the Cambridge approach	117
4.3. The modern thermomechanical approach to modelling rate independent materials – “hyper-plasticity”	118
4.4. The thermomechanical approach to Cambridge models	120
4.5. Modelling Reynolds’ dilatancy	123
5. Conclusions	124
Bibliography	127

CHAPTER 1

Interface behaviour of soils

R. G. ROBINSON

1. Introduction

A need to estimate the frictional resistance at the interface between dissimilar materials exists in many engineering disciplines. The interfacial friction of concern to the geotechnical engineer is that which arises between solid surfaces and soils. The importance of friction between soils and solid materials has been recognized, as early as the 18th century by Coulomb (1776) while developing the earth pressure theories. The materials used in engineering construction may be soft or hard, and extensible or inextensible. Knowledge of interfacial friction is essential for the design of a variety of structures like pile foundations (positive or negative drag), retaining structures, reinforced earth structures, etc.

A simple empirical law, known as Coulombian friction law, is routinely used to describe the shear strength of soils and interfaces. In this law, the interfacial frictional resistance τ is expressed as,

$$\tau = c_a + \sigma_n \tan \delta, \quad (1.1)$$

in which σ_n stands for normal stress acting on the interface, δ for friction angle and c_a for adhesion between soil and the solid surface.

In the case of cohesionless soil-solid surface interface, the value of c_a is equal to zero. Considerable work has been done on the interfacial friction between cohesionless soils and solid surfaces over the past five decades commencing with Meyerhof (1948). Several types of apparatus were developed to evaluate the interfacial friction and attempts have been made to identify the factors influencing it. However, many issues need to be resolved.

This paper is mainly concerned with the interfacial friction between cohesionless soils and relatively hard and non-deformable solid surfaces. Unless otherwise specified, the term solid material in this paper refers to non-deformable material. The information available in the literature dealing with interfacial friction is briefly reviewed and few issues which need further study are brought out.

2. Apparatus types reported in the literature

Meyerhof (1948) is one of the earliest researchers who determined the interfacial friction angle of sand on brass sections from constant rate of strain shear tests using a shear box apparatus. Kézdi (1957) used a similar type of direct shear box of 300×300 mm size and evaluated the δ value for sandy gravel on a concrete

surface. The credit for the first systematic study on the interface friction between soils and various construction materials goes to Potyondy (1961). He used a strain controlled shear box of 36 cm² shearing area and stress controlled shear box with 80 cm² shearing area for the study. The specimens of construction materials were placed in the lower portion of the box and the soil in the upper box. A schematic representation of this modified direct shear apparatus is shown in Figure 1(a). In the

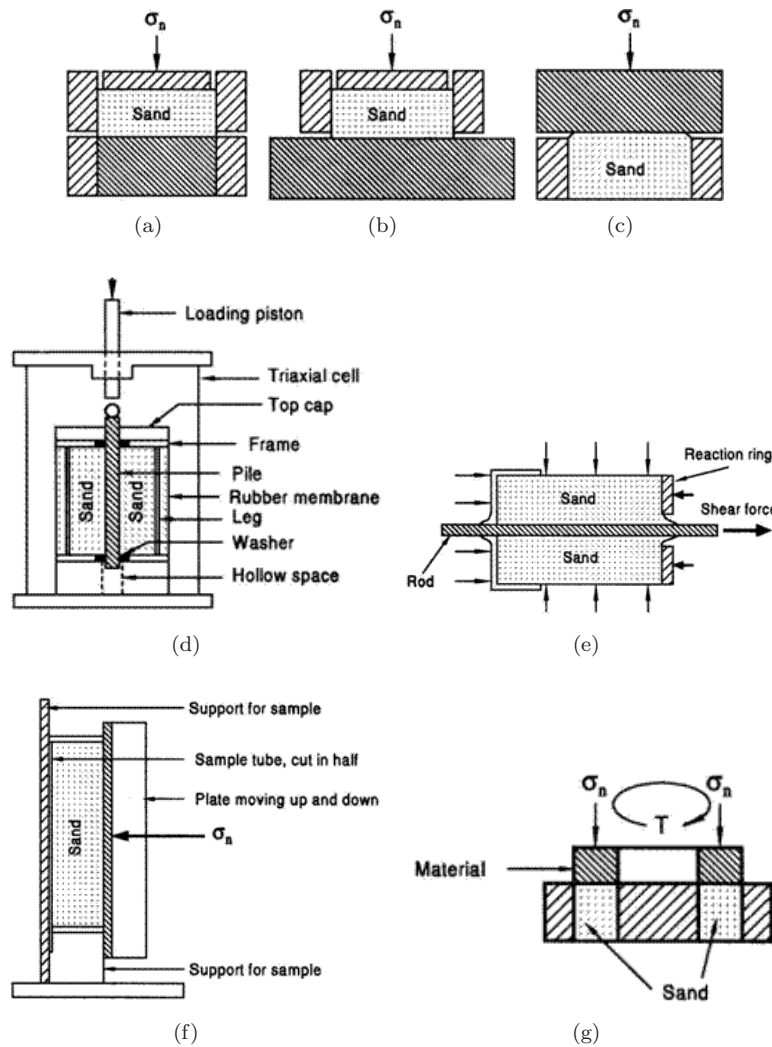


FIGURE 1. Schematic diagram of apparatuses used to evaluate δ

modified direct shear apparatus reported above, the interface area decreases during shear. Rowe (1962) rectified this drawback by replacing the bottom half of the shear box with a test block of sufficiently larger size than the interface dimensions (Figure 1(b)). Silberman (1961) utilized a shear box in which the upper box was

replaced with the test material (Figure 1(c)). This mode is the reverse of the configuration adopted by Potyondy (1961).

While the above studies used the direct shear apparatus, Coyle and Sulaiman (1967) designed a miniature pile testing apparatus by modifying a large triaxial cell (Figure 1(d)). Though the idea of designing this apparatus was to get a constant interface area, the δ values obtained from this apparatus may be more realistic for pile-sand interfaces than those determined from a direct shear set-up. Brumund and Leonards (1973) used a cylindrical device to investigate static and dynamic friction between sands and rods of various construction materials (Figure 1(e)). Heerema (1979) devised a system using a steel tube that was cut in half lengthwise (Figure 1(f)). A flat steel plate is pressed against the soil sample contained in this split tube by applying normal stress. The test material was moved up and down and all the forces and displacements were continuously recorded. Yoshimi and Kishida (1981) utilized a ring torsion apparatus, in which a ring shaped metal specimen was placed on the prepared sand in an annular container in order to have an unlimited circumferential deformation (Figure 1(g)). A constant vertical load was applied through the metal specimen and static torque T was applied so that the metal surface moved at a rate of about $0.6 \text{ mm}/\text{min}$ in circumferential direction. The deformation of sand and slippage at the soil-metal contact were measured using X-ray radiography.

3. Factors influencing interfacial friction

Several studies were reported in the literature, which have examined the influence of various soil parameters such as grain size and shape, density of the granular soil and the solid material properties such as surface roughness and hardness. The influence of other factors like normal stress, deformation rate, type of apparatus and size effects have also been the focus of studies reported in the literature. Not infrequently, the results of studies on the same factor have differed. The reports of several studies on each of these factors influencing δ are brought out in this section.

Table 1: Results of triaxial and soil-steel friction tests (Noorany, 1985)

Soil Type	Soil Condition	ϕ [degrees]	δ [degrees]
Silica sand	Loose	35	21
	Dense	40	20
Calcareous sand from Guam	Loose	46	18
	Dense	49	18
Calcareous sand from Florida	Loose	44	20
	Medium	45	20
	Dense	47	23

3.1. Density. It is well demonstrated in the literature that the angle of internal friction ϕ of sand increases with density (Burmister, 1948; Bolton, 1986). Attempts to study the influence of density on the interfacial friction angle δ between sands and solid surfaces have yielded contradictory conclusions. The studies of Noorany (1985), Yoshimi and Kishida (1981) and Broms (1963) indicated that

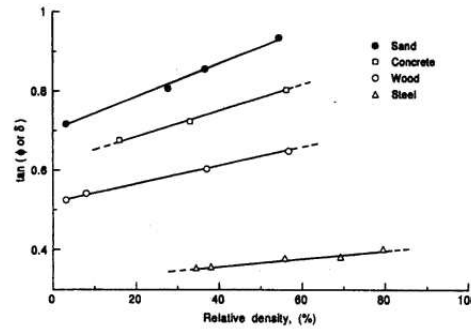


FIGURE 2. Influence of density on friction angle obtained from direct shear apparatus (after Acar et al., 1982)

the friction angle δ is independent of the sand density. Typical results of Noorany (1985) are given in Table 1. On the other hand, many others showed that the friction angle δ increases as the density of sand increases. Typically, data from Acar et al. (1982) is reproduced in Figure 2.

3.2. Normal stress. The peak angle of internal friction of granular material is generally assumed to be constant over the stress range of interest in geotechnical engineering (Taylor, 1948; Bishop and Eldin, 1953). The failure envelope for granular materials is in fact curved and hence decreases with the increase in normal stress (Bolton, 1986). Similar results have been reported by Acar et al. (1982) on uniform quartz sand for stress levels in the range 100 to 300 kPa. However, an assumption of linear behaviour is justifiable at low stress levels as has been confirmed by O'Rourke et al. (1990) from tests on Ottawa sand at stress levels less than 70 kPa. The influence of normal stress on δ depends on the material characteristics of the granular material. For all particulate materials the deviation from a simple frictional behaviour is due to crushing and breaking of grains (Lambe and Whitman, 1969). Hence at low stress levels (with less crushing) δ is constant and at higher stress levels it decreases due to crushing. From this it can be inferred that δ , which derives from the characteristics of both granular material and solid surfaces can be influenced by the normal stress level used for its evaluation.

Potyondy (1961) observed that the friction angle δ decreases with the increase in normal stress in the range 48.7 to 146 kPa. Acar et al. (1982) and Schultz and Horn (1967) corroborated the results of Potyondy (1961). Panchanathan and Ramaswamy (1964) also concluded that δ decreases with the increase in normal stress for most of the surfaces tested. But for soft materials like soft wood they found that the sand grains bite into the fibers of wood resulting in increase in the friction angle with normal stress increase. Everton (1991) also observed that δ was strongly affected by the normal stress level (Jardine et al., 1993).

Tejchman and Wu (1995) observed that the effect of normal stress on δ values was most pronounced at low normal stress levels ($\sigma_n < 100$ kPa). In this range the friction angle was seen to decrease with increase in normal stress. The normal stress has only a minor effect on the δ values in the range 100 to 400 kPa. However,

O’Rourke et al. (1990), Abderrahim and Tisot (1993), Heerema (1979) and Uesugi and Kishida (1986a, b) concluded that the normal stress has no influence on the δ values.

In summary, the influence of normal stress (within the normal engineering range) on δ values can either be to decrease the δ values or to have no influence. In the case of soft solid surfaces δ can increase with the increase in normal stress. Thus the influence of normal stress depends on the properties of sand (mainly its tendency to crushing), stress level and the material hardness. Clearly, more research is required into this aspect of interface behaviour.

3.3. Deformation rate. Of the few studies, which considered the rate of deformation as an influencing factor, the results of Heerema (1979) and Lemos (1986) are significant. Heerema (1979) varied the deformation rate from 0.7 to 600 mm/sec on a steel-sand interface. He observed that δ was independent of deformation rate and obtained a constant δ value of 25° for all deformation rates. Lemos (1986) sheared sand against a steel surface in a ring shear apparatus. A test was carried out along a displacement of 273 mm in six stages in which the deformation rate ranged from 0.0038 to 133 mm/min. The ultimate shear resistance at all stages was approximately constant and was not affected by the deformation rate. These studies show that the deformation rate has no influence on the measured friction angle of sands.

3.4. Size of apparatus. Laboratory studies on interfacial friction use relatively small size apparatus. It is essential to know the influence of size of apparatus. The tests performed by Brumund and Leonards (1973) using a 51 mm diameter rod (contact area 400 cm²) showed no appreciable difference in the computed values of coefficient of friction compared to the values obtained using a 28 mm diameter rod (area 225 cm²). Uesugi and Kishida (1986b) compared the results obtained from the simple shear apparatus with interface areas of 40 cm² and 400 cm². The results showed a reasonable agreement with each other showing that the size of apparatus has no influence on the δ values. Jewell and Wroth (1987) suggested that a ratio of shear box length L_b to average particle size D_{50} in the range 50-300 would be most likely yielding the same results. O’Rourke et al. (1990) have concluded from the results on Ottawa sand-HDPE interface using direct shear box of sizes ranging from 60 × 60 mm to 305 × 305 mm that the effect of size of apparatus on δ is insignificant for the sands tested.

It may be concluded that size of apparatus, with a minimum size of 60 × 60 mm, has no influence on δ values obtained between sands (particle size less than 22 mm) and solid surfaces. For particle sizes more than sand size the size of apparatus has to be chosen considering the particle size of the granular material as is specified for evaluation of angle of internal friction (BS: 1377, 1990).

3.5. Grain size and shape. Rowe (1962) showed that the friction angle between quartz sand and quartz block decreases as the particle size of the sand increases. This phenomenon was attributed to the larger particles being able to roll more easily than the smaller particles, perhaps as a result of their centre of gravity being further away from the plane of shear (Lambe and Whitman, 1969). Hence the

measured interfacial friction angle, which involves both rolling and sliding components, is smaller for the larger particles. Rowe’s observation was further confirmed by Kishida and Uesugi (1987), Uesugi and Kishida (1986b), Jardine and Lahane (1994) and Fioravante et al. (1995). The result of Rowe (1962) is reproduced in Figure 3. Uesugi and Kishida (1986b) observed that the coefficient of friction

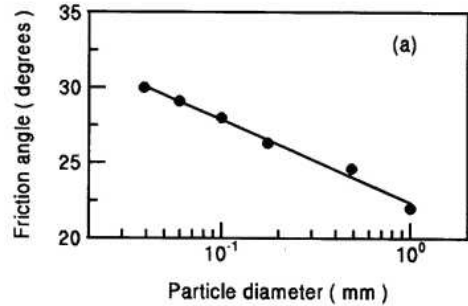


FIGURE 3. Influence of particle size on δ (after Rowe, 1962)

between steel and sand for angular particles was higher than that for round particles. The test results of Brumund and Leonards (1973) support this observation. O’Rourke et al. (1990) also concluded the same from the direct shear test results on sand-polymer interfaces. Paikowsky et al. (1995) observed that Ottawa sand yielded higher friction angle than glass beads. This increase in δ values for the sand with respect to the glass beads was attributed to the effect of grain shape.

To sum up it can be said that as the particle size of sand decreases δ value increases. The interfacial friction angle values for angular particles are higher than those for rounded particles.

3.6. Type of apparatus. It was brought out earlier that several types of apparatus are available to evaluate the friction angle. There have been some attempts to study the influence of type of apparatus on the measured δ values. In these studies the major influencing factors such as surface roughness, sand density, sand type, normal stress etc. were kept the same with the type of apparatus different. It was seen that the δ values obtained were different even though the interface conditions remained the same.

Kishida and Uesugi (1987) compared the coefficient of friction values obtained from direct shear apparatus with simple shear apparatus. They noted that the values obtained from simple shear apparatus and direct shear apparatus are essentially the same. The end restraints (rigid or deformable boundary) appeared to have no influence on the δ values. Abderrahim and Tisot (1993) compared δ values obtained from the direct shear apparatus, the ring shear apparatus and a mini pressure meter probe. Divergent results were obtained with the three apparatus. The friction at the interface measured with the mini pressure meter probe was greater than the value measured with the ring shear apparatus and less than that measured with direct shear apparatus. Tejchman and Wu (1995) conducted interface shear tests between sand and steel from three types of apparatus viz: plane strain apparatus,

4. QUANTIFICATION OF INTERFACE ROUGHNESS AND EMPIRICAL CORRELATIONS 79

parallelly guided direct shear apparatus and a model silo. The results showed that the coefficient of friction $\tan \delta$ and the corresponding displacements are different. The results mentioned above show that the δ values are strongly influenced by the type of apparatus used for their evaluation. This suggests that the friction angle values for design should not be selected without considering the type of field situation emulated by the apparatus type for the determination of δ .

4. Quantification of interface roughness and empirical correlations

The surface roughness of the solid material has a very significant influence on the friction angle δ . In the earlier studies the type of construction material was considered to be important. Potyondy (1961) determined the friction angle between sand and smooth and rough surfaces of the commonly used construction materials as steel, wood and concrete. The test results were expressed in the form of interfacial-to-internal friction angle ratio δ/ϕ . These values are commonly used in design (NAVDOCKS, 1962). This practice of assigning values to δ arbitrary fractions of the angle of internal friction ϕ , of the soil, irrespective of the soil-solid material interface roughness, is currently being critically reviewed.

Esashi et al. (1966) showed that skin friction between sands and construction materials could be correlated to the quantified surface roughness regardless of the type of the solid material (Yoshimi and Kishida, 1981). Yoshimi and Kishida (1981) measured the interfacial shear resistance between solid surfaces (steel, brass, aluminium, wood and concrete) possessing a wide range of surface roughness and sands of different types (Toyoura sand, Tonegawa sand, Nigigata sand and Soma sand). They correlated the coefficient of friction with the surface roughness. The surface roughness was quantified by using R_{\max} ($L = 2.5$ mm), defined as the vertical distance between the highest peak and the lowest trough along a gauge length L of 2.5 mm of the surface profile (Figure 4).

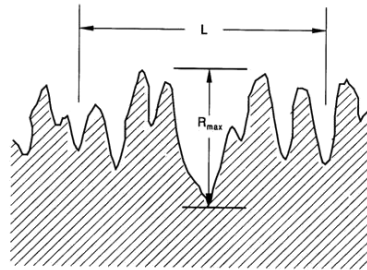


FIGURE 4. Typical surface profile showing R_{\max}

R_{\max} ($L = 2.5$ mm) is a parameter of roughness only and does not involve grain size. Allowing for the effect of grain size on the friction angle Kishida and Uesugi (1987) defined a normalized roughness R_n . Normalized roughness R_n is defined as

$$R_n = \frac{R_{\max}(L = D_{50})}{D_{50}}, \tag{1.2}$$

where R_{\max} ($L = D_{50}$) is the relative height between the highest peak and the lowest valley along a surface profile over a gauge length L equal to D_{50} size of sand (D_{50} is the size at which 50% of the particles are finer by weight). A bilinear correlation was obtained between coefficient of friction of dense Toyoura sand and normalized roughness over a wide range of sand diameters.

Uesugi and Kishida (1986b) estimated the coefficient of friction between sands of different angularity and steel as a function of modified roundness and normalized roughness R_n as shown in Figure 5. The modified roundness of a particle is defined as

$$R_i = \frac{1}{2} \left(\frac{r_2 + r_4}{l_1} + \frac{r_1 + r_3}{l_2} \right), \quad (1.3)$$

where r_1, r_2, r_3, r_4, l_1 and l_2 are defined in Figure 6. The modified roundness values of Toyoura, Fujigawa and Seto sand were estimated to be 0.27, 0.19 and 0.17, respectively.

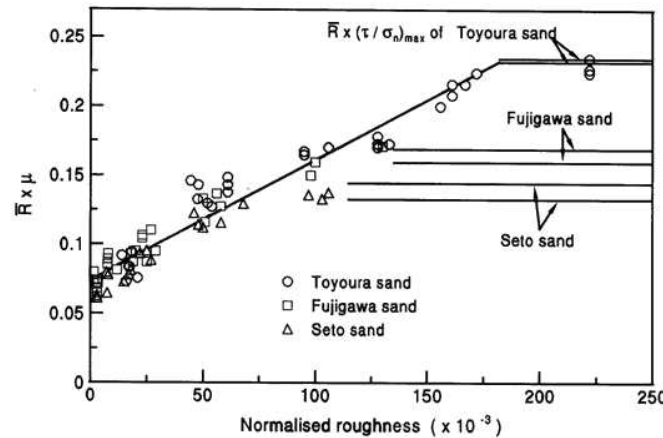


FIGURE 5. Coefficient of friction multiplied by modified roughness as function of normalised roughness (after Uesugi and Kishida, 1986b)

5. Limiting values of δ

The dependence of δ on surface roughness has been well demonstrated (Potyondy, 1961; Subba Rao et al., 1998; Yoshimi and Kishida, 1981; Uesugi and Kishida 1986a,b, to name a few). As the roughness increases, δ values increase and tend to a constant value.

Potyondy (1961) reported a value of δ approximately equal to 0.99ϕ for rough concrete-sand interface. Similarly Panchanathan and Ramaswamy (1964) observed that for very rough surfaces the friction angle ϕ is as much as the value of sand. Recent studies using simple shear apparatus also show that the limiting maximum value of δ , denoted as δ_{lim} , is the peak angle of internal friction of the sand (Kishida and Uesugi, 1987; Uesugi and Kishida, 1986a,b; Uesugi et al., 1990). Everton (1991) also observed from direct shear tests that $\delta_{lim} = \phi$, (Jardine et al., 1993).

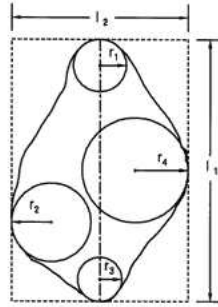


FIGURE 6. Modified roundness (after Uesugi and Kishida, 1986b)

While the above mentioned studies report that δ_{lim} is the peak angle of internal friction of sand, the studies of Yoshimi and Kishida (1981) using ring torsion apparatus show that it is the critical state angle of internal friction of sand.

Theoretically, one may assume that for very smooth surfaces, with the roughness equal to zero, the friction angle is equal to zero. But, experimental studies on interfacial friction between highly polished surfaces and sand show that the friction angle for very smooth surfaces is not zero but has a value of about $5-7^\circ$ (Tatsuoka and Haibara, 1985; Paikowsky et al., 1995).

6. Analysis of past studies

Table 2 summarises the results reported in the literature by various authors. Based on the results of the experimental investigations contained in Table 2, the following three general observations can be drawn:

- (1) Value of δ depends on surface roughness.
- (2) The maximum limiting value of δ could be either the peak angle of internal friction ϕ or the critical state angle of internal friction ϕ_{cv} .
- (3) With regards to density, Yoshimi and Kishida (1981) and Noorani (1985) report that δ is independent of density while the findings of Acar et al. (1982), Levacher and Siefert (1984), Desai et al. (1985), O'Rourke et al. (1990), Uesugi et al. (1990), and Lahane et al. (1993), contradict this view.

While observation (1) is logical and conclusive, observations (2) and (3) involve inconsistent findings regarding the magnitude of δ and the role of density and therefore require reconciliation.

Examining the details of experimental procedures adopted in the several studies, it is seen that whenever it was reported that the maximum limiting value of δ is not greater than the critical state friction angle of the sand mass ϕ_{cv} and that δ was independent of soil density, the material was placed on the free surface of the prepared soil. Normal stress was then applied through the material. Figure 7(a) schematically describes the material surface/granular soil interaction present in this situation which can be described as type A.

On the other hand, in those studies where it was observed that δ is equal to the peak angle of internal friction ϕ_p and that δ increases with density, it is seen that

TABLE 2. Analysis of published interface friction test results

Author(s)	Type of testing apparatus	Results of investigation	Remarks
Potyondy (1961)	Direct shear apparatus with the sand on the top of test material.	Value of δ increases with density and $\delta = \phi$ for very rough surfaces.	Sand was placed above the test material.
Broms (1963)	Direct shear mode by sliding the material over the sand.	Value $\delta = 23^\circ$ was obtained irrespective of sand density.	Test material was placed above the sand.
Yoshimi and Kishida (1981)	Ring shear with the test material on top of sand.	Density has no influence and $\delta = \phi_{cv}$ for very rough surfaces.	Test material was placed above the sand.
Acar et al. (1982)	Similar to Potyondy.	Value of δ increases with density.	Sand was placed above the test material.
Desai et al. (1985)	Translational test box.	Value of δ increases with density.	Sand was placed above the test material.
Noorany (1985)	Similar to Broms.	Influence of density is negligible.	Test material was placed above the sand.
O'Rourke et al. (1990)	Similar to Potyondy (1961).	Value of δ increases with density.	Sand was placed above the test material.
Uesugi et al. (1990)	Simple shear with the sand on top of the test material.	Value of δ increases with density $\delta_{lim} = \phi_p$.	Sand was placed above the test material.

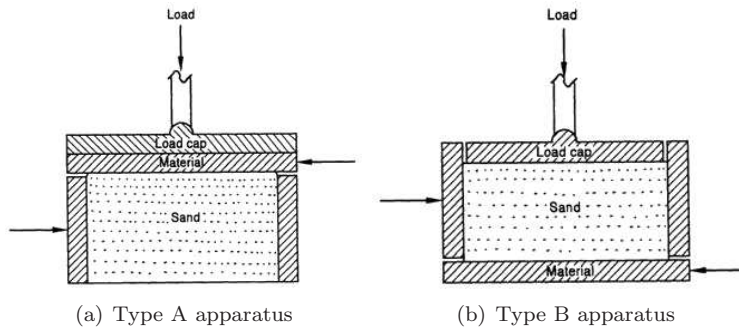


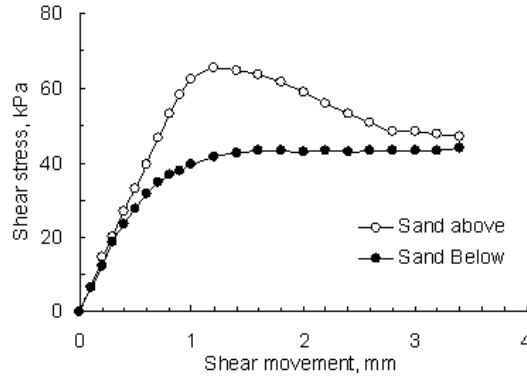
FIGURE 7. Schematic diagram of apparatuses

the soil was placed on the material prior to being prepared to a desirable density. The idealization labeled type B in Figure 7(b) is representative of this interactive system.

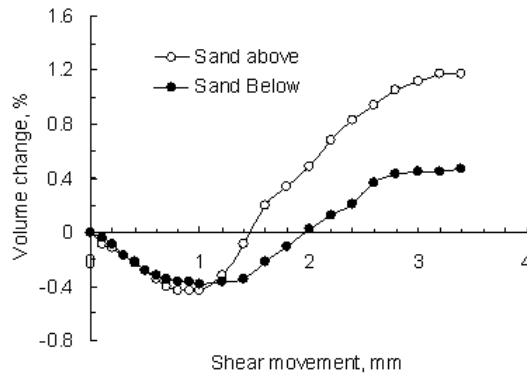
7. Effect of mode of shear on shear stress-movement curves

Apart from the magnitude of the friction angle being affected by the mode of shear, as discussed above, the shape of shear stress-movement curve is also affected

by the mode of shear. Typical result from a modified direct shear test for the sand-concrete interface is shown in Figure 8(a) and Figure 8(b) (Robinson, 1998). The relative density of the sand used is 85%. It can be seen that for the Type B case, a well defined peak is observed and at large movements, the shear stress for both Type B and Type A are practically the same. There is also a notable difference in the volume change behaviour during shearing. The dilation for Type B case is more than that for Type A case.



(a) Shear stress-movement curve



(b) Volume change-movement curve

FIGURE 8. Typical shear-movement and volume change-movement in Type A and Type B mode of shear

8. Modeling of interfaces

For the analysis and design of many structures, accurate interface models are necessary as the behavior of structures is significantly affected by the response of the interface between the structure and adjacent soil. Studies of the behavior of retaining walls have shown that accurate modeling of the response of wall backfill

interfaces is necessary to obtain adequate estimates of earth pressure magnitudes (Clough and Duncan 1969, 1971). Many studies have shown that the pre- and post-construction stress paths followed by the interface may be complex, often involving simultaneous changes in normal and shear stresses, as well as unloading and reloading Gómez et al. (2003).

Many models are proposed in the literature. Clough and Duncan (1971) developed a hyperbolic model for interfaces that has been used extensively in soil-structure interaction analyses of geotechnical structures. Other researchers have developed constitutive models for soil-structure interfaces that do account for complex stress paths using nonlinear elasticity, plasticity theory, damage theory, and the disturbed state concept (Drumm et al., 2000; Boulon et al., 1995). Gómez et al. (2003) reviewed the available interface models and developed an extended hyperbolic model to account for additional factors.

9. Looking forward

The behaviour of interface between soils and solid surface is very complex. Both the type of soil and the type of solid material affect the interface behaviour. In addition, it is seen that the mode of configuration also affects the interface behaviour and is situation dependent. Though some interface models are available they do not account for all the influencing factors. Therefore, there is a need to develop interface models capable of explaining the results reported in this paper.

Bibliography

Abdereahim, A. and Tisot, J.P. (1993). “Friction at the Cohesionless Soil-Structure Interface: Effect of Various Parameters according to a Classic Study and a New Approach”, *Geotechnical Testing Journal*, ASTM, 16(1), 122–130.

Acar, Y.B., Durguroglu, H.T. and Tumay, M.T. (1982). “Interface Properties of Sand”, *Journal of Geotechnical Engineering*, ASCE, 108(4), 648–654.

Bishop, A.W. and Eldin, G. (1953). “The Effects of Stress History on the Relation between ϕ and Porosity in Sand”, *Proceedings, 3rd International Conference on Soil Mechanics and Foundation Engineering*, Zürich, 1, 100–105.

Bolton, M. D. (1986). “The Strength and Dilatancy of Sands”, *Geotechnique*, 36(1), 65–78.

Boulon, M., Garnica, P., and Vermeer, P. A. (1995). “Soil-structure interaction: FEM Computations.”, *Mechanics of geomaterial Interfaces*, Studies in Applied Mechanics 42, A. P. S. Selvadurai and M. J. Boulon, eds., Elsevier, Amsterdam, 147–171.

Broms, B.B. (1963). “Discussion on Bearing Capacity of Piles in Cohesionless Soils”, *Journal of Soil Mechanics and Foundations Division*, ASCE, 89(6), 125–126.

Brumund, W.F. and Leonards, G.A. (1973). “Experimental Study of Static and Dynamic Friction between Sand and Typical Construction Materials”, *ASTM Journal of Testing and Evaluation I*, (2), 162–165.

BS: 1377-Part 7. (1990). *Determination of Shear Strength by Direct Shear* (Small Shear Box Apparatus).

Burmister, D.M. (1948). “The Importance and Practical Use of Relative Density in Soil Mechanics”, *ASTM Proceedings*, 48, 1249–1268.

Clough, G. W. and Duncan, J. M. (1969). “Finite element analyses of Port Allen and Old River Locks.” *Rep. No. TE-69-3*, U.S. Army Engineers Waterways Experiment Station, Vicksburg, Miss.

Clough, G. W. and Duncan, J. M. (1971). “Finite element analyses of retaining wall behavior.” *J. Soil Mech. Found. Div., Am. Soc. Civ. Eng.*, 97(12), 1657–1673.

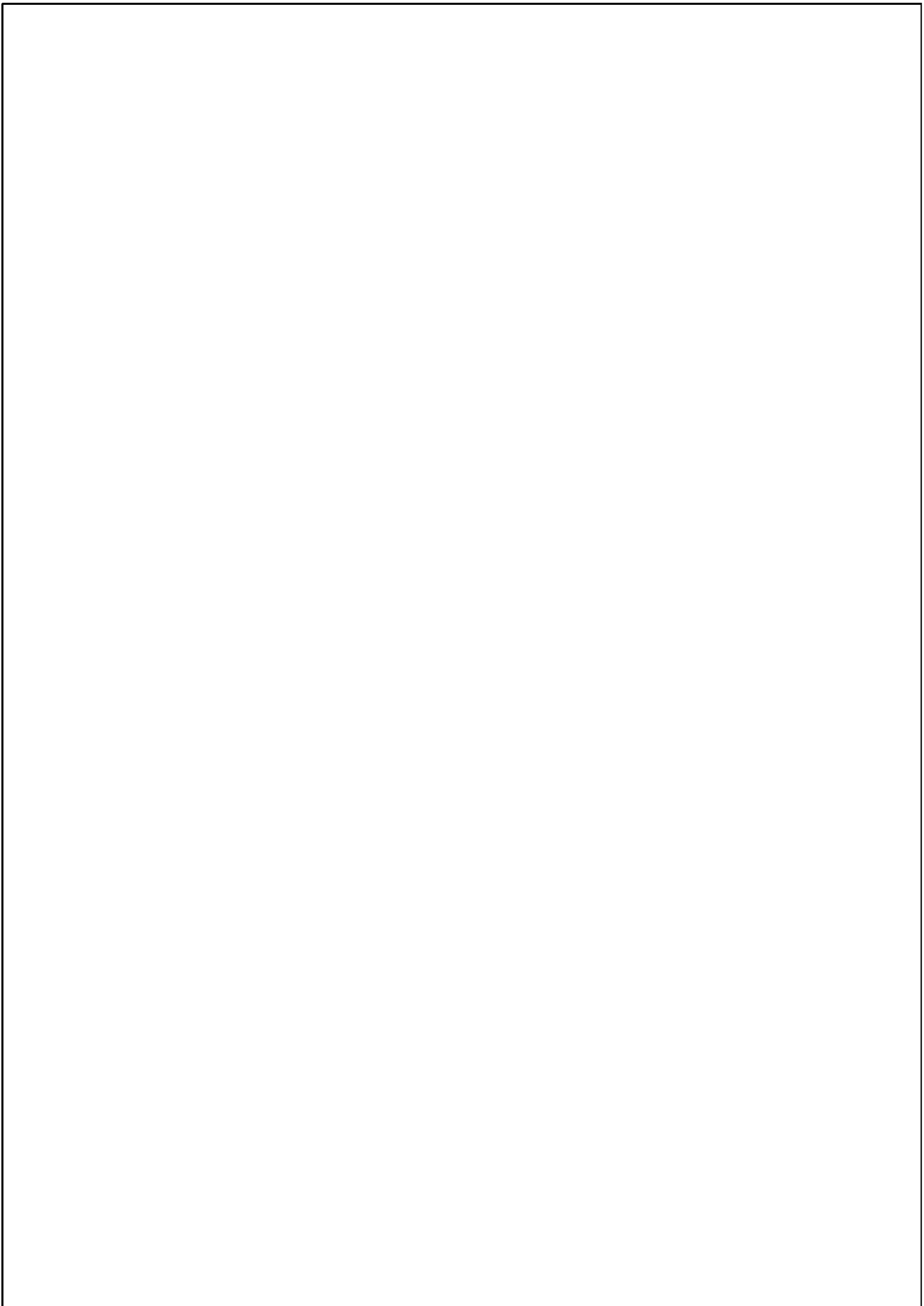
Coulomb, C. A. (1776). “Essai sur Une Application des Regles des Maximis et Minimis a Quelques Problems de Statique Relatif a L’architecture”, *Mem. Acad. Royal Pres.*, Divers Say., Paris.

Coyle, H.M. and Sulaiman, I.H. (1967). “Skin Friction for Steel Piles in Sand”, *Journal of Soil Mechanics and Foundations Division*, ASCE, 93(6), 261–278.

Drumm, E. C., Fishman, K. and Zaman, M. (2000). “Modeling of interfaces and joints” *Modeling in geomechanics*, M. Zaman, G. Gioda, and J. Booker, eds., Wiley, New York, Chap. 16.

- Esashi, Y., Kataoka, T. and Yasuda, M. (1966). “Uplift Resistance of Piles: Part 1, Cohesionless Soil”, *Report of Central Research institute of Electrical Power industry (66037)*, 1-60 (in Japanese) - vide Yoshimi and Kishida (1981).
- Everton, S.J. (1991). “Experimental Study of Frictional Shearing Resistance between Non-Cohesive Soils and Construction Materials”, *MSc (Engg) Dissertation*, University of London (Imperial college).
- Fioravante, V., Ghionna, V.N., Jamiolkowski, M. and Pedroni, S. (1995). “Load Carrying Capacity of Large Diameter Bored Piles in Sand and Gravel”, *Proceedings, X Asian Regional Conference on Soil Mechanics and Foundation Engineering*, Beijing, China, 2, 3–15.
- Gómez, J. E., Filz, G. M., Ebeling, R. M (2003). “Extended Hyperbolic Model for Sand-to-Concrete Interfaces” *Journal of Geotechnical and Geoenvironmental Engineering*, 129(11), 993–1000.
- Heerema, E.P. (1979). “Relationship between Wall Friction, Displacement Velocity and Horizontal Stress in Clay and in Sand for Pile Driveability Analysis”, *Ground Engineering*, 12(9), 55–60.
- Holtz, R. D. (1977). “Laboratory Studies of Reinforced Earth using a Woven Polyester Fabric”, *Proc. Int. Conf. Fabrics in Geotechnics*, 3, 149–154.
- Ingold, T.S. (1984). “A Laboratory Investigation of Soil-Geotextile Friction”, *Ground Engineering*, 17(2), 1–28.
- Jardine, R.J., Lehane, B.M. and Everston, S.J. (1993). “Friction Coefficients for Piles in Sands and Silts”, *Proceedings, Conference on Offshore Site Investigation and Foundation Behaviour*, London, 28, 661–677.
- Jewell, R.A. and Wroth. C.P. (1987). “Direct Shear Tests on Reinforced Sand”, *Geotechnique*, 37, 53–68.
- Kezdi, A. (1957). “Bearing Capacity of Piles and Pile Groups”, *Proceedings 4th International Conference on Soil Mechanics and Foundation Engineering*, London, 2, 46–51.
- Lambe, T.W. and Whitman, R.V. (1969). *Soil Mechanics*, Wiley and Sons., New York.
- Lemos, L. (1986). “The Effect of Rate on Residual Strength of Soil”, *Thesis submitted to the Imperial College of Science and Technology at the University of London*, in partial fulfillment of the requirements for the degree of Doctor of Philosophy, – vide Paikowsky et al. (1995).
- Levacher, D.R. and Sieffert, J.G. (1984). “Tests on Model Tension Piles”, *Journal of Geotechnical Engineering*, ASCE, 110(12), 1735–1748.
- Meyerhof, G.G. (1948). “An Investigation of the Bearing Capacity of the Shallow Footings on Dry Sand”, *Proceedings, 2nd International Conference on Soil Mechanics and Foundation Engineering*, 1, 237–243.
- Murthy, B.R.S., Sridharan, A. and Bindumadhava (1993). “Evaluation of Interfacial Frictional Resistance”, *Geotextiles and Geomembranes*, 12, 235–253.
- Navdocks (1962). *Design Manual DM-7, Soil Mechanics, Foundations and Earth Structures*, US Navy - vide Nayak (1996).
- Noorany, I. (1985). “Side Friction of Piles in Calcareous Sands”, *Proceedings, 11th International Conference on Soil Mechanics and Foundation Engineering*, San Fransisco, 3, 1611–1614.

- O'Rourke, T.D., Druschel, S.J. and Netravalli, A.N. (1990). “Shear Strength Characteristics of Sand-Polymer Interfaces”, *Journal of Geotechnical Engineering*, ASCE, 116(3), 451–469.
- Paikowsky, S.G., Player, C.M. and Connors, P.J. (1995). “A Dual Interface Apparatus for Testing Unrestricted Friction of Soil along Solid Surfaces”, *Geotechnical Testing Journal*, ASTM, 18(2), 168–193.
- Potyondy, J.G. (1961). “Skin Friction between Various Soils and Construction Materials” *Geotechnique*, 11(4), 39–353.
- Robinson, R. G. (1998). “Some studies on the interfacial friction between soils and solid surfaces”. A thesis submitted for the degree of Doctor of Philosophy in Indian Institute of Science, Bangalore.
- Rowe, P.W. (1962). “The Stress-Dilatancy Relations for Static Equilibrium of an Assembly of Particles in Contact”, *Proceedings, Royal Society of London, Series A*, 269, 500–527.
- Schultz, E. and Horn, A. (1967). “The Base Friction for Horizontally Loaded Footings in Sand and Gravel”, *Geotechnique*, 17, 329–347.
- Silberman, J.O. (1961). “Some Factors Affecting the Frictional Resistance of Piles Driven in Cohesionless Soils”, *Thesis presented to Cornell University, Ithaca, NY*, in partial fulfillment of requirements for the degree of Master of Science, vide Broms (1963).
- Subba Rao, K.S., Allam, M.M. and Robinson, R.G. (1998). “Interfacial Friction between Sands and Solid Surfaces”, *Geotechnical Engineering Proc. Instn. Civ. Engrs*, 131, 75–82.
- Tatsuoka, F. and Haibara, O. (1985). “Shear Resistance between Sand and Smooth or Lubricated Surfaces”, *Soils and Foundations*, 25,(1), 89–98.
- Taylor, D.W. (1948). *Fundamentals of Soil Mechanics*, Wiley and Sons. Inc., New York.
- Tejchman, J. and Wu, W. (1995). “Experimental and Numerical Study of Sand-Steel Interfaces”, *International Journal for Numerical and Analytical Methods in Geomechanics*, 19, 513–536.
- Uesugi, M. and Kishida, H. (1986a). “Influential Factors of Friction between Steel and Dry Sands”, *Soils and Foundations*, 1986, 26(2), 33–46.
- Uesugi, M. and Kishida, H. (1986b). “Frictional Resistance at Yield between Dry Sand and Mild Steel”, *Soils and Foundations*, 26(4), 139–149.
- Uesugi, M., Kishida, H. and Uchikawa, Y. (1990). “Friction between Dry Sand and Concrete under Monotonic and Repeated Loading”, *Soils and Foundations*, 30(1), 125–128.
- Yoshimi, Y. and Kishida, H. (1981). “Friction between Sand and Metal Surface”, *Proceedings, 10th International Conference on Soil Mechanics and Foundation Engineering*, Stockholm, 1, 831–834.



CHAPTER 2

Consolidation behaviour of reclamation fill made of lumps

R. G. ROBINSON

1. Introduction

Many countries often create additional land through land reclamation by filling sea or lakes. For example, Casagrande (1949) reported the design and construction of Logan Airport dredged fill. Whitman (1970) reported many cases of hydraulic fills that were used to raise the swampy or submerged land to create new sites. In Halmstad harbour situated in south-western Sweden, stiff silty clay dredged from harbour approach was deposited between two breakwaters to create new land (Hartlen and Ingers, 1981). In some countries, land reclamation form one of the major civil engineering activities. Typically, Singapore has increased its land area by about 17% since 1960 to 2001 (Lui and Tan, 2001). This paper is relevant to a major reclamation work in Singapore.

In the past, inland hill-cut materials and local sand deposits were used as fill materials while reclaiming many sites in Singapore. These are now virtually exhausted and reclamations in the last 15 years have relied mainly on imported sand from neighboring countries. This has spurred a search for alternate materials in huge volumes that can meet future reclamation needs. On the other hand, large volumes of unwanted soils are obtained from inland construction activities, maintenance of navigation channels and coastal construction activities, which need to be disposed off. These materials, comprising mainly highly plastic marine clay in the form of lumps, if used for reclamation, can solve the problem of finding suitable dumping grounds and at the same time becomes material of value as fills for land reclamation.

Research on the use of marine clay for land reclamation has been in progress in Singapore for more than a decade (Karunaratne et al., 1990 and Tan et al., 2000). Initially hydraulic fill using clay slurry was used, but it was recognized that after consolidation, the resulting fill volume is small. Also, using the marine clay in the form of slurry requires double handling, as the water content of the clay must first be introduced and then subsequently reduced as part of the reclamation process.

Another fill is hydraulically transported dredged clay and this often consists of clay balls in addition to the clay slurry. Mendoza and Hartlen (1985) performed laboratory tests to compare the compressibility characteristics of clay slurries and mixtures of clay balls of 5 to 50 mm in diameter. The study brought out the advantage of using a mixture of clay balls and slurry, instead of slurry alone. Another



FIGURE 1. View of dredged clay lumps placed in a barge before dumping in the sea

alternative is to use the clay lumps directly as reclamation fill, by dumping from barges. This approach was adopted in Halmstad harbor of Sweden, to create approximately 1.2 km^2 industrial area (Hartlen and Ingers, 1981).

Bo et al. (2001) compared the use of slurry and large clay lumps as reclamation fills and concluded that reclamation using clay lumps is easier than using slurry. A scheme using lumpy fill is now being used in Singapore for the 1500 hectares Pulau Tekong/Ubin, which began in the year 2000. For this project, dredged and excavated lumps are transported and dumped using bottom-opening barges. A view of the lumps dredged from the seabed and placed in the barge before dumping is shown in Figure 1. When such clay lumps are dumped in the sea, large inter-lump voids are expected.

A schematic of the lumpy fill scheme is shown in Figure 2. Sand is used as a topping fill and also as a surcharge to accelerate the consolidation process. Little information is known about the mechanics of lumpy fills. Issues that need to be addressed include the consolidation pressure required to close inter-lump voids, the equilibrium state of the lumpy fill under different consolidation pressures, swelling of clay lumps, etc. An understanding of the behaviour of lumpy fill and the influence of these factors would provide significant opportunity to further optimize the design. Towards this purpose, experiments were conducted on lumpy fills in which the inter-lump voids were filled with water. Clay lumps made of undisturbed Singapore marine clay were used. This paper reports the experimental results and highlights the need for further research.

2. Experimental programme

The lumps in the field are often very large and volume in excess of $1\text{-}2 \text{ m}^3$ are very common when clamshell grabs of volume ranging from 10 to 24 m^3 are used (Figure 3). However, in the present study small lumps of uniform sizes were used so as to conduct the experiments under controlled conditions. The dredged clay lump of lower member of Singapore marine clay was cut at the site into lumps of

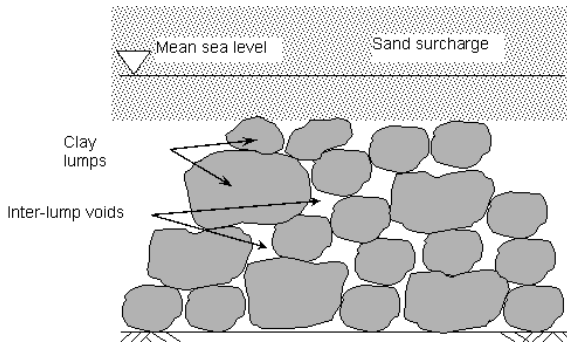


FIGURE 2. Typical land reclamation scheme using clay lumps



FIGURE 3. Clay lump of Singapore marine clay dredged from the seabed

200 mm and transported to the lab. The lumps were further cut into small cubical lumps of required size using a thin wire cutter. Cylindrical Perspex containers were used as cells for performing consolidation tests on the lumpy fill. A view of the experimental set-up is shown in Figure 4. The lumps were placed in the container and allowed to swell to the specified degree of swelling (defined later) after adding water. Then consolidation test was performed in the conventional way by subjecting the fill to step loading. The settlement of the fill was monitored during the consolidation process. In some cases, the pore water pressure developed inside the lump and in between the lumps was also measured using miniature pore pressure transducer. Falling head permeability tests were conducted at the end of consolidation.

As a result of the removal of overburden stress during dredging operations in the field, suction equivalent to the mean overburden pressure would develop in the lumps. When placed back in water during the filling process, these lumps would swell due to the suction in the soil. However, as the lumps in the field could be very large in some cases, the time required for full swelling will take long time due to the low permeability of clay. If the time between placing the lumps in water and the application of surcharge is short, the lumps will be in a partially swollen state.



FIGURE 4. Experimental set-up for the lumpy fill experiments

To study the influence of swelling of clay lumps on the consolidation behaviour, experiments were conducted using lumps that were subjected to degree of swelling of 0%, 50% and 100%. Degree of swelling is defined as

$$U_s = \frac{w - w_i}{w_f - w_i} \times 100, \quad (2.1)$$

where w_i , w_f and w are the water contents at the initial stage, final stage and at any time t , respectively.

Before conducting the test, a relationship between U_s and time t was established by submerging clay lumps in water and monitoring their weights till they reached constant weight. The time t_{50} for a degree of swelling of 50% was then obtained from the U_s - t relationship. For a 25 mm cubical lump, t_{50} was found to be 20 min.

Three-dimensional swelling behaviour of clay lumps were studied on reconstituted clay lumps of Kaolinite and Singapore marine clay. Miniature pore pressure transducers were used to monitor the rate of dissipation of suction during the swelling of clay lumps. Lumps with sizes ranging from 100 mm to 400 mm were used. Finite element analysis was carried out to simulate the swelling of clay lumps when submerged in water. Detailed description of experimental procedure and finite element analysis are given in Robinson et al. (2004).

Experiments were also conducted to evaluate the end state of the lumpy fill, subjected to a degree of swelling of 100%, using 50 mm cubical lumps. Miniature cone penetrometer was used to evaluate the shear strength profile of the fill under different surcharge loadings.

3. Results and discussions

3.1. Fully swollen state. Figure 4 shows the state of a lumpy fill immediately after placing in water. Large inter-lump voids are clearly visible. As the

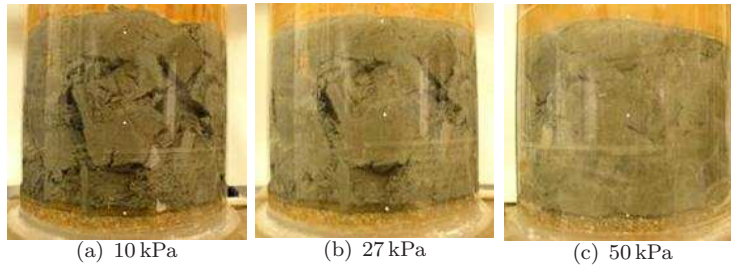


FIGURE 5. View of the lumpy fill under different consolidation pressures

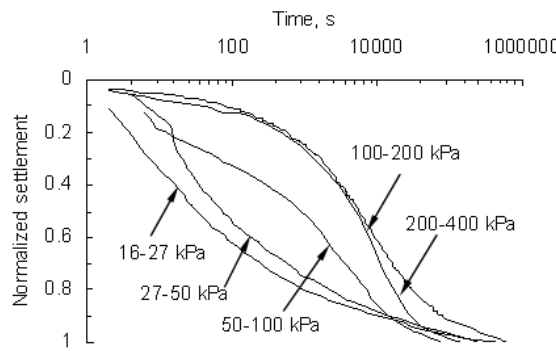


FIGURE 6. Typical time-settlement curves

surcharge pressure was increased, the size of the inter-lump voids decreased as seen in Figure 5(a) to 5(c). When the pressure reached a value of 50 kPa, the inter-lump voids are visibly closed and the fill begins to look more like homogeneous clay. Typical time-settlement curves obtained under different step-loadings are shown in Figure 6. The settlement values are normalized with the final settlement under each loading to facilitate comparison. Under small surcharge loadings, the rate of settlement is faster due to the presence of inter-lump voids, which permits practically free drainage of water. As the consolidation pressure is increased, the rate of settlement decreases markedly. For pressures less than 50 kPa, the shape of the time-compression curve in the logarithmic time plot is concave, in marked contrast to those observed for homogeneous clays, following the classic Terzaghi’s model. As the lumpy fill is a double porous system consisting of inter-lump voids and intra-lump voids, double porosity model should be adopted (Yang et al., 2002) for more realistic analysis. Beyond a consolidation pressure of 50 kPa, the rate of settlement is much slower due to the closure of the inter-lump voids and the shape of the curve started changing. Typical S-shaped curves are obtained for pressures beyond 100 kPa. The variation of pore water pressure with time for the load increment from 25 kPa to 50 kPa is shown in Figure 7(a). It is expected for homogeneous clay that immediately after the application of load the pore pressure increases to a value equal to the applied pressure increment. The pore pressure in between the lumps

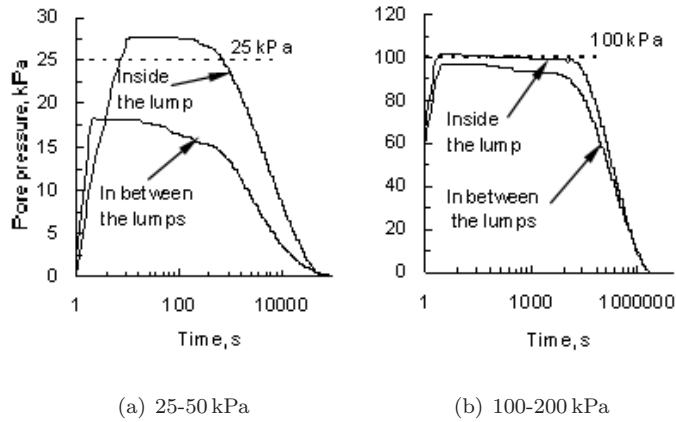


FIGURE 7. Excess pore pressure under various pressure increments

(inter-lump) increases after the application of the load but reaches a maximum value much less than the applied pressure increment and dissipates at a faster rate. On the other hand, the pore pressure inside the lump reaches a maximum value more than the applied pressure increment. This is attributed to the difference in permeability of the inter-lump voids and intra-lump voids. Under a pressure increment of 100 to 200 kPa (Figure 7(b)), the pore pressure in the inter-lump voids and inside the lump are close to each other and the maximum pressure is approximately equal to the applied pressure increment, similar to the case of a homogeneous clay. This is due to the fact that the inter-lump voids, by now, are practically closed and the fill behaves more like homogeneous clay. The variation of permeability with consolidation pressure is shown in Figure 8. The permeability of the soil in the undisturbed and remoulded state are also plotted. Drastic reduction in permeability of about two orders of magnitude was observed under a consolidation pressure of 50 kPa. However, the value is still higher than those corresponding to the homogeneous clay. This suggests that even though the photograph (Figure 5(c)) shows substantial closing of inter-lump voids under 50 kPa, the fill is not homogeneous, in terms of permeability. Under a consolidation pressure of 100 kPa, the permeability of the fill has now reduced to a value comparable to the homogeneous clay. The time-compression curves, beyond a consolidation pressure of 100 kPa, also look like those obtained for homogeneous clays. It appears therefore that for the fill made of undisturbed clay lumps, the consolidation pressure required to close the inter-lump voids is about 100 kPa.

3.2. Influence of degree of swelling. The influence of degree of swelling, on the consolidation behaviour of the lumpy fill, was studied through visual observations and from e - $\log \sigma'_v$ plots. As it is difficult to measure the inter-lump and intra-lump voids separately, the global void ratio, defined in the conventional way, is used to interpret the results. The e - $\log \sigma'_v$ plots of the lumpy fill subjected to different degree of swelling are shown in Figure 9. The initial void ratio of the fill before the start of the test is 3.84. The effect of swelling is clearly evident. Under

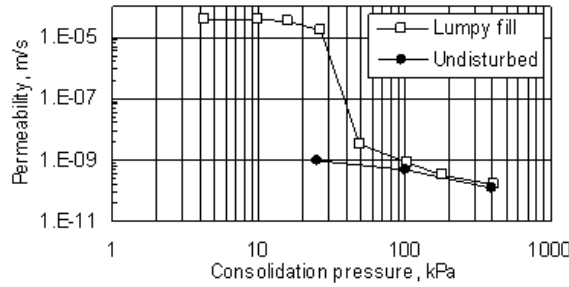


FIGURE 8. Variation of permeability with pressure

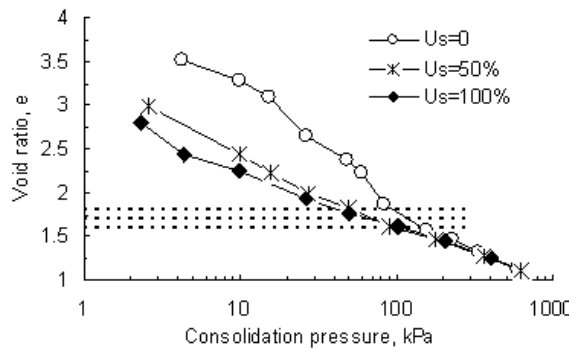


FIGURE 9. Influence of U_s on consolidation behaviour

small consolidation pressures, the void ratio of the fill made of lumps with $U_s = 0\%$ is considerably higher than those corresponding to the lumps subjected to swelling. When the clay lumps are subjected to swelling, the water content increases with a consequent reduction in shear strength and stiffness. Therefore the lumps cannot withstand the high contact stresses and slips at the contact points to form a stable configuration leading to reduction in inter-lump voids. But the lumps which were not subjected to swelling are much stronger and are able to withstand higher pressure without deformation and slippage. This is clearly seen in Figure 10(a), 10(b) and 10(c), which shows the photographs of the lumpy fill under 50 kPa with different degree of swelling. Under the same consolidation pressure of 50 kPa, the inter-lump voids of the fully swollen lumps are visibly closed but large inter-lump voids can still be seen for the fill in which the lumps were not allowed to swell. The above results show that the degree of swelling has a direct influence on the pressure required to close the inter-lump voids. Therefore it is important to study the swelling behaviour of clay lumps.

3.3. Swelling of clay lumps. The variation of negative pore water pressure (suction) with time at the centre of the clay lump of different sizes when submerged in water is shown in Figure 11 for the Kaolinite lumps. The suction values u are normalized with the initial suction u_0 present in the lump before submerging in

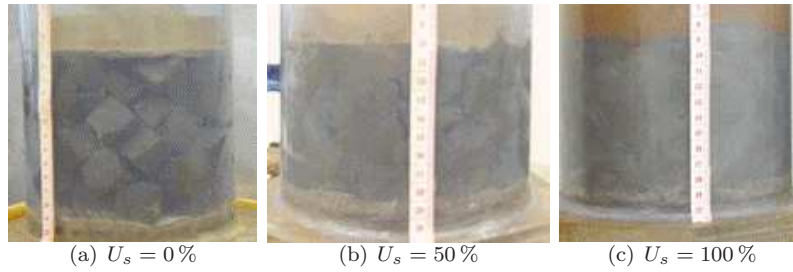


FIGURE 10. View of the lumpy fill under consolidation pressure of 50 kPa with various U_s

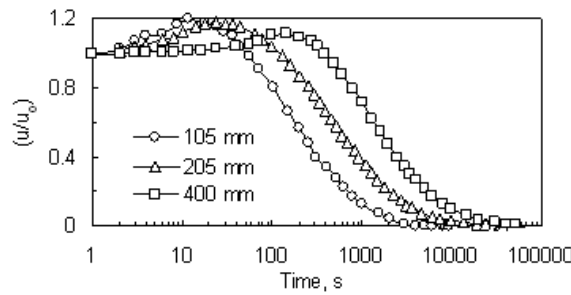


FIGURE 11. Dissipation of suction during swelling of clay lumps made of kaolinite

water. The suction values increases initially before dissipating showing the existence of Cryer-Mandel effect during three-dimensional swelling of clay lumps. Similar results were obtained for the lumps made of Singapore marine clay. The increase in suction at the centre of the lump is 15-20% for Kaolinite and 18-20% for the Marine clay. The time required for reaching the peak increases as the lump size increases. Also, as expected, the rate of dissipation of suction decreases as the size of the lump increases due to the increase in drainage path.

3.3.1. *Finite element analysis.* Finite Element Analysis using a non-linear elastic model was carried out in order to verify the experimental results obtained from this test. Detailed description of the finite element analysis is given in Robinson et al. (2004). Due to symmetry half the lump was modeled using axi-symmetric elements and 380 eight node quadrilateral consolidating elements were used. In the analysis, deformation has been coupled with Biot’s pore pressure dissipation equations (Biot, 1941). The effective bulk modulus K' was assumed to be similar to the elastic part of Cam clay model and is given by

$$K' = \frac{(1 + e)p'}{\kappa}, \quad (2.2)$$

where p' , is the mean effective normal stress, e is the void ratio and κ is the slope of the swelling curve in the e - $\log \sigma'_v$ plot. It was found that increases with over-consolidation ratio (OCR) very similar to that observed by Al-Tabbaa (1987)

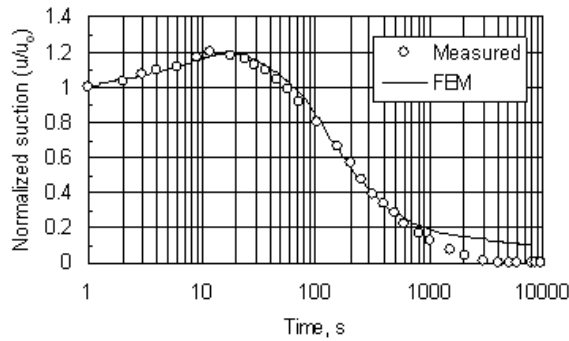


FIGURE 12. Comparison of measured suction with finite element analysis

and Stallebrass (1990). Curve fitting of the data yielded the following relationship between κ and OCR

$$\kappa = 0.005 + 0.10 \log(\text{OCR}). \quad (2.3)$$

The permeability change with void ratio and anisotropy in permeability were also considered in the analysis. The ratio of horizontal permeability k_h to vertical permeability k_v is 1.96. The values of k_h and k_v were obtained by performing consolidation tests under vertical drainage and radial drainage as described in Robinson and Allam (1998). Equation (2.4) is the relationship obtained between e and k_v (in m/s) from the falling head permeability tests conducted for this clay (Robinson et al., 2004)

$$e = 11.9 + 1.22 \log_{10} k_v. \quad (2.4)$$

The results obtained from the finite element analysis are compared with those obtained from the experiments in Figure 12. The experimental values are very close to those predicted by the finite element analysis over a wide range. Towards the end, the predicted suction deviates significantly from the measurements. It was found that small cracks occurred in the sample towards the end of the test. The cracks increase the global permeability of the lump leading to faster rate of dissipation of suction in the experiments than that predicted by the FEM results.

3.4. Shear strength profiles of the lumpy fill. The shear strength profiles obtained using cone penetration tests under surcharge pressures of 50 kPa, 100 kPa, 200 kPa and 360 kPa are shown in Figure 13(a)-13(d). Under consolidation pressures of 50 kPa and 100 kPa, the shear strength is not uniform with depth. This suggests that even though the lumpy fill appears to be uniform from visual observations and inferred from permeability measurements under a consolidation pressure of 100 kPa, the fill is highly heterogeneous in terms of strength.

The shear strength values predicted based on SHANSEP concept (Ladd et al., 1977) for the normally consolidated state ($\text{OCR} = 1$) and with the respective OCR values corresponding to the vertical normal stress are also plotted in Figure 13(a)-13(d). This shows that at consolidation pressures of 50 kPa and 100 kPa, the shear strength values mostly lying in between the normally and over consolidated state. This is consistent with the findings of Karthikeyan et al. (2004) who reported the

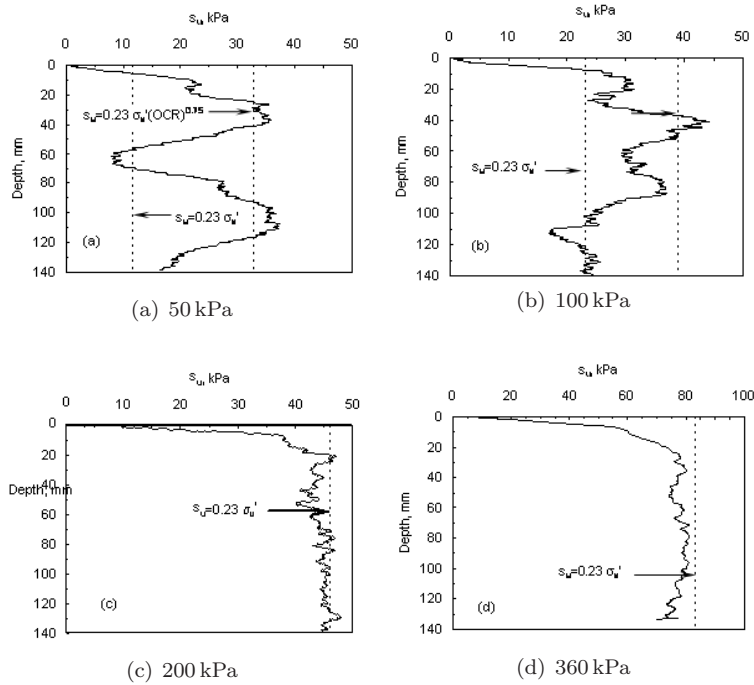


FIGURE 13. Shear strength profiles under various consolidation pressures

presence of zones of normally consolidated and overconsolidated states, based on an extensive site investigation on a reclaimed land using dredged clay lumps.

When the consolidation pressure applied is equal to the preconsolidation pressure (Figure 13(c)), the strength profile is almost uniform. This suggests that to make the fill uniform, consolidation pressure equal to or greater than the preconsolidation pressure (Figure 13(d)) of the lump should be applied to the fill.

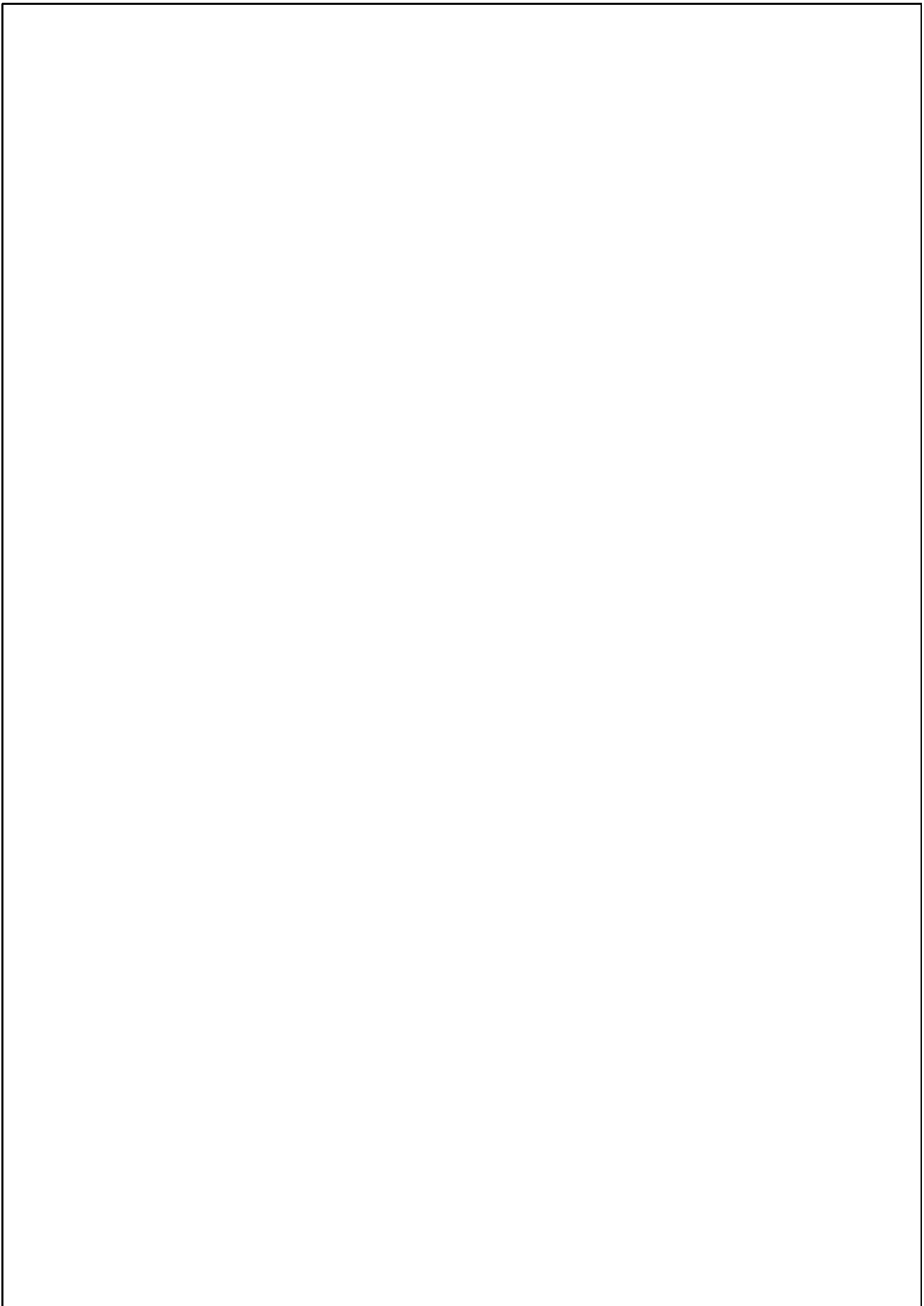
4. Some research issues

Consolidation behaviour of homogeneous clays is understood quite significantly. In this case the porosity is practically the same. However, the lumpy fill is a double porous system consisting of both inter-lump and intra-lump voids. Therefore, during the compression process, settlement is enhanced by closing of both the voids. Limited studies exist that explains the consolidation behaviour of dual porous system consisting of deformable lumps.

5. Conclusions

Laboratory studies using small lumps showed that degree of swelling has a strong influence on the behaviour of lumpy fill. The surcharge pressure required to close the inter-lump voids of fully swollen lumps is considerably less than that required for lumps that were not subjected to swelling. Non-linear finite element

analysis using pressure dependent bulk modulus is able to predict the dissipation of pore pressure inside the lumps during swelling. The end state of a lumpy fill is heterogeneous when the consolidation pressure is less than the preconsolidation pressure of the lumps, but lies within the range for NC and OC state. A model that is capable of explaining the consolidation behaviour of lumpy fill is needed.



Bibliography

- Al-Tabbaa, A. (1987). Permeability and stress-strain response of speswhite kaolin. PhD thesis, University of Cambridge, UK.
- Biot, M. A. (1941). General theory of three-dimensional consolidation. *Journal of applied physics*. 37, pp. 369-392.
- Bo, M. W., Bawajee, R. and Choa, V. (2001). “Reclamation using dredged materials”. Proceedings of the international conference on Port and Maritime R & D and Technology, Singapore, Vol.1, pp.455-461.
- Casagrande, A. (1949). Soil Mechanics in the Design and Construction of Logan Airport. *Boston Society of Civil Engineers Journal*, pp. 176-205.
- Hartlen, J. and Ingers, C. (1981). Land Reclamation using fine-grained dredged material. Proc., 10th International conference on Soil Mechanics and Foundation Engg, Stockholm, Vol. 1, pp. 145-148.
- Karthikeyan, M., Dasari, G. R. and Tan, T. S. (2004). In-situ characterization of a land reclaimed using big clay lumps, *Canadian Geotechnical Journal*, Vol. 41, No. 2, pp. 242-256.
- Karunaratne, G. P., K. Y. Yong, T. S. Tan, S. A. Tan, K. M. Liang, S. L. Lee, and A. Vijiaratnam (1990). “Layered clay-sand scheme reclamation at Changi South Bay”. Proceedings of 10th Southeast Asian Geotechnical Conference, 16-20 April, Taipei, Vol.1, pp.71-76.
- Ladd, C. C., Foott, R., Ishihara, K., Schlosser, F. and Poulouse, H. G. (1977). Stress-deformation and strength characteristics. SOA report. Proceedings, 9th International Conference on Soil Mechanics and Foundation Engineering, Tokyo, 2, 421-494.
- Lui, P. C., and Tan, T. S. (2001). “Building Integrated large-Scale Urban Infrastructures: Singapore’s Experience”. *Journal of Urban Technology*, Vol.8, No.1, pp.49-68.
- Mendoza, M. J., and Hartlen, J. (1985). “Compressibility of clayey soils used in land reclamation”. Proceedings of the Eleventh International Conference on Soil Mechanics and Foundation Engineering, San Francisco, Vol.2, pp.583-586.
- Robinson, R. G., and Allam, M. M. (1998). Analysis of consolidation data by a non-graphical matching method. *Geotechnical Testing Journal*, ASTM, 21(2): 140-143.
- Robinson, R. G., Dasari, G. R. and Tan, T. S. (2004). Three-dimensional swelling of clay lumps. *Géotechnique*, Vol. 54, No. 1, pp. 29-39.
- Stallebrass, S E (1990). “Modelling the effect of recent stress history on the deformation of overconsolidate soils”, PhD thesis, City University, UK.

Tan, T. S., Leung, C. F. and Yong, K. Y. (2000). “Coastal reclamation projects in Singapore”. In Proceedings, Coastal Geotechnical Engineering in Practice, Vol.2, IS-Yokohama, Japan, Edited by A.Nakase and T.Tsuchida, pp.119-125.

Whitman, R. V. (1970). Hydraulic fills to support structural loads. Journal of the Soil Mechanics and Foundations Division. Proc. Americal Society of Civil Engineers. ASCE, Vol. 96, SM 1, pp. 23-47.

Yang, L. A., Tan, T. S., Tan, S. A. and Leung, C. F. (2002). One-dimensional self-weight consolidation of a lumpy clay fill. Géotechnique, 52(10), 713-725.

CHAPTER 3

Modelling the behaviour of soils and granular materials

I. F. COLLINS

1. Historical introduction

Leonardo da Vinci had something to say about most aspects of science. For example he noted that; “every heap of sand, whether it be on level ground or sloping, will have its base twice the length of its axis”. This reflects the fundamental fact that the “strength” of sands is governed by critical angles rather than by critical stress levels as in metals and most crystalline solids. Coulomb /1736-1806/ was the first to devise a design procedure based upon the concept that soil strength involves critical angles. He was concerned with designing retaining walls for military fortifications. His procedure was based upon the “failure criterion”, which now bears his name:

$$|\sigma_t| = c + \sigma_n \tan \varphi, \quad (3.1)$$

where σ_t and σ_n are the shear and normal stresses on the failure plane (Figure 1). The cohesion c and friction angle φ were assumed to be a material constants. The cohesion is the shear strength of the material at zero normal stress. Coulomb, wrongly, identified this with the adhesion of the material. Whilst this model is still widely used in geotechnical design procedures, it is now well appreciated that c and φ are not material constants, but depend on the history of the material deformation.

The true granular nature of soils, sands and other geomaterials was recognized by Osborne Reynolds /1842-1912/. He performed a famous experiment (1885), in which a leather bag was filled with lead shot and water. A standpipe was attached, which enabled the pressure in the water to be measured. When squeezed, it was found that the level of water in the standpipe went down indicating that water actually flowed into the bag. This counter-intuitive observation is explained by realising that the individual shot particles have to move apart in order to roll past each other, so that extra void space is created and this is filled by water from the standpipe. Another simple example of this phenomena is when the sand becomes “dry” under one’s foot when walking on a “wet” beach. The shear strains induce a local volume increase (i.e. a dilation) and the surface water drains downwards into the newly created voids. Although critical to the successful modelling of granular materials, as will be seen, “Reynolds dilatancy” is largely ignored in modern continuum, constitutive models of sands and other particulate materials.

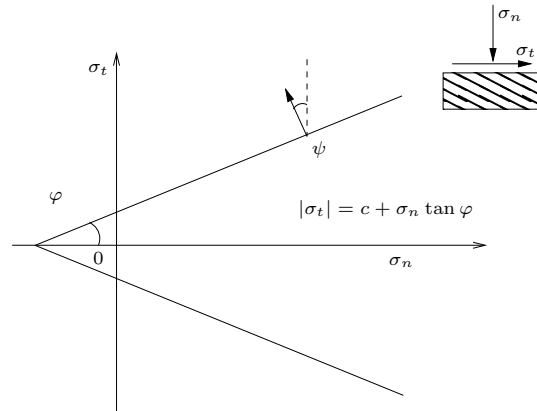


FIGURE 1. Coulomb model

Modern theories of soil mechanics are based upon the pioneering ideas of Terzaghi /1883-1963/, who is regarded as the “father of soil mechanics”. His most important contribution is that of “effective stress”. He proposed that the stress in a saturated soil should be regarded as the sum of the pore pressure u in the water and an effective stress σ'_{ij} borne by the solid particles, so that:

$$\sigma_{ij} = \sigma'_{ij} + u\delta_{ij}, \quad (3.2)$$

where compressive stresses are taken as positive. When first proposed in the 1930’s, this decomposition was the subject of heated debate as described in detail by de Boer (2000), but it has stood the test of time and is now the “foundation concept” of modern soil mechanics.

Casagrande (1947) was one of the first to conduct systematic series of experiments on soils. In particular he found that any sheared sand sample would eventually reach a critical voids ratio, irrespective of the starting conditions. The voids ratio e and specific volume v are two alternative measures commonly used to describe the “dilatant state” of a granular material defined by:

$$e = \Delta V_V / \Delta V_S, \quad (3.3)$$

$$v = \Delta V / \Delta V_S = 1 + e, \quad (3.4)$$

where ΔV , ΔV_V , ΔV_S are, respectively the total volume, volume of the voids and volume of the solid phase. Taylor (1948) was the first to attempt to relate the “strength” of a granular material, as represented by the stress ratio σ_t / σ_n to the degree of dilation. He modelled the Reynold’s effect by considering the sliding of two “saw tooth” surfaces over each other (Figure 2) and deduced the formula:

$$\sigma_t / \sigma_n = \tan \varphi + \tan \psi, \quad (3.5)$$

where φ is the friction angle of the sliding surfaces, and the dilation angle ψ is defined by $\tan \psi = \delta y / \delta x$ (see Figure 2). This equation is an example of a “stress-dilatancy relation”, which demonstrates that the strength of a soil continuum, depends not only on the interface friction between the individual grains, but also the dilatancy induced by the relative motion of these grains. More sophisticated

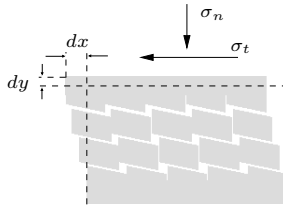


FIGURE 2. Taylor’s interlocking model – the serrated block model provides a simple analogy of the effects of volume change and induced dilatancy and anisotropy

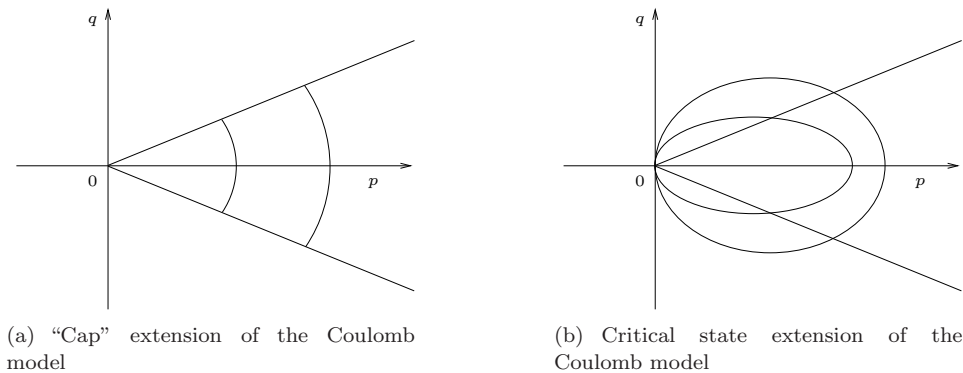


FIGURE 3. Extensions of the Coulomb model

relations, deduced by considering the shearing of idealised arrays of spherical particles were subsequently proposed by Rowe (1962) and Horne (1965). The first attempts at using elastoplasticity theory, which was proving highly potent in explaining the behaviour of metals, to construct constitutive models of soils were made by Drucker, Gibson and Henkel (1957) in the USA and Roscoe, Schofield, Wroth and Burland at Cambridge in the UK – see Schofield and Wroth (1968). The former used the Coulomb model to provide a yield surface governing plastic behaviour under shear, together with a “cap” to model plastic behaviour under compression (Figure 3(a)). The Cambridge models were more sophisticated. The “Coulomb line” was regarded as an “ultimate failure line” and not a yield locus. Yielding was governed by a family of closed yield loci, with normal flow rules, all of which intercepted the “Coulomb line” at points where the plastic volume change (i.e. dilation) is zero (Figure 3(b)). A deformed soil element eventually reached this ultimate line, irrespective of the starting state, in accord with the Casagrande’s findings. This line is, unfortunately, universally known as the “critical state line”, although there is nothing “critical” about it. These early “critical state models” were also notable for the use of energy arguments. The shape of the yield loci was deduced from an expression for the rate of energy dissipation, which was based upon experimental observations in the laboratory, and could also be interpreted in

terms of frictional energy dissipation. Although the mathematical arguments used can now be seen to be seriously flawed, the advent of these physically based models was a major advance. Unfortunately many of the extensions of these early models have lost sight of the need for an underlying physical, conceptual model and are really only recipes for reproducing limited sets of experimental data. These issues are discussed in detail in Sections 3 and 4.

2. Material properties and experimental techniques

2.1. Material properties. Whilst the granular nature of sand is obvious, the fine structure of clays is more complex. At the micron level, clays are constructed of basic platelets comprising layers of silica and alumina crystals. The strength of these platelets is determined by the manner in which these crystal layers are arranged. In a “strong clay” such as kaolin, which is used for making china, the two types of crystal layers are arranged alternately, where as in montmorillinite the basic plate unit consists of single layers of alumina between two layers of silica. The bonding between adjacent silica layers is relatively weak, and can admit water molecules, which results in the clay swelling. These platelets are arranged in a flocculated manner forming “clay particles” known as “peds”, which can be regarded as the “grains” of a clay. From a modelling perspective, the essential difference between clays and sands, is that in sands the grains are of the order millimetres and are elastic/brittle, where as clay grains are of the order of microns, are loosely configured and ductile, and are able to absorb water. For future reference we also note that the flocculated nature of the platelets in a clay ped, means that these particles are able to store elastic energy as the platelets tend to bend under applied loads.

2.2. Laboratory experiments. One of the main problems faced by mechanicians, who want to improve the modelling of sands, clays and other geomaterials, is the limited range of experiments that can be performed on such materials, and the inherent complexity of performing these experiments. The laboratory test most widely used by geotechnical engineers is the “triaxial test”, where a cylindrical specimen can be subjected to axial and radial loading histories. (The use of the word “triaxial” is misleading, as the system actually only has two degrees of freedom. About a dozen “true triaxial” apparatus do exist in the world, but they are significantly more difficult to construct and operate.) Saturated specimens are either loaded “slowly” in so called “drained tests”, the drainage valves are open so that water can drain out and the pore pressure has time to adjust back to its initial value, or “quickly” in “undrained tests” where the drainage valves are kept closed, so that the total volume of the specimen cannot change. The latter test is particularly relevant to earthquake problems. One of the main disadvantages of the triaxial test, from a modelling perspective, is that the symmetry of the apparatus enforces the coincidence of the principal axes of stress and strain rate. The coincidence or non-coincidence of the principal axes of effective stress and plastic strain rate is central to elastoplastic, model construction and is still largely unresolved. The other main laboratory test of value to the modeller is the “direct simple shear” test, though the basic test is limited by the amount of shear strain that can be imposed. This is overcome in the “hollow cylinder, torsional device”, where an annulus of

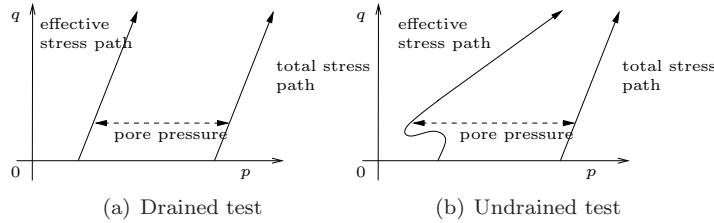


FIGURE 4. Typical triaxial test results

material is subjected to shear strains of up to 200%. These shear tests are not subject to the principal axes coincidence problem discussed above. An excellent account of experimental soil mechanics is given in the book by Bardet (1997).

The standard notation for presenting the results of triaxial results is to define the pressure, shear stress, volume and shear strains by:

$$p = \frac{1}{3}(\sigma_1 + 2\sigma_3), \tag{3.6a}$$

$$q = (\sigma_1 - \sigma_3), \tag{3.6b}$$

$$e_v = (e_1 + 2e_3), \tag{3.6c}$$

$$e_\gamma = \frac{2}{3}(e_1 - e_3), \tag{3.6d}$$

where the suffices 1 and 3 refer to the axial and radial components respectively. The definitions are chosen so that these components are work conjugate. Note that from now on all “stresses” are to be interpreted as “effective stresses” and the “prime” notation introduced in (3.2) is dropped. Typical results for drained and undrained tests in the case when the radial stress is held constant, where $dq = 3dp$, are illustrated in Figure 4. Since the pore pressure is constant in a drained test, the effective and total stress paths are parallel. In an undrained test the effective stress exhibits an “S-shaped” curve. The effective pressure initially decreases and the pore pressure increases, but of further deformation the stress path turns upwards and becomes close to a radial line through the origin. This decrease in effective pressure is important as the sample is behaving more like a fluid and can lead to “liquefaction”, which is one of the most destructive consequences of earthquakes, e.g. Ishihara (1993). Two further problems with laboratory testing should be noted. Ideally the deformation of the specimen should be homogeneous, so that it is a genuine “element test”. Unfortunately the deformations are inherently unstable. For example the deformation of specimens of dense sand or over-consolidated clays (clays which have in the past been subjected to high pressure, such as due to an overlying ice sheet) localise and the deformation is concentrated in shear bands. This is a subject which has much interest for the applied mathematician – see the book by Vardoulakis and Sulem (1995) for example. It is also of great practical importance, since such failures frequently occur in practice and must be designed against. Conversely, specimens of loose sand exhibit barrelling inhomogeneities at strains of around 15% and the results at higher strains are meaningless. This is one reason for the current interest in the torsional shear apparatus. The second problem

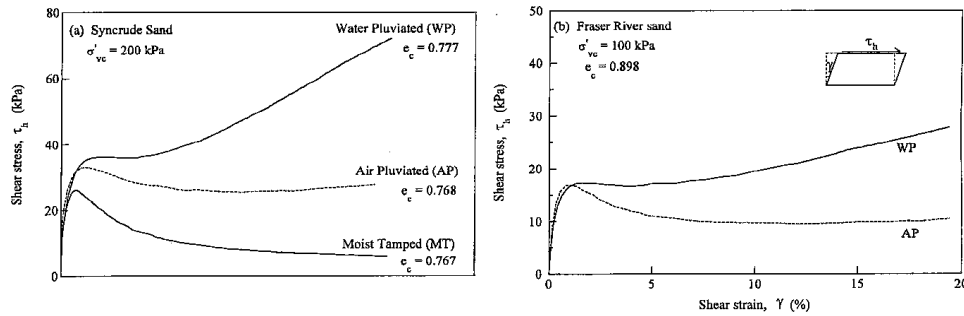


FIGURE 5. Dependence of effective stress path on preparation procedure, after Vaid et al. (1999)

arises from the observation that the response of the specimen is highly dependent on the preparation procedure. In one of the commonest such procedures, known as “moist tamping”, successive layers of moist sand are poured into the test cell and then tamped in order to achieve the desired initial voids ratio (porosity). Due to the presence of significant capillary action it is possible to generate very loose samples, with voids ratios much larger than those which actually occur in nature. Undrained tests on such samples exhibit significant liquefaction, and for a time there was much interest in such experiments. However it is now appreciated that such specimens are highly unrealistic. Specimens prepared by “wet or dry fluviation” do not exhibit such catastrophic loss of strength. In these procedures either (a) water is put in the cell first and then dry sand is carefully poured afterwards – “wet pluviation”, or (b) the order is reversed – “dry pluviation”. This phenomena has been carefully studied by Vaid et al (1999), and one of his figures is reproduced here in Figure 5. The lesson for the modeller is that the “internal structure” of a granular material has a highly significant effect on its macro-behaviour.

2.3. Discrete element methods of simulation (DEM). The first computer simulation of the behaviour of the deformation of granular materials was developed by Cundall and Strack (1979), and now there are a number of commercially available simulation codes. The grains are treated as individual rigid, elastic or elastoplastic particles, and the motion of an assembly of such particles is solved incrementally, using Newton’s laws of motion and appropriate interparticle contact laws. From the constitutive modelling perspective the most important observation is that the transfer of stress through the assembly is highly inhomogeneous. The bulk of the load is carried by the “force chains” as illustrated in Figure 6. The interparticle contact stress is frequently 8-10 times larger than the mean value. These chains tend to align themselves with the greater compressive principal stress. The force chain network is often referred to as the “strong network”, whilst the set of particles which carry lower than average stresses form the complementary “weak network”. Most of the elastic energy stored in the compressed grains occurs in the strong network, whilst most of the frictional dissipation occurs in the weak network. The high values of the normal component of the contact stresses in the force chains, prevents significant interparticle slip.

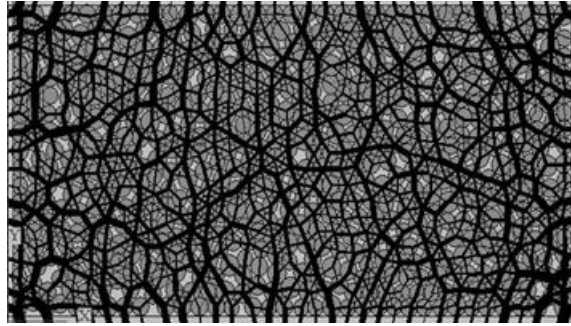


FIGURE 6. DEM simulation of isotropic compression, showing weak and strong networks (force chains) – the thickness of lines in proportional to contact force

Whilst there have been many studies of the mechanics of assemblies of various types of particles using DEM simulations, they have, to date, provided little information of value to the continuum constitutive modeller. Indeed many argue that a continuum approach is inappropriate to granular materials. However from the view point of a geotechnical engineer, such continuum “engineering” models are a necessity. In practice the engineer will have little detailed knowledge of the micro-structure of the soil, so that what is required are models which pick out the “essential features” of the micro-mechanical behaviour, i.e. those which significantly effect the material’s response at the macro-level. Some ideas along these lines have been proposed by Radjai et al (1998) and Thornton and Antony (2000). They noted that the mean stress distribution in the weak network is effectively isotropic and the deviatoric part of the stress is entirely carried by the force chain network, which forms the “backbone” of the granular assembly. This suggests the use of “bi-modal” models, in which two stress systems are required to describe the behaviour in a representative continuum element. Some developments along these lines have been suggested by Collins (2005a). This issue is discussed further in Section 4.

3. Some extant theories of soil mechanics

3.1. Coulomb models. The early attempts at constructing theories of soils, which lead to the posing of boundary value problems, were based upon the theory of rigid perfectly-plastic solids, which had been developed so successfully in the context of metal forming and structural analysis. In particular attention was concentrated on the extremum principles which enabled one to calculate upper and lower bounds to the failure load, and on the theory of sliplines, which took advantage of the hyperbolic nature of the governing equations for plane strain deformations to obtain quasi-analytic solutions to a large number of important engineering problems. The Mises or Tresca yield conditions for the plastic deformation of metals were replaced by the Coulomb condition as in (3.6a). In (1965) the English translation of the Russian book by Sokolovskii was published. It describes a number of “solutions” to practical geotechnical problems, such as slope and foundation failures. However

his solutions were only “partial” in the sense that he only considered stress fields which satisfied equilibrium and the yield condition in the deforming region. To demonstrate that the solution is unique it is necessary to also demonstrate the existence of a kinematically admissible velocity field, which is one which satisfies all kinematic boundary conditions, and is compatible with the assumed yield condition via a “normal or associated flow rule” – see below. In addition, it is necessary to demonstrate that the stress field is “statically admissible”, in the sense that the yield condition is not violated in any proposed rigid regions of the solution. Sokolovski’s “solutions” did not satisfy either of these two conditions.

In constructing a rigid perfectly plastic model it is necessary to formulate a flow rule as well as a yield condition. In metal plasticity it had been found experimentally that a “normal flow rule” was highly realistic. If the yield condition is given by $f(\sigma) = 0$, then the normal flow rule takes the form:

$$\dot{\epsilon}^p = \dot{\lambda} \frac{\partial f}{\partial \sigma}. \quad (3.7)$$

This equation requires the direction of the vector of plastic strain rate components to be normal to the yield surface. This is illustrated in Figure 1 for the Coulomb model. This condition is sufficient to guarantee uniqueness of the solution to the rigid plastic collapse problem, and the validity of the associated extremum principles (limit theorems). The parameter $\dot{\lambda}$ is unspecified, so that the magnitude of these strain rates is not determined by the constitutive law, reflecting the fact that plastic deformations are rate-independent. In Figure 1 it can be seen that this strain rate vector has a shear component $\dot{\epsilon}_\gamma^p$ and that its volumetric component $\dot{\epsilon}_v^p$ is dilatant, since it is in the direction of negative normal stress¹ σ_n . The ratio of these two components defines the “dilation angle” ψ

$$\tan \psi \equiv -\frac{\dot{\epsilon}_v^p}{\dot{\epsilon}_\gamma^p}. \quad (3.8)$$

For a Coulomb material the normal flow rule requires the dilation angle ψ to be equal to the friction angle φ . As already noted dilation is an essential feature of granular materials. However where as the friction angle for sand is in the range 35°-45°, the dilation angle is rarely greater than 10°. The normal flow rule assumption is hence quite unrealistic for granular materials. This has serious consequences for a rigid perfectly-plastic modelling approach, as the uniqueness and associated extremum principles are no longer valid. A rigid plastic model can be viewed as the limit of a family of elastic/hardening models in which the elastic stiffness is infinite and the hardening modulus is zero. Boundary value problems for elastic/hardening plastic materials must be formulated incrementally, and it is necessary to follow the deformation from the initial state to the final “failure state” in which the deformations become unbounded. In general this final failure state will depend on the initial state and the loading path. The incremental problem is unique even if the flow rule is non-normal, except when bifurcations occur as when the deformation becomes localized and shear bands form. Perfectly plastic models, with normal flow rules, where the failure state is independent of the loading history are hence the exception rather than the rule.

¹We are taking compressive stresses and strains as positive.

Another problem with the Coulomb model arises from the interpretation of the cohesion. Well defined granular materials, such as sand, have no cohesion, so that $c = 0$ in (3.6a). Clays which have been undisturbed for many years develop significant chemical bonds between the “peds” and have a true cohesion. However reconstituted, saturated or partially saturated clays also exhibit an “apparent cohesion”. This is due to the large surface tension forces that can develop at an air-water-solid interface and which induce negative pore pressures (suctions). These forces are inversely proportional to the size of the voids between the solid particles. Since the dimensions of voids in clays are of the order of microns, the corresponding surface tensions are significant, producing pore suctions of the order of 140 kPa, which is sufficient to support a vertical cliff 14 meters high. It is hence customary when modelling reconstituted clays to put the true cohesion to zero in the same way as for sands.

3.2. Double shearing models. Another difficulty which arises when trying to generalize classical slipline theory to Coulomb materials is that the stress and velocity characteristics do not coincide. Elementary stress analysis shows that in plane strain, the yield condition (3.6a) is attained on line segments which make an angle of $\pi/4 - \varphi/2$ with the direction of maximum compressive principal stress. These are the stress characteristics used by Sokolovskii described above. At failure it is observed that the deformation is isochoric, so that the corresponding velocity characteristics are the zero-extension directions and hence are at angles of $\pi/4$ to the principal strain rate axes. If we assume the material is isotropic, the principal axes of stress and plastic strain rate coincide, so that these two sets of characteristics only coincide in the frictionless limit where $\varphi = 0$ as in the case of metals. We are hence left in the unsatisfactory position of having a model in which the failure condition develops on one line segment, but failure occurs by shearing on another. Spencer (1964, 1982) following earlier work by Mandel and de Josselin de Jong, proposed a modified model in which the deformation is the sum of two shearing motions on the two Sokolovskii stress characteristics. This gets over the above objections. The principal axes of stress and plastic strain rate do not now coincide, even though the material is isotropic. This however does not violate the basic coincident axis theorem for isotropic materials, since the constitutive model is a relation between three tensors: the plastic strain rate, stress and stress-rate. The theory hence falls outside the scope of traditional plasticity models, in which the stress rate does not figure in the flow rule. This theory is the forerunner of an extended family of models for rate-independent theories, now termed “hypo-plastic”. This theory has many mathematical attractions and has been developed by a number of researchers. However many of the resulting solutions turn out to be unstable, and it is not widely used in geotechnical modelling. Another reason for this is that it is essentially an isotropic theory and experiments and DEM simulations conclusively demonstrate that significant anisotropy is induced at very small strains (of around 2%). Collins (1990) has also shown that the critical state models, to be discussed shortly, provide an alternative explanation for the non-coincidence of the two sets of characteristics.

3.3. Cap models. Another shortcoming of the Coulomb criterion, is that it does not predict yielding under isotropic compression. As already noted Drucker

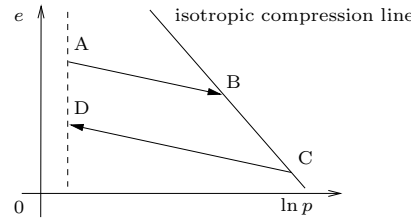


FIGURE 7. Loading/unloading paths in e - $\ln p$ plane

et al. (1957) suggested a modification in which a “cap” is added to the Coulomb failure lines as shown in Figure 3(a), so that two separate yield criteria and hardening rules are required. Whilst this approach still remains popular in the USA, the critical state models, described in the next section are far superior in many respects. For example yielding under shear and under isotropic compression are modelled by the same yield locus.

3.4. Critical state models. The critical state models are the most successful of the extended Coulomb models. They were developed during the 1960’s in Cambridge, principally by Roscoe, Schofield, Wroth and Burland – see Schofield and Wroth (1968). See the recent book by Schofield (2005) for an intriguing historical account of the development of these models. They are often referred to as the “Cambridge” models. As well as including Coulomb’s ideas of failure, they take account of the influence of the voids ratio on the material behaviour and are able to predict the different behaviours of “loose” samples, which contract upon shearing, and “dense” ones, which dilate in apparant accord with Reynolds’s experiments. (We use the qualifier “apparant” since, as will be seen, the dilatant behaviour predicted by the Cambridge models has nothing to do with the ideas of Reynolds.) They also model Casagrande’s findings that the soil sample eventually reaches a “critical state”, with a constant voids ratio, which is independent of the initial conditions. The original models have been found to work best for clays and we will initially concentrate on the behaviour of clays. The typical behaviour of clays under isotropic compression is illustrated in Figure 7 in an e - $\ln p$ diagram. Let us assume the sample is initially at a voids ratio e_1 and effective pressure p_1 corresponding to the point A. Upon loading the sample follows the straight line AB, and if it is unloaded it returns to A, so that the deformation is elastic. However upon reaching B the sample follows the fixed line BC, where both plastic and elastic strains occur. If it is then unloaded from C it follows the line CD, which is parallel to AB. This is the elastic unloading (or swelling line). The loading cycle is completed at D, so that the voids ratio of the sample has been reduced to e_2 , but the pressure is unchanged. Instead of using e , one could equally well use the specific volume $v = 1 + e$, and increasingly researchers are using $\ln v$ instead of v . It is found that experimental points fit a straight line in $\ln v$ - $\ln p$ space, just as well as in a e - $\ln p$ diagram. The use of $\ln v$ has many theoretical advantages as it can be interpreted as a volumetric strain.

For ease of presentation we will present the basic concepts of critical state soil mechanics (CSSM) in terms of triaxial tests using the nomenclature introduced in (3.6a). In these models the “state” of the soil sample is determined if we know the voids ratio e , the effective pressure p and the shear stress q . The hardening properties of CSSM models are determined by the changes in the volume, i.e. in e . Unlike metals there is no shear hardening. The yield loci of the most widely used model, known as “Modified Cam Clay” are shown in Figure 8. These loci consist of a family of ellipses, all of which have the pressure axis as a principal axis, and all of which pass through the origin. The “critical state lines” (CSL’s) are defined to be the straight lines, which intercept the ellipses at the points where the tangents are horizontal. The slope of the lines is denoted by $\pm M$, where M is a dimensionless material constant, which is an effective “friction coefficient”. The equation of the family of ellipses can be written:

$$q = \pm M \sqrt{p(p_c - p)}, \quad (3.9)$$

where p_c is the intercept on the p axis and is hence the yield pressure under isotropic compression ($q = 0$), often referred to as the pre-consolidation pressure. This pressure p_c acts as a label, defining a particular ellipse, and since the voids ratio e decreases as p_c increases, it follows that the expansion of the elliptical yield loci corresponds to densification of the sample. The plastic deformation is assumed to be governed by the normal flow rule. Hence at points to the right of the CSL the volumetric part of the plastic strain rates are contractive, so that the voids ratio will decrease and the yield loci will expand. However at points to the left of the CSL, this strain rate component is dilative, and the yield loci will hence contract. This is illustrated in Figure 8 for the case of a drained test performed at constant pressure. In all cases the stress path must eventually terminate at the CSL, where $q = \pm Mp$, and where the volumetric part of the plastic strain rate is zero. The yield loci can hence no longer change and the sample will continue to shear, but at constant volume and at constant stress levels (i.e. e , p and q are all constant). This is the definition of a “critical state”. The behavior to the right of the CSL is typical of “loose samples” which contract upon shearing. Clays which exhibit this behavior are termed “lightly over-consolidated”. On the other hand the behavior to the left of the CSL is typical of dense samples or “heavily over-consolidated clays”, whose pre-consolidation pressure p_c is significantly larger than the current pressure value. This situation occurs when the ground has been covered by an ice sheet at some time in its history or in deep excavations.

This model also gives a satisfying new interpretation of “Coulomb failure”. The Coulomb failure line has been superseded by the critical state line. When the soil reaches this line it “fails” by shearing without any changes in stress. However it is not a yield line, and many of the difficulties encountered by early workers, who attempted to construct a plasticity theory using the Coulomb criterion as a yield condition, are overcome. The normal flow rule requires the strain rate vector to be normal to the elliptical yield loci, not to the Coulomb line. This development also meets the objections regarding the non-coincidence of stress and velocity characteristics in plane strain problems discussed above in Section 3.2. At a point on the CSL the stress is subject to two constraints (a) because it lies on the CSL and (b) because it lies on an elliptical yield locus. Each constraint yields

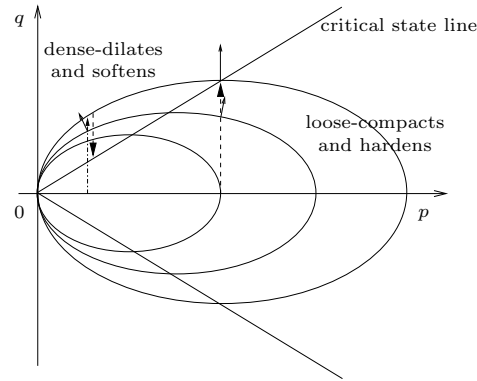


FIGURE 8. Modified Cam Clay model – both loose and dense specimens end up on CSL

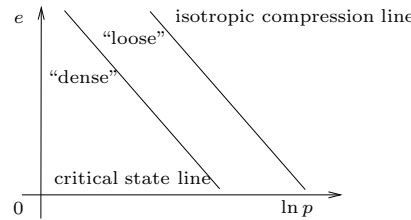


FIGURE 9. Isotropic and critical state lines in $e-\ln p$ plane

a family of stress characteristics, so that there are actually two families of stress characteristics. Those used by Sokolovskii correspond to constraint (a) whilst the new family resulting from (b), which, as a result of the normal flow rule assumption, do coincide with the velocity characteristics. There is hence no paradox. When at the critical state, the model assumes a unique relation between the critical state pressure p_{csl} and the voids ratio e . This relation is given by a straight line in $e-\ln p$ space, which is parallel to the isotropic compression line (ICL), as shown in Figure 9. This embodies Casagrande’s findings that the ultimate behaviour is independent of the initial conditions. Material states between the CSL and ICL represent “loose” states, since they have to compact to reach the CSL, on the other hand states below the CSL have to dilate. It is very important to appreciate that “loose” and “dense” behaviour depends on the current pressure as well as on the voids ratio. Increasing the pressure at constant voids ratio converts an initially “dense” sample to one which exhibits “loose” behaviour.

Whilst this model was a big advance at the time, it is now appreciated that it has many shortcomings. It has been found to reproduce the behaviour of lightly over-consolidated clays, which are necessarily on the loose side of critical, very well. However it fails to predict the detailed behaviour of heavily over-consolidated, i.e. “dense” clays, and of sands, whatever the initial density. It is essentially an isotropic theory, where as, as already noted, granular materials exhibit pronounced

anisotropic behaviour very early in a deformation. Also the normal flow rule assumption is at odds with many experimental observations. It also assumes the critical state lines in both, e - $\ln p$ and q - p space are unique. Experimental results are inconclusive on this issue, and is a subject of much current debate, e.g. Chu (1995), Chu and Lo (1994), Mooney et al (1998).

Various extensions of the basic theory have been proposed, and here we mention just a few. Many experiments have shown that the behaviour of sands depends just on the “distance” of the current state from the CSL in e - $\ln p$ space. Been and Jefferies (1985) hence proposed that this distance could be used as a “state parameter”, viz: $\zeta \equiv e - e_{csl}$ where the two voids ratios are evaluated at the same pressure. The resulting models are able to reproduce some of the observed behaviour sands in triaxial tests, subjected to monotonic loading, but these models are still isotropic. Anisotropy can be included by allowing the yield loci to rotate in the q - p plane, e.g. Dafalias (1986), whilst cyclic loading has been modelled by using two families of yield loci, which expand and translate according to some complex hardening laws, e.g. Hashiguchi (1989).

A major objection to all these models, is that, with the notable exception of the original Cambridge models, they are mostly in the nature of “recipes”, in which yield loci, flow and hardening rules are chosen to provide “models”, which predict the behaviour observed in the limited range of laboratory experiments. There is seldom any discussion of the underlying physics of the model. In the writer’s view such “recipe” models are of dubious value, and pose the question: “What validity do they have when used as the basis for solving complex, engineering boundary value problem?”

4. Thermomechanical approaches to the constitutive modelling of soils

4.1. The Cambridge approach. The original approach to critical state soil mechanics (Schofield and Wroth (1968), Roscoe and Burland (1968), see also Muir Wood (1990, 2002), Schofield (2005)) was based on the plastic work equation:

$$\widehat{W}^p \equiv p\dot{e}_v^p + q\dot{e}_\gamma^p = Mp\dot{e}_\gamma^p, \quad (3.10)$$

where we are again using the standard notation for triaxial tests. This relation equates, the rate of plastic work, to the rate of energy dissipation. The latter being assumed to be entirely due to frictional shearing, M being the effective frictional coefficient. In using (3.10) the rate of elastic work is tacitly assumed to be balanced by the rate of change of the recoverable, elastic free energy. This equation can be rewritten:

$$\eta \equiv \frac{q}{p} = M + \tan \psi, \quad (3.11)$$

ψ is the dilation angle defined in (3.8).

In this form the relation is equivalent to Taylor’s (1948) classical stress-dilatancy equation. It can be interpreted as stating that the strength of the material as exhibited by the stress ratio η is the the some of two terms: M , which arises from internal friction and $\tan \psi$, which is due to the dilation. Schofield and Wroth (1968) then identified this dilation angle with the normal to the plastic potential function,

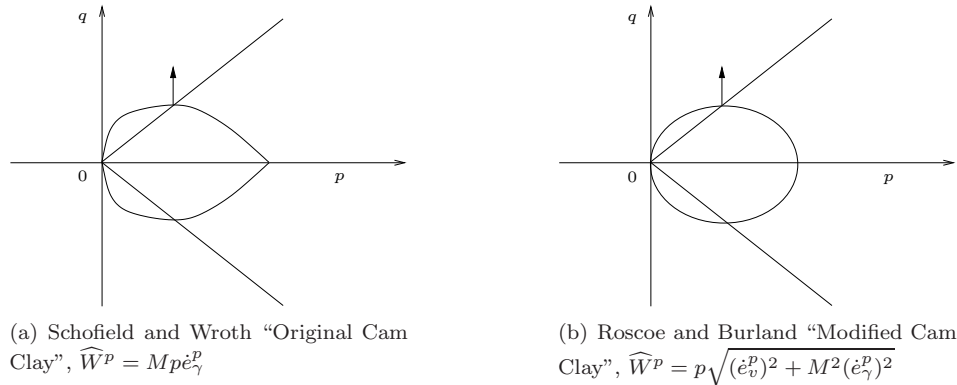


FIGURE 10. Original and modified Cam Clay models

so that (3.10) can again be rewritten:

$$\frac{q}{p} = M + \frac{dq}{dp}, \tag{3.12}$$

which integrates to give $q = Mp \ln(p_c/p)$. Drucker’s postulate, or the maximum work hypothesis, was then invoked to identify the plastic potential and the yield locus, so that the flow rule is “normal”. The yield loci given by (3.12) and illustrated in Figure 10, determine the model now known as “Original Cam clay”. These yield loci have a vertex on the pressure axis, where $p = p_c$. As explained above this consolidation pressure p_c is assumed to be a unique function of the voids ratio e . This function describes the expansion or contraction of the yield loci. It should be noted that although this, and the other classical critical state soil models are frequently referred to as being “isotropic hardening models”, they do in fact contain a “volumetric kinematic hardening” component in the sense that they translate along the pressure axis as well as expand isotropically. Of course they still describe isotropic material behaviour. This observation is important since the physical origins of kinematic and isotropic hardening are very different.

However some of the specific properties of the model, such as the vertex, were deemed to be unsatisfactory by some, and Burland (1965) and Roscoe and Burland (1968) produced the “Modified Cam Clay” model, by postulating a plastic work equation, which includes volumetric dissipation:

$$\widehat{W}^p = p\dot{e}_v^p + q\dot{e}_\gamma^p = p\sqrt{(\dot{e}_v^p)^2 + M^2(\dot{e}_\gamma^p)^2} \tag{3.13}$$

which, using the procedure described above, predicts the yield loci of (3.9) and associated flow rule of the “Modified Cam Clay” model already discussed in Section 3.3 and also illustrated in Figure 4.1. The yield loci are now elliptical, and do not have vertices, but the stress-dilatancy relation is now markedly different from that proposed by Taylor and is found not to be as realistic. Nevertheless the new yield loci are found to be more in accord with experiment, at least for lightly over-consolidated clays.

4.2. A critique of the Cambridge approach. Here we are concerned with the validity of the arguments, illustrated above, which were used to establish the yield condition and flow rule, from a postulated dissipation function. Although they have been used by many subsequent workers, they are open to a number of major criticisms. The modern theory of thermomechanics of elastic/plastic materials – sometimes referred to as “hyper-plasticity” (Houlsby and Puzrin 2000, 2006) will be used in the next section to overcome these various difficulties.

- (a) The plastic work equations (3.10) and (3.13) identify the plastic work rate \widehat{W}^p with the rate of dissipation function $\widehat{\Phi}$. This is not generally true. In the current class of models, which are assumed to be isothermal, in which a soil state is defined by the elastic and plastic strains, the free energy function in general, depends on the plastic as well as the elastic strain. The free energy Ψ is frequently assumed to be decoupled and can be written as the sum of two state functions: the elastic free energy $\Psi^e(e^e)$ and the plastic free energy $\Psi^p(e^p)$ (Collins and Houlsby (1997), Collins and Kelly (2002), Ulm and Coussy (2003)). The plastic work equation should hence be written:

$$\widehat{W}^p = \dot{\Psi}^p + \widehat{\Phi}, \quad (3.14)$$

where $\widehat{\Phi} \gtrsim 0$.

Physically this extra term Ψ^p represents that proportion of the elastic energy stored at the micro-level, within the elastically deformed grains, that is not recovered during elastic unloading. Instead it is trapped as a result of the “grain rearrangement” associated with the plastic deformation. It is frequently referred to as “frozen elastic energy” or “stored plastic work” (Coussy (1995), Ulm and Coussy (2003), Collins (2005b)). It can only be recovered under reversed plastic loading. It would seem to be of more importance in clays than sands, since, in addition to the effect of grain rearrangement, energy can be stored at the micro-level within elastically deformed platelets within the flocculated particle structure. The rate of change of the plastic part of the free energy can be used to define the shift or back stresses p^s and q^s :

$$\dot{\Psi}^p = p^s \dot{e}_v^p + q^s \dot{e}_\gamma^p \quad (3.15)$$

These stresses control the kinematic aspects of the material hardening.

- (b) The use of the current pressure p in the expression for dissipation means that the dissipation mechanism is unaffected by pre-consolidation, so that the material has no memory. Whilst this would seem appropriate for sands at confining pressures low enough not to induce crushing, it would not seem apt for clays or crushable sands, whose structure is significantly affected by prior consolidation. In fact the modern hyper-plastic, thermo-mechanical procedure when applied to the dissipation functions in (3.10) and (3.13), results in open ended, “Coulomb-type” yield loci, with no pre-consolidation pressure as shown by Collins and Hilder (2002).
- (c) Similarly the “dissipative stresses” p^D and q^D can be defined by:

$$\widehat{\Phi} = p^d \dot{e}_v^p + q^d \dot{e}_\gamma^p. \quad (3.16)$$

Thus, whilst it is the inner product of the plastic strain rate with the actual stress, which gives the plastic work rate, it is the inner product with the dissipative stress, which gives the dissipation rate. The rate independence of a material requires its dissipation function to be homogeneous of degree one in the plastic strain rates. One of the most powerful and useful results of hyper-plastic thermomechanics is that for such materials, the dissipative stresses must lie on a yield locus, whenever dissipation occurs, and that the plastic strain rates are always given by a normal flow rule in “dissipative stress space”. The yield function in “true stress space” can then be found by using the shift stresses. When the dissipation function involves the actual pressure, the flow rule is no longer normal in true stress space as shown by Collins and Houlsby (1997) and Collins (2005a). The flow rule is hence determined by the two thermodynamic potentials Ψ^p and $\hat{\Phi}$ and one does not have to invoke any extraneous postulate such as Drucker’s or any other “normality rule”. Details of the hyper-plastic arguments are given in the next section.

- (d) The use of the simple frictional dissipation rate function in (3.10) used to generate the original Cam clay model, actually violates the second law of thermodynamics, as volume changes do not dissipate any energy, so the model cannot model isotropic compression. This fault is corrected in the modified Cam clay model in (3.13).

Although the models’ flow rules predict dilative behaviour on the dense side of critical, this dilation has nothing to do with the ideas of Reynolds, which envisages dilation occurring as a result of concomitant, shear deformations. Dilation in the Cambridge models is due to the recovery of stored plastic work. In addition, as already noted, the whole model structure is isotropic and based upon “normal flow rule plasticity theory”, in violation of observations. These ideas are discussed in the next section where it is shown that the concepts of the flow rule, Reynolds dilatancy and induced anisotropy are intimately interconnected.

4.3. The modern thermomechanical approach to modelling rate independent materials – “hyper-plasticity”. As already stated, this approach starts by postulating forms of the free energy Ψ and rate of dissipation potential $\hat{\Phi}$ and deducing the form of the constitutive equation. In the case of a rate independent material, this means deducing the yield function and flow rule. This procedure was developed in reasonable generality by Ziegler (1983). Recently the theory has been made more rigorous notably by Rajagopal and Srinivasa (1998, 2002). Text book accounts can be found in the books by Maugin (1992, 1999).

The first step is to stipulate the “state” or “internal” variables which uniquely define the current state of the model material. It is clearly impractical to specify the position and orientation of each and every particle, so that it is necessary to use sample statistical parameters. The voids ratio e or specific volume v is an uncontroverted choice, though $\ln v$ is a more useful parameter as it can be interpreted as a volume strain. Shear strains are more problematic and require the stipulation of some reference state. The use of the zero stress reference state is also problematic since it does not lie in the elastic domain. The critical state is a possible reference

state, as in the Been and Jefferies “state parameter” models, but this presumes the existence and uniqueness of such a state. Most theories are expressed in terms of elastic and plastic strains e^e and e^p , defined with respect to the initial state. However it must be appreciated that the use of these strains is an assumption. Attempts at understanding the significance of this assumption have been made by Nicot and Darve (2006) and Collins and Einav (2005), whilst more general formulations are discussed in Collins (2005a). The free energy and dissipation potentials will be written:

$$\Psi(e^e, e^p) = \Psi^e(e^e) + \Psi^p(e^p), \quad (3.17)$$

and

$$\widehat{\Phi}(\dot{e}^p) = \frac{\partial \widehat{\Phi}}{\partial \dot{e}^p} : \dot{e}^p. \quad (3.18)$$

The first relation embodies the “decoupled assumption” Mroz (1973), Ulm and Coussy (2003), and the separate elastic and plastic parts of the free energy function are also assumed to be state functions. For rate independent materials the dissipation rate function must be a homogeneous function of degree one. The second relation in (3.17) then follows from Euler’s Theorem. The basic work rate equation (3.14) can now be rewritten:

$$\widehat{W}^p = \sigma : \dot{e}^e + \sigma : \dot{e}^p = \frac{\partial \Psi^e}{\partial e^e} : \dot{e}^e + \frac{\partial \Psi^p}{\partial e^p} : \dot{e}^p + \frac{\partial \widehat{\Phi}}{\partial \dot{e}^p} : \dot{e}^p. \quad (3.19)$$

Equating the elastic and plastic strain rate terms, gives the relations:

$$\sigma = \frac{\partial \Psi^e}{\partial e^e}, \quad (3.20)$$

$$\sigma = \frac{\partial \Psi^p}{\partial e^p} + \frac{\partial \widehat{\Phi}}{\partial \dot{e}^p}. \quad (3.21)$$

The first relation is the classical elasticity law. The second relation does not, in general, follow from (3.19) because the dissipation potential $\widehat{\Phi}$ is a function of the plastic strain rates \dot{e}^p . The stronger result in (3.20) is an example of Ziegler’s hypothesis. It is equivalent to stating that not only the entropy production, and hence the dissipation rate, is positive, as required by the Second Law of Thermodynamics, but that it is also maximal. This stronger hypothesis is required to produce unique constitutive formulations. So far, no counter example has been found to this stronger requirement. See Rajagopal and Srinivasa (1998) for a comprehensive discussion of these issues.

The total stress is hence the sum of two stresses, which we will term the shift and dissipative stresses respectively:

$$\sigma^s = \frac{\partial \Psi^p}{\partial e^p}, \quad (3.22)$$

$$\sigma^d = \frac{\partial \widehat{\Phi}}{\partial \dot{e}^p}, \quad (3.23)$$

so that

$$\widehat{\Phi} = \sigma^d : \dot{e}^p \geq 0. \quad (3.24)$$

The shift stress is that part of the stress which produces the “stored plastic work” or “frozen elastic energy” already discussed, whilst the dissipative stress is that

part which produces energy dissipation. The variation of the shift stress with the deformation induces kinematic hardening represented by the translation of the yield surface, whilst the dissipative stress governs the isotropic hardening component in which the yield surface expands or contracts.

Normally $\widehat{\Phi}$ depends on the plastic strain, which determines the isotropic hardening law, and the plastic strain-rate. Since $\widehat{\Phi}$ is homogeneous of degree one in the plastic strain rates, its Legendre (or Legendre-Fenchel) transform $F(e^p, \sigma^d)$ is singular. It is hence zero valued with a non-unique inverse (c.f. Sewell (1987), Maugin (1992, 1999)), hence:

$$F(e^p, \sigma^d) = 0, \tag{3.25}$$

$$\dot{e}^p = \dot{\lambda} \frac{\partial F}{\partial \sigma^d}. \tag{3.26}$$

where $\dot{\lambda}$ is an undertimed multiplier. This is, of course just the yield condition and normal flow rule of classical plasticity theory, except that it is formulated in dissipative and not true stress space. The yield condition and flow rule in true stress space are

$$F^*(e^p, \sigma) = F(e^p, \sigma - \sigma^s) = 0, \tag{3.27}$$

$$\dot{e}^p = \dot{\lambda} \frac{\partial F^*}{\partial \sigma}. \tag{3.28}$$

The flow rule is hence still normal in true stress space since the shift stress depends only on the plastic strain.

This argument has to be modified however, if the rate of dissipation potential depends additionally on components of the stress tensor, as in the frictional dissipation potentials in (3.10) and (3.13). In this situation, the potential is of the form $\widehat{\Phi}(\sigma, e^p, \dot{e}^p)$ and the dual dissipative yield condition is $F(\sigma, e^p, \sigma^d) = 0$, and the flow rule is still given by (3.27) with σ being treated as a passive parameter. However, the yield condition and flow rule in true stress space now become:

$$F^*(e^p, \sigma) = F(\sigma, e^p, \sigma - \sigma^s) = 0, \tag{3.29}$$

and

$$\dot{e}^p = \dot{\lambda} \frac{\partial F^*}{\partial \sigma} - \dot{\lambda} \frac{\partial F}{\partial \sigma}, \tag{3.30}$$

so that the flow rule is non-normal, but differs from the classical formulation as it does not use a potential function and involves an additive correction factor. The true stress space yield condition is obtained from the dissipative yield condition, by performing a shift, translation operation, as usual in kinematic hardening models, but in addition the yield surface undergoes a distortion. Some examples are given in Section 4.4. This result was first given in Collins and Houslyby (1997), and in greater generality in Collins (2005a). These considerations show why non-normal flow rules are necessary in materials exhibiting frictional dissipation.

4.4. The thermomechanical approach to Cambridge models. Under tri-axial conditions the basic plastic work equation (3.19) can be written:

$$\widehat{W}^p = p \dot{e}_v^p + q \dot{e}_\gamma^p = p^s \dot{e}_v^p + p^d \dot{e}_v^p + q^d \dot{e}_\gamma^p, \tag{3.31}$$

where $p^s = \frac{\partial \Psi^p(\epsilon_v^p)}{\partial \epsilon_v^p}$ is the shift pressure, and p^d and q^d are the dissipative pressure and shear stress respectively. Here we are assuming that the plastic shear strains do not induce any “frozen elastic energy” so that there is no q^s term. A view supported by the experiments of Luong (1986) and Okada and Nemat-Nasser (1994). It follows that:

$$p = p^s + p^d, \tag{3.32}$$

$$q = q^d. \tag{3.33}$$

In order to generate the modified Cam clay model we will choose the dissipation potential to be:

$$\widehat{\Phi} = p^{cd} \sqrt{(\dot{\epsilon}_v^p)^2 + M^2(\dot{\epsilon}_\gamma^p)^2}, \tag{3.34}$$

where p^{cd} is that part of the consolidation pressure which causes dissipation. From (3.24) the dissipative stresses are hence given by:

$$p^d = \frac{\partial \widehat{\Phi}}{\partial \dot{\epsilon}_v^p} = (p^{cd})^2 \frac{\dot{\epsilon}_v^p}{\widehat{\Phi}}, \tag{3.35}$$

$$q^d = \frac{\partial \widehat{\Phi}}{\partial \dot{\epsilon}_\gamma^p} = (Mp^{cd})^2 \frac{\dot{\epsilon}_\gamma^p}{\widehat{\Phi}}. \tag{3.36}$$

Eliminating the plastic strain rates gives the elliptical, dissipative yield condition and associated flow rule:

$$\left(\frac{p^d}{p^{cd}}\right)^2 + \left(\frac{q^d}{Mp^{cd}}\right)^2 = 1, \tag{3.37}$$

and

$$\tan \psi \equiv -\frac{\dot{\epsilon}_v^p}{\dot{\epsilon}_\gamma^p} = \frac{M^2 p^d}{q^d}, \tag{3.38}$$

which using (3.32) gives the elliptical yield loci in true stress space:

$$\left(\frac{p - p^s}{p^{cd}}\right)^2 + \left(\frac{q}{Mp^{cd}}\right)^2 = 1. \tag{3.39}$$

When $q = 0$, yielding occurs when $p = p^s \pm p^{cd}$, so that if we insist that the yield loci all go through the origin, $p^s = p^{cd}$ and the consolidation pressure is $p^c = 2p^s$, and (3.39) reduces to (3.9), the yield condition for modified Cam clay. Note that if we do not make this assumption, we can generate “bubble models” in which both ends of the yield locus translate. The true yield locus is found from the dissipative yield locus by a simple translation. The locus does not distort and the flow rule remains normal. This, of course, is because the pressure in the dissipation function in (3.34) does not depend on the actual pressure. It is also important to note that on the critical state line, where the dilation angle is zero and there is no plastic volume change, $p^d = 0$, so $p = p^s$. The pressure on the critical state line is hence equal to the shift pressure. This is a general feature of these models, and demonstrates that the pressure-volume relation at the critical state is determined by the free energy function and is independent of the dissipation mechanisms. In passing we note that this result is an added argument for the assumption that the plastic part of the free energy is independent of the plastic shear strain.

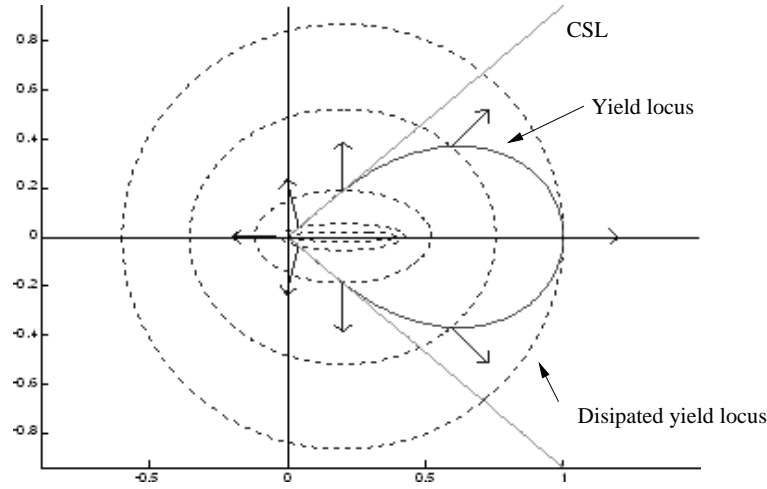


FIGURE 11. Example of model with non-associated flow rule – elliptical dissipative loci also been shifted ($\alpha = 0.1$, $\gamma = 0.4$, $r = 0.5$)

There are, however, still a number of unsatisfactory aspects to this model. For example, for sands, the ratio of the consolidation pressure p^c to the critical state pressure p^s , is frequently much higher than 2. In addition, the dissipation function in (3.34) does not model friction as it does not involve the current pressure. Accordingly Collins and Hilder (2002) proposed a generalised family of models, in which this dissipation function (3.34) is replaced by:

$$\widehat{\Phi} = \sqrt{(A\dot{e}_v^p)^2 + M^2 (B\dot{e}_\gamma^p)^2}, \tag{3.40}$$

where

$$A = (1 - \gamma)p + p^s, \tag{3.41}$$

$$B = (1 - \alpha)p + \alpha p^s. \tag{3.42}$$

This model introduces two new parameters α and γ , both of which lie in the range $[0, 1]$, and are both 1 for modified Cam clay. It is found that $\gamma = 2/r$, where $r = \frac{p^c}{p^s}$ is the “spacing ratio”. As γ decreases from 1 the yield loci become more elongated, and the ratio of stored to dissipated plastic work decreases. In the limit where $\gamma = 0$, the Coulomb model is recovered with the straight line Coulomb loci, and no plastic work is stored. The second parameter is the “tear drop” parameter. As α decreases from 1, the yield loci become more tear drop shaped, as shown in Figure 11. Since the dissipation function now depends explicitly on the pressure, the elliptical dissipative yield loci distort when transformed to true stress space and the flow rule is non-normal. Collins (2005) has shown that these two parameters can be directly related to the bi-modal model of Radjai et al. (1998) discussed above in Section 2.3. The modified Cam clay model and Coulomb models are the limiting cases, where the continuum element is all force chains and has no force chains respectively.

4.5. Modelling Reynolds’ dilatancy. Although the Cambridge models do predict dilatant behaviour on the dense side of the critical state line, the above thermomechanical analysis shows that this dilatancy is due to the recovery of stored plastic work (frozen elastic energy), arising from the prior compression of the sample. This dilatant behaviour is completely different from that described by Reynolds in which the dilatant behaviour is induced by the shear of the grain assemblies. We hence recognize that there are two reasons for dilation in a granular medium, so that we can write the plastic volume strain rate as:

$$\dot{\epsilon}_v^p = \dot{\epsilon}_{vc}^p + \dot{\epsilon}_{vi}^p, \quad (3.43)$$

where $\dot{\epsilon}_{vc}^p$ is the volume strain rate associated with changes in frozen elastic energy, and is given by the plastic flow rule. The second term $\dot{\epsilon}_{vi}^p$ is the plastic volume strain rate induced by the shear deformations, and is given by:

$$\dot{\epsilon}_{vi}^p = -\dot{\epsilon}_\gamma^p \tan \theta, \quad (3.44)$$

where θ is termed the “induced dilatancy angle”. It is a function of the plastic shear strain and of the polydiversity of the grain assembly.

As noted by Reynolds, the work associated with this induced deformation is zero. This can be seen by considering the deformation of an assembly of smooth, rigid particles, in which case there is no dissipation and no work stored – see also Kanatani (1982), Goddard and Bashir (1990) and Houlsby (1993). The applied work has to overcome gravity and inertia, both of which are zero in a standard quasi-static analysis. The standard plastic work equation (3.31) can now be written

$$\widehat{W}^p = p\dot{\epsilon}_v^p + q\dot{\epsilon}_\gamma^p = p^s\dot{\epsilon}_{vc}^p + (p^d\dot{\epsilon}_{vc}^p + q^d\dot{\epsilon}_\gamma^p) + (p^r\dot{\epsilon}_{vc}^p + q^r\dot{\epsilon}_\gamma^p), \quad (3.45)$$

where the last term in the work equation is the zero-valued “constraint” work associated with the induced deformation, so that:

$$(p^r\dot{\epsilon}_{vc}^p + q^r\dot{\epsilon}_\gamma^p) = 0, \quad (3.46)$$

and hence

$$q^r = p^r \tan \theta, \quad (3.47)$$

where the last equation follows from (3.44). By equating like terms in the identity (3.45) it also follows that:

$$p = p^r = p^s + p^d, \quad (3.48)$$

$$q = q^r + q^d, \quad (3.49)$$

and hence that:

$$\eta \equiv \frac{q}{p} = \frac{q^d}{p} + \tan \theta. \quad (3.50)$$

This is essentially Taylor’s result – see Section 1. The strength of the granular material consists of two terms, the first coming from the dissipation produced by frictional shearing between the grains, and the second coming directly from Reynolds dilatancy. The dissipation function (3.34) can now be generalised to:

$$\widehat{\Phi} = p^{cd} \sqrt{(\dot{\epsilon}_{vc}^p)^2 + M^2(\dot{\epsilon}_\gamma^p)^2} = p^{cd} \sqrt{(\dot{\epsilon}_v^p + \dot{\epsilon}_\gamma^p \tan \theta)^2 + M^2(\dot{\epsilon}_\gamma^p)^2}, \quad (3.51)$$

Applying the standard hyper-plastic procedure, gives families of yield loci, which rotate and deform in the (p, q) stress plane, demonstrating that the response is now

anisotropic as shown in Figure 12. Thus Reynolds induced dilatancy is also accompanied by induced anisotropy. This is because as a shear deformation proceeds, the distribution of contact normals on an individual grain becomes anisotropic with a bias in the direction of the maximum compressive continuum stress. The induced dilatancy angle θ hence also determines the degree of anisotropy. The critical state line of the isotropic theory is replaced by two lines: the “Reynolds-Taylor line” (RTL), where $\dot{e}_{vc}^p = 0$, and the “Phase transition line” (PTL), where $\dot{e}_v^p = 0$. Taylor’s stress dilatancy holds on the RTL, where the stored plastic work is constant and the only source of dissipation is due to shear. Ultimately the induced dilation and anisotropy must cease so that $\theta = 0$, and the material eventually reaches an amorphous, unstructured isotropic state (i.e. the critical state). However, as already noted, in practice some form of instability or bifurcation often occurs before this state is achieved. Since the material is anisotropic, the application of an isotropic pressure, does not produce an isotropic deformation, and vice versa. The kinematic normal compression line (KNCL) illustrated, corresponds to isotropic deformation states. For further details of these anisotropic models, see Collins and Muhunthan (2003), Collins and Tai (2005) and Collins et al (2007), whilst some three dimensional extensions can be found in Collins (2003).

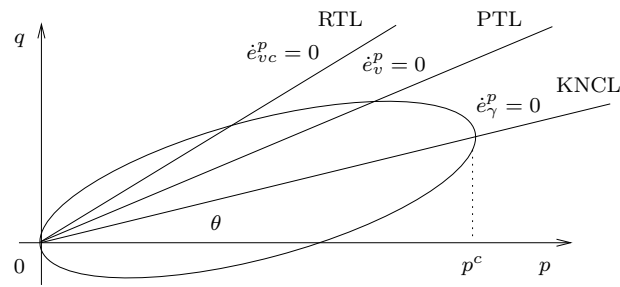
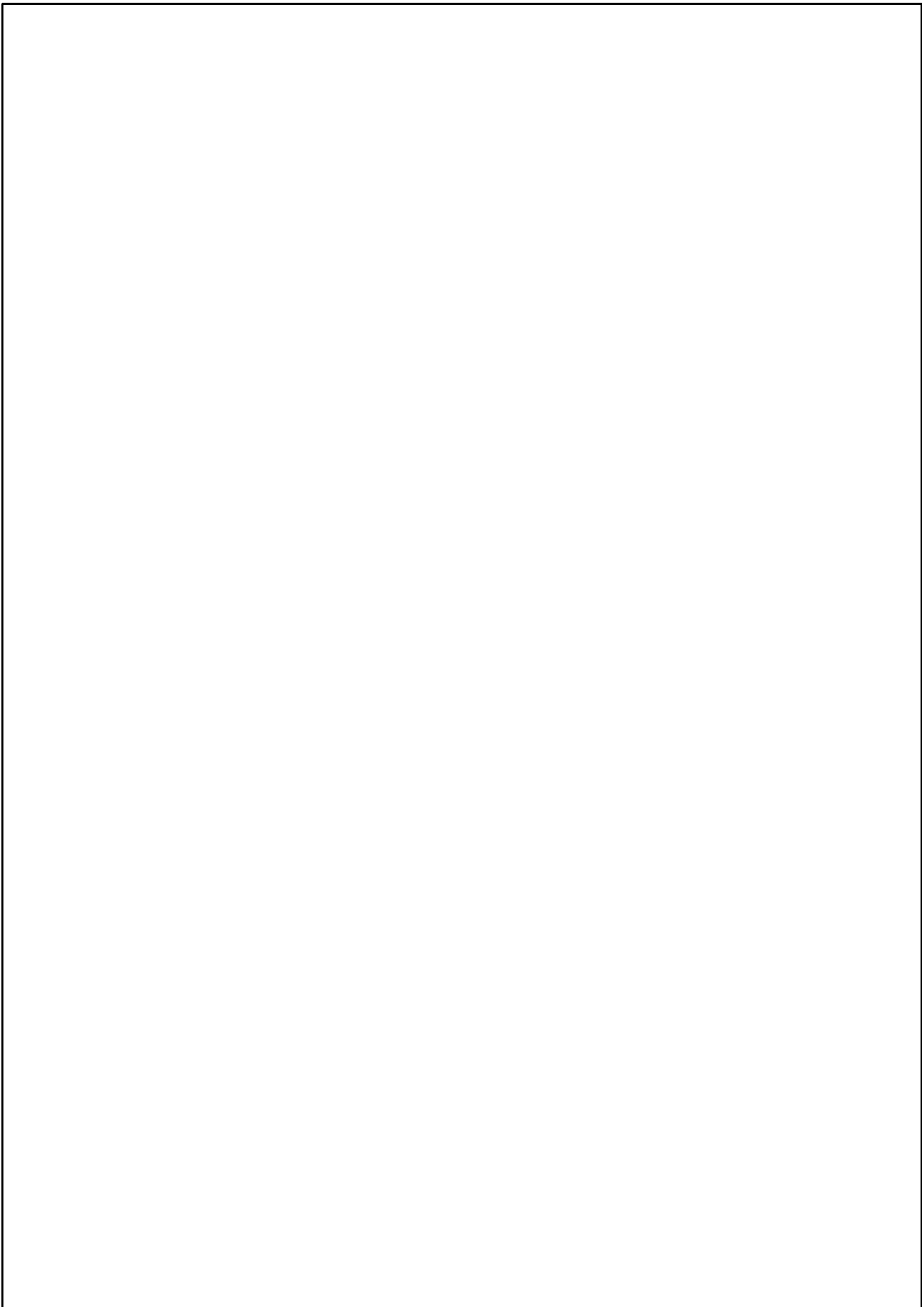


FIGURE 12. Rotated modified Cam clay model – when on RTL material is behaving in manner envisaged by Reynolds

5. Conclusions

This review has been written with the aim of demonstrating the power of the modern thermomechanical procedures to generate, physically meaningful, constitutive models for soils and granular media. It has also been written from the point of view of a “plastician” whose goal is to formulate models which are “sufficiently simple” so as to be of practical value to practising engineers, particularly geotechnical engineers. There are of course many other approaches. Some for example start from the view point of a fluid dynamicist who is interested in granular flows as in hoppers, avalanches or debris flows. Others use much more sophisticated generalized continuum models, such as Cosserat or micro-polar continua or mixture theory – these have much intrinsic interest, but have yet to make much impact in engineering applications. There is also much interest from physicists in applying ideas from statistical physics to understand the self selecting formation and destruction of force chains. It is a very rich area for research which requires input

from a wide range of disciplines. Whilst small strain theory is sufficient for most geotechnical applications, modern torsional shear apparatus are capable of strains of 250 %, and indeed, such strains are needed to determine the final critical state behaviour. There is hence a need for a finite strain constitutive formulation.



Bibliography

- Bardet, J.-P. (1997). *Experimental soil mechanics*. Prentice Hall, New Jersey.
- Been, K and Jefferies, M.G. (1985). A state parameter for sands. *Geotechnique* 35, No 2, 99-112.
- Burland, J.B. (1965). The yielding and dilation of clay. *Correspondence, Geotechnique*, 15, 211-214.
- Casagrande, A. (1947). Classification and identification of soils. *Proc. ASCE*, 73, 783-810.
- Chu, J. (1995). An experimental examination of the critical state and other similar concept for granular soils. *Can. Geotech. J.* 32, 1065-1075.
- Chu, J. and Lo, R. (1994). Asymptotic behaviour of a granular soil in strain path testing. *Geotechnique*, 44, No 1, 65-82.
- Collins, I.F. (1990). Plane Strain Characteristics Theory for Soils and Granular Materials with Density Dependent Yield Criteria. *J. Mech. Phys. Solids*, 38, 1-25.
- Collins, I.F. (2003). A systematic procedure for constructing three-dimensional critical state models. *Int. J. Solids Structures* 40, 4379-4397.
- Collins, I.F. (2005a). Elastic/plastic models for soils and sands. *Int. J. Mech Sci.* 47, 493-508.
- Collins, I.F. (2005b). The concept of stored plastic work or frozen elastic energy in soil mechanics. *Geotechnique* 55, No 5, 373-382.
- Collins, I.F. and Einav, I. (2005). On the Validity of Elastic/Plastic Decompositions in Soil Mechanics. *Proceedings of the Symposium on Elastoplasticity for Professor K. Hashiguchi Retirement Anniversary*. Kyushu University, Japan, Feb 28, 2005 ed: T. Tanaka and T. Okayasu 193-200.
- Collins, I.F. and Hilder, T. (2002). A theoretical framework for constructing elastic/plastic constitutive models for triaxial tests. *Int. J. Numer. Anal. Methods Geomech.* 26, 1313-1347.
- Collins, I.F. and Houlsby, G.T. (1997). Application of thermomechanical principles to the modelling of geotechnical materials. *Proc. Roy. Soc. Lond. A* 453, 1975-2001.
- Collins, I.F. and Kelly, P.A. (2002). A thermomechanical analysis of a family of soil models. *Geotechnique*, 52, No 7, 507-518.
- Collins, I.F. and Muhunthan, B. (2003). On the relationship between stress-dilatancy, anisotropy, and plastic dissipation for granular materials. *Geotechnique*, 53, No 7, 611-618.
- Collins, I.F. and Tai, A. (2005a). What has thermo-mechanics to offer geomechanics? *Proceedings of 11th International Conference on Computer Methods and Advances in Geomechanics*, Ed. G. Barla and M. Barla, Torino, Italy, 19-24 June, 1, 281-288.

- Collins, I.F. and Tai, A. (2005b). Energy methods for constitutive modelling in geomechanics. *Modern Trends in Geomechanics*, Ed: W. Wu and H. S. Yu, 3-15.
- Coussy, O. (1995). *Mechanics of porous continua*. Chichester, New York, Wiley.
- Cundall, P.A. and Strack, O.D.L. (1979). A discrete numerical model for granular materials. *Geotechnique*, 29, No 1, 47-65.
- Dafalias, Y.F. (1986). An anisotropic critical state clay plasticity model. *Mechanics Research Communications*, 13, 341-347.
- De Boer, R. (2000). *Theory of porous media*. Springer, Berlin.
- Goddard, J.D. and Bashir, Y. M. (1990). On Reynolds dilatancy. *Recent Developments in Structured Continua*, Vol 2, eds. D. DeKee and P.N. Kaloni, New York, Longmans, 23-35.
- Horne, M.R. (1965). The behaviour of an assembly of rotund, rigid, cohesionless particles II. *Proc. Roy. Soc. London, Series A*. 286, No 1404, 79-97.
- Houlsby, G.T. (1993). Interpretation of dilation as a kinematic constraint. *Modern approaches to plasticity*, Ed D. Kolymbas, New York: Elsevier 119-38.
- Houlsby, G.T. and Puzrin, A.M. (2000). A thermomechanical framework for constitutive models for rate-independent dissipative materials. *Int. J. Plasticity*, 16,1017-1047.
- Houlsby, G.T. and Puzrin, A.M. (2006). *Principles of Hyperplasticity: An approach to plasticity theory based upon thermodynamic principles*. Springer, Berlin.
- Ishihara, K. (1993). Liquefaction and flow failure during earthquakes. *Geotechnique* 43, No 3, 351-415.
- Jefferies, M. G. (1993). Nor-sand: a simple critical state model for sand. *Geotechnique*. 43, No1, 91-103.
- Kanatani, K-I. (1982). Mechanical foundation of the plastic deformation of granular materials. *Proc. IUTAM Conf. on Deformation and Failure of granular materials*, Delft, 119-127.
- Klotz, E.U and Coop, M.R. (2002). On the identification of critical state lines for sands. *Geotechnical Testing Journal*. 25, No 3, 1-13.
- Lade, P. (1975). Elastoplastic stress strain theory for cohesionless soil with curved yield surfaces. *Int. J. Solids Struct.* 13, 1019-1035.
- Leroueil, S. (1997). Critical state soil mechanics and the behaviour of real soils. *Symposium on Recent Developments in Soil and Pavement mechanics*, Rio de Janeiro, Brazil. 1-40.
- Lubliner, J. (1990). *Plasticity theory*. Macmillan, New York.
- Luong, M.P. (1986). Characteristic threshold and infrared vibrothermography of sand. *Geotechnical Testing J. ASTM*, 80-86.
- Maugin, G. A.(1992). *The thermomechanics of plasticity and fracture*, Cambridge, Cambridge University Press.
- Maugin, G.A. (1999). *The thermomechanics of nonlinear irreversible behaviors*. World Scientific Press.
- Mroz, Z. (1973). *Mathematical models of inelastic material behaviour*, University of Waterloo Press.
- Mooney, M.A., Finno, R.J. and Viggiani, M.G. (1998). A unique critical state for sands? *ASCE, J. Geotech. and Geoenv. Eng.* 124, No 11, 1100-1107.

- Mroz, Z. (1998). Elastoplastic and viscoplastic constitutive models for granular materials behaviour of granular materials, Cambou, B (ed) CISM courses and lectures No 385, Springer, Wien, New York, 269-337.
- Muir Wood, D. (1990). Soil behaviour and critical state soil mechanics. Cambridge, Cambridge University Press.
- Muir Wood, D. (2002). Constitutive cladistics: the progeny of critical state soil mechanics. Constitutive and centrifuge modeling: two extremes, Ed S. Springman, Swets &Zeitlinger, Lisse.
- Nicot, F. and Darve, F. (2006). On the elastic and plastic strain decomposition in granular materials. *Granular Matter*, 8, Issue 3-4, 221-237.
- Okada, N and Nemat-Nasser, S. (1994). Energy Dissipation in inelastic flow of saturated cohesionless granular media, *Geotechnique*, 44, No1,1-19.
- Radjai, F., Wolf, D.E., Jean, M. and Moreau, J-J (1998). Bimodal character of stress transmission in granular packings. *Phys. Rev. Letters*, 80, No 1, 61-64.
- Rajagopal, K.R. and Srinivasa, A.R (1998). Mechanics of inelastic behaviour of materials-Part I, *Int. J. Plasticity*, 14, 969-995.
- Rajagopal, K.R. and Srinivasa, A.R (1998). Mechanics of inelastic behaviour of materials-Part II, *Int. J. Plasticity*, 14, 945-967.
- Rajagopal, K.R. and Srinivasa, A.R (2002). On thermomechanical restrictions of continua, *Proc Roy. Soc. Lond. A* 460, 631-651.
- Reynolds, O. (1885). On the dilatancy of media composed of rigid particles in contact. With experimental illustrations. *Phil. Mag.* 20, 469-482.
- Roscoe, K.H. and Burland, J.B. (1968). On the generalized stress-strain behaviour of “wet clay”. *Engineering Plasticity*, ed J Heyman and F.A.Leckie, Cambridge, Cambridge University Press, 535-609.
- Rowe, P.W. (1962). The stress-dilatancy relation for static equilibrium of an assembly of particles in contact. *Proc. Roy. Soc. A.* 269, 500-527.
- Schofield, A. N. and Wroth, C. P. (1968). *Critical state soil mechanics*, New York, London, McGraw-Hill.
- Schofield, A. N. (2005). *Disturbed soil properties and geotechnical design*. Thomas Telford, London.
- Sewell, M.J. (1987). *Maximum and minimum principles*. CUP, Cambridge.
- Sokolovskii, V.V. (1965). *The statics of granular media*. Pergamon Press, Oxford.
- Spencer, A.J.M. (1964). A theory of the kinematics of ideal soils under plane strain conditions. *J. Mech. Phys. Solids* 12, 337-351.
- Spencer, A.J.M. (1992). Deformation of ideal granular materials. *Mechanics of Solids*, the Rodney Hill 60th Anniversary Volume, Ed. H. G. Hopkins and M. J. Sewell. Pergamon Press, Oxford, 607-652.
- Taylor, D.W. (1948). *Fundamentals of soil mechanics*. New York, John Wiley.
- Ulm, F-J, and Coussy, O. (2003). *Mechanics and durability of solids*, Vol 1. New Jersey, Prentice Hall.
- Vaid, Y.P., Sivathayalan, S. and Stedman, D. (1999). Influence of specimen-reconstituting method on the undrained response of sand. *Geotechnical Testing Journal*. 22, No 3, 187-195.
- Vardoulakis, I and Sulem, J. (1995). *Bifurcation analysis in geomechanics*. Glasgow, Blackie Academic.

Ziegler, H. (1983). An introduction to thermomechanics (2nd edition). Amsterdam, North Holland.

Part 3

Hypoelasticity and viscoelasticity

2000 *Mathematics Subject Classification.* 74A20, 74A15, 74C05, 74C10

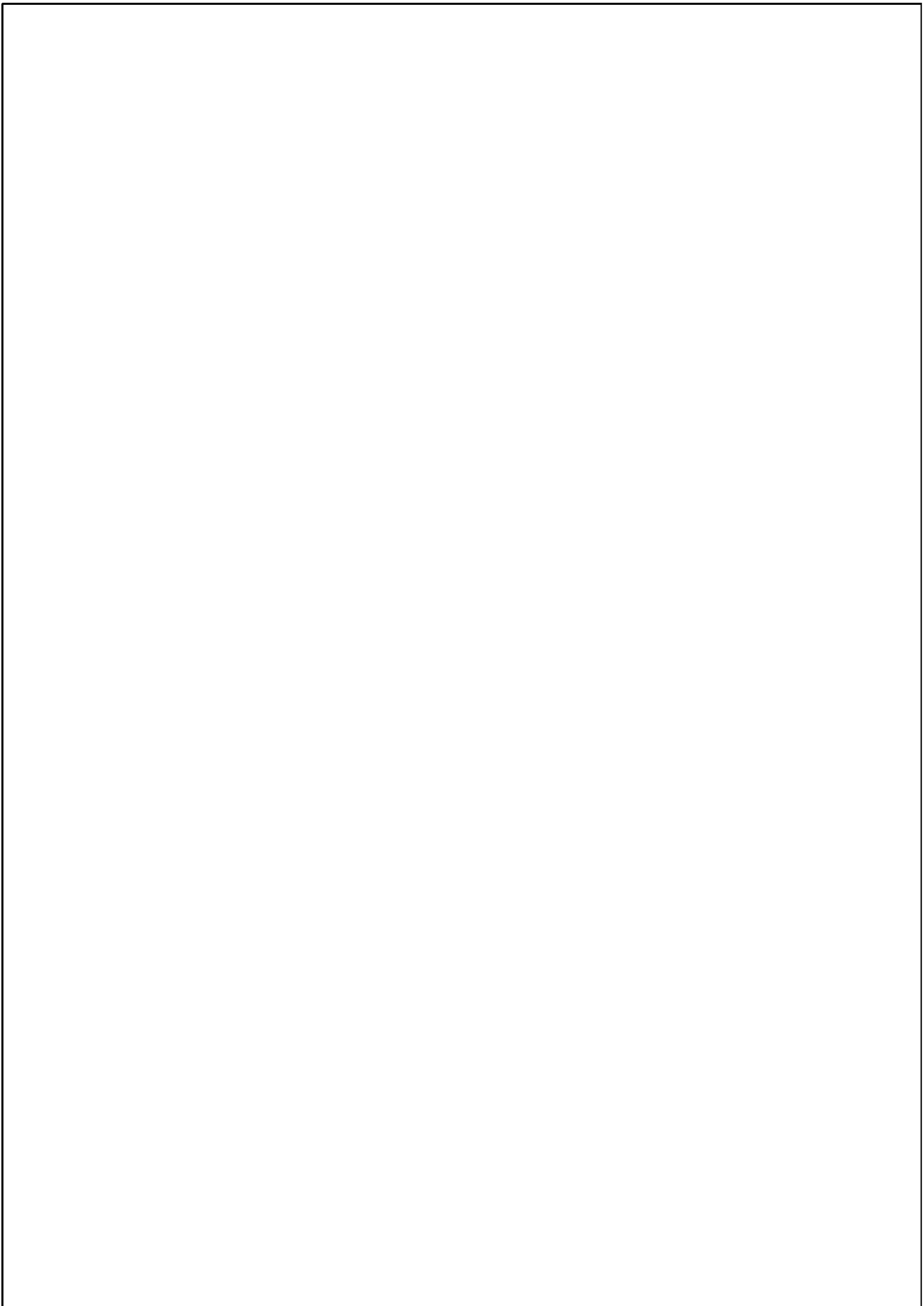
Key words and phrases. elasticity, plasticity, hypoelasticity, viscoelasticity

ABSTRACT. The first chapter is devoted to the discussion of plasticity and elasticity. It is shown that a certain set of rate theory type constitutive equations can give rise to both elastic behavior and plastic yield in infinitesimal strain both in loading and unloading. A thermodynamics is also developed for the unified theory of elasticity and plasticity in infinitesimal strain. Finally a thermodynamics of hypoelasticity is discussed.

The second chapter provides a short overview of viscoelasticity.

Contents

Chapter 1. Hypoelasticity	
B. BERNSTEIN	135
1. Introduction	135
2. Equations of hypoelasticity	136
3. Plasticity	137
3.1. A simple one dimensional model	137
3.2. A three dimensional model	138
3.3. Thermodynamics	139
4. Hypoelasticity	141
4.1. Thermodynamics of hypoelasticity	142
5. Concluding Remarks	144
Bibliography	145
Chapter 2. Viscoelasticity	
B. BERNSTEIN	147
1. Introduction	147
2. Elastic solid	148
3. Viscous fluid	149
4. Viscoelasticity	149
5. Energy	150
6. General theory	152
7. Conclusion	154
Bibliography	155



CHAPTER 1

Hypoelasticity

B. BERNSTEIN

1. Introduction

Hypoelasticity was introduced by Truesdell [6] in 1955 as a (non-thermal) theory involving rate type equations which show no time effects. I am told that it is used to describe behavior of asphalt. But Truesdell’s interest was in generalizations of mathematical models – he was interested in theory for its own sake.

The idea of hypo-elasticity is basically simple. Let us look at a one dimensional situation, where ϵ is strain and σ is stress. Linear elasticity would then involve a relation of the form

$$\sigma = \mu\epsilon$$

where μ is a modulus – an elastic modulus. Since classical elasticity is to hold for small strains, we can think of this equation as holding when ϵ and σ are small perturbations about zero strain and zero stress respectively. Carrying this further, ϵ and σ could be replaced by their changes, $\Delta\epsilon$ and $\Delta\sigma$ respectively.

Divide by the time interval Δt in which these changes occur, and with the usual limiting process, we arrive at

$$\dot{\sigma} = \mu\dot{\epsilon}.$$

This form allows large changes, for which μ need not be a constant. Let μ depend on σ and we have the prototype for hypo-elasticity

$$\dot{\sigma} = \mu(\sigma)\dot{\epsilon}.$$

It turns out, then, once the proper three dimensional properly invariant equations are formulated, the resulting theory of hypoelasticity is one possible generalization of linear elasticity. Indeed, in the same year, 1955, Noll [3] showed that every elastic material for which the stress-strain relation is invertible is also a hypo-elastic material. So, hypoelasticity appears to be more general than elasticity, a property which was very important to Truesdell and his school.

Indeed, Truesdell had a classification of the elasticity-hypoelasticity: The most general of these theories, according to Truesdell, was hypoelasticity. Less general was Cauchy elasticity, in which stress was a function of deformation gradient, but a strain energy function did not necessarily exist. At the lowest rank of the hierarchy stood Green elasticity, which was Cauchy elasticity with a strain energy.

To summarize, here is the ranking and the rationale of the terminology of Truesdell:

- (1) Hypoelasticity – less than elasticity – a rate theory.

- (2) Elasticity – Cauchy elasticity.
- (3) Hyperelasticity – more than elasticity – Green elasticity.

Although the embedding of a strain energy in one of the thermodynamic potentials (Hemholtz, Gibbs, etc.) is often not carried out, without a thermodynamic potential, it is unreasonable to expect to be able to construct a thermodynamic theory. Thus, according to this classification, it appears that only the hyper-elastic theory (of those under discussion) allows of a thermodynamic theory. Professor Rajagopal and I [5] have just turned that last statement on its head by constructing thermodynamics for hypoelasticity.

Related to these matters is also plasticity, although the plasticity that I have in mind is one which deals with infinitesimal strain. Nevertheless, as I shall show you, plasticity can arise as a type of singular behavior in a rate theory with no time-dependence, as does hypoelasticity. In the process of this lecture, I shall also show you the construction of a thermodynamic theory of elasticity and plasticity which agrees with the first and second laws.

2. Equations of hypoelasticity

Let us now turn to the proper formulation of the hypoelastic equations. We shall use Cartesian tensor notation in which, although we write all indices as subscripts, we do sum out on repeated indices in a term.

First we must define some symbols, to this end:

$$\begin{aligned}
 \sigma_{ij} & \quad \text{stress tensor,} \\
 s_{ij} = \sigma_{ij} - \frac{1}{3}\delta_{ij}\sigma_{kk} & \quad \text{stress deviator,} \\
 v_i & \quad \text{velocity vector,} \\
 d_{ij} = \frac{1}{2}(v_{i,j} + v_{j,i}) & \quad \text{rate of deformation,} \\
 \omega_{ij} = \frac{1}{2}(v_{i,j} - v_{j,i}) & \quad \text{rate of rotation,} \\
 p & \quad \text{pressure,} \\
 \rho & \quad \text{mass density.}
 \end{aligned}$$

Of course δ_{ij} is the Kroneker delta, i.e. the unit matrix,

$$\delta_{ij} = \begin{cases} 0 & \text{if } i \neq j, \\ 1 & \text{if } i = j, \end{cases}$$

and the comma denotes partial differentiation. For example, if the spatial Cartesian coordinates are x_i , $i = 1, 2, 3$,

$$\begin{aligned}
 p_{,i} & \equiv \frac{\partial p}{\partial x_i}, \\
 v_{i,j} & \equiv \frac{\partial v_i}{\partial x_j}.
 \end{aligned}$$

Let us define the hypoelastic equations. For these equations, there is a fourth order tensor valued function of σ_{ij} ,

$$A_{ijkl} = A_{jikl} = A_{jilk}$$

such that the equations of hypoelasticity become

$$\dot{\sigma}_{ij} = \sigma_{ik}\omega_{jk} + \sigma_{jk}\omega_{ik} + A_{ijkl}d_{kl},$$

where the dot stands for material derivative. In our treatment, we assume that there is also a relation of density or specific volume to pressure p . Since this can be a standard type relation, the discussion of it here will distract us from treatment of shear (stress deviator) and so we shall not deal with it here. The terms in ω_{ij} are needed for proper geometric invariance and if put on the right hand side, then together with the material derivative, they would make up what is called the corrotational derivative. They are of second order and hence are dropped in the case of infinitesimal displacement, but they are necessary for finite strain.

In the general theory of hypoelasticity the assignment of the A_{ijkl} as functions of stress is left open, except for requiring this assignment to be isotropic. Later we shall look at some restrictions on such assignment, these restrictions resulting from thermodynamic considerations.

3. Plasticity

Now let us change pace and talk about plasticity. In the theory of perfect plasticity, which is a theory of infinitesimal strain, the stress-strain relation is that of elasticity as long as the stress, or, actually some function of the stress remains below a critical value, perhaps known as the yield condition, and above which other conditions hold – e.g. the yield condition remaining constant. To be more specific, we deal with the von-Mises yield condition, which is as follows: There is a critical value $k > 0$ such that the yield condition is

$$s_{ij}s_{ij} = 2k^2.$$

As long as $s_{ij}s_{ij} < 2k^2$, the stress-strain response is elastic. When equality is reached, the von-Mises condition continues to hold and a set of rate equations, known as the Prandtl-Reuss equations, takes over. But there is a concept which is not usually too well defined, namely loading and unloading. The Prandtl-Reuss equations hold at the yield condition during loading. During unloading, there is a return to elastic behavior, albeit with permanent set. But hold on – we will have a definition of loading and of unloading before our hour is up.

3.1. A simple one dimensional model. We shall start with a simple one dimensional model (see Bernstein [2]): Let ϵ be shear strain and let s be shear stress. We consider the following constitutive equation:

$$\frac{ds}{dt} = \sqrt{1 - s^2}\dot{\epsilon}$$

This has solutions

$$s = \sin(\epsilon - c)$$

But it also has a two singular solutions:

$$s = 1 \quad \text{and} \quad s = -1.$$

Now consider ϵ to be varied. As long as s remains between $s = -1$ and $s = 1$, this equation obeys a Lipschitz condition, and therefore follows a unique path in ϵ, s space. Such we may call an elastic regime. When s reaches one of the singular

values, say $s = 1$, which it does exactly, not asymptotically at $\epsilon - c = \frac{\pi}{2}$, it stays there as long as ϵ is increasing. This is a plastic regime.

Now we are going to consider reversing the direction of $\dot{\epsilon}$, but first we need to say something more about the plastic regime. We need to introduce the concept of stability: When ϵ is increasing, and s is perturbed (only downwards is possible), s will come right back up to the yield value. Upon decreasing ϵ , however, s will continue to fall: the stable solution will be to return to an elastic regime, albeit in general not the one which in which it entered the yield condition in the first place.

Perhaps the sine function is not what most people have in mind for an elastic regime. Indeed, if we replace the equation by

$$\frac{ds}{dt} = \sqrt{1 - s^{2n}} \dot{\epsilon}$$

then the elastic regimes straighten out for large enough n . This is fine for the one-dimensional situation.

3.2. A three dimensional model. For the three dimensional situation, we shall deal here only with the shear part and ask you to believe that the pressure-volume part can be added.

Consider now the strain deviator ϵ_{ij} . We assume a strain potential function $\varphi(\alpha)$ where

$$\begin{aligned} \alpha &= \sqrt{\epsilon_{ij}\epsilon_{ij}}, \\ s_{ij} &= \frac{\partial\varphi}{\partial\epsilon_{ij}}, \end{aligned}$$

and let $\beta = \sqrt{s_{ij}s_{ij}}$. Then

$$\beta = \varphi'(\alpha)$$

which, when solved for α is expressed as $\alpha = \psi(\beta)$.

After a bit of manipulation, we get

$$\frac{\psi(\beta)}{\beta} s_{ij} = \epsilon_{ij}.$$

But we want a rate equation, and so we take the time derivative and after some algebra, we arrive at the following rate equation:

$$\dot{s}_{ij} = \frac{\beta}{\psi(\beta)} \dot{\epsilon}_{ij} + \frac{1}{\beta^2} \left[\frac{1}{\psi'(\beta)} - \frac{\beta}{\psi(\beta)} \right] s_{ij} s_{kl} \dot{\epsilon}_{kl}.$$

Multiplying both sides by s_{ij} and summing out on the indices yields

$$\frac{d\beta^2}{dt} = \frac{2}{\psi'(\beta)} s_{ij} \dot{\epsilon}_{ij}.$$

We can now choose the function $\psi(\beta)$ so that the equations are those of an elastic-plastic material. Indeed, first choose ψ to be

$$\psi(\beta) = \frac{k\sqrt{2}}{2\mu} \sin^{-1} \frac{\beta}{2k\sqrt{2}}$$

which results in

$$\frac{d\beta^2}{dt} = \sqrt{1 - \frac{\beta^2}{2k^2}} s_{ij} \dot{\epsilon}_{ij}.$$

Thus, when β^2 reaches the value $2k^2$ which, as s did in the one-dimensional case, $\frac{d\beta^2}{dt}$ will be zero, and so the von-Mises yield condition will be reached. Loading now can be defined as $s_{ij}\dot{\epsilon}_{ij}$.

Again, during loading, the yield condition will be stable. On the onset of unloading, however, the stable solution will be a return to an elastic regime.

Actually, we can play around with ψ : In fact, the way to do this is to pick $\psi'(\beta)$. Given a positive integer n , we can pick ψ so that

$$\psi'(\beta) = \frac{1}{2\mu\sqrt{1 - \left(\frac{\beta^2}{2k^2}\right)^n}}$$

which will straighten out the elastic regime curves, and give the yield behavior

$$\frac{d\beta^2}{dt} = \sqrt{1 - \left(\frac{\beta^2}{2k^2}\right)^n} s_{ij}\dot{\epsilon}_{ij}.$$

But there are still the equations for s_{ij} . Remember, they are

$$\dot{s}_{ij} = \frac{\beta}{\psi(\beta)}\dot{\epsilon}_{ij} + \frac{1}{\beta^2} \left[\frac{1}{\psi'(\beta)} - \frac{\beta}{\psi(\beta)} \right] s_{ij}s_{kl}\dot{\epsilon}_{kl}.$$

During yield, we set $\frac{1}{\psi'(\beta)} = 0$, and $\beta^2 = 2k^2$ to get

$$\dot{s}_{ij} = \frac{k\sqrt{2}}{\psi(k\sqrt{2})} \left[\dot{\epsilon}_{ij} - \frac{1}{2k^2} s_{ij}s_{kl}\dot{\epsilon}_{kl} \right]$$

which are the well known Prandtl-Reuss equations. And so we have recovered elasticity and plasticity of infinitesimal strain in a single set of equations.

3.3. Thermodynamics. Now let us see how all of this plays out thermodynamically [1]. To construct the thermodynamics, we need to be sure what will be taken as state variables. Indeed, we shall take stress deviator s_{ij} and temperature T as state variables. I ask that you take my word that we can also include pressure or mass density as state variables in a fairly straightforward way, but doing so will just distract us now. So let us stick with the stress-deviator and temperature.

The thermodynamic potential which is the most appropriate here is the Gibbs function, $G(s_{ij}, T)$, which we take to depend on s_{ij} through the invariant β

$$G = G(\beta, T).$$

We write down some relationships, which we then replace by their time derivatives as rate equations. Indeed, we write

$$\begin{aligned} \epsilon_{ij} &= -\frac{\partial G}{\partial s_{ij}}, \\ \eta &= \frac{-\partial G}{\partial T}, \\ E &= G + T\eta + s_{ij}\epsilon_{ij}, \\ \psi &= -\frac{\partial G}{\partial \beta} \end{aligned}$$

where η is entropy density, T is temperature, and E is internal energy. After some manipulation, we arrive at the following rate equation:

$$\dot{s}_{ij} = \frac{\beta}{\psi} \dot{\epsilon}_{kl} + \frac{1}{\beta^2} \left[\frac{1}{\psi_{,\beta}} - \frac{\beta}{\psi} \right] s_{ij} s_{kl} \dot{\epsilon}_{kl} - \frac{\psi_{,T}}{\beta \psi_{,\beta}} s_{ij} \dot{T}.$$

We now use the energy balance equation, which is the following:

$$\dot{E} = s_{ij} \dot{\epsilon}_{ij} - q_{i,i}$$

where q_i is the heat flux vector. And we need to non-dimensionalize our equations. To this end let $k(T)$ be the temperature dependent yield stress and let

$$\begin{aligned} S_{ij} &= \frac{s_{ij}}{k\sqrt{2}}, \\ B &= \sqrt{S_{ij}S_{ij}}, \\ H(B, T) &= G(\beta, T), \\ \Theta(B, T) &= \psi(\beta, T) \end{aligned}$$

in which case the rate equation becomes

$$\dot{S}_{ij} = \frac{B}{\Theta} \dot{\epsilon}_{ij} + \frac{1}{B^2} \left[\frac{1}{\Theta_{,B}} - \frac{B}{\Theta} \right] S_{ij} S_{kl} \dot{\epsilon}_{kl} - \frac{\Theta_{,T}}{B\Theta_{,B}} S_{ij} \dot{T},$$

and the equation for B becomes

$$\frac{dB^2}{dt} = \frac{2}{\Theta_{,B}} \left[S_{ij} \dot{\epsilon}_{ij} - B\Theta_{,T} \dot{T} \right].$$

So the yield condition is $B = 1$. If we take ψ as before, we get for this last equation

$$\frac{dB^2}{dt} = \frac{4\mu}{k\sqrt{2}} \sqrt{1 - B^{2n}} \left[S_{kl} \dot{\epsilon}_{kl} - B\Theta_{,T} \dot{T} \right]$$

This tells us that yield is stable when the expression in the brackets is positive and unstable when the expression in the brackets is negative. So we have a definition of loading and unloading

$$\begin{aligned} \left[S_{kl} \dot{\epsilon}_{kl} - B\Theta_{,T} \dot{T} \right] &> 0 \quad \text{loading} \\ \left[S_{kl} \dot{\epsilon}_{kl} - B\Theta_{,T} \dot{T} \right] &< 0 \quad \text{unloading} \end{aligned}$$

But this is not the end: If we go back to the balance of energy equation, we may consider two conditions; at first $B^2 < 1$, in which case the chain rule of calculus applies. One obtains

$$\dot{E} = s_{kl} \dot{\epsilon}_{kl} + T\dot{\eta}$$

which, when placed into the energy balance,

$$\dot{E} = s_{ij} \dot{\epsilon}_{ij} - q_{i,i}$$

results in

$$T\dot{\eta} + q_{i,i} = 0.$$

So there is no entropy production except that due to heat flow.

On the other hand, during yield, $B = 1$, we have to differentiate differently: First we set B to the constant value, $B = 1$ and then differentiate. So $G = G(1, T)$ depends only on temperature for this analysis. When we do so, we get

$$\dot{E} = k\sqrt{2}\Theta_{,T}\dot{T} + T\dot{\eta}$$

which then results in the following

$$T\dot{\eta} + q_{i,i} = k\sqrt{2}\left(S_{ij}\dot{\epsilon}_{ij} - B\Theta_{,T}\dot{T}\right).$$

Isn't this interesting? The condition for stability of yield now comes into the entropy production. If the expression in brackets is positive during yield, (loading), yield is stable and produces entropy: the second law is upheld by positive entropy production. On the other hand, should this expression become negative (unloading), the stable solution dictates a return to an elastic regime, in which case there is zero entropy production. We need add only positive thermal conductivity, $q_i T_{,i} \leq 0$ so that we get always

$$\dot{\eta} + \frac{q_{i,i}}{T} = \dot{\eta} + \left(\frac{q_i}{T}\right)_{,i} + \frac{q_i T_{,i}}{T^2}.$$

So positive entropy production and positive thermal conductivity ($q_i T_{,i} \leq 0$) gives agreement with the second law. The theory agrees with the laws of thermodynamics.

4. Hypoelasticity

Now to hypoelasticity. What we have done in the case of small strain can be carried over to large strain, with appropriate modifications. Indeed, let us consider what we need to do for a thermodynamic approach. We need to:

- choose our state variables,
- choose the appropriate thermodynamic potential in terms of which we will state conservation of energy,
- choose the rate equation for stress (deviator),
- establish that the second law holds.

In 1984, Olsen and Bernstein [4] did just that for a thermodynamic set of equations which follows pretty much what was just done for the case of infinitesimal strain, but which treats large deformation in hypoelasticity. We now present the essence of this contribution.

Choose as state variables the stress deviator and temperature. Then assume given a Gibbs free energy function $G(s_{ij}, T)$ which depends only of the invariant $\beta = \sqrt{s_{ij}s_{ij}}$. Again, let $\eta = -\frac{\partial G}{\partial T}$ be the entropy density. The internal energy will then be given by

$$E = G - s_{ij}\frac{\partial G}{\partial s_{ij}} + T\eta.$$

Note that this time, we do not assume that the derivative of the Gibbs function with respect to stress is strain. Instead, let these derivatives remain as functions of stress and temperature, but we make the terms involving s_{ij} balance the work terms in the energy balance, i.e.

$$-\rho s_{ij}\left(\frac{\partial G}{\partial s_{ij}}\right)' = s_{ij}d_{ij}$$

Then the balance of energy becomes

$$\rho T \dot{\eta} + q_{i,i} = 0$$

or

$$\rho \dot{\eta} + \left(\frac{q_i}{T} \right)_{,i} = - \frac{q_i T_{,i}}{T^2}.$$

which, when positive thermal conductivity is $q_i T_{,i}$ is assumed, gives agreement with the second law. It remains only to complete the algebra and to replace the time derivative of stress by the corotational derivative and to define $\psi = -\frac{\partial G}{\partial \beta}$ to arrive at the constitutive equation

$$\dot{s}_{ij} - s_{ik} \omega_{jk} - s_{jk} \omega_{ik} = \frac{1}{\rho} \left[\frac{1}{\beta^2} \left(\frac{1}{\beta^2} - \frac{\beta}{\psi} \right) s_{ij} s_{kl} + \frac{\beta}{\psi} \varphi_{ijkl} \right] d_{kl} - \frac{1}{\beta} \frac{\psi_{,T}}{\psi_{,\beta}} \dot{T} s_{ij}$$

where

$$\varphi_{ijkl} = \frac{1}{2} \delta_{ij} \delta_{kl} + \frac{1}{2} \delta_{jk} \delta_{il} - \frac{1}{3} \delta_{ij} \delta_{kl}.$$

Bernstein and Olsen were also able to show that this model was definitely not elastic by applying conditions derived by in 1960.

4.1. Thermodynamics of hypoelasticity. The latest addition to these studies is to be published in *Zeitschrift fur Angewandte Mathematik und Physik* under the title of Thermodynamics of Hypoelasticity, by B. Bernstein and K.R. Rajagopal.

The stress deviator is traceless, $s_{ii} = 0$. This relation uses up one of its three invariants. Of the other two, we have dealt with β . We have one more, which we call γ ,

$$\begin{aligned} \beta &= \sqrt{s_{ij} s_{ij}} \\ \gamma &= \sqrt[3]{s_{ik} s_{kl} s_{lj}}. \end{aligned}$$

So that G depends on s_{ij} through its two invariants, β and γ .

We proceed pretty much as before, except that we make two assumptions and ask when they tie together:

- the constitutive relation

$$\dot{s}_{ij} = s_{ik} \omega_{jk} + s_{jk} \omega_{ik} + v A_{ijkl} d_{kl} + a_{ij} \dot{T} + \dot{v} b_{ij},$$

- the Gibbs function depending on s_{ij} and T ,
- conservation of energy.

If we put all this into our equations and define

$$\varphi_{ij} = - \frac{\partial G}{\partial s_{ij}},$$

we get after some manipulation

$$\rho T \dot{\eta} + q_{i,i} - \rho r = s_{ij} d_{ij} - \rho s_{ij} \dot{\varphi}_{ij}.$$

So, if we want the second law to hold, we need to have

$$s_{ij} d_{ij} - \rho s_{ij} \dot{\varphi}_{ij} \geq 0$$

But if the right hand side of this is greater than zero, we could reverse the path and thus make it less than zero. So the only way we are going to satisfy the second law is to make it zero.

After using the constitutive equation in this last relationship and doing some tensor algebra, we come up with restrictions on the A_{ijkl} which make this last condition hold. For A_{ijkl} we have the following

$$\begin{aligned} \tilde{A}_{ijkl} = & A_1 \delta_{ij} \delta_{kl} + \frac{A_2}{2} (\delta_{ik} \delta_{jl} + \delta_{il} \delta_{jk}) + A_3 \delta_{ij} s_{kl} + A_4 s_{ij} \delta_{kl} \\ & + \frac{A_5}{4} (\delta_{ik} s_{jl} + \delta_{jk} s_{il} + \delta_{il} s_{jk} + \delta_{jl} s_{ik}) + A_6 \delta_{ij} s_{kl}^2 + A_7 \delta_{kl} s_{ij}^2 \\ & + \frac{A_8}{4} (\delta_{ik} s_{jl}^2 + \delta_{jk} s_{il}^2 + \delta_{il} s_{jk}^2 + \delta_{jl} s_{ik}^2) \\ & + A_9 s_{ij} s_{kl} + \frac{A_{10}}{2} (s_{ik} s_{jl} + s_{jk} s_{il}) \\ & + A_{11} s_{ij} s_{kl}^2 + A_{12} s_{ij}^2 s_{kl} + \frac{A_{13}}{4} (s_{ik} s_{jl}^2 + s_{jk} s_{il}^2 + s_{il} s_{jk}^2 + s_{jl} s_{ik}^2) \\ & + A_{14} s_{ij}^2 s_{kl}^2 + \frac{A_{15}}{2} (s_{ik}^2 s_{jl}^2 + s_{jk}^2 s_{il}^2). \end{aligned}$$

After making it traceless by subtracting its traces, and using that last relation, we come up with the following restrictions on the A_k : Let P and Q be defined respectively by

$$\begin{aligned} P &= -G_{,\beta\beta} - \frac{\gamma}{\beta} G_{,\beta\gamma}, \\ Q &= -\frac{\beta}{\gamma^2} G_{,\gamma\beta} - \frac{1}{\gamma} G_{,\gamma\gamma}. \end{aligned}$$

Then these are conditions that must be satisfied:

$$\begin{aligned} PA_2 + Q \frac{\beta^2}{6} A_5 + \left(P \frac{\beta^2}{2} + Q \frac{\gamma^3}{3} \right) A_8 + (P\beta^2 + Q\gamma^3) A_9 + \left(P \frac{\beta^2}{2} + Q \frac{\gamma^3}{3} \right) A_{10} \\ + \left(P\gamma^3 + Q \frac{\beta^4}{6} \right) A_{12} + \left(P \frac{\gamma^3}{3} + Q \frac{\beta^4}{12} \right) A_{13} + \left(P \frac{\beta^4}{4} + 2Q \frac{\beta^2 \gamma^3}{9} \right) A_{15} = 1 \end{aligned}$$

and

$$\begin{aligned} QA_2 + PA_5 + Q \frac{\beta^2}{6} A_8 + Q \frac{\beta^2}{6} A_{10} + (P\beta^2 + Q\gamma^3) A_{11} \\ + \left(P \frac{\beta^2}{2} + Q \frac{\gamma^3}{3} \right) A_{13} + \left(P\gamma^3 + Q \frac{\beta^4}{6} \right) A_{14} + \left(P \frac{\gamma^3}{3} + Q \frac{\beta^4}{12} \right) A_{15} = 0. \end{aligned}$$

These are two conditions on the ten coefficients, a grossly undetermined system. Actually, it is even more so. Because of the volume of material presented here in a relatively short time, I have not discussed the restrictions on the temperature and volume terms. In fact, these add two more restrictions, but also add four more coefficients. And all of these coefficients are functions of the invariants, the temperature and, actually, also the volume. The Bernstein-Olsen results fit in very

nicely by choosing

$$A_2 = \frac{\beta}{\psi},$$

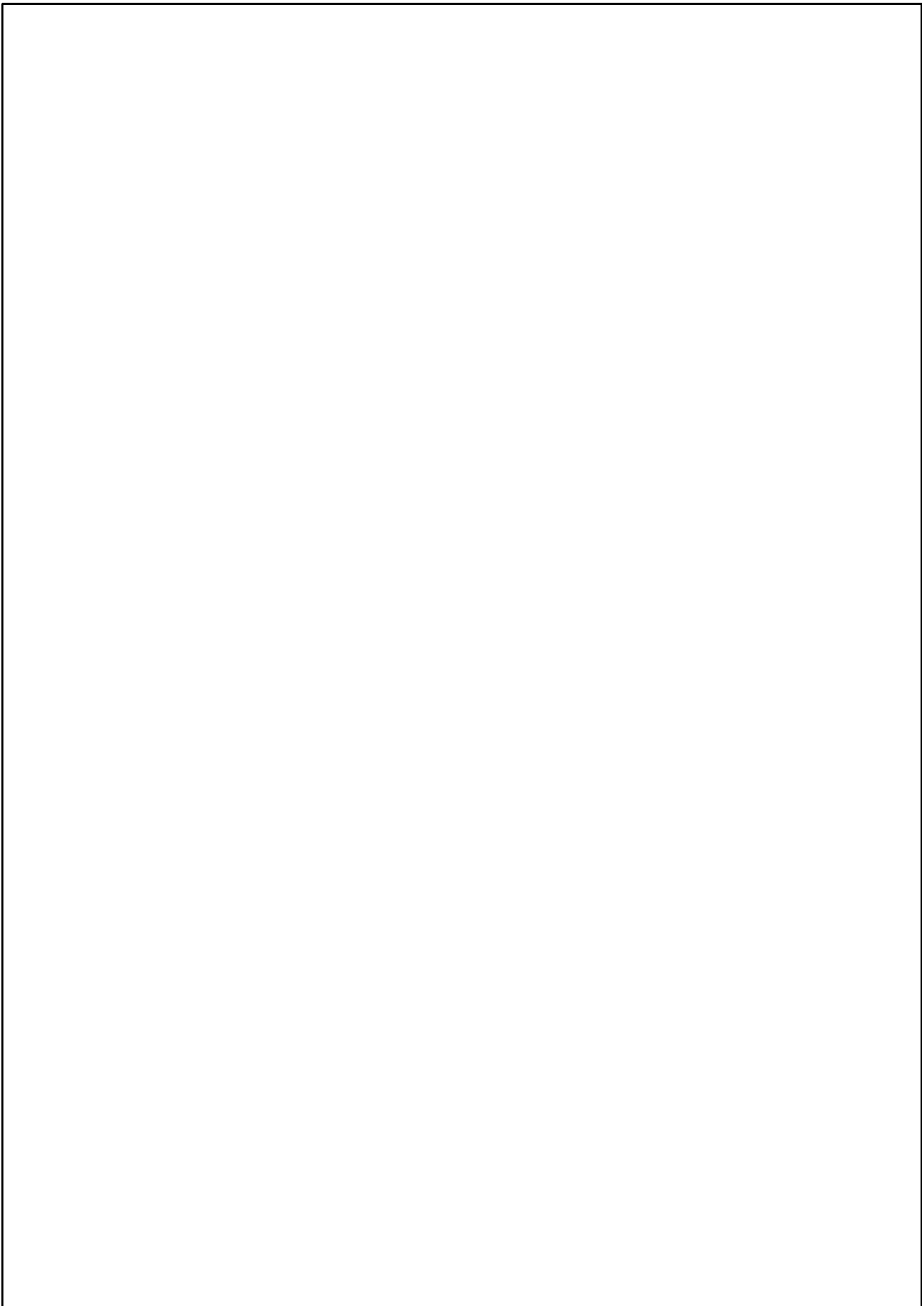
$$A_9 = \frac{1}{\beta^2} \left(\frac{1}{\psi_{,\beta}} - \frac{\beta}{\psi} \right).$$

5. Concluding Remarks

- Hypoelasticity is a rate theory of stress versus strain.
- Hypoelasticity is considered more general than Cauchy elasticity, in which there stress is a function of strain.
- Nevertheless under appropriate restrictions, one may construct a thermodynamic theory of hypoelasticity.
- The theory presented here involves a severely underdetermined set of restrictions which arise from the requirement that the theory fit the laws of thermodynamics.
- Because hypoelasticity is path reversible, obeying the second law, as formulated here, gives no entropy production except that due to heat flow, as in an elastic theory.
- The theory of elasticity and perfect plasticity can be formulated in a single set of equations. These can be made into a thermodynamic theory in which loading and unloading is well defined. The definition even includes dependence on temperature changes.
- In the elasticity-plasticity equations given here, agreement with the second law follows from the assumption that the stable path will be taken both in loading and unloading.

Bibliography

- [1] B. Bernstein. A unified thermodynamic theory of elasticity and plasticity. *Journal of Elasticity*, 13(4):411–427, 1983.
- [2] B. Bernstein. A unified theory of elasticity and plasticity. *Int J. Engineering Science*, 15:645–660, 1977.
- [3] Walter Noll. On the continuity of the solid and fluid states. *J. Ration. Mech. Anal.*, 4:3–81, 1955.
- [4] E.T. Olsen and B. Bernstein. A class of hypo-elastic non-elastic materials and their thermodynamics. *Arch. Ration. Mech. Anal.*, 86(3):291–303, 1984.
- [5] K.R. Rajagopal and B. Bernstein. Thermodynamics of hypoelasticity. *Zeitschrift fur Angewandte Mathematik und Physik*, to appear
- [6] Truesdell. Hypo-elasticity. *J. Ration. Mech. Anal.*, 4:83–133, 1955.



CHAPTER 2

Viscoelasticity

B. BERNSTEIN

1. Introduction

It is common to think of certain substances as elastic solids and to think of others as viscous fluids. But today we deal with media which can behave as either one, depending on conditions, and, indeed, in appropriate senses, commonly exhibit behavior which lies in between that of an elastic solid and that of a viscous fluid and which show elastic behavior and viscous fluid behavior in appropriate limiting senses. These are known as viscoelastic substances and include polymers, which are in common use today. Indeed, it can be argued that the substances which are, in fact, viscoelastic comprise very many material. Indeed, if one considers viscoelasticity as giving us a point of view for mathematical description of material behavior, then one might even argue that this point of view is general enough to cover all materials.

In setting theories for material behavior, energetic aspects, i.e. thermodynamic aspects are too often placed in the background or even ignored completely.

What I shall present to you today is a thermodynamic theory of viscoelastic behavior which has had a certain amount of success and of which I am an author [1, 2, 3], and for which there is experimental evidence for some predictions of the theory [5]. In its full version, it deals with large deformations and material time dependence. And let me repeat that it is a thermodynamic theory: It obeys the laws of thermodynamics, including the second law. It is my contention that a theory of material behavior should address thermodynamics for at least two reasons:

- (1) The world, if not the universe, operates thermodynamically and so ignoring thermodynamics leave a theory incomplete.
- (2) There can be many ways to formulate mechanical relationships so that one needs criteria to select from many formulations those which have the best hope of describing reality and thermodynamic restrictions provide one important set of criteria – obeying the first and second laws.

In the case of large strains in a three dimensional world, there are geometric invariance considerations which introduce a complexity which can mask the physical assumptions at first. So, in presenting the theory, I will initially present the theory in a boiled down version which can omit the three dimensional non-linear considerations in order to bring out the physical assumptions. Then, once we have these considerations in mind, we shall see how they fit into the properly invariant three dimensional theory with large strains.

First, we introduce the limited cast of characters that we need for the simplified theory. We have, to begin with, strain γ , stress σ , temperature ϑ , and heat flux Q , which is the rate at which heat is being removed. We also need the rate of deformation $\dot{\gamma}$.

2. Elastic solid

First let us consider the elastic solid. The stress-strain relation takes the form

$$\sigma = \mu\gamma$$

where μ is an elastic modulus. We now do the thermodynamics of this simple model: First of all, the elastic modulus can depend on temperature ϑ , and the Helmholtz free energy $A(\gamma, \vartheta)$ obeys

$$\sigma = \frac{\partial A}{\partial \gamma}$$

which results in A taking the form

$$A = \frac{1}{2}\gamma^2 + h(\vartheta)$$

where h is some function of ϑ . The entropy s assumed to satisfy

$$s = -\frac{\partial A}{\partial \vartheta}$$

and the internal energy E is assumed given by

$$E = A + \vartheta s.$$

Using the principle of balance of energy, we equate the rate of change in internal energy to the sum of the work done by the stresses and the rate of heat added, viz.

$$\dot{E} = \sigma\dot{\gamma} - Q.$$

So

$$\dot{E} = \dot{A} + \dot{\vartheta}s + \vartheta\dot{s} = \frac{\partial A}{\partial \gamma}\dot{\gamma} + \frac{\partial A}{\partial \vartheta}\dot{\vartheta} + \vartheta\dot{s} + \dot{\vartheta}s = s\dot{\gamma} - s\dot{\vartheta} + \vartheta\dot{s} + \dot{\vartheta}s = \sigma\dot{\gamma} + \vartheta\dot{s}.$$

Putting these last two equations together yields

$$\vartheta\dot{s} + Q = 0$$

or

$$\dot{s} + \frac{Q}{\vartheta} = 0$$

which tells us that the production of entropy for an elastic material is due only to heat flow. Contrast this to the viscous fluid, which we shall introduce next.

3. Viscous fluid

In the viscous fluid we have a parameter η , called *viscosity* and the stress is proportional to the rate of strain, or rate of deformation $\dot{\gamma}$

$$\sigma = \eta \dot{\gamma}.$$

In general, η is a function of the temperature ϑ , i.e. $\eta = \eta(\vartheta)$, as is the Helmholtz free energy $A = A(\vartheta)$. The entropy is then given by $s = -dA/d\vartheta$, and the internal energy is given by $E = A + \vartheta s$. The balance of energy is then $\dot{E} = \sigma \dot{\gamma} - Q$, which then sorts out as

$$\overline{A + \vartheta s} = \frac{dA}{d\vartheta} \dot{\vartheta} + \dot{\vartheta} s + \vartheta \dot{s} = -s \dot{\vartheta} + s \dot{\vartheta} + \vartheta \dot{s} = \eta \dot{\gamma}^2 - Q$$

Which sorts out to

$$\dot{s} + \frac{Q}{\vartheta} = \frac{\eta}{\vartheta} \dot{\gamma}^2 \geq 0$$

so that the second law is satisfied. Note that entropy is produced now not only by heat flow, but by viscous flow and is positive if anything happens.

4. Viscoelasticity

In the case of a viscoelastic substance, we have time dependence. This manifests itself as a dependence of the appropriate variables on time history. In particular, there is what is called a *relaxation modulus* $G(t, \vartheta)$, where t is time. The modulus is measured as follows: start with the material sample at rest and assume that it can be considered as always having been at rest, i.e. it can be assumed that the sample has forgotten its past history. Load the sample to a fixed strain at an experimental time taken as $t = 0$, i.e. to a given value of γ , and measure the stress as a function of time t . Then $\frac{\sigma}{\gamma}$ will give G .

Generally it is expected, at least at fixed ϑ , that G will be a sum or integral of decaying exponentials

$$G = \sum_n a_n e^{-t/\tau_n}$$

where the τ_n are called the *relaxation times*¹. The stress in a general deformation history is then given at present time t by

$$\sigma = G(0)\gamma(t) + \int_{-\infty}^t \dot{G}(t - \tau)\gamma(\tau) d\tau$$

where we have omitted ϑ for simplicity, but we understand that it is still there. Consider now the motion given by

$$\gamma = \begin{cases} 0 & \text{if } t < 0 \\ \gamma(t) & \text{if } t > 0 \end{cases}$$

¹Sometimes G is expressed as an integral

$$G(t) = \int_0^\infty H(\tau) e^{-t/\tau} d\tau$$

instead of a sum.

Then one gets

$$\sigma = G(0)\gamma(t) + \int_0^t \dot{G}(t - \tau)\gamma(\tau) d\tau.$$

So, if the modulus is changing slowly, i.e. if \dot{G} is not large, one can envision a period of time in which G can be neglected and the material will appear to be elastic with elastic modulus $\mu = G(0)$. To turn this around, we can say that whatever the decay rate of G , at the initial time $t = 0$ and for some time afterwards, the material will appear to be elastic – time in which the elastic approximation holds is always there, but it may be long or short depending on the rate \dot{G} .

Note that we have made no assumption about $G(+\infty)$. We get an approximate elastic interval of time no matter what $G(+\infty)$ is. To get fluid behavior, we need to assume that $G(+\infty) = 0$, i.e. that relaxation is eventually complete. Doing so, we find that after an integration by parts gives

$$\sigma = \int_0^\infty G(t - \tau)\dot{\gamma}(\tau) d\tau$$

so that if G is replaced by a delta function, we recover the viscous fluid with viscosity being the area under the curve of the relaxation modulus. If the rate at which the relaxation modulus decays with time is fast enough, we will see apparent viscous fluid behavior. Since the fluid point of view is unifying, we adopt it.

5. Energy

Now let us turn to the energies. We take as our Helmholtz free energy

$$A = -\frac{1}{2} \int_{-\infty}^t \dot{G}(t - \tau, \vartheta) [\gamma(t) - \gamma(\tau)]^2 d\tau + h(\vartheta),$$

$$\frac{\partial}{\partial \vartheta}(-\dot{G}) \geq 0$$

where h is some given function of ϑ , and proceed as before. The algebra is a bit more complex than before, but the steps are essentially the same. We come out with the following where we have kept the dot to mean the derivative with respect to present time t :

$$s = \frac{1}{2} \int \frac{\partial}{\partial \vartheta} \dot{G}(t - \tau, \vartheta) [\gamma(t) - \gamma(\tau)]^2 d\tau - h'(\vartheta),$$

$$E = A + \vartheta s,$$

$$\dot{E} = \sigma \dot{\gamma} + \vartheta \dot{s} - \frac{1}{2} \int_{-\infty}^t \ddot{G}(t - \tau, \vartheta) [\gamma(t) - \gamma(\tau)]^2 d\tau.$$

After putting this into the energy balance equation, we get, after simplifying,

$$\dot{s} + \frac{Q}{\vartheta} = \frac{1}{2\vartheta} \int_{-\infty}^t \ddot{G}(t - \tau, \vartheta) [\gamma(t) - \gamma(\tau)]^2 d\tau.$$

Since G is a sum of decaying exponentials, $\ddot{G} \geq 0$ and so the second law holds.

Now let us look at a special case, namely when G is proportional to temperature, in analogy to the perfect gas or ideal rubber. Write

$$G(t - \tau, \vartheta) = \vartheta \bar{G}(t - \tau).$$

Then the internal energy becomes

$$E = h(\vartheta) - \vartheta h'(\vartheta).$$

So, as in an ideal gas, the internal energy is a function of temperature alone. So during an isothermal stress relaxation, there is no work being done, the internal energy is not changing and so no heat is flowing. What is happening?

Go back for a moment to an ideal gas. Suppose that it is originally at room temperature and that it is compressed and then allowed to remain at rest in contact with its isothermal surroundings which we call the room. During rapid compression, the work put in goes into internal energy. It gets hot. Then it cools to the room temperature: at which time the internal energy, depending only on temperature, returns to its original value. When the pressure is released, energy is recovered in the form of work. Where does it come from? It initially comes from internal energy, the lowering of which causes the gas to cool. Then the cooled gas returns to room temperature by removing energy from the room in the form of heat flow.

What is different about our material? As it relaxes, no energy is flowing. But it is losing its ability to give back work and then remove the energy from the room in the form of heat flow.

One other comment may be of interest. Note that if we define Σ by

$$\Sigma = \frac{1}{2} \int \frac{\partial}{\partial \vartheta} \dot{G}(t - \tau, \vartheta) [\gamma(t) - \gamma(\tau)]^2 d\tau$$

then $s + \Sigma = -h'(\vartheta)$.

Consider, now, a stress relaxation experiment. Since for times $t < 0$ and $\tau \leq t$ we have $\gamma(t) - \gamma(\tau) = 0$, and thus $\Sigma = 0$. The load is put on, the temperature returns to room temperature and $s + \Sigma$ is the same as it was originally. But now, $\Sigma > 0$ and so s has decreased. As time goes on, Σ decays toward zero, and so s rises to its original value.

Perhaps more importantly, one should note that if $\Sigma > 0$, and nothing else is changing, then Σ is changing. Equilibrium is possible only if $\Sigma = 0$. So we are dealing with thermodynamic non-equilibrium. We proposed that Σ be called *entaxy*, i.e. internal form.

One more refinement should be mentioned, namely time-temperature superposition. The time seen by the material is that on a temperature dependent clock. The higher the temperature, the faster the relaxation. Let $b_T(\tau)$ be the time read by the material clock at laboratory time and let

$$\beta(t) = \int_0^t b_T(\xi) d\xi$$

be the material time when the laboratory time is t . Then the Helmholtz free energy becomes

$$A = -\frac{1}{2} \int_{-\infty}^t \dot{G}(\beta(t) - \beta(\tau), \vartheta) [\gamma(t) - \gamma(\tau)]^2 b_T(\tau) d\tau + h(\vartheta)$$

and, except for such modifications, nothing important changes.

6. General theory

The next task is to carry over our these ideas to a theory which

- (1) allows finite strain,
- (2) is properly invariant,
- (3) is three dimensional.

To these ends, then, we consider a motion, which is a time dependent mapping of the material points into space. We choose a reference configuration, which is just some mapping of material points into space. We suppose, then, that X_α , $\alpha = 1, 2, 3$, varies over a given material region in the reference configuration and that $x_i = x_i(X, t)$ maps the material point X into the spatial point x_i at time t . The deformation tensor is given by

$$x_{i\alpha} = \frac{\partial x_i}{\partial X_\alpha}.$$

For elastic behavior, the reference configuration is conveniently taken to be a stress-free configuration, if one exists and the Helmholtz free energy is then a function of the deformation gradient with respect to the stress-free configuration. The Helmholtz free energy, being a scalar, depends on the deformation gradient through its right Cauchy-Green tensor

$$C_{\alpha\beta} = x_{i\alpha}x_{i\beta}$$

which is the part of the deformation which is invariant to rigid motions in space. The stress σ_{ij} is then given by

$$\sigma_{ij} = 2\rho x_{i\alpha}x_{j\beta} \frac{\partial A}{\partial C_{\alpha\beta}}$$

where ρ is mass density. The entropy density, as before, $s = -\partial A/\partial\vartheta$ and the internal energy density is $E = A + \vartheta s$. For heat transfer, we introduce the heat flux vector, q_i . The integral of q_i over the surface of a volume is the rate at which heat leaves the volume. So we now balance energy by setting the rate of change of internal energy equal to the work rate plus the rate of heat added. After some algebra, one arrives at the entropy production equation

$$\rho\vartheta\dot{s} + q_{i,i} = 0$$

which then can be written

$$\rho\dot{s} + \left(\frac{q_i}{\vartheta}\right)_{,i} = \frac{-q_i\vartheta_{,i}}{\vartheta^2}.$$

So as long as heat flows against the temperature gradient, as in Fourier’s law, we have agreement with the second law of thermodynamics. We also observe that for an elastic material, entropy production is the result of heat flow – no viscosity.

But we need to get to large strain viscoelasticity. For such, we need a constitutive law for history dependence. So we made some assumptions and did some experiments. We came up with the stress depending on the history of strain through a single integral in time. And the strain dependence of the integrand was taken to be relative strain, i.e. $x_{ij}(t, \tau) = x_{i\alpha}X_{\alpha j}$, where the later is the matrix inverse of $x_{i\alpha}$. The concept was that the material wants to return to every configuration that it had in the past as if it were a preferred configuration, but it cannot and so

it compromises and gives a weight to each such past configuration, with the more recent counting more than the less recent, (fading memory) and adds the weighted contributions.

The assumption led to the result that from single step stress relaxation results, one could predict the stress history in any other motion. This concept seemed to be verified experimentally as shown by the data of Zapas and Craft [5].

In fairness, I must add that we also want the predictions to hold when the strain is reversed. This turned out not to hold for the original materials tested, but recently there have been some results on branched polymers for which the strain reversal seems to hold [4].

Since most of the thermodynamic notions have already been developed in the linear case, let us end by stating how they carry over to the non-linear situation.

We assume that there is a scalar function of relative strain and time t , which we shall call $U(x_{ij}(t, \tau), t)$ with the following properties:

- $U \geq 0$,
- $U(\delta_{ij}) = 0$,
- $U_* = \frac{\partial U}{\partial t} \leq 0$.

There is a time-temperature superposition constant, $b_T(t)$ so that the effective time to which the material responds is

$$\beta(t) = \int_0^t b_T(\tau) d\tau.$$

We define a quantity Σ called *entaxy* which has dimensions of entropy, by

$$\Sigma = \int_{-\infty}^t U(x_{ij}(t, \tau), \beta(t) - \beta(\tau)) b_T(\tau) d\tau.$$

The Helmholtz free energy is given by an expression of the form

$$A = \Phi(v, \vartheta) + \Sigma$$

where $v = \frac{1}{\rho}$ is the specific volume and Φ is some given function.

The stress is given by

$$\sigma_{ij} = \rho x_{i\alpha} \frac{\partial A}{\partial x_{j\alpha}}(t)$$

where one can use any reference configuration X_α .

For the balance of energy, one winds up with

$$\rho \vartheta \dot{s} + q_{i,i} = -\rho \vartheta \int_{-\infty}^t U_* b_T(t) b_T(\tau) d\tau$$

which gives positive entropy production and, along with positive thermal conductivity, agreement with the second law. As in the linear case, this is a non-equilibrium theory. It can be shown that if $\Sigma > 0$ and no motion is occurring and temperature is not changing, then $\Sigma \downarrow 0$. The only possibility of nothing changing is when $\Sigma = 0$. So is the seat of the non-equilibrium behavior. Furthermore, when $\Sigma = 0$, it can be shown that there is no shear stress. This is a fluid theory in the sense that it cannot support a shear stress in thermodynamic equilibrium.

7. Conclusion

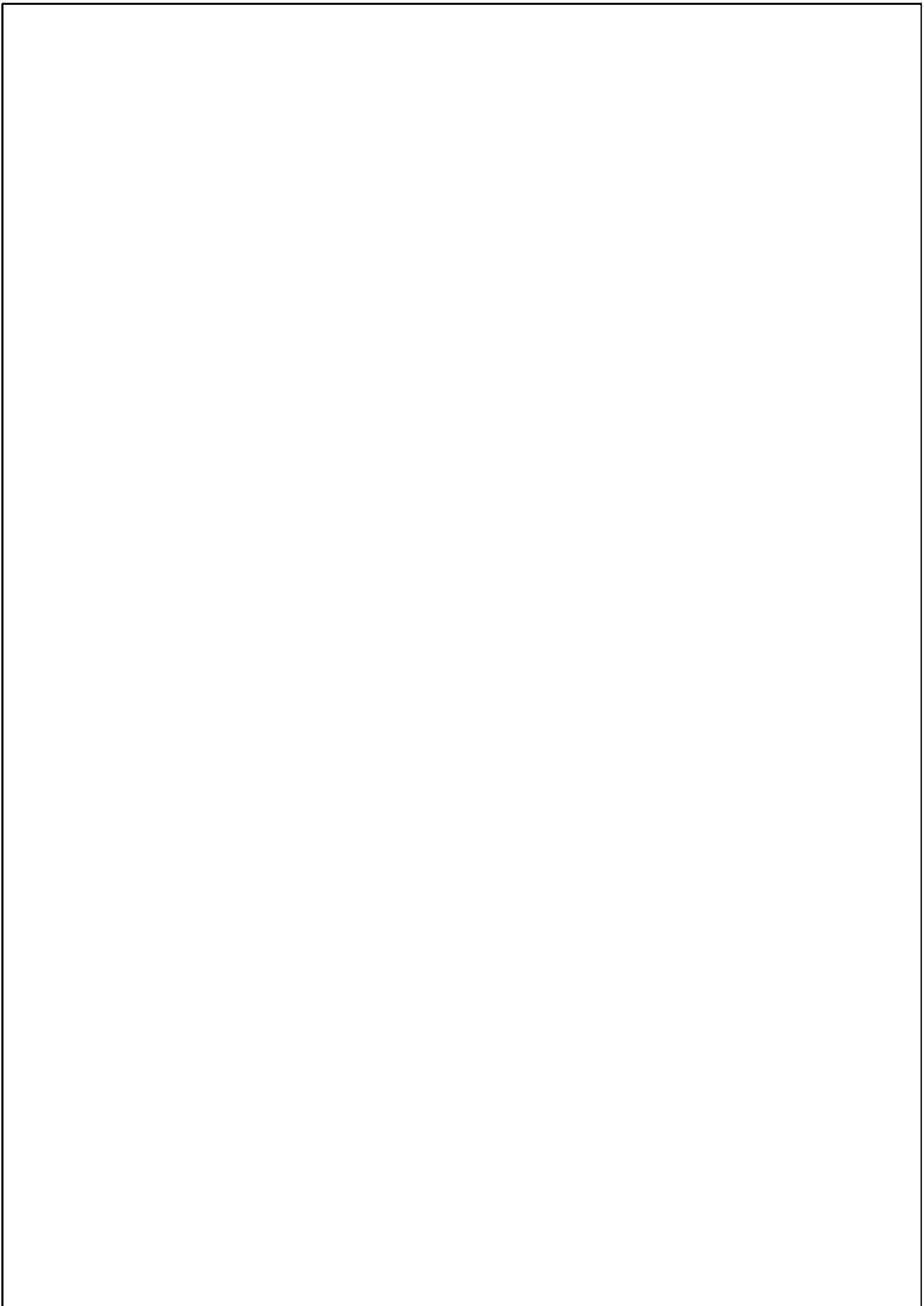
In concluding, let us summarize some features of this theory.

- It is a theory of non-equilibrium thermodynamic behavior.
- It is a fluid theory in the sense that shear stresses are not supported in thermodynamic equilibrium.
- It obeys the first and second laws of thermodynamics.
- Internal energy depends only on temperature. This means that in and isothermal stress relaxation, no heat is flowing. It is just losing its ability to remove energy from its surroundings and return it as heat.

One final remark is in order: Recent experiments [4] which have shown that the theory works better for branched polymers than it does for linear polymers seems counter intuitive to me. But such is the experimental evidence.

Bibliography

- [1] B. Bernstein. Time dependent behavior of an incompressible elastic fluid : Some homogeneous deformation histories. *Acta Mechanica*, 2:329–354, 1966.
- [2] B. Bernstein, E.A. Kearsley, and L. Zapas. Thermodynamics of perfect elastic fluids. *J. Research N.B.S.*, 68B:103–113, 1964.
- [3] B. Bernstein, E.A. Kearsley, and L.J. Zapas. Elastic stress-strain relations in perfect elastic fluids. *Trans. Soc. Rheology*, 9:27–39, 1965.
- [4] J. Shieber and D. Venerus. Pompom theory evaluation in double step strain. *J. Rheology*, 47:413, 2003.
- [5] E.A. Zapas and T. Craft. Correlation of large longitudinal deformations with different strain histories. *J. Research N.B.S.*, 69A:541–546, 1963.



(Eds.) J. Málek, V. Průša and K. R. Rajagopal

Reviews in geomechanics

Published by
MATFYZPRESS
Publishing House of the Faculty of Mathematics and Physics
Charles University, Prague
Sokolovská 83, CZ – 186 75 Praha 8
as the 226. publication

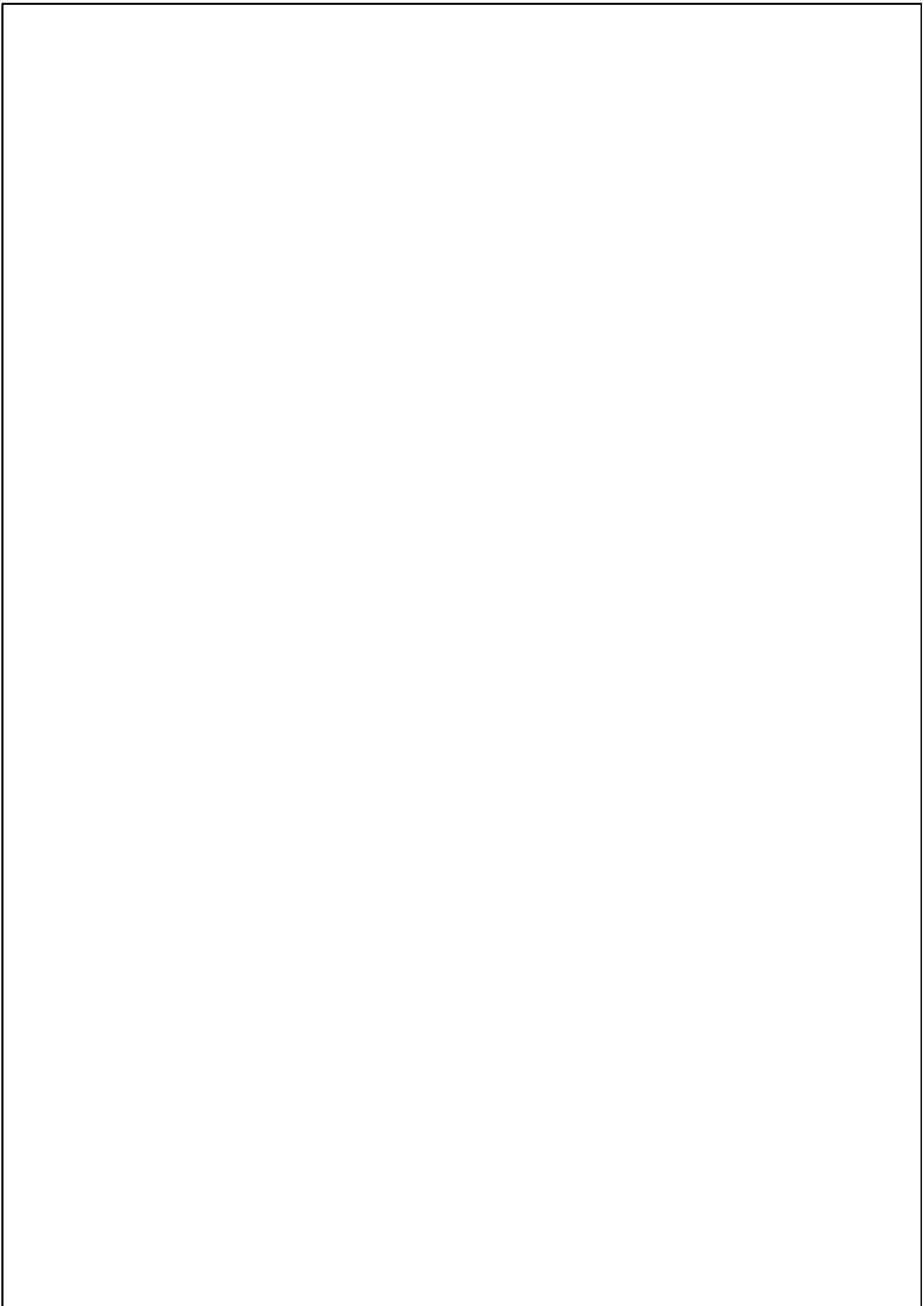
The volume was typeset by the authors using \LaTeX

Printed by
Reproduction center UK MFF
Sokolovská 83, CZ – 186 75 Praha 8

First edition

Praha 2007

ISBN 978-80-7378-032-6



JINDŘICH NEČAS

Jindřich Nečas was born in Prague on December 14th, 1929. He studied mathematics at the Faculty of Natural Sciences at the Charles University from 1948 to 1952. After a brief stint as a member of the Faculty of Civil Engineering at the Czech Technical University, he joined the Czechoslovak Academy of Sciences where he served as the Head of the Department of Partial Differential Equations. He held joint appointments at the Czechoslovak Academy of Sciences and the Charles University from 1967 and became a full time member of the Faculty of Mathematics and Physics at the Charles University in 1977. He spent the rest of his life there, a significant portion of it as the Head of the Department of Mathematical Analysis and the Department of Mathematical Modeling.

His initial interest in continuum mechanics led naturally to his abiding passion to various aspects of the applications of mathematics. He can be rightfully considered as the father of modern methods in partial differential equations in the Czech Republic, both through his contributions and through those of his numerous students. He has made significant contributions to both linear and non-linear theories of partial differential equations. That which immediately strikes a person conversant with his contributions is their breadth without the depth being compromised in the least bit. He made seminal contributions to the study of Rellich identities and inequalities, proved an infinite dimensional version of Sard's Theorem for analytic functionals, established important results of the type of Fredholm alternative, and most importantly established a significant body of work concerning the regularity of partial differential equations that had a bearing on both elliptic and parabolic equations. At the same time, Nečas also made important contributions to rigorous studies in mechanics. Notice must be made of his work, with his collaborators, on the linearized elastic and inelastic response of solids, the challenging field of contact mechanics, a variety of aspects of the Navier-Stokes theory that includes regularity issues as well as important results concerning transonic flows, and finally non-linear fluid theories that include fluids with shear-rate dependent viscosities, multi-polar fluids, and finally incompressible fluids with pressure dependent viscosities.

Nečas was a prolific writer. He authored or co-authored eight books. Special mention must be made of his book “Les méthodes directes en théorie des équations elliptiques” which has already had tremendous impact on the progress of the subject and will have a lasting influence in the field. He has written a hundred and forty seven papers in archival journals as well as numerous papers in the proceedings of conferences all of which have had a significant impact in various areas of applications of mathematics and mechanics.

Jindřich Nečas passed away on December 5th, 2002. However, the legacy that Nečas has left behind will be cherished by generations of mathematicians in the Czech Republic in particular, and the world of mathematical analysts in general.

JINDŘICH NEČAS CENTER FOR MATHEMATICAL MODELING

The Nečas Center for Mathematical Modeling is a collaborative effort between the Faculty of Mathematics and Physics of the Charles University, the Institute of Mathematics of the Academy of Sciences of the Czech Republic and the Faculty of Nuclear Sciences and Physical Engineering of the Czech Technical University.

The goal of the Center is to provide a place for interaction between mathematicians, physicists, and engineers with a view towards achieving a better understanding of, and to develop a better mathematical representation of the world that we live in. The Center provides a forum for experts from different parts of the world to interact and exchange ideas with Czech scientists.

The main focus of the Center is in the following areas, though not restricted only to them: non-linear theoretical, numerical and computer analysis of problems in the physics of continua; thermodynamics of compressible and incompressible fluids and solids; the mathematics of interacting continua; analysis of the equations governing biochemical reactions; modeling of the non-linear response of materials.

The Jindřich Nečas Center conducts workshops, house post-doctoral scholars for periods up to one year and senior scientists for durations up to one term. The Center is expected to become world renowned in its intended field of interest.